PARAMETRIC MECHANICAL DESIGN AND OPTIMISATION OF THE CANTERBURY HAND

A thesis submitted in partial fulfilment of
the requirements for the degree of
Master of Engineering (Mechanical)

In the

Department of Mechanical Engineering
University of Canterbury
Christchurch, New Zealand

by
Christopher S. Green B.E. Mech (Hons)

University of Canterbury
2002

Abstract

As part of worldwide research humanoid robots have been developed for household, industrial and exploratory applications. If such robots are to interact with people and human created environments they will require human-like hands. The objective of this thesis was the parametric design and optimisation of a dexterous, and anthropomorphic robotic end effector. Known as the ‘Canterbury Hand’ it has 11 degree of freedoms with four fingers and a thumb. The hand has applications for dexterous teleoperation and object manipulation in industrial, hazardous or uncertain environments such as orbital robotics.

The human hand was analysed so that the Canterbury Hand could copy its motions, appearance and grasp types. An analysis of the current literature on experimental prosthetic and robotic hands was also carried out. A disadvantage of many of these hand designs was that they were remotely powered using large, heavy actuator packs. The advantage of the Canterbury Hand is that it has been designed to hold the motors, wires, and circuit boards entirely within itself; although a belt carried battery pack is required. The hand was modelled using a parametric 3D computer aided design (CAD) program. Two different configurations of the hand were created in the model. One configuration, as a dexterous robot hand, used Ø13mm 3 Watt DC motors, while the other used Ø10mm, 0.5 Watt DC motors (although this hand is still slightly too large for a general prosthesis). The parts within the hand were modelled to permit changes to the geometry. This was necessary for the optimisation process. The bearing geometry of the finger and thumb linkages, as well as the thumb rotation axis was optimised for anthropomorphic motion, appearance and increased force output. A design table within a spreadsheet was created to interact with the CAD models of the hand to quickly implement the optimised geometry. The work reported in this thesis has shown the possibilities for parametric design and optimisation of an anthropomorphic, dexterous robotic hand.

Acknowledgements

I would first like to thank Dr Dunlop for this interesting thesis. His help has been invaluable in shaping the design of the Canterbury Hand. I would also like to thank the technicians Andy Cree and Ken Brown who have given me insight into the practicalities of building a mechanical hand. While he was here the store man Geoff Leathwick was very helpful in helping me find local and international manufacturers for the tiny components I needed to make for this hand. Paul Southward and Adam Latham were very helpful in setting up the computers and necessary programs. Thank you also to all the various postgraduates, staff and lecturers of the mechanical engineering department who have all been friendly and accommodating with me.

Various postgraduates in particular have been of help during this thesis. I would like to thank Eric Hung who has patiently listened and acted as a sounding board for my ideas. Angleo Garcia, Henry Chen, and Eric Hung for helping me do an enormous amount of scanning. Ian McMillan for his help with various Solidworks problems and explaining that a five bar linkage is in fact unstable until singularity. Michael Fielding for describing how his hexapod robot HAMLET worked and how it might apply to the robotic hand design. Justin Stevenson for his help in CorelDraw. Jens Roesner was very helpful in getting me started on the VBA programming used in optimising the hand. Simon Ferguson for generously sharing his research on prosthetics and robotic hands. Thank you also to David Stewart who started me on the road of 3D CAD designing. Lastly I would like to thank my parents, Gary and Suzanne Green, for their emotional and economic support during this thesis. Also to my brother Lyndon and sister Charlotte for keeping me sane. We should all be blessed with such a wonderful family.

Contents

List of Figures

List of Pictures

List of Tables

Nomenclature

Acronyms

2D	Two-dimensional
3D	Three-dimensional
AIST-MITI	National Institute of Advanced Industrial Science and Technology (AIST) Ministry of International Trade and Industry (MITI).
AMF	American Machine and Foundry
AMMIS	Articulated Manipulator for Minimally Invasive Surgery
A/D, ADC	Analogue to Digital Converter
AEC	Active Electromechanical Compliance
ABS	Acrylonitrile/butadiene/styrene
AMA	Antagonistic Muscle like Actuator
AMF	American Machine and Foundry
ANS	American Nuclear Society's
ASME	The American Society of Mechanical Engineers
BIWA	Body in white assembly
BOD	Bearing Outer Diameter
BOM	Bill of Materials
BMES	Biomedical Engineering Society
BUAA	Beijing University of Aeronautics and Astronautics
CA	California
CAT	Centre for Advanced Technology
CB	Circuit Board
CAD	Computer Aided Drawing
CAE	Computer Aided Engineering
CAM	Computer Aided Manufacture]
CATIA	Computer-Aided Three-dimensional Interactive Application
CM	Carpo-Metacarpal
CNC	Computer Numerical Control
CS	Counter Sunk
CTSD	Crew and Thermal Systems Division

CUHK	The Chinese University of Hong Kong
D/A, DAC	Digital Analogue Converter
DALSA	Dexterous Articulated Linkage for Surgical Applications
DC	Direct Current
DIP	Distal Interphalangeal
DIST	Dipartimento di Informatica, Sistemistica e Telematica
DLR	Deutschen Zentrum für Luft und Raumfahrt (German Aerospace Centre)
DMOS	Diffusion Metal Oxide Semiconductor
DOF	Degree of Freedom
DOTS	Double Octagon Tactile Sensor
DSP	Digital Signal Processor
DXF	Drawing Exchange Format
EDS	Electronic Data Systems
EDM	Electro Discharge Machine
EMBS	Engineering in Medicine and Biology Society
EMG	Electromyographic
ETL	Electro technical Laboratory
ETS	Engineering Test Satellite
EXOS	Explore your OS
ENOVIAPM	ENOVIA Product Management
EVA	Extra Vehicular Activity
FBI	Federal Bureau of Investigation
FDM	Fused Deposition Modelling
FEA	Finite Element Analysis
FOS	Factor of Safety
FPGA	Field Programmable Gate Array
FRIEND	Functional Robot Arm with user interface for disabled people
FSR	Force Sensing Resistors
FZK	Forschungszentrum Karlsruhe
GA	Genetic Algorithm or Georgia Arizona
GE	General Electric
GUI	Graphical User Interface
HRL	Harvard Robotics Lab

IBM	International Business Machines Corporation
ICAR	International Conference on Advanced Robotics
ICECS	International Conference on Electronics, Circuits and Systems
ICRA	International Conference on Robotics and Automation
ID	Inside Diameter
IECON	Industrial Electronics Society Conference
IEE	Institution of Electrical Engineers
IEEE	The Institute of Electrical and Electronics Engineers
IFAS	Institut für fluidtechnische Antriebe und Steureungen (Institute of Fluid Power Drives and Controls)
IFMA	Institut Français de Mécanique Avancée (French Institute for Advanced Mechanics)
IFToMM	International Federation for Theory of Machines and Mechanisms
IGES	Initial Graphics Exchange Standard
IP	Inter-Phalangeal
IRE	Investigative Reporters and Editors
IROS	Intelligent Robots and Systems
I/O	Input/Output
IP	Interphalangeal
IROS	Intelligent Robots and Systems
ISAC	Intelligent Soft Arm Control
ISATP	International Symposium on Assembly and Task Planning
ISO	International Organisation for Standardisation
ISS	International Space Station
JPL	Jet Propulsion Laboratory
LED	Light Emitting Diode
LH	Left Handed
LMS	Laboratoire de Mécanique des Solides
LVDT	Linear Variable Differential Transformer
MAC	Man and Computer
MARCUS	Manipulative Automatic Control and User Supervision
MCP	Metacarpophalangeal, see also MP
MHS	Micromechatronics and Human Science
MIA	Mechanical Impedance Adjustor

MIS	Minimally Invasive Surgery
MIT	Massachusetts Institute of Technology
MIMO	Multiple Input Multiple Output
MP	Metacarpo-Phalangeal, see also MCP
MPMS	Multiple Prehensile Manipulator System
NASA	National Aeronautics and Space Administration
NASDA	National Space Development Agency of Japan
NELCON	New Zealand National Electronics Conference
NTU	National Taiwan University
NZ	New Zealand
OCEANS	Open Architectures and Network Programming,
OD	Outside Diameter
OS	Operating System
PaT	Payload Tutor
PC	Personal Computer
PCB	Printed Circuit Board
PCD	Pitch Circle Diameter
PDM	Product Data Management
PETP	Polyethylene terephthalate
PIP	Proximal Interphalangeal
PLM	Product Lifecycle Management
PMA	Pneumatic Muscle Actuator
POSTECH	Pohang University of Science and Technology
P. R. China	Peoples Republic of China
PSD	Position Sensing Device
PSoC	Programmable System on a Chip
PTFE	Polytetrafluoroethylene, otherwise known as Teflon
PUMA	Programmable Universal Machine for Assembly
PVDF	Polyvinylidene fluoride
PWM	Pulse Width Modulation
RAC	Raytheon Aircraft Company
RH	Right Handed
ROV	Remote Operated Vehicle
RPI	Rensselaer Polytechnic Institute

RTV	Room-Temperature Vulcanising
RUR	Rossum’s Universal Robots
RWTH	Rheinisch-Westfälische technische Hochschule
RSJ	Robotics Society of Japan
SCARA	Selective Compliance Assembly Robot Arm or Selective Compliant Articulated Robot for Assembly
SCROLLIC	Synchronously Closing with rolling constraints
SDPSI	Stock Drive Products Sterling Instrument
SPDM	Special Purpose Dexterous Manipulator
SDSU	San Diego State University
SEKON	Senter for Kompetanse og Næringsutvikling
SICE	Society of Instrument and Control Engineers
SMA	Shape Memory Alloy
SMC	Systems, Man, and Cybernetics
SMT	Surface Mount
SMA	Shape Memory Alloy
STEP	Standard for the Exchange of Product data
TD	Terminal Device
TDT	Tension Differential type Torque
TENCON	International Conference on Electrical and Electronic Technology
TNZ	Team New Zealand
TRN	Technology Research News
TUAT	Tokyo University of Agriculture and Technology
TUM	Technische Universität München
UA	University of Alberta
UK	United Kingdom or University of Kentucky
UMDH	Utah/MIT Dexterous Hand
UOC	University of Canterbury
UPP	Universal Pulse Processor
USA	United States of America
USC	University of Southern California
USSR	United Soviet States of Russia
USTB	University of Science and Technology Beijing
VBA	Visual Basic Application

WABOT	Waseda Robot
WABIAN	Waseda Biped Humanoid
WAM	Waseda Automatic Manipulator
WENDY	Waseda Engineering Designed Symbiont

Symbols

º	Degree
g	Gram
kg	Kilogram
kPa	Kilopascal
lbs	Pounds
m	Metre
mm	Millimetres
mN	Milli-Newton
mNm	Milli-Newton metres
MPa	Mega Pascal
ms	Millisecond
N	Newton
Nm	Newton metres
Pa	Pascal
Psi	Pounds per square inch
s	Second
X	Variable

Abbreviations

B	Breadth
e.g.	exempli gratia (for example)
etc	et cet·er·a (and so forth)
GND	Ground
Inc.	Incorporated
i.e.	id est (that is)
L	Length
Ltd.	Limited

No.	Number
Mod.	Modulus
p.	Page
pp.	Pages
Rx	Receive
Tx	Transmit
Vol.	Volume
wrt	With Relation To

Glossary

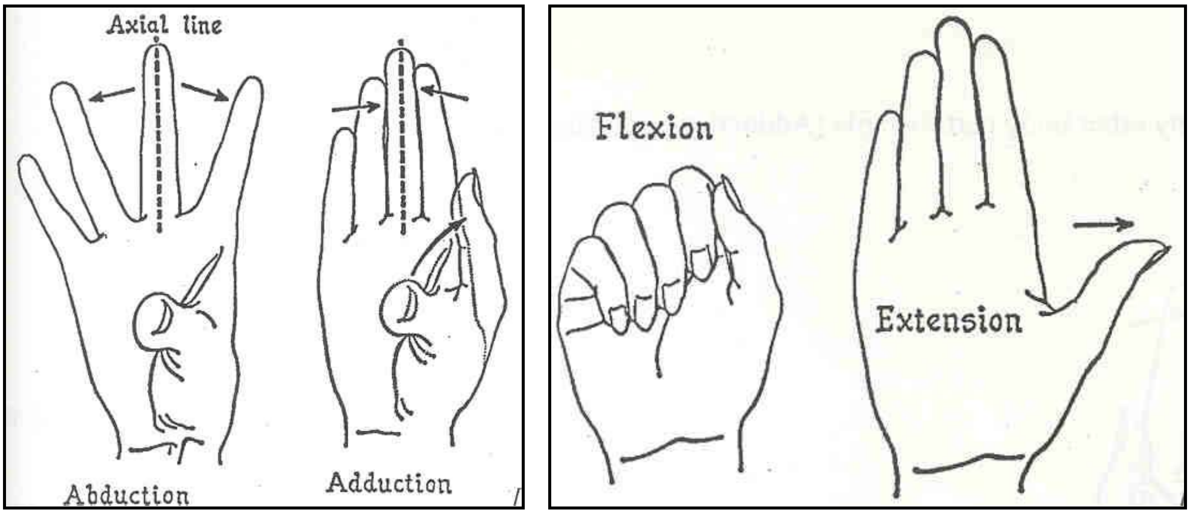

Picture 1 Hand Motions [Basmaginan & Slonecker, 1989]

Abduction	To bring a limb away from the body
Addendum circle	Diameter of circle around outer edge of gear teeth
Adduction	To bring a limb or any other body part towards the body
Antagonistic	When used with tendons: one tendon opposes the other tendons motion.
Anthropomorphic	Has human like attributes, behaviour or characteristics
Anodise	Oxide Coating
Carpal Bones	The bones of the wrist.
Circumduction	Movement of digit a so its end traces a circle in space
Compliance	The fingers will move about an object to comply with its shape
Flexion	The action of bending or closing a limb.
Extension	The action of extending or straightening a limb.
Degree of Freedom	This means an independent component of motion within a system.
Distal	Far or farther from the trunk
Distal Link	Is the fingertip linkage in the Canterbury Finger.
Dorsiflexion	The hand rotates up at the wrist (opposite to the palm).
Medial	Towards the mid-line of the body

Medial Link	The middle link in the Canterbury Finger. It is between the Proximal and the distal link.
Metacarpal Block	The metacarpal block is attached to the Canterbury finger and houses the motors and the drive screws that move the finger.
Opposition	Circumduction and flexion of the thumb, usually describes when the thumb touches the tip of a finger
Palmar flexion	The wrist rotates the hand down in the direction of the palm.
Phalange (Phalanx)	Any bone of the fingers or toes.
Pitch	Up and down motion of a joint or an angular displacement along the lateral axis.
Pronation	Turning the forearm so the palm faces posteriorly (towards the body)
Proximal	Near or closer to the trunk
Proximal Link	The link closest to the Metacarpal block.
Quadrature	The process of making something square i.e. Square Waves for encoder output
Radial Deviation	Abduction of the wrist, where the thumb side of the palm moves towards the radius of the forearm
Rocker Plate	A rocker plate within the proximal link that helps produce the curling action of the finger.
Roll	Rotation of the joint about a longitudinal axis i.e. in line with the arm.
Singularity	The area in a robotic joint’s range of motion that must be avoided due to two possible solutions to the movement. This is a point where function ceases to be analytic (differentiable). This is a problem in the movement area of the finger and the thumb linkage models.
Supination	The turning of the forearm so the palm faces anteriorly (away from the body)
Ulnar Deviation	Adduction of the wrist, where the little finger side of the palm moves toward the ulna of the forearm
Underactuated	The manipulator has more motions (degrees of freedom) than are powered by the actuators. Usually for reasons of compliance

Whiffle Tree A Differential mechanism that slits one link into two or more new ones. It attempts to keep the force equal in each new link.

Yaw Side to side motion. It can also be an angular rotation around a vertical axis.

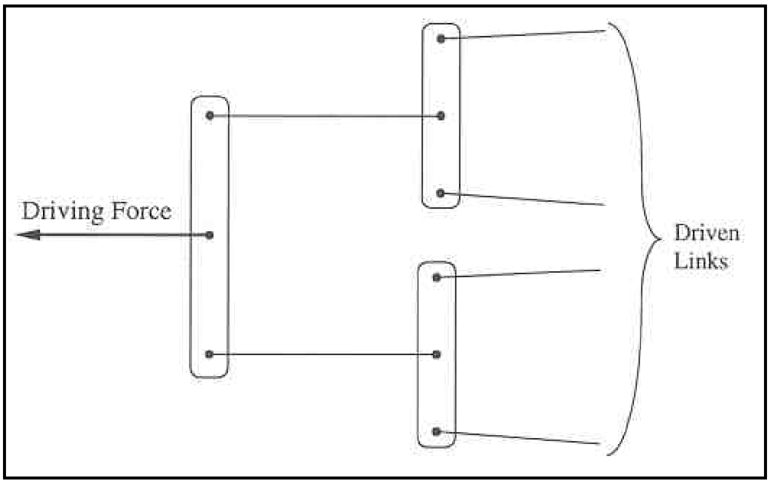

Picture 2 Example of Whiffle Tree Mechanism [Ward, 1996]

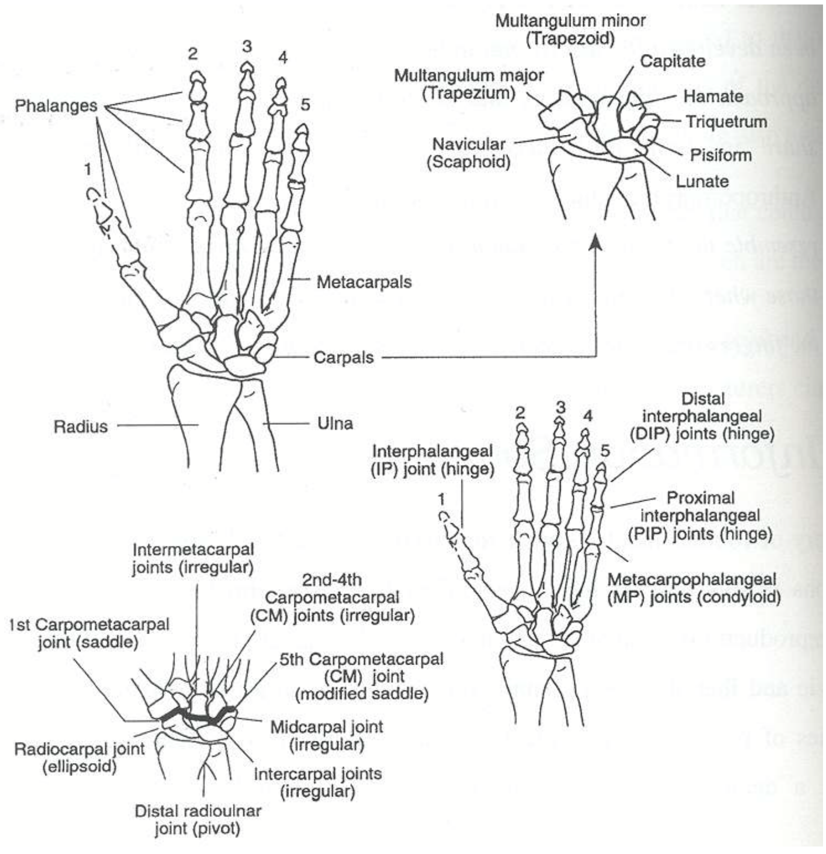

Picture 3 Bones and Joints within the skeletal human hand [MacKenzie & Iberall, 1994]

Chapter 1:   Introduction

Futuristic humanoid robots have long been a part of science fiction. They have appeared in such famous films as 'The Terminator', and 'Star Wars'. The idea of an artificial human like robot has become an accepted feature in literature and the public consciousness. It has also become an objective that roboticists around the globe strive to create. Such a robot will require a highly dexterous multifingered manipulator if it is to successfully interact with the outside world. For it to grasp manmade objects and to interact with society the manipulator will also need to replicate the motion and appearance of the human hand. The question becomes, to what purpose would such a humanoid robot be used for? The answer is, whatever humans do right now that they want something or someone else to do for them.

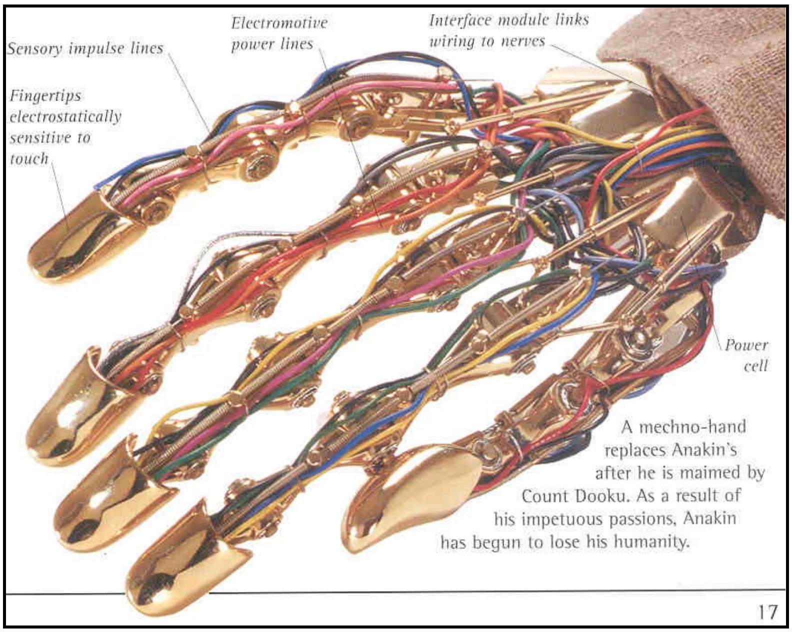

Figure 1.1 Anakin's Prosthetic hand from Star Wars Attack of the Clones [Reynolds, 2002]

Robot hands and arms have been in common use for over fifty years. This is a relatively short period in comparison to the millennia that the human hand has taken to evolve. Even in this short period their applications have become widespread and multifaceted. They have been used for industrial applications, such as handling radioactive materials in nuclear power plants, assembly lines for car manufacture, and the layout of microchip circuit boards. Remotely controlled robot hands have facilitated the exploration of the oceans and outer space. The robot arm on the space shuttle, for example, has been used to deploy satellites in orbit for a number of years. Later developments have included rugged bomb disposal robots. Remotely controlled they can be used to explode or defuse bombs without once placing the fragile human operator in any danger. Some of the latest research for example has been for household cleaning robots and robots that would patrol at night as building security.

Figure 1.2 Bomb Disposal Robot [BBC News, May 2002]

The key idea is that robots and in particular robotic hands have been used in repetitive and hazardous situations instead of humans. Thus they save peoples time and lives for more productive pursuits. The objective of this thesis was the parametric design and optimisation of a robotic manipulator called the ‘Canterbury Hand’. This thesis is part of ongoing research into artificial hands that is being undertaken at the Mechanical Engineering department at the University of Canterbury. This hand design presented here is dexterous, anthropomorphic (that is human shaped) and highly compact.

When beginning the design of the hand various constraints had to be considered. To make the hand compact it had to hold the motors, circuit boards and the wiring entirely within itself. The hand had to utilise the linkage arrangement of the original Canterbury Finger design [Ward, 1996]. Since there were two types of DC motors (from the Mini motor and Maxon motor companies) that had been previously bought for the hand the design had to incorporate each kind of motors in two different hand designs. The first hand design was to use the Ø13mm 3 Watt DC motors from Maxon in a robotic manipulator. The second hand design was to use the Ø10mm, 0.5 Watt DC motors from Mini motor as a prosthetic device. Due to the complexity of the hand design it was parametrically modelled in a 3D Computer Aided Design (CAD) program called SolidWorks. Both designs were modelled as two configurations of a single CAD model. The reason for doing this was to reduce the design time by utilising the parametric attribute of the CAD program. Both hands would have the same features in their creation, though they would use them with different dimensions and additional features.

Both hands designed using this process have the same characteristics and shape though they are of different sizes. The ‘Canterbury Hand’ can be described as an eleven degree of freedom (DOF) multifingered robotic manipulator. The hand is anthropomorphic (human shaped) and has four fingers and a thumb. Each of the fingers is a two DOF linkage mechanism that is actuated by two DC electric motors. It is actuated via a lead screw and drive nut transmission system from the motors, which are located within the finger’s metacarpal assembly. The thumb is a single DOF linkage mechanism that is also directly actuated by a DC motor. The hand has two other mechanisms that are located within the palm of the hand. They are a finger spreading mechanism (1 DOF), and a thumb rotation mechanism (1 DOF). Each of the digits in the hand has human like motions. The fingers can spread apart so that different types of grasps can be made. The thumb for can rotate about the palm so as to oppose the fingers for grasp manipulation.

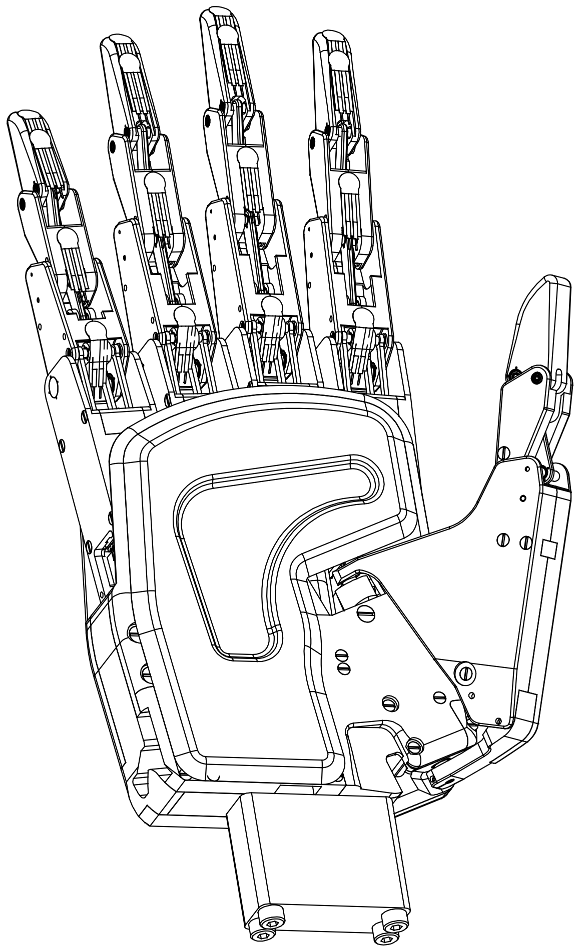

Figure 1.3 The Canterbury Hand (Mini motor Configuration)

The complexity of the geometry involved in the finger and thumb linkage arrangements and the aligning of the thumb rotation axis required the design to be optimised. The optimisation process was an iterative one based on modifying the geometry and evaluating the results. This meant that the CAD design of the hand had to be able to incorporate any changes in the linkage and thumb axis geometry. Since the CAD package was parametric and feature based it could automatically allow for low-level changes for such things as dimension size or for small changes in configurations. However the complexity of the hand design required a CAD structure that could make smart changes. For example, if a modification was placed in the index fingers linkage bearing geometry, the hand design would need to automatically select the correct bearing size, and to modify the surrounding geometry. These design decisions were made using logical functions in the design table spreadsheets within the part models and in the structure of the CAD model. To help implement these changes quickly, instead of laboriously changing each part model or having extremely long rebuild times, a design table in a spreadsheet was created. This program (written in VBA called 'Configure') was used to interact with the design tables within the part models of the hand and to update them. Using this program the optimised geometries were implemented into the hand design.

The thesis initially began as work experience in the summer of 1998, which included the SolidWorks modelling of previous students designs of the Canterbury Finger. It was officially begun mid year in 1999 and has continued since then until the middle of 2002. In that time the design and the optimisation of the Canterbury hand has been completed. The results of which are presented here. This thesis not only presents the results of the work it also attempts to explain the reasons and the method behind them. This is necessary due to the complexity of the design and because other researchers will carry on this work. To detail this work the thesis has been separated into a number of Chapters. This Introductory chapter introduces the concept of what the Canterbury Hand is, why it was designed, and how this thesis is constructed.

Chapter two 'Research' summarises the investigations that were made for this thesis. The purpose of the research was to give an overview of previous research on the Canterbury hand, human hand anthropometrics, and hand prostheses. This research helped shape the design of the hand. A comparison is also made of the Canterbury hand with current experimental prosthetic and robotic manipulators, to evaluate the design and to ascertain its degree of uniqueness. The detailed review of robotic hands is given in the compendium [Green, 2002].

The third Chapter ‘The Canterbury Hand CAD Model’ describes what Computer Aided Design (CAD) design is, and describes a number of CAD software packages, and how they are used in industry. CAD was used in the design of the Canterbury Hand due to the designs complexity, its need for accuracy and to save time in the design process. SolidWorks was selected as the CAD software for the Canterbury Hand design model. SolidWorks is a feature-based parametric solid modeller, which is fully associative, able to be constructed with, or without constraints and can utilise relations to implement the users design intent. The organisation of the parametric model of the Canterbury hand, and the innovative CAD features that were used in its design and optimisation was described in this chapter as well.

The ’Design of the Canterbury Hand’ is described in chapter four. This chapter describes the design objectives for the Canterbury hand. The Canterbury Hand is an 11-degree of freedom mechanism. It is comprised of four fingers of two degrees of freedoms each, and a single degree of freedom thumb. It also has a single degree of freedom thumb rotation mechanism and a single degree of freedom finger spreading mechanism that is housed within a palm assembly. This chapter explains the design features of these mechanisms, what decisions were made when creating them (with regard to the objectives) and how they interact within the hand.

The ‘Background Theory behind the mechanisms within the hand is descried in chapter five. The movements, force output and singularities within the finger and thumb linkage mechanisms are described. The finger spreading and the thumb rotation mechanisms are also explained as to why they work. The background theory section is necessary for the description of the next chapter.

Chapter six describes the ‘Optimisation of the Canterbury Hand’ for the finger, thumb and thumb axis geometry. The finger and thumb linkage bearing geometry needed to be optimised so as to give the maximum anthropomorphic working area, grip force and prehensile interaction within the hand model. The thumb axis needed to be optimised so that it had a maximum grip volume and an anthropomorphic appearance for the thumbs rotation motion. The method, guidelines and results of the optimisation process are given. The results are compared against the Bain [1997] and Ward [1996] finger geometries to help evaluate their effectiveness.

The thesis is concluded in chapter seven, ‘Conclusions and Recommendations’. This chapter evaluates how the hand will perform once it is manufactured and how it may be tested. It also summarises how the hand design compares to other experimental dexterous manipulators. It also makes recommendations as to what design improvements could be made to the Canterbury hand design. After the concluding chapter the references, for the thesis are given.

Chapter 2: Research

The research objective for this thesis focused on areas that would aid in the development of the design of the Canterbury hand. The research for the design began by reviewing the preceding work on the hand. Many of the design choices behind the current Canterbury hand design followed from this examination. Later research was focused on three particular areas; they were the human hand, prosthetic hands and multifingered robotic hands.

The original design brief for the Canterbury hand project was to create a robotic manipulator that had an anthropomorphic appearance and motions that mimicked the human hand. The human hand was investigated, and anthropometrics data found so as to objectify its capabilities, and to incorporate them into the design. This data was also used to optimise the hand so that the fingers, thumb and hand were scaled to human size. The types of grasps the human hand made were also investigated so that the hand design could accomplish them.

One of the goals of the continuing Canterbury hand development at the University of Canterbury is the eventual creation of a prosthetic hand device. Thus research into current and experimental prosthetics was made. The mini motor hand design was created to be a prosthetic. Unfortunately the results showed it to be too large and heavy. However this information will be useful, as the hand once manufactured will serve as a test bed for technologies that will eventually go into the future prosthetic.

Research was made on multifingered robotic hands for inspiration and later comparison for the Canterbury hand. The history of robotics and robotic manipulators is a relatively recent one. Only over the last fifty years has there been developments towards making robotic manipulators for useful applications outside of entertainment and art. It was found that robotic manipulators with large numbers of DOF’s have been part of recent robotic hand developments. Anthropomorphic manipulators in particular have been created and are potentially the most useful for telemanipulation and interacting with people.

On analysing the various experimental prosthetic and robotic hands it was found that a large number were remotely actuated, usually by a large, heavy and bulky actuator system outside of the hand, or in a forearm. The advantage the Canterbury hand has over these hand designs is that all of its actuators are located within the hand itself. Also unlike SMA and tendon systems the directly driven linkage system of the Canterbury hand will have few maintenance problems and losses due to friction. It will also be less costly than a fully gear driven hand design. Though the Canterbury hand utilises a reasonably well-known linkage arrangement, it is a unique robotic hand design.

2.1 Brief History of the Canterbury Hand

The Canterbury Hand originated from discussions between Dr Reg. Dunlop of Canterbury University and Dr Marko Vuskovic of the San Diego State University (SDSU) after reviewing the problems associated with the Belgrade/USC hand model III being built at SDSU.

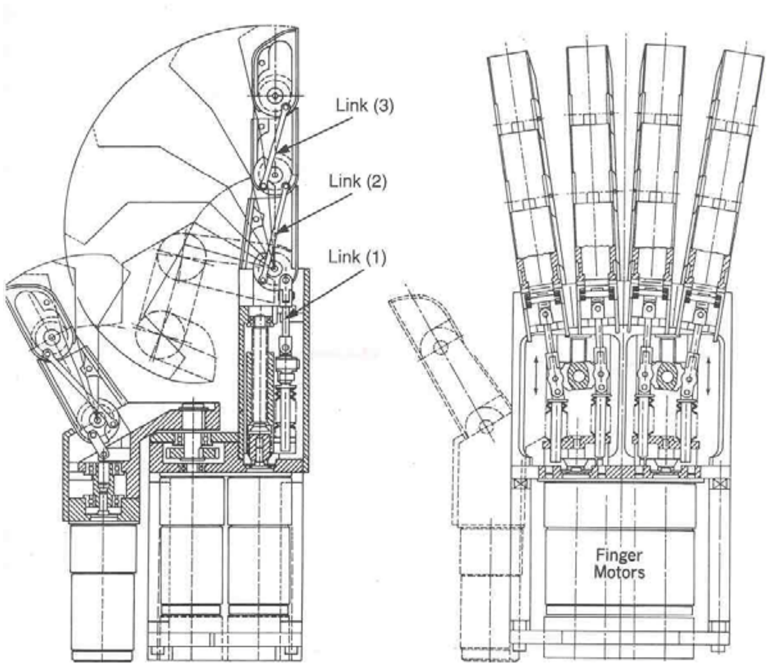

Figure 2.1 Belgrade/USC Hand Model II Cross Sections [Rosheim, 1994]

The Belgrade/USC hand had problems with backlash, friction, and jamming of the drive nut and linkage when trying to release a grip. It was decided that instead of the drive screw and nut being offset from the finger linkages with a single actuator link as in the Belgrade/USC hand, the Canterbury finger would have the drive screw in line with a pair of actuator links. The Belgrade/USC model III hand also required a large motor force on the lead screw to provide the force output from the fingers. This was because the radius of the rotating joints in the finger limited the force's moment from the drive screw. For the Canterbury finger the pivot point was moved to the top edge of the finger to increase the leverage distance for the finger curl. To reduce the cross sectional size of the linkages it was decided that the

Canterbury finger linkages would be placed under tension when holding a load. Lastly the Belgrade/USC hand's fingers only had a single degree of freedom curl motion. This limits the finger positions and the grasp types that the hand could make. The Canterbury hand would be more dexterous with at least two degrees of freedoms for each of the fingers.

With these proposals in mind Dunlop launched a feasibility study for developing a new hand. Two French students Laurent Magnier and Hugues Monier [1993] from the Mechanical Engineering Department at Ecole Nationale D'Ingenieurs Saint-Eterne, France reviewed alternative drive systems for the Canterbury finger. They settled on the two-degree of freedom finger linkage arrangement (see Figure 2.2) that was proposed by Dr Dunlop. The top motor would drive the finger curl, while the bottom motor would drive the finger rotation motion.

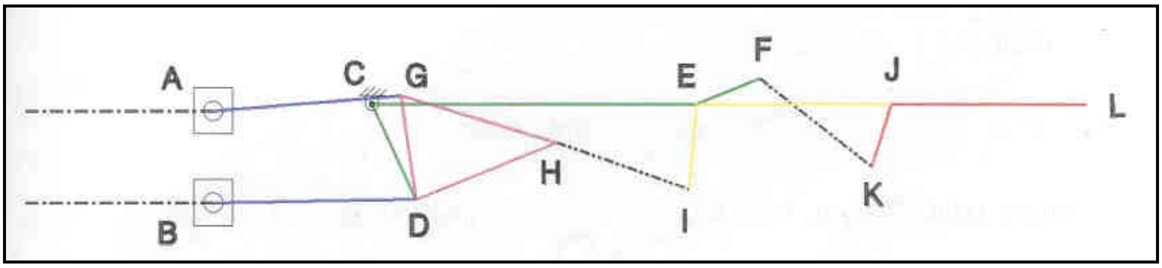

Figure 2.2 Schematic of Canterbury Finger Geometry [Monier & Magnier, 1993]

Since this feasibility study there has been almost continuous work on developing the Canterbury hand. Derek Ward [Ward, 1996] designed, built and tested the prototype Canterbury finger and control system. This finger had problems with its weight, appearance and it's ease of assembly. It also had a reduced working area due to a singularity at the distal joint, and insufficient gripping output force.

Dietmar Traub [Traub, 1996] from 'Fachhochschule für Technik', Esslingen, Germany worked on trying to reduce the size and weight of the finger by using carbon fibre for the linkage material. Overall it was found that carbon fibre was a difficult material to work with and gave results that made it not the most appropriate material. While multiple windings of the carbon fibre increased its strength and repetition introduced better techniques it still tended to fracture under loads comparable to that which the finger would be put under.

Andrew Bain's thesis [Bain 1997] was on the creation of a genetic algorithm program in Mat Lab that would optimise the finger geometry. He also conceptualised a single degree of freedom thumb linkage design. Various finger and thumb geometries were found but were unfortunately found later to be unsuitable.

Rodney Elliot [Elliot, 1998] assessed four techniques for signal parameterisation of the real time Electro Myographic (EMG) signals measured on a persons forearm muscles for six different hand grasps. EMG signals are the voltages appearing at the surface of the skin as a result of contracting muscles. Elliot recommended that more research was needed in classifying forearm muscle function for optimum electrode placement, and in alternative signal classification techniques, before the most reliable technique could be determined. It is in this area that Simon Ferguson is currently completing a doctoral thesis.

Judith Taylor [Taylor, 1998] worked on extending the position control software for Ward's prototype finger, including adding a Hall effect switch within the metacarpal block. Taylor also replaced the acrylic finger linkages with aluminium and simplified the rocker links into a single solid link.

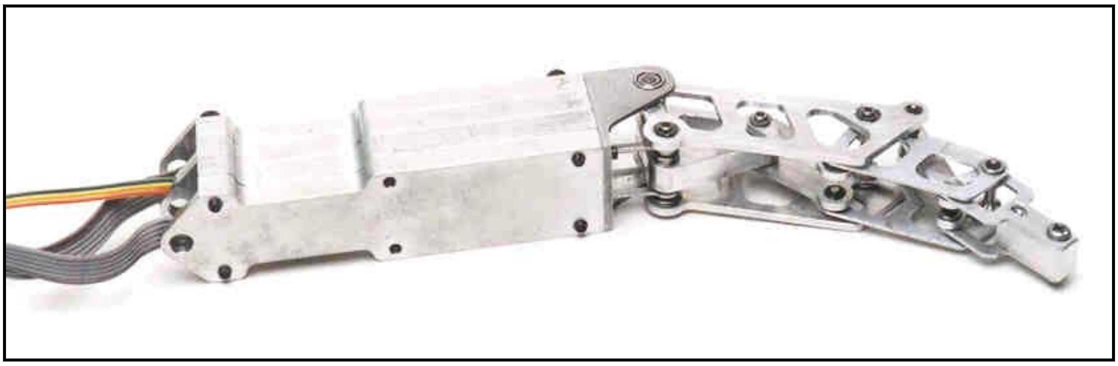

Figure 2.3 Taylor's modified Ward Finger

David Stewart [Stewart, 1999] helped create the Solid Works models of the Ward and Traub fingers. SolidWorks was used, as it was a better 3D Solid Modelling CAD platform than Microstation (which till then had been previously used for modelling the finger).

Didier Lamalle from the IFMA (Institut Français de Mécanique Avancée) undertook a project designing a plastic bearing-testing device, with the ultimate aim of implementing them in the Canterbury finger [Lamalle, 1999]. Unfortunately there was insufficient time for anything but initial testing, which indicated that plastic bearings would not be suitable for the finger. It was decided that miniature ball bearings would be used in future finger designs.

There are four Canterbury hand projects that are currently being worked on at the same time as this thesis. Simon Ferguson is working on the interpretation of EMG signals for real time grasp classification using pattern recognition algorithms. Thomas Cannariato and Olivier Marc from the National Engineering School of Saint-Etienne are currently working on the circuit board programming for the Canterbury Finger for a new microchip from Cyprus Microsystems (the PSoC, or Programmable System on a Chip). Marlene Helfert from Damstadt University is working on the dynamics and gripping forces of the Canterbury Hand. Helfert's special topic is the forces involved in gripping and throwing a ball with the Canterbury Hand. Fabien Orivel from the IFMA in France is working on creating the engineering drawings for the Canterbury Hand as well as its motor control program.

2.2 The Human Hand

The human hand is a highly complex manipulator that has taken millions of years to evolve. It has become over that period specialised towards using tools as opposed to its original form that was used for tree dwelling. For example, the claws of the fingers have become nails and the finger pads have become specialised for grasping. Additional extrinsic muscles evolved on the forearm for more independence of the fingers. Only over the last few thousand years has humanity's life style changed. The human skeletal structure (including the hand) is still that of a bipedal humanoid evolved for walking long distances, while carrying light loads. Modern civilisation has changed from this to one that has little walking but higher load demands.

The human hand is a highly complex five-digit manipulator. It can make a large variety of grasps and grip forces for manipulating an object. This requires a large amount of processing power in the brain. It has been estimated that controlling the hands requires power equivalent to the legs and the trunk of the body combined. The hand consists of bones, ligaments, tendons as well as the circulation system for the skin and muscles. To provide feedback to the brain of the grasped objects there are thousands of sensors in the skin, muscles and joints of the hand. These sensors measure temperature, pressure, slip, force, and tactile sensations. The skin of the hand is also specialised for gripping. It was found [MacKenzie & Iberall, 1994] that the coefficient of static friction was greater on the palm of the hand than it was on the back of the hand. The distal pulp/pads on the fingers have special epidermal ridges with self-lubricating glands whose sticky excretions help increase the friction on a gripped object.

The following sections describe the basic characteristics of what the hand is and how it works. This information was useful in determining the objectives for the design and optimisation of the hand.

2.2.1 Skeleton

The upper arm consists of only a single bone called the humerus. The forearm consists of two parallel bones, the Ulna and the Radius. These connect to the Carpal bones of the wrist. The carpal bones consist of eight bones that form two rows. The four proximal carpal bones are the scaphoid, lunate, pisiform, and triangular bones. The four distal carpal bones are the trapezium, trapezoid, capitate, and hamate bones. The bones are articulated with one another at joints. These joints allow for some sliding and twisting between the bones. The carpal bones are also connected to ligaments that help to stabilise the wrist joints.

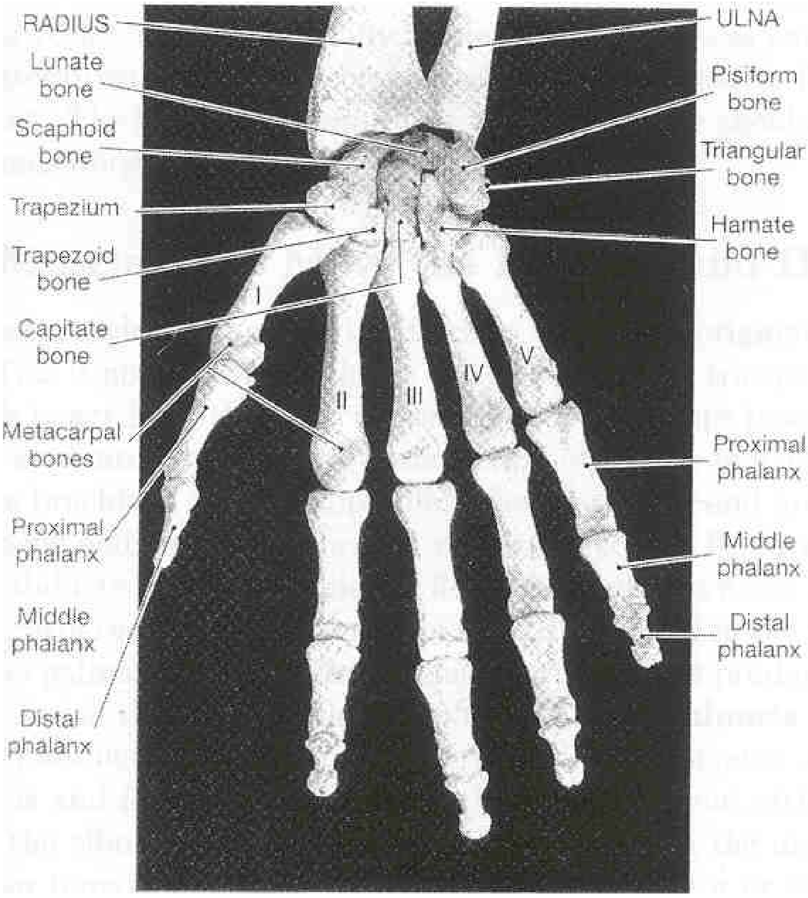

Figure 2.4 Bones of the Hand [Martini, 1998]

The hand has five metacarpal bones articulated with the distal carpal bones of the wrist to support the hand. Each finger is comprised of a proximal, medial and distal phalange. The thumb has only a proximal and distal phalange. This gives a total of fourteen finger bones in the hand. The phalanges are articulated to each other at the Distal Interphalangeal (DIP) and Proximal Interphalangeal (PIP) joints. The finger phalanges are articulated to the metacarpal bones at the Metacarpo-Phalangeal (MP) joint.

2.2.2 Muscles

The muscles of the body work by contraction and consist of bundles of fibre tissues. These muscle fibres can shorten their length by a third when contracting, which brings the bones they are fastened to closer together. The motions produced in the body are always from muscle contraction. If motions occur in an opposite directions it is from an opposing muscle i.e. extension muscles and flexion muscles. This section will deal only with the muscles that move the hand. The wrist is controlled by a combination of numerous muscles that will not be dealt with here. It should be mentioned though that the wrist has a range of different motions, including rotation (pronation and supination), flexion and extension, and deviation (adduction and abduction).

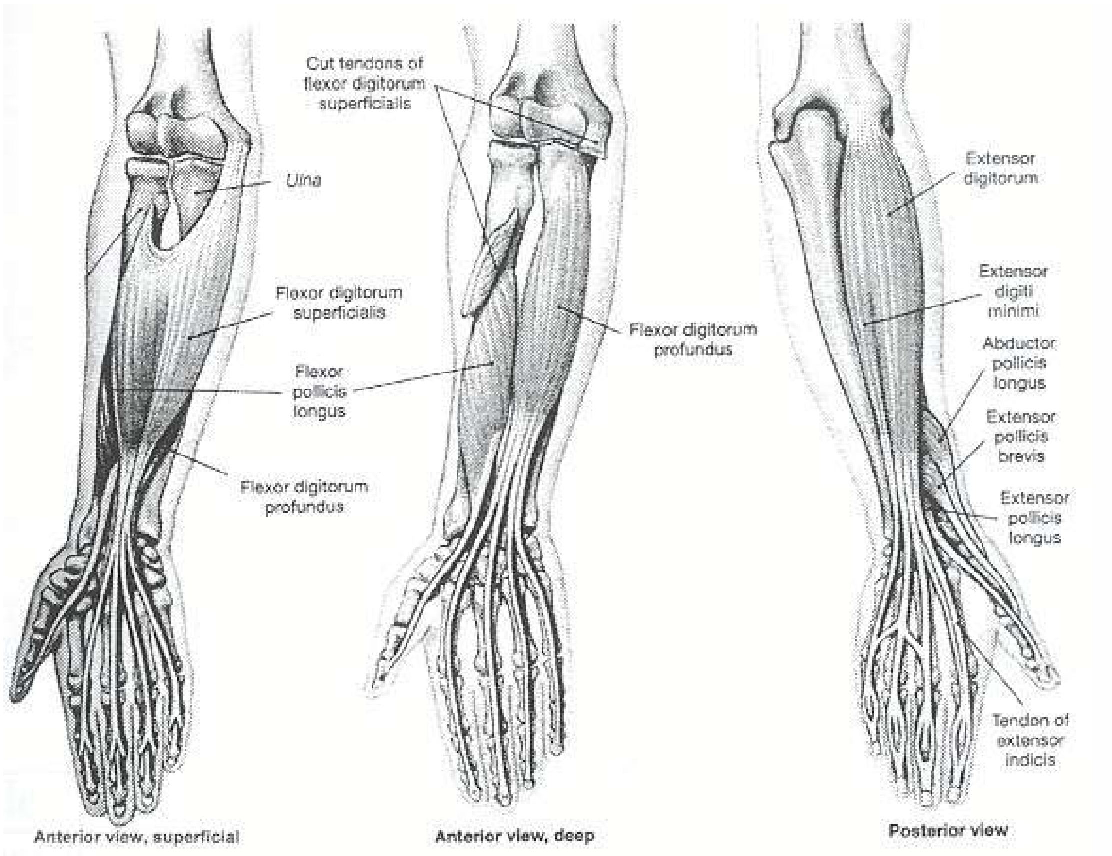

Figure 2.5 Extrinsic Muscles of the Hand [Martini, 1998]

There are three sets of muscles that move the hand and the fingers. They are the extrinsic flexors (flexor digitorum profundus, and the flexor digitorum superficialis), the extrinsic extensors (principally the extensor digitorum) and the intrinsic muscles (lumbricals and interossei). The extrinsic muscles are used for providing strength and crude control of the hand and fingers. They are located in the forearm and reach to the wrist. In particular the extrinsic flexors originate anterior forearm, while the extrinsic extensors originate on the posterior forearm.

Only their tendons pass on into the hand. These tendons move through sheaths for lubrication and to reduce friction, and insert into the phalanges of the finger. The extrinsic finger flexor muscles have greater mechanical force than the extrinsic finger extensors. The reason for this is that there usually is much less force required in opening the hand compared to what is needed to keep a grip on a heavy object. The hand has evolved to reflect this physical reality.

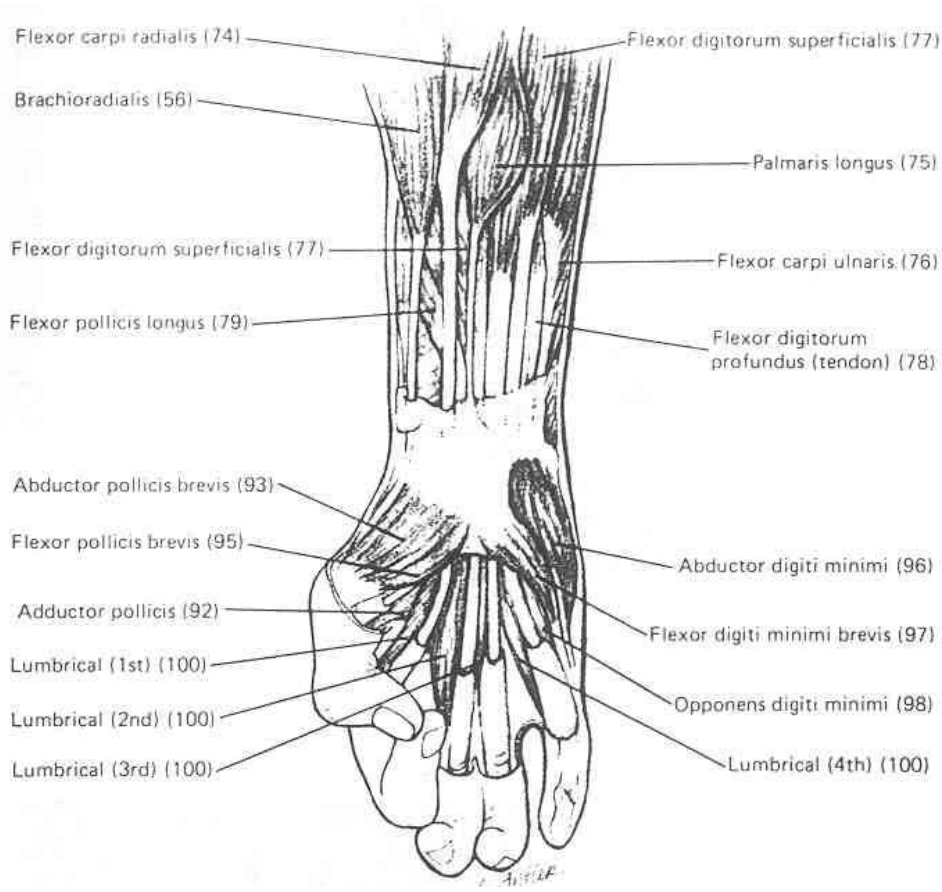

Figure 2.6 Muscles within the Hand Detailed [Solomon, Schmidt, & Adiagna]

The intrinsic muscles are located in the hand after the wrist on the carpal and metacarpal bones, and are used for precise control of the fingers. They are also used for curving the palm to wrap around objects being grasped. Only tendons pass over the phalanges. This is because there are no muscles originating on the finger phalanges. The intrinsic muscles within the hand of the index finger produce more force in a lateral pinch than in an enclosing grasp. However on average the fingers and the thumb have greater strength in a power grasp than in a pulp pinch grasp. So the digits in the hand have different functionality for different grasp types.

Table 2.1 Muscles that Move the Fingers and Hand [Martini, 1998, p.348]

Muscle	*Action*
Abductor Pollicis Longus	Abducts Thumb
Extensor Digitorum	Extends fingers and hand
Extensor Pollics Brevis	Extends thumb, abducts hand
Extensor Pollicis Longus	Extends thumb, abducts hand
Extensor Indicis	Extends and adducts little finger
Extensor Digiti Minimi	Extends little finger
Flexor Digitorum Superficialis	Flexes fingers
Flexor Digitorum Profundus	Flexes distal phalanges
Flexor Pollicis Longus	Flexes thumb

2.2.3 Characteristics

This section will summarise the general properties of the human hand. The values presented here depend on the occupation, age and sex of the test subjects. They also depend on the age of the survey. Over the last hundred years people on average have grown taller and their hand sizes have grown to match this. The results presented here are the average measurements for male test subjects, aged 20 to 29 years. These are taken and averaged from the more recent sources where possible. The original data for these values will be given in the compendium [Green, 2002]. Individual hands will of course differ to the values given here.

2.2.3.1 Size

The following tables give basic dimensions for the average hand. A number of different anthropometrics books were consulted for the sizes of the fingers. Unfortunately many of the references used different methods for measuring the hand. For example finger lengths could be measured from the web above the knuckles to the fingertip. Another method would measure this same distance from the fingertip to the middle of the knuckle. Many of the systems took only selective measurements. For example they only measured the index finger or gave a single width for all the fingers in the hand. The only source that had measured all of the quantities accurately for the hand was Bain [1997]. A couple of measurements were missed by Bain's thesis. These have been substituted using values from other sources [Pheasant, 1986 and Dreyfuss, 1967]. It should be noted that the measurements (though mostly from Bain) were compared against other sources. On the whole the values matched or were only a few millimetres off. The measurements for the size of the hand were later used to scale the finger, thumb and hand designs in the optimisation process.

Fingers

The finger length values were given by Bain [1997]. They were measured from the fingertips and the middle of the knuckle joints for references.

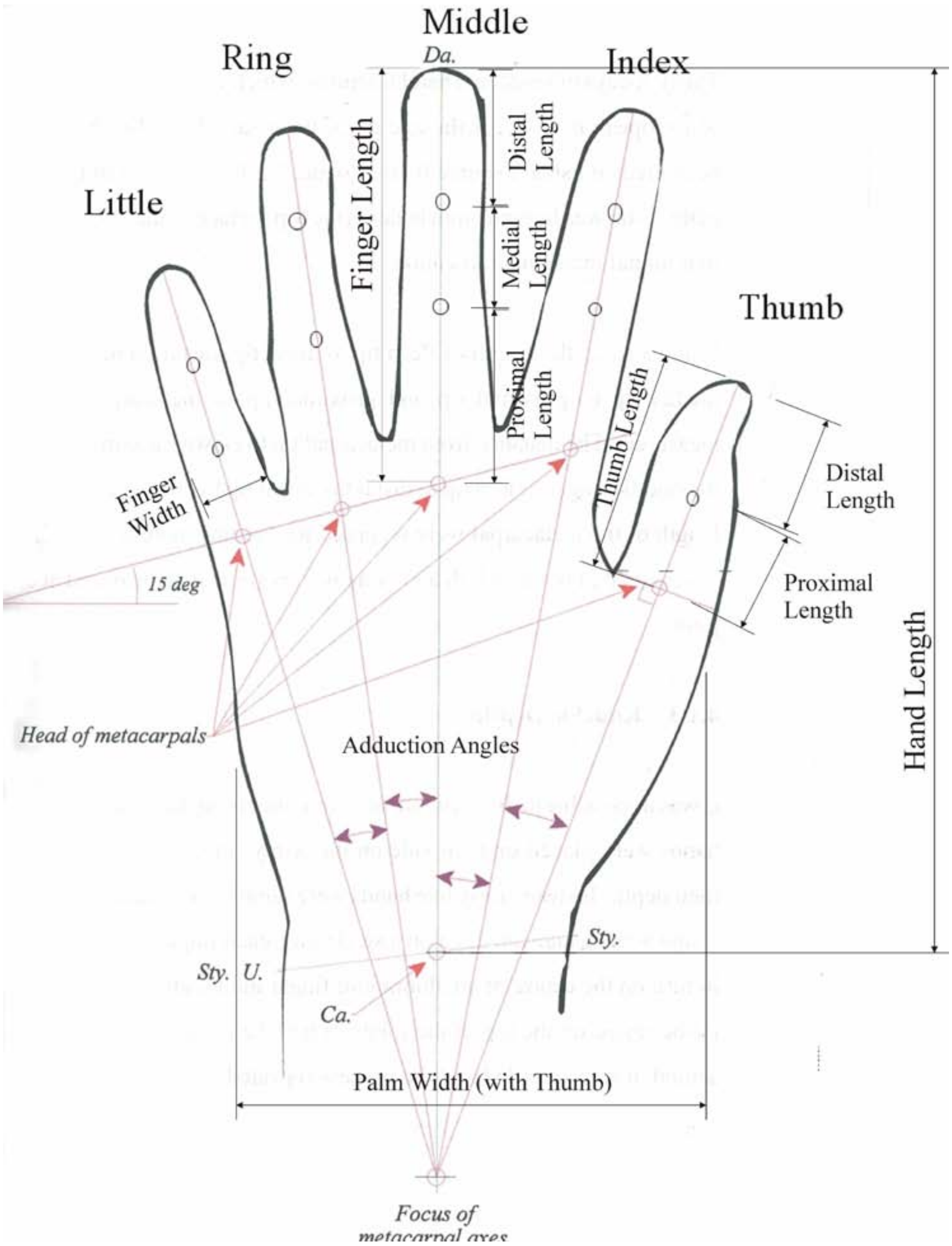

Figure 2.7 Overview of Hand Measurement Scheme [modified from Bain, 1997]

Table 2.2 Finger Lengths

Finger	*Distal (mm)*	*Medial (mm)*	*Proximal (mm)*	*Total Length (mm)*
Index	24	24	41	89
Middle	26.5	28.5	46.5	101.5
Ring	27	28	43	98
Little	23	20	35	78

The widths of the finger phalanges were measured slightly differently to each other. The Distal and Medial phalanges were measured with the flesh around the phalange included. The distal link was measured from the bone.

Table 2.3 Finger Widths

Finger	*Distal (mm)*	*Medial (mm)*	*Proximal (mm)*
Index	19	22	17.5
Middle	19	22	17
Ring	18	21	16.2
Little	16	18	15

The finger depths were taken from a sample of thirty people [Bain, 1997]. The reason for taking a large sample was due to problems differentiating widths of fingers on the X-rays. Measurements were taken using a digital gauge mounted on a steel plate. Each finger joint was measured at the top of their joints at a reasonable pressure of the probe.

Table 2.4 Finger Depths

Finger Depths	*Distal (mm)*	*Medial (mm)*	*Proximal (mm)*
Index	12.5	17	25.9
Middle	13	17.6	26.6
Ring	12	16.5	25
Little	11.1	14.4	23

Thumb

The thumb measurements given in the below tables were provided by Bain's [1997] thesis. As before measurements were taken from X-ray photographs.

Table 2.5 Thumb Measurements

Thumb	*Distal (mm)*	*Proximal (mm)*	*Metacarpal (mm)*	*Total (mm)*
Lengths	34	32	50	116
Widths	20	24.4	~	~
Depths	16	23.3	~	~

Palm

The palm measurements given below are taken as being separate from the Hand measurements as they do not include the fingers and the thumb. The length of the palm for example was measured from the wrist line to the web of tissue under the proximal phalange of the middle fingers. The depth of the palm was taken from the top of the knuckles at the top of the palm.

Table 2.6 Palm Measurements

Measurement	*Size (mm)*
Length	107
Width (Without thumb)	89
Wrist Width	67.8
Depth	33

Hand

Ward [Vanriper, et al., 1992] gives the maximum dimensions of the hand as being length 190mm, and width 90mm. Wards palm depth of 28mm does not include the thumb. When this is compared against the values given by Bain [1997] given in the table below it can be seen that the values are reasonably close to each other in size. The depth of the thumb was taken from [Pheasant, 1986] and is taken from the fleshy base of the thumb metacarpal to the top of the palm.

Table 2.7 Overall Hand Measurements

Overall Hand Measurement	*Size (mm)*
Length from middle finger tip to wrist	191
Width including thumb	106.5
Depth including thumb	51

2.2.3.2 Mobility

This section attempts to separate the basic motions of the hand and wrist so as to identify them. The mobility of the thumb and fingers were used later as goals to which the motions of the Canterbury Hand would try to implement in its design.

Finger

The first measurements given below are for the maximum flexion angle each individual phalange of the finger can make as measured from the axis line of the finger. Ward [1996] found the flexion rotation to be approximately 90º for each of the phalanges and the maximum adduction between the fingers to be 25º.

Table 2.8 Finger Flexion for Individual Joints [Panero & Zelnik, 1979]

Maximum Flexion from finger axis	*Angle (º degrees)*
Distal	45
Medial	110
Proximal	90

The measurements of the adduction angle for the individual fingers had not been referenced by any anthropometrics source. Instead appropriate measurements were taken from the author's hands using a shadow ray tracing method. The values from this method are approximately the same as Ward's values.

Table 2.9 Adduction Angle of Fingers

Adducted Finger (wrt Middle finger)	*Maximum Adduction Angle (º degrees)*
Little	45*
Ring Finger	20
Index Finger	20

Note: For this the middle finger adduction angle was taken to be stationary. The angle of maximum adduction was taken between the adducted finger and the middle finger.

Thumb

The flexion for each of the thumb phalanges as they rotate from the axis of the extended thumb was found experimentally. The thumb, unlike the fingers, does not have its phalanxes curl until they are perpendicular to each other. Instead the proximal phalanx only curls 45º from the metacarpal as it opposes the palm.

Table 2.10 Thumb Flexion for Individual Joints

Maximum Flexion from thumb axis	*Angle (º degrees)*
Distal	90
Proximal	45

The thumb also moves from its CM (Carpo-Metacarpal) joint with two degrees of freedom. This joint allows the flexion/extension of the thumb in the plane of the palm as well as a swivelling abduction/adduction motion below the palm. The table also gives the thumb's metacarpal resting angle. Though not strictly a motion it was a useful for positioning the thumb axis in the design of the palm assembly.

Table 2.11 Thumb Motion around palm

Thumb Motion	*Angle (º degrees)*
Maximum Extension (in plane of hand)*	80
Maximum Adduction (below plane of hand)	85
Thumb metacarpal Resting Angle (from middle finger axis)	30

* - Referenced from [Dreyfuss, 1967]

Wrist and Forearm

The wrist has several motions and constraints to its movements. This information is presented in the tables below. While this data was not used in the design it will become useful for a future wrist mechanism for the hand design.

Table 2.12 Wrist Motions

Wrist Motion	*Maximum Angle (º degrees)*
Palmar Flexion*	65
Dorsiflexion*	70
Radial Deviation^	27
Ulnar Deviation^	47

* - referenced from [Panero, Zelnik, 1979]

^ - referenced from [Pheasant, 1986]

The forearm can rotate the wrist in the hand towards (pronation) and away (supination) from the body. As can be seen this motion is approximately 90º on either side.

Table 2.13 Forearm Motions of the Wrist [Panero, Zelnik, 1979]

Forearm Motion	*Maximum Angle of Rotation (º degrees)*
Supination	90
Pronation	90

Note: Measurements were taken from the fist perpendicular to the ground.

2.2.3.3 Dexterity

The hand has a number of joints that allow the bones in the hand to move with respect to each other. The DIP, PIP (Distal Interphalangeal and Proximal Interphalangeal) joints in the finger for example each have 1 degree of freedom (DOF). The MP (Metacarpo-Phalangeal) joint is considered to have 2DOF. However these motions are complicated to measure as many of the motions are coupled with each other. From the values above it would be reasoned that each finger has 4DOF. In reality these motions are not all individually controllable. The flexors tendons for example tend to work together when a finger is closed. Thus estimating the dexterity of the hand is difficult. Depending on the reference quoted the hand dexterity may from 20 to 27DOF. The following table gives a range of values for the hands total mobility from some different sources.

Table 2.14 Total Dexterity of the Human Hand

Hand Mobility (DOF)	*Reference*
21	[Shimoga& Khosla, 1994]
22	[Andeen, 1988]
20	[Rosheim, 1994]
23+	[MacKenzie & Iberall, 1994]

The last reference [MacKenzie & Iberall, 1994] gives a listing of each degree of freedom for each joint within the hand, which probably indicates it is one of the more accurate estimations.

2.2.3.4 Forces

It has been stated [Kyberd, 1995] that 80% of grips require only 10N of force. It has also been stated the average (20-39 year old) male hand gives a maximum grip strength of 1040N to 1100N [Nieman, D.C., 1990]. An average female hand at the same age will give a grip strength of 600N to 630N. These tests involved the grip force between the medial (and proximal) phalanges of the fingers and the palm of the hand.

2.2.3.5 Speed

It has been reported that speeds of 10Hz are possible with the human hand [Bekey et al., 1990]. The time taken for the finger to pass through its full range of movement and return to its rest position is approximately 0.3 seconds.

2.2.3.6 Weight

The average hand is reported to weigh 400-500g [Ward, 1996]. This mass does not include the weight of the extrinsic muscles in the forearm though. Since a prosthetic hand would be a dead weight on the arm, it should ideally weigh less than a human hand.

2.2.4 Grasps

2.2.4.1 Prehension

Prehension may be defined as the "application of functionally effective forces by the hand to an object for a task, given numerous constraints" [Iberall & MacKenzie, 1990, p.15].

- The task that the prehension of the object is for may or may not be readily definable. For example definable tasks are object manipulation or transport. A less definable and arbitrary task is the touching of the object for texture or temperature.
- The forces of the hand are constrained by how the object is gripped to fulfil the task.
- One of the most fundamental prerequisite constraints for a task is that the object not be dropped. Therefore the hand usually needs to apply forces in a stable grasp (one with opposition with the thumb) to oppose the effect of gravity. A stable grasp should also allow the increase of grasping forces to prevent movement of the object from an applied force.
- Other constraints depend on the size and friction of the object as well as properties of the hand.

2.2.4.2 Grasp Types

There are several systems of hand grasp classification. These all share common grasp types. The generic system in particular gives the most common grasp types, and because of this will be the only classification scheme described in detail.

There are several others including the Cutkosky and Howe classification [Iberall & MacKenzie, 1990], as well as the MacKenzie and Iberall [1994] system. (See Appendix for these systems). The Cutkosky and Howe Classification have divided the hand into two hierarchies of grasps: Power and Prehension. Power grasps have increased power and object size for their grasps. They may be identified as using the palm to grip the object. Precision grasps use only the fingers for the grasp. They have an increased dexterity and use smaller object sizes than the power grasps. Between these two main types are 16 particular grasp types.

The MacKenzie and Iberall system is a later development than the Cutkosky and Howe classification. It has identified four main types of grasps. These types are Palm opposition, Pad Opposition, Side Opposition, and Virtual fingers. Palm opposition has the object upon the palm of the hand. Pad opposition has only the pads of the fingers and thumb holding an object in a grasp. Side opposition uses the sides between the fingers to hold an object in the hand. A virtual finger grasp uses gravity to hold an object to the hand. They include hook grasps where the weight of the object is held across the fingers as well as the flat hand posture that has the object balanced across the palm like a waiter carrying a platter.

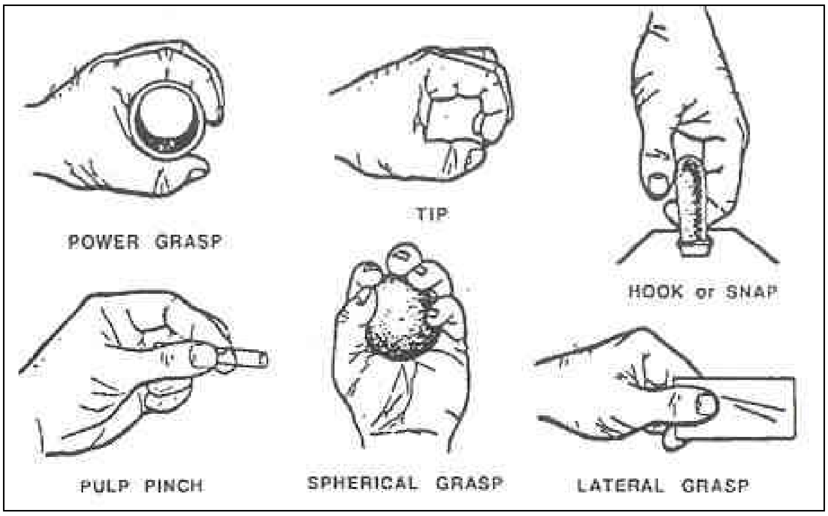

Figure 2.8 Schlesinger's /Generic Grasp System [Iberall & MacKenzie, 1990]

The generic system [Bekey, et al., 1993] is a simplification of these systems into six basic and commonly used grasp types. They are Fingertip Prehension, Lateral Prehension, Palmar Prehension, Spherical Grasp, Cylindrical Grasp, and Hook Grasp.

Fingertip Prehension

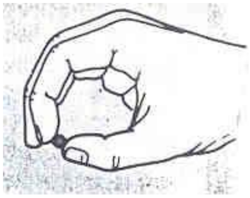

This grips otherwise known as a tip or precision pinch is used for picking up small items. It uses the thumb and the index finger and may involve using the tips of the fingernails. For example, lifting a pin from a flat surface. It is not very stable however.

Lateral Prehension

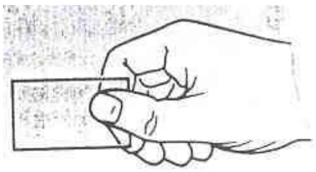

Otherwise known as the key pinch. The pulp of the side of the thumb is opposed to the radial side of the medial phalange of the index finger. For example, turning a key.

Palmar Prehension

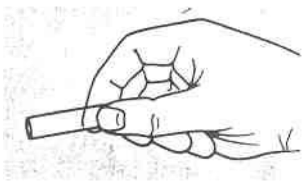

This versatile grasp, otherwise known as the pad-to-pad grasp, is the one most used by the hand for picking up and holding objects. In it the pulps of the index and the thumb oppose the object in a pinch. This grasp is stable and can also be used for large objects.

Spherical Grasp

Otherwise known as a precision grip. The fingers are flexed and are used for holding round objects against the palm. For example holding a petanque ball. If three fingers are used (around a smaller object) it would be called the three-jawed chuck grasp.

Cylindrical Grasp

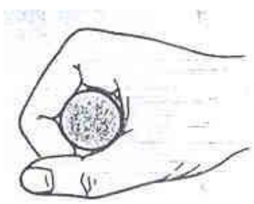

Otherwise known as a Squeeze grip, the Coal hammer, and the power grasp. The fingers are fully flexed and the flexed thumb opposes the object. This is the simplest grasp type because the whole palm gives stability to the grasped object. For example, grasping a stair rail.

Hook Grasp Otherwise known as the Snap grasp. In this grasp the fingers are all flexed (and be able to be flexed) at their interphalangeal joints and extended at the metacarpo-phalangeal joint. The function of the fingers is vaguely like a hook as the object is held within the crook of the fingers by gravity. For example, carrying a suitcase.

Figure 2.9 Assorted Generic Hand Grasps [Solomon, Schmidt, & Adiagna]

2.2.4.3 Patterns of Grasping

From experiments it was found that the hand makes four patterns of motion when grasping an object [Kaneko, 2000]. They are the Direct Grasp, Sliding Based Grasp, Rolling Based Grasp and the Regrasping based grasp.

1. Direct Grasp The hand directly grasps the object without any re-grasping motion.

2. Sliding Based Grasp This pattern uses the sliding motion between the finger and the object to make the grasp. The fingertips push under the object and lift it into the palm.

3. Rolling Based Grasp The object is rolled up over the thumb or index finger into the palm. The object is then held in an enveloping grasp.

4. Regrasping based grasp The object is picked up by the thumb, index (or middle) finger and then the remaining fingers hook under the object and squeeze it until the fingertip grasp is broken. The object then comes into contact and is held within the palm.

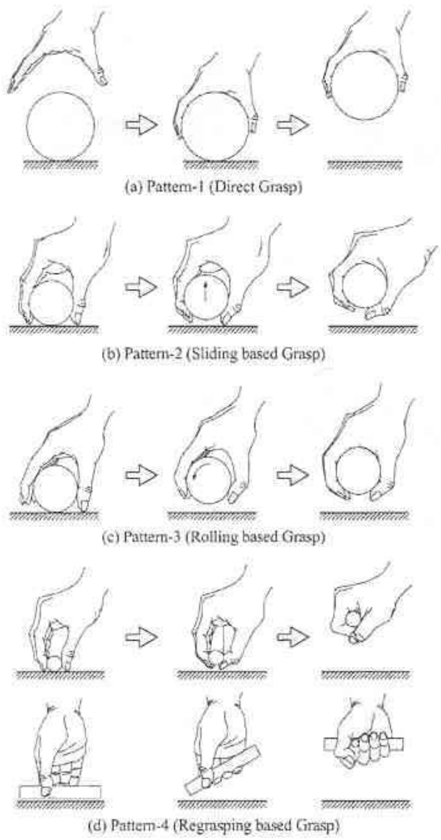

Figure 2.10 Grasping Patterns [Kaneko, et al., 2000]

The pattern used for an object depends on its size and its contact friction. Large objects are directly grasped irrespective of their shape or contact friction. As the size decreases the other patterns are used according to the graspers personal choice. When objects have low surface friction sliding based grasps are often used. For objects with significant friction rolling based grasp and regrasping based grasps are used. Regrasping based grasps are used for very small objects in particular.

2.3 Prosthetic Hands

2.3.1 History of Prosthetics and Robotic Hands

The human hand is a highly complex manipulator with multiple digits, variable compliance, and redundant degrees of freedom. It has the ability and the sensitivity to manipulate very delicate objects as well as being strong and rugged enough to hold very heavy ones (i.e.100kg). It has been estimated that the hand has over 20 degrees of freedom, with a grip force of over 500N. These abilities allow it to manipulate a wide variety of objects and tools. The hand contributes about 90% of the function of the upper limb [Magee, 1992]. It has been argued that the evolution of the human hand, and its subsequent effect on mans ability to manipulate his surroundings was one of the chief reasons for the ascendancy of the human race. It is no wonder that when a hand is lost there is great personal loss for the individual. Not only is their ability to manipulate the environment impaired but there is also loss of coordination, apprehension (tactile feedback) personal expression and body aesthetic. Social and emotional problems can occur for the disabled individual as well.

To help compensate for a lost limb prostheses have been invented. This is a relatively new technology. While evolution has taken millions of years and many thousands of generations to create the human hand, the field of prosthetics has only been around for hundreds of years.

The first prostheses created were mainly for aesthetic reasons and had only limited functions. Examples of this are the metal gloves that knights used in medieval times to replace their lost hands. Eventually body powered prosthetics were created. These gave the prosthetic arm and hand, motions that were driven by the human body. An example of this is the copper artificial arm created by Kreigseissen. However it wasn’t until after the American Civil War when anaesthesia and antisepsis was discovered that a prosthetics industry was established.

By the early twentieth century external power sources began to be included in prosthetic designs. It wasn't until the 1950's and 1960's that externally powered prosthetics were regularly used. Due to the minimal weight tolerance and the difficulty in replenishing power sources externally powered prostheses have been mainly restricted to electric actuators. In the United States this was driven by the need to help bilateral arm amputees, who were the victims of war and accident. In Europe it was from the thalidomide tragedy that affected children. The externally powered prosthetics were powered by a motor with batteries and operated by electromyographic (EMG) signal or by control switches.

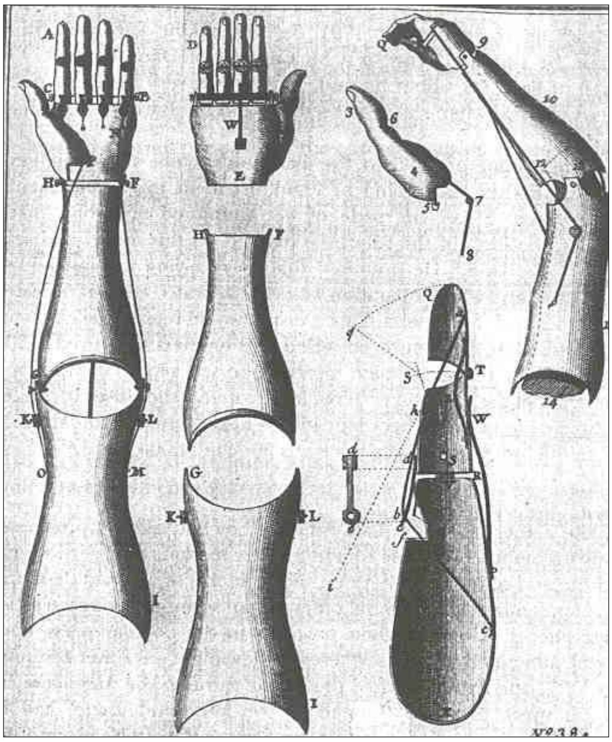

Figure 2.11 Copper Artificial Arm [Benhamou, 1994]

Prosthetics (especially externally powered) are price sensitive and rely on technology created from other sources. Recent developments in microelectronics and battery technology for example have been derived from the PC and Cell phone markets, giving better control and sensory feedback to prosthetic users. While the numbers of externally powered prostheses is increasing it has been estimated [LeBlanc] that 90% of arm amputees use body powered type prostheses. The reasons for this are mainly due to their better comfort, cost, weight, function and reliability. As advances in smaller actuators, batteries, and microchips continue, lighter and more functional externally powered prosthetic hand alternatives will begin to dominate the market.

Table 2.15 History of Prosthetic Developments

Year	Event
Ancient Greeks	Descriptions of mechanical limbs
500BC	Earliest reference to a prosthesis was to Hegesistratus when cut off his foot to escape chains and then made a wooden foot for himself
218BC	Roman General Marcus Sergius fitted with iron hand to hold his shield

14^{th} Century Earliest existing examples of mechanical limbs, e.g. medieval knights fitted with prosthetic hands from their armourers that resemble metal gloves

1400 Alt-Ruppin hand prosthesis

Figure 2.12 Alt-Ruppin hand [Muilenburg & LeBlanc, 1989]

1476 Clockmaker Ulrich Wagner created an artificial hand (unknown design)

1509 Spring loaded metal hand device built for German knight, Goetz von Berlichingen, which had functionality and aesthetic appeal and weighed approximately 1500grams

1560 Hand for a below elbow amputee designed by Le Petit Lorrain

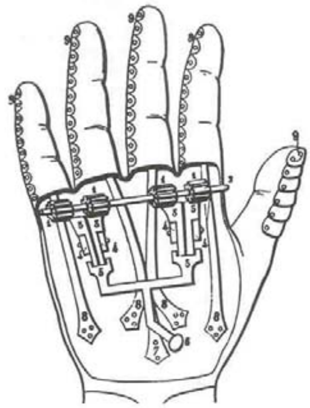

Figure 2.13 Hand for a below elbow amputee [Benhamou, 1994]

1732 Copper artificial arm for a below the elbow amputee made by Kreigseissen

1760 The ‘silver arm’ is created by Pieere Joseph Laurent de Villedeuil for a soldier who lost both his arms while loading a cannon

1792 An artificial arm is created in Switzerland weighing only 480grams

1812 Ballif Arm - body powered prosthesis

1890’s Split Hook developed by D.W. Dorrance

19^{th} Century First pneumatically powered hand

1919 Electrical prosthetic hand developed though not usable with available batteries

1922 First electrically powered hand

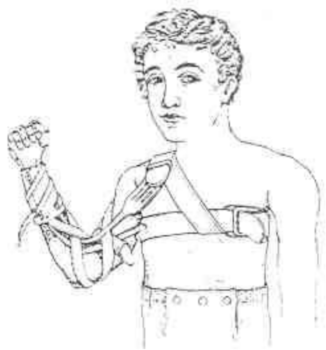

Figure 2.14 Ballif Arm [Muilenburg & LeBlanc, 1989]

1948 First myoelectric hand demonstrated at the Exportmesse in Hannover. Developed by Reinhold Reiter of Munich. (USSR)

1949 Vaduz electric hand patented

1955	First portable myoelectric hand design (Roehampton). Earlier myoelectric amplifiers were too large to be portable.
1961	Kobrinski publishes a paper on the first EMG hand (Russian)
1965	Otto Bock Orthopaedic Industries develops an electric hand that grips with two fingers and a thumb
1969	First Southampton hand – a four DOF hand with adaptive control
1970	First commercial myoelectric hand, outside of Russia
1971-73	Simpson hand (Scotland) – a gas powered hand for use by children
1978	Self contained (externally powered) Utah Arm prototype prosthetics
1980	First Utah arm fittings with myoelectric elbow.
1988	Utah Arms fitted regularly across US, Canada and Europe
1992	Jacques Monestier a sculptor creates a 'golden' arm for 'below the elbow' amputees cast from a bronze/beryllium alloy

The facts for this table was compiled from a variety of sources including, [MacKenzie & Iberall, 1994], [Kyberd, 2000], [Ward, 1996] and [Benhamou, 1994].

2.3.2 Current Upper Extremity Prosthetic Devices

There are various kinds of upper body prostheses; there are above the elbow prosthetics, forearm prostheses, hand/wrist prostheses and partial hand prostheses. These may be separated again on their type of function. There are; Cosmetic, Passive, Body Powered and Externally powered prostheses. The body powered and the externally powered prostheses are the two main types of controlled upper body prostheses.

The upper extremity prosthetic ends in a hand attachment. This is also known as the terminal device (TD). The terminal devices are designed so that they can be fitted into a number of different arm/wrist prostheses types. The terminal devices are dependent on the type of prosthesis used and may be separated into the same types (Cosmetic, Passive, etc). There are also partial hand prostheses. However these are dependent on the level and the location of the amputation. They will not be covered in much detail here as this thesis concentrates on a whole hand prosthetic design.

After a hand is lost to disease or trauma the brain eventually loses a lot of its old pathways. A large amount of mental and physical effort is required to move a prosthetic hand. It has required that the numbers of motions (DOFs) for prostheses be reduced for ease of use. Most prosthetic TDs only have one to two degrees of freedom. These may be mounted on movable wrists that allow additional motions.

The method of operation for each type of TD is similar but this also depends on the particular manufacturer, and also the size of the person's hand. Children's terminal devices are smaller sized and usually are more anthropomorphic (to avoid social stigma). Generally TD's may be separated into Hooks (which are body-powered), Hands (body powered and myoelectric), Grippers and custom devices.

Figure 2.15 Range of Terminal Devices for Prosthetic Arms [Sears, et al., 1987]

2.3.2.1 Cosmetic

Cosmetic prostheses are used to represent the lost limb. They have little to no motion beyond pushing and pulling. This type of prosthesis is the earliest and simplest type of prosthesis, i.e. Hegesistratus' wooden foot. Cosmetic terminal devices are made to aesthetically resemble the human hand. Examples of these are wooden, PVC plastic, and soft foam hands. Modern cosmetic hands include sophisticated latex hands that mimic the hand's look and texture. Gloves (flesh covered etc) that cover the terminal device may also be thought of as being included as being of a cosmetic type. Many of these hands are bendable, so as to grasp objects. (This technically would then classify them as Passive terminal devices.)

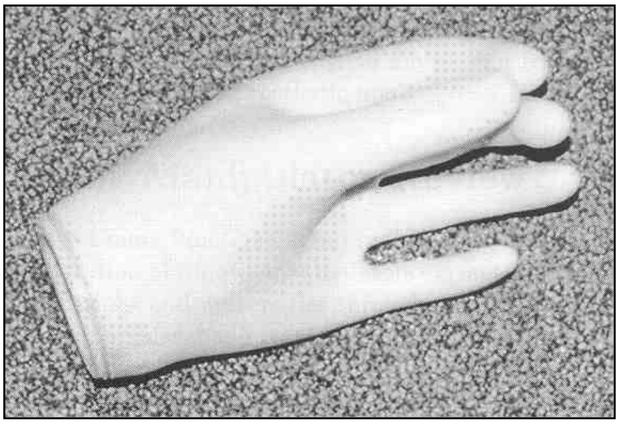

Figure 2.16 Glove for a Terminal Device [Elliot, 1998]

2.3.2.2 Passive

The second type is a passive prosthetic. These prostheses require manual manipulation of the grasping hand by the non-prosthetic hand if they are to be used. This hand type has been used quite often throughout history i.e. Berlichngen hand.

Examples of passive devices are the bendable or modifiable TD hands discussed above. Other examples are the special TD attachments. These may be used for sports jobs and other activities. For example special TD attachments include baseball, bowling, skiing, fishing and driving. Partial hand prostheses are usually passive devices (due to the lack of room for an actuator). However they can also be cable driven or wrist driven.

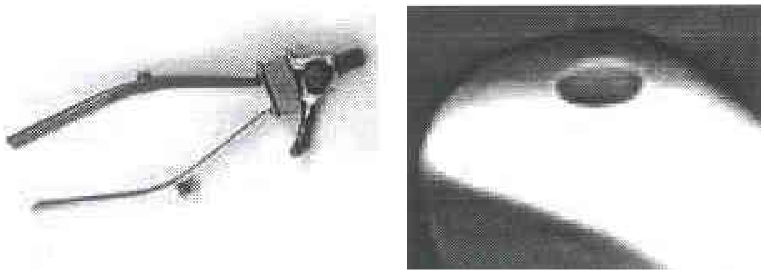

Figure 2.17 Baseball glove holder attachment and Fishing Hand attachment

2.3.2.3 Body powered

A body-powered prosthesis uses the body to activate/transmit motion to the arm and the hand. They also try to maximise the indirect sensory feedback to the amputee. This type of prosthesis is also known as a functional or internally powered prosthesis. There are four different body sources for the motion. They are the wrist joint, forearm, biceps and the shoulder/thoracic muscles. The two methods commonly used for control are by arm-flexion or by shrug control. Arm flexion involves the arm pulling a cable to control the hand. Shrug control is when the shoulders are rounded to produce the motion. In this case the shoulder is used to transmit the force by a shoulder harness and cable to the terminal device. Body-powered prostheses are the most commonly used by amputees. An example of a historical body powered prosthesis is the Ballif Arm.

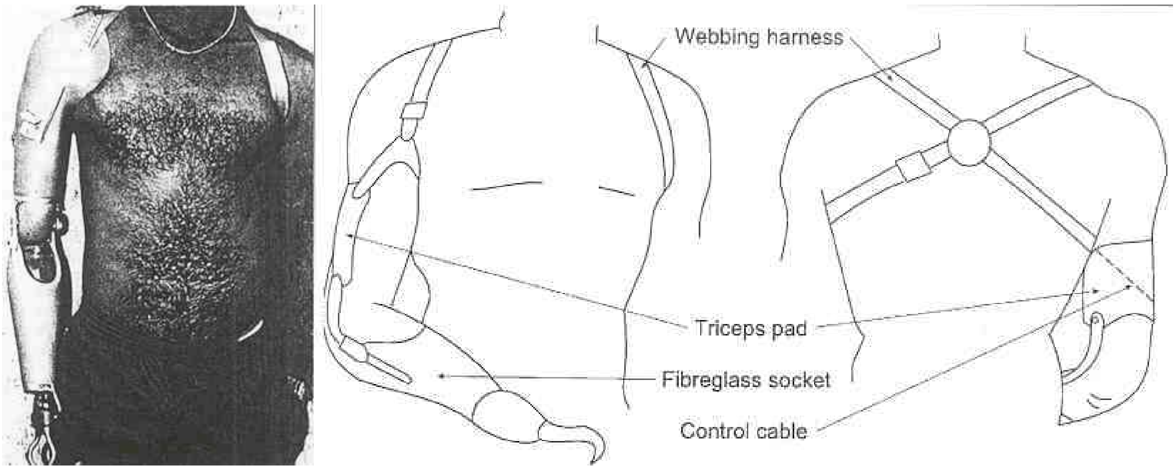

Figure 2.18 Body Powered Prosthetic Arm & Harness [Muilenburg, & LeBlanc, 1989]

The terminal device for the modern body powered prosthesis is usually of a Hosmer Dorrance manufactured type. These may be separated into hooks and hands. Both types either have a voluntary opening or a voluntary closing function. Most amputees choose the voluntary open type, even though the voluntary closing type is more analogous to the human hand. However this would avoid having to continuously pull to hold an object, and worry about an open hand when it is not being used.

Hooks

The prosthetic split hook has one degree of freedom and is made of two curved (aluminium or steel) jaws. Within the jaws are bonded neoprene grip inserts for assisting in gripping an object. The jaws are usually held closed (if voluntary open type) by two large rubber bands. They screw in to the amputee’s wrist socket for attachment. Since the hook is body driven a particular motion is needed to open the hook. Since this is usually a shoulder harness, a rounding of the shoulder is used to open the hand (via a stainless steel control cable). The shoulder harness resembles a figure of eight when worn.

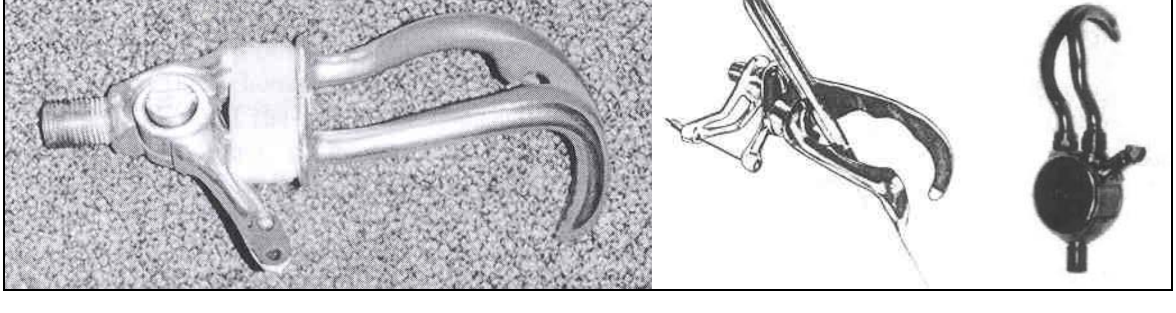

Figure 2.19 Range of Body Powered Hook Designs [Elliot, 1998] [Sears, et al., 1987]

There are various manufactures for these hooks, Hosmer, Sierra, Contourhook, Hugh Steeper etc. The hooks themselves have a variety of shapes and usually have either canted jaws, or are lyre shaped.

Hands

Most body powered prosthetic hands have a standard threaded shaft for connection to the wrist device. They have a three-jawed chuck or palmar prehension and like the hooks are cable operated. Like the hooks there are various manufacturers/types for body-powered hands, i.e. Dorrance, Sierra, Becker, and Robin-Aids.

2.3.2.4 Externally Powered

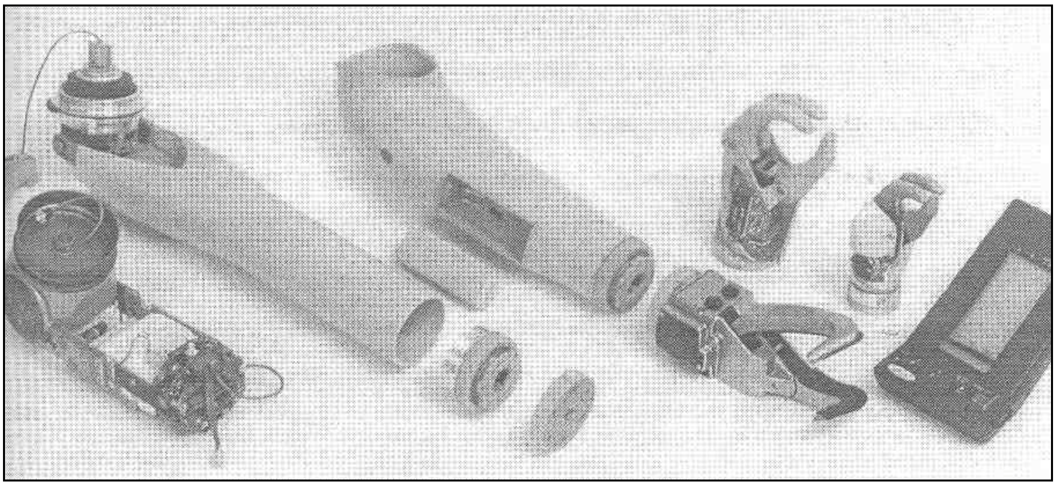

Figure 2.20 Externally Powered Hands disassembled [Steeper, 1993]

Externally powered prostheses use energy from some power source outside the body for the motion of the prosthetic. This power source may be batteries, a compressed air cylinder etc. However these prostheses are not as commonly used as body powered prosthetics though their use is increasing. Many externally powered prostheses are controlled by electromyographic (EMG) signals, and are known as myoelectric prostheses. These signals are read of the muscles and are used to drive motors. The muscles read off the user depend on their level of amputation. These can include muscles on the forearm, triceps, and the biceps. Typically these devices have one or two degrees of freedom. An example of an externally powered prosthetic is the Utah arm and hand.

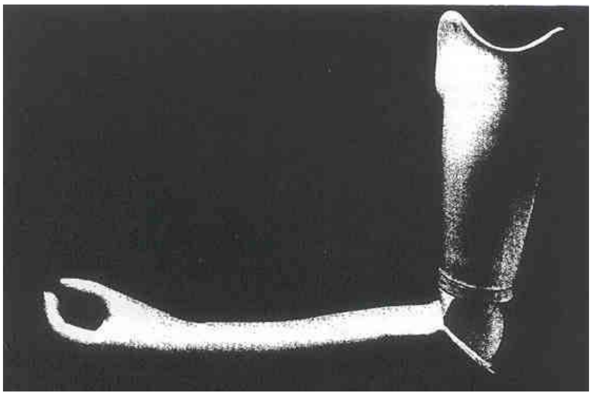

Figure 2.21 Utah arm and hand [Sears, et al., 1989]

A simple and typical myoelectric hand can be described as a single one-degree of freedom gripper. They consist of two fingers and a thumb that are controlled through an electrical and mechanical system. Two sets of pressure sensitive electrodes are moulded into the socket to which the myoelectric hand attaches. By pushing the stump against one set of electrodes, an electrical circuit is closed and the hand opens (through a motor and reduction gearbox). By pushing the stump onto the other electrodes the hand closes. The hand is held in place by a collar. The wrist/socket also holds the battery packs and also a third set of electrodes for an optionally powered wrist.

There are a variety of externally powered hands. Other than myoelectric control there are also switch controlled servo powered electric hands. There also a number of different manufacturers for these varieties of hands. These include Hugh Steeper Ltd, Otto Bock, Systemteknik (children's hands) and Variety Ability Systems Inc. Some particular electric hands are the Griefer pincer, Utah Arm, Utah Arm model 2, VASI hands, electrohand 2000 and the Motion Control hand (from Motion Control Products).

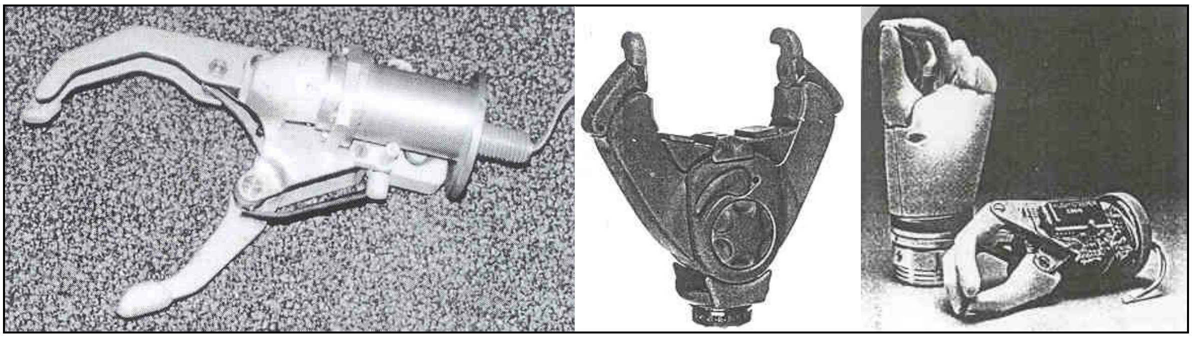

Figure 2.22 Range of Myoelectric Hands [Elliot, 1998] [Sauter, 1999]

2.3.3 Motivation for New Prosthetic Hand Devices

In the US there are 102,000 people with upper extremity amputations. Partial hand amputation is the most common at 61,000 followed by the loss of one arm at 25,000 [LaPlante, & Carlson, 1996]. These figures were verified by another report [LeBlanc, 1973], which stated that of the 350,000 persons with amputations in the US 30% had upper limb loss. Of this 30% wrist and hand amputations made up 10%. Of all persons with upper limb amputation 70% were amputations to the elbow. This suggests that well over 70,000 people in the US have wrist and hand amputations. This is a relatively small market of people most of whom already have had prosthetic devices fitted.

Further surveys [Silcox, Rooks, et al., 1993] [Atkins, Heard, & Donovan, 1996] have shown that 30% to 50% of prosthetic users chose not to wear their prosthetic hand regularly. The reasons for this were due to the hand being too heavy, having too low a functionality and had a robot like motion [Kyberd, Beard, Davey and Morrison, 1998]. When this is looked at in conjunction with the fact that 90% of users wore body-powered prostheses, it can be seen that there is room in the market for a lightweight, functional myoelectric hand. A survey of below elbow amputees found that a myoelectric prosthesis took twice as long as a hook, for an objects manipulation, and five times as long as with a normal hand. Also they weigh approximately 25% more and only give 75% the force of a hook terminal, body powered prosthesis.

Yet 60% of those preferred the myoelectric prosthesis compared to the conventional prosthetic hands. The reasons for this may be the lack of a body harness, better cosmetic appearance and the greater comfort of the myoelectric hands. However there are disadvantages, mostly that the hands weigh more, are not designed for heavy work and that they cost more. The greatest drawback with satisfaction with current myoelectric hands is that they lack sensory feedback (other than audio and visual) to the user. This rejection of conventional hand prosthetics has led to many developments worldwide. Many of the latest experimental prosthetic hand designs are discussed in the compendium [Green, 2002].

2.4 Robotic Hands

2.4.1 Comparison of Robotic End Effectors with the Canterbury Hand

As part of this thesis experimental prosthetic and multifingered robotic hand designs were investigated. The hand designs found with this research are summarised in detail within the compendium [Green, 2002].

It was noticed after the research that the clear majority of the experimental prosthetic and robotic hands in the literature were actuated outside of the hand. This was especially true for hydraulic and pneumatically actuated hand designs, which had very large and bulky actuation systems. The hands for these systems could be made quite small and light with a large number of motion freedoms. Several of these hands even used pneumatic muscles to create human like motions in the hand. Even though these hands were light and small they still required the actuator system that could be weighty and not easily transportable. Examples of Hydraulic hands are the many industrial robot grippers, as well the Hydraulic JPL Hand. Pneumatically actuated hands via McKibben muscles are becoming more popular, with such examples as the Bionic hand, (with flexible fluidic actuators) and the Shadow Robot hand.

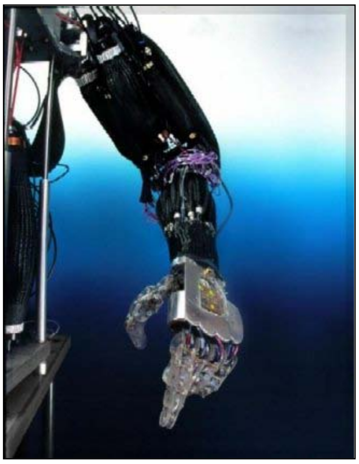

Figure 2.23 Shadow Robot hand [Wood, 2002]

Other methods of actuation were by an electric motor or by Smart Metal Alloy SMA actuators. This last type of actuator works by the heating and cooling of a Nitinol SMA wire. As the wire is heated the SMA wire goes through a thermo elastic martensite transformation (to austenite) that causes it to contract. As the wire cools it transforms back to martensite it causes the wire to expand back to its original shape. SMA actuated hands are very light, small and self-contained. However they are also very experimental with only a small number of hands using this type of actuation. Also these hands tend to have only incorporated a limited number of freedoms and fingers into their design so they are comparatively in a more primitive stage of development. Unfortunately they also have a number of problems. The SMA wires need regular replacement, as they tend to wear out quickly. Also the force output produced by the actuators is currently too small for the hands to be useful for anything but small light objects. The fingers extension and flexion times tended to be slow as well. (The opening times in particular were slow, as the wires needed a number of seconds to cool down.) Examples of SMA actuators are the Shape memory alloy finger and the Bendbots hand.

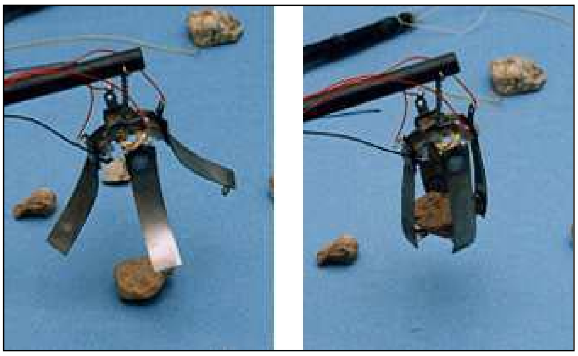

Figure 2.24 Bendbots Hand [Discover 1998]

The most common form of actuation is by electric motor. The motor transmission system for the fingers motion is usually either by cable, tendon, gear or linkage systems. This does not exclude other transmission systems such as the Minnac linear actuators of the Omni hands, or mixed systems like the flexible drive screws and finger linkages of the Robonaut hand. Traditionally most experimental robotic hands have been cable or tendon operated such as the Salisbury hand or the Utah/MIT hand. Usually the motors for these types of transmission systems are remotely located from the hand, for example the Salisbury hand. Or they are located in a large forearm such as the JPL hand. The actuation packages for these hands tend to be large, heavy and not easily transportable. The reason for the remotely located actuator pack is that the large numbers of cables in the hand have to be sorted, routed and connected to the phalanges. There usually is insufficient space within the hand for holding the cabling and the motors. This complexity can lead to coupling, and limitations between the motions of the various digits.

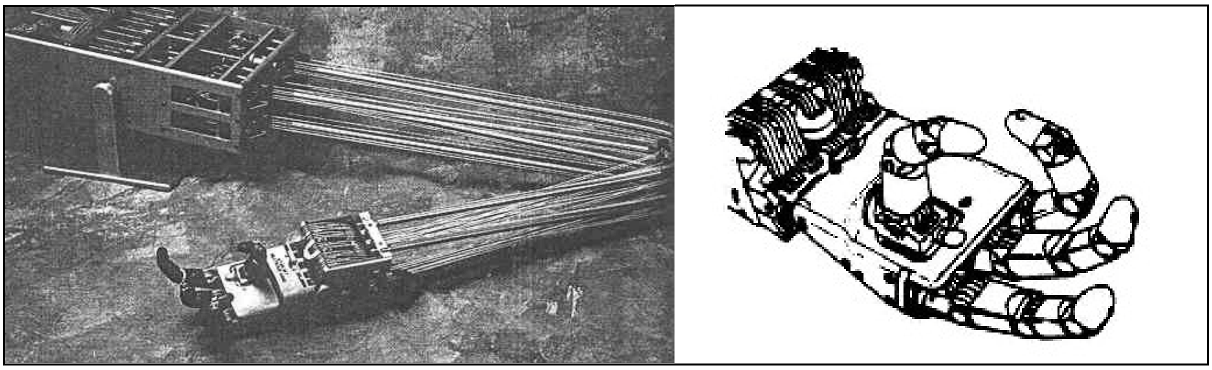

Figure 2.25 Utah Hand [Rosheim, 1994] [Farry, et al., 1996]

Tendon and Cabling hands have various other limitations that limit their use as a robotic end effector. The tendons/cables tend to have large frictional losses even with lubrication and low friction sheaths. They tend to stretch and break over time, requiring maintenance. The stretching/compliancy in the cabling can lead to a loss of accuracy. This can be actively controlled though it increases the complexity of the control system. Another problem of cabling and tendon based systems are their kinematic inefficiency. Usually pulleys are located within the finger joints over which the tendons move. This means that only half the radius of the finger is used to give a rotational moment/lever effect for the finger phalanges. This means that for a given motor the fingers are giving half the possible output force that they are capable of. Thus for a larger force output the motor size needs to be increased, which in turn increases the size and mass of the robotic hand.

However tendon based hands do have several advantages such as quick response, low weight and compactness of the hand mechanism. Some of the new cable hands have chosen to directly drive the fingers using only limited cabling in the fingers. In the case of the Barrett hand for example motors behind the fingers via a pair of antagonistic cables directly actuate the fingers. The Barrett hand though has a limited 4DOF so it has sacrificed its dexterity for compactness. Overall hydraulic, pneumatic and electrically driven tendon based hands have been described in their articles without much focus on their actuation source or how large this system is in relation to the hand. While the hand is reasonably compact and lightweight these actuation sources usually are not. They would act as a large constraint on how the hand is used, either as a prosthetic or as a robotic end effector.

Another method to transfer the actuation to the hand is by gears, such as the NTU hand or the DALSA manipulator. These fingers require a large amount of expense in the manufacture/purchase of the gears and their accurate location in the hand. The gearing of the fingers also leads to backlash, which in turn leads to problems with accuracy.

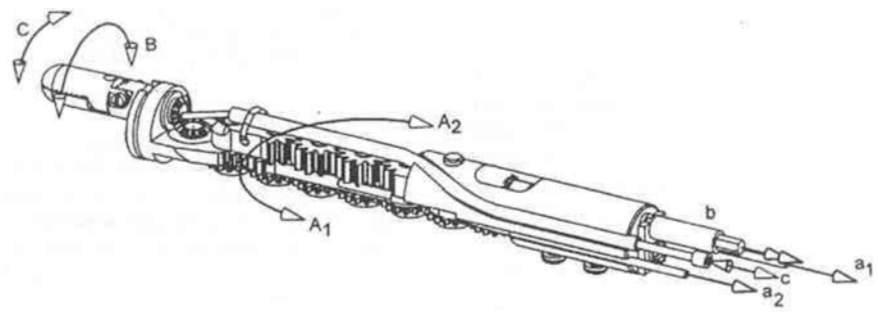

Figure 2.26 DALSA Manipulator [Minor & Mukherjee, 1999]

Linkage driven systems have the potential for being more compact. This is because the linkages can use the whole width of the finger to be more kinematically efficient. The linkages can then be directly driven, as the actuators do not need to be as large and can be fitted within the hand. The hands are also more accurate and simpler to control than tendon hands. They do not have the same frictional or maintenance problems as well. Examples of these kinds of hands include the Belgrade/USC model II hand and the Southampton hand designs. However these systems tend to be more limited for their motions compared to tendon based systems. The joints tend to be limited to revolute joints (i.e. Bearings on shafts), as the linkages motions are more easily controlled if they have two-dimensional motions.

The Canterbury Hand design is a directly driven mechanical hand that has all the DC motors located within the hand and drives the fingers via linkages. An analogy is that these motors act like the intrinsic muscles in the human hand by moving the hand from within. Unlike the human hand, and most other hand designs the Canterbury hand does not need to locate any actuators within the forearm or outside of itself. This means the hand is very compact compared to most pneumatic, hydraulic and tendon driven hand designs. Once completed the only components that will be outside the Canterbury hand is a battery pack with the DSP control board. Even though it does not have the same grip force as pneumatic and hydraulic hands it should be sufficient for the minimum grip strength. The hand will also cost less than a gear driven hand and will not have the same problems with backlash, or with overcoming the finger inertias.

The Canterbury Hand will have 11DOFs. This compares well with most hand designs. While it does not have as many motion freedoms as some tendon based hands it will be more robust and compact. It will not have as many compliance, frictional or maintenance problems. Compared to other linkage-based hands it is also highly dexterous. For example the Belgrade/USC model II hand has only four degrees of freedom. It also is kinematically efficient as the linkages unlike the Belgrade/USC hand design will be under tension when gripping an object.

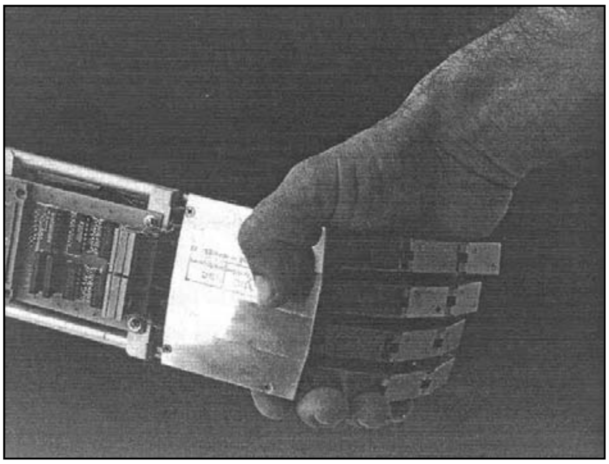

Figure 2.27 Belgrade/USC Hand Model II [Bailon, Vuskovic & Ivokovic, 1995]

The Canterbury Hand's directly driven anthropomorphic linkage mechanism also makes it reasonably unique. The exceptions to its uniqueness are the Southampton finger and

Robonaut hand designs that utilise similar yet different finger linkage mechanisms. Unlike the Southampton finger it will be more anthropomorphic. And unlike the Robonaut hand it is more compact as it does not require a forearm to house its actuators. Also the finger spreading and thumb rotation mechanism are compact and individualistic design solutions for these motions. Overall the Canterbury hand compares well to other multifingered dexterous robotic manipulators. While the Canterbury Hand is too large and heavy for use as a prosthetic device, the design when it is eventually refined does have applications in this area.

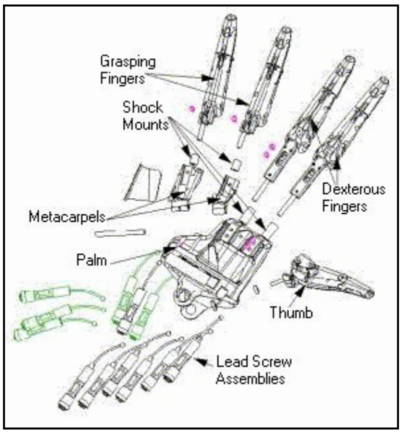

Figure 2.28 Robonaut hand exploded diagram [Lovchik & Diftler, 1999]

2.5 Research Summary

This chapter has summarised research made into prosthetic hand devices. It has described the reasons and history behind these developments. Since the design objectives for the Canterbury hand included making the appearance and motion of the hand as anthropomorphic as possible, the human hand was investigated. This included the anatomy, typical hand and finger sizes as well as the expected grasps and motion of the hand. It has also found that the Canterbury Hand is a unique robotic hand design that has a number of design advantages over other manipulators.

Chapter 3: The Canterbury Hand CAD Model

3.1 Design Methodology of the Canterbury Hand

The Canterbury hand was created entirely within the CAD software program SolidWorks (from SolidWorks Corporation). CAD or computer aided design is the name given to using a computer program to create computer models of a design, component lists and engineering drawings. In particular SolidWorks creates feature-based parametric solid models, which are fully associative, able to be constructed with or without constraints and can utilise relations to implement the users design intent. SolidWorks was chosen because it is the main CAD software used within the Mechanical Engineering Department at the University of Canterbury. Because of its functionality, process sensitivity and ease of use, another CAD package was not deemed necessary. As already mentioned SolidWorks is a fully associative, feature-based parametric solid CAD modeller that can utilise constraints and relationships as directed by the user's design intent.

As part of the design brief, two hand designs were to be created in Solidworks. The first was a Robotic Hand that would use the larger Maxon Motors. The second hand, which was to be a prosthesis prototype, was to use the smaller Mini Motors. Both motor types had already been selected and purchased for use in the Canterbury Hand. It was decided that the two hands would be created as two different configurations of the same model. This would save design time and would force the model to be more robust to changes in the design.

The bearing geometry of the fingers and the thumb models needed to be optimised. This meant that the CAD models would have to be able to cope with different bearing placements while giving a manufacturable and robust design. The widths of the spacers, shafts, and the finger linkages would also need to change with the different bearing sizes.

The lack of constraints could easily cause the CAD models to go unstable unless some design rules were applied. These were implemented as logical functions within the design tables. These functions would automatically update the dimensions and configurations of the parts within the model when changes were made to the bearing geometry in the spreadsheet. The need for optimisation, flexibility and the inherent complexity and size of creating a CAD assembly model of a robotic hand dictated that it would have to be built with particular methods in mind.

There are four basic structures of organisation in the creation of the models for the Hand, and in the models associated within it. The first structure type was the one used for the finger and thumb assembly models. The second and third types are the palm assembly and hand assembly models. The fourth structural type was the one used for the linked models of the finger and thumb assembly. This final model was used in the optimisation of the hand geometries.

3.1.1 Finger and Thumb Assembly Structure

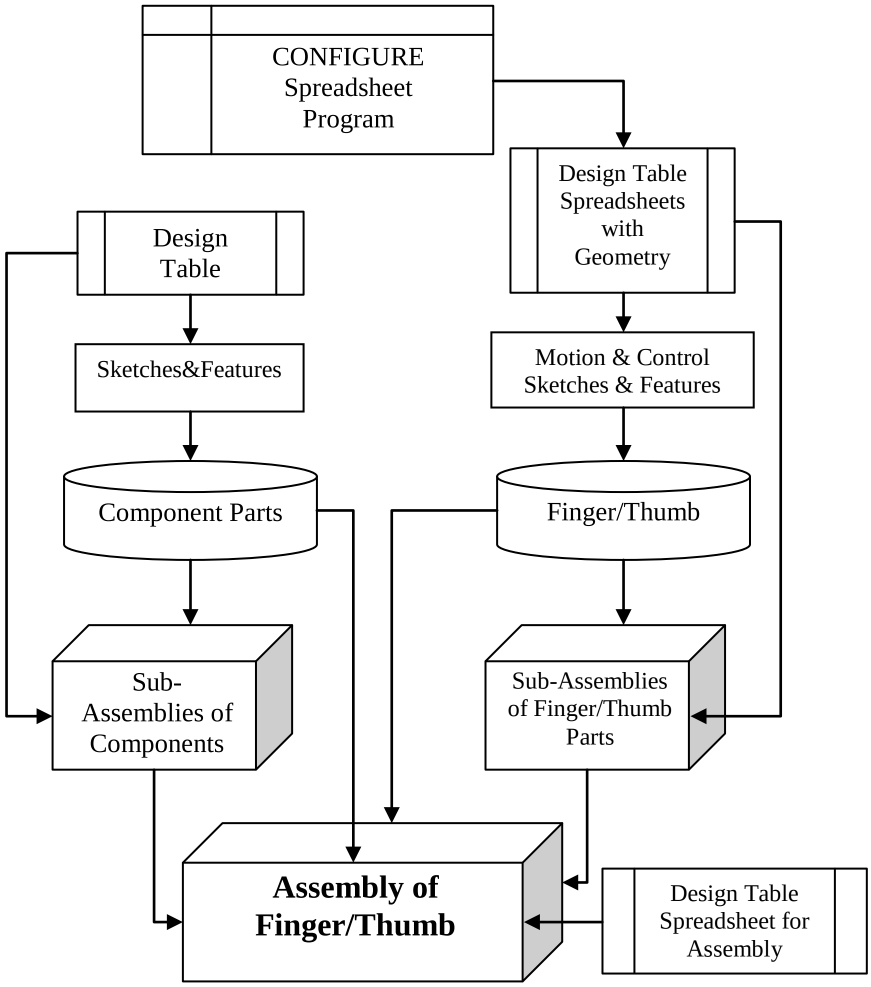

Figure 3.1 shows the structure of the Canterbury Finger and Canterbury Thumb models. As can be seen they both use the same structure. The main assembly model of the finger and thumb were based on the Bottom-up method. That means components were created first and then inserted into the assembly.

Figure 3.1 CAD structure of the Canterbury finger and thumb models

The reason Bottom up assembly was used for the creation process is that it is faster than using derived components and it cuts down on the number of parts used. Components derived from the main assembly need to be updated as they are rebuilt, or when the assembly changes. This makes for a more time intensive model. They are also limited to having every derived feature in the model's configurations being dependent on the current geometry within the main assembly. For example, the hand assembly could have four different fingers. Each finger could have been created with geometry derived from the main hand assembly. For this to work there would need to be four separate models for every finger model that used derived geometry. This is wasteful and computationally inefficient.

The structure of the main assembly of the finger and the thumb can be separated into two different types of models. That is models that have features dependent on geometry changes and models that do not. The models that are independent of geometry changes are called components in the structure diagram. They only have a simple use within the main assembly. Briefly the embedded design table spreadsheets control the sketches, features and configurations of the component parts and sub-assembly models. These components are then used within the main assembly model.

The finger/thumb models that are dependent on geometry have a different type of structure. A VBA program written in Excel called 'Configure' controls the changes in the geometry within these models. It does this by interacting with the imbedded spreadsheets within the parts and assemblies. It was designed for the quick utilisation of the optimised geometry (for the finger, thumb and thumb axis) within the hand. Before this program the models within the hand would have been manually and individually opened, their design tables modified, and the model updated. Originally there was a separate system to control the thumb rotation axis and the thumb web geometry via top down assembly using equations within the hand assembly. Both of these methods were slow, tedious and prone to human error. The equations controlling the thumb axis method had problems when rebuilding the thumb model. The Configure program replaces these two methods, by automatically updating the geometry of the finger and thumb models. It is automated and interacts with the logical functions within the design spreadsheets, and it does not require user supervision once it has begun.

Other than the interaction with the Configure program, the structure of the Finger and Thumb models is the same with the component models. That is their design table drives the features, parts, and configurations of the parts and subassemblies. The parts and subassemblies of the finger and thumb models are then used within the Main assembly.

The structure diagram shows that the main assembly also has a design table spreadsheet. It is used to create the different configurations of geometry and finger/thumb type. Briefly the main types of configurations are split between whether the models use the Maxon or Mini motors. For the fingers this is subdivided between the Index/Ring, the Middle and the Little Finger geometries. The thumb only has a single geometry each for the Maxon and Mini motor geometries.

Some comments should also be made on the nature of why the models were placed as they were in the main assembly. Solidworks will not allow parts within subassemblies to be separately moved in an assembly model. That means that only the parts and subassemblies that were used as movable sections, or that act as foundations, were used in the main assembly. All non-moving parts attached to the movable models were kept as sub-parts within them. This method kept the number of models in the main assembly to a minimum and reduced waiting time. While the hand model moves as the real mechanical hand would, many of the small moving parts, such as bearings, do not. This is an acceptable compromise when creating the CAD model. To have these smaller components moving in the main assembly would slow the model down considerably, and be unwieldy for user modification.

3.1.2 Palm Assembly Structure

The palm assembly uses a mixed bottom-up, and top-down assembly method. This was chosen because of the complexity of the hand geometry that was used in the creation of the palm assembly. Like the Finger and thumb organisation structure there are two types of parts in the Palm assembly. The first are the component parts. Again these models are independent of the changes made to the thumb axis, or the finger/thumb bearing geometry. Like the other structure these components are inserted using the bottom up method. They include such things as the screws, bearings and the finger’s rotation shafts.

The other type of parts are the Derived hand parts. These are all derived from a single model called the palm base part. The base part incorporates all the geometry of the finger placement, thumb location and hand actuator placements using motion and control sketches. These sketches, the configurations and the features of the palm base are controlled from a design table. The two configurations for the palm base are whether the hand is using Maxon or Mini motors. The ‘Configure’ program opens and modifies the geometry of the palm assembly using this design table. The geometry that ‘Configure’ controls are the thumb axis, plus a few dimensions relating to the sizing of the thumb and the fingers. Each of the derived hand parts features and sketches was controlled by their own design table spreadsheets. This was to set out the two configurations of the palm, and to control the dimensions of the derived parts from a single source. A design table was also used in the main palm assembly. It controls which configuration of the derived parts and components is used within the two configurations of the palm.

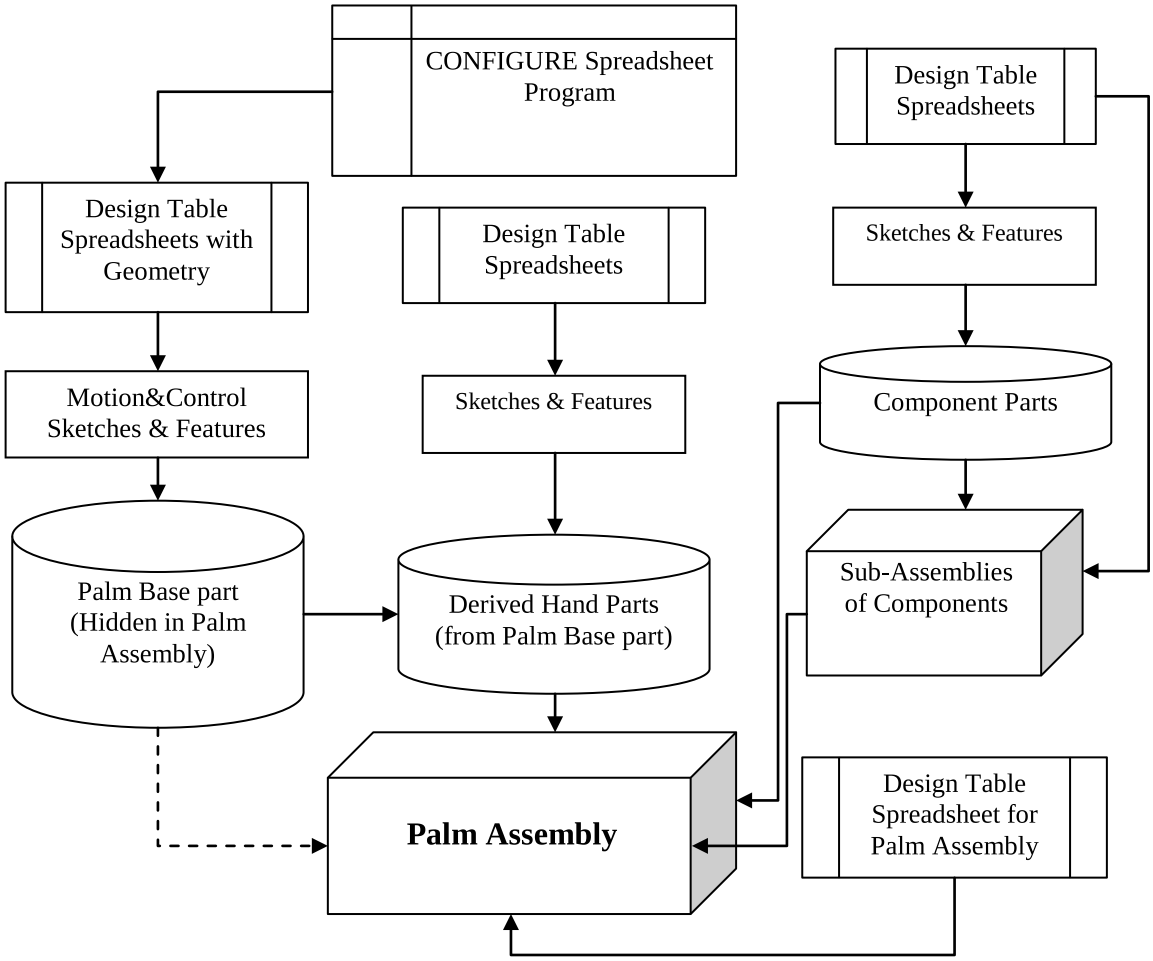

Figure 3.2 Palm Assembly CAD structure

The reason for using a base part is that the palm of the hand is so complex it would have been far too time consuming to create the individual parts using the bottom up method. The palm base could have been created from a single part with multiple configurations, but this would have made the palm even more unwieldy for making design changes. The idea of using a base part in a model's design is to contain the complexity so that the end design is as simple as possible. In fact each individual palm sub-part only required a small number of reduction operations after the base part was added. This made it simple to keep track of design changes. Also only the base part needs to be modified for changes to propagate to all the hand's palm models. There are some problems with this method as it relies on certain geometrical features within the base part to remain constant. If they do not then the relationships that the sketches and features relied upon within the derived parts can dangle. A dangling relationship means that SolidWorks cannot find one or more of the features that made up the relationship.

Another feature of the structure of the palm assembly figure is the dashed line from the palm base part into the Palm Assembly. This represents that the palm base part was added to the palm assembly but was hidden from view. The palm assembly is made of many derived sub-parts. The palm base part, which forms these subparts is exactly the same size, and fills the same location as the palm assembly. When it is in view the result looks rather ugly on the screen. The reason why it is still in the main assembly is that the derived parts do not lose their external reference to it. Also it is always easier to access a part for editing from the main assembly than it is to access it separately in another window.

3.1.3 Hand Assembly Structure

The hand assembly uses a bottom up assembly method. From the structure diagram it can be seen that it was formed partly by the subassemblies that made up the finger and the thumb. The subassemblies of the finger rotation, and thumb rotation mechanisms (hand actuators) were also inserted. The Palm assembly model forms the rest of the hand. The palm was fixed and acts as the reference ground upon which the fingers and the thumb move against. Hand Motion control parts are used to create the motions of the hand. The hand's design tables control the sketches in the assembly as well as the configurations of the hand's models.

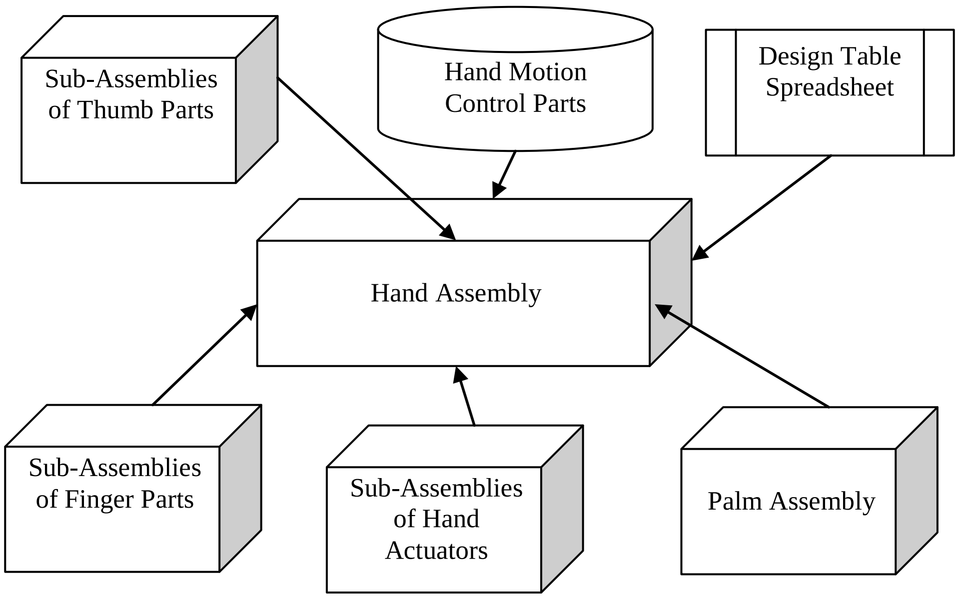

Figure 3.3 Hand Assembly CAD structure

It should be noted that the Hand assembly is separate from the Finger and Thumb Assembly models. Only the subassemblies and parts of the Finger and Thumb models are used in the Canterbury Hand Assembly. The reason for doing this was due to the way parts move within SolidWorks. The parts cannot move within a subassembly model when manipulating it from an assembly. SolidWorks treats the subassembly and the parts within it as a single model. For the hand to have full motion it must use the separated parts and subassemblies of the finger and thumb models in the hand assembly.

The subassemblies of the hand actuators, (i.e. the motors that control the finger spreading motion and the thumb's rotation), could have been placed within the palm assembly. However, the process of creating the hand model meant that the palm assembly was created last. It was easier to design the hand to have these components located separately in the main assembly. It gave the hand model the same stability, but better manipulability for making changes to the actuator positions. The actuators are mated to the sketches within the assembly for location. These sketches use the same geometry as that used within the Palm Base Part and are controlled by the main design table. The sketches are meant to be independent of changes made to the thumb and finger geometries using the Configure Program. The design table also controls the configurations that make up the components of the hand. The two configurations of the hand model are the Maxon motor hand, and the Mini motor hand.

The thumb curl, finger spread, and each individual finger's flexion motion was linked to the motion control board. This was inserted in the hand assembly structure as the Hand Motion Control Parts. The motions made on this board are only implemented once the hand is rebuilt. The thumb's metacarpal rotation though was done as a separate and freely manipulated motion.

3.1.4 Linked Finger Assembly and Linked Thumb Assembly Structure

The Configure Program was used to implement the optimised geometries within the finger and the thumb designs. However to optimise the geometry a new set of models was created. These are the linked finger and the linked thumb models. As the diagram (Figure 3.4) shows they both had the same structure. Like the assembly structure of the unlinked finger and thumb assembly, they have two sets of structures in their design. The first types are the component models. They are independent of changes in the linkage bearing geometry. The other model types are those that are dependent on geometry changes.

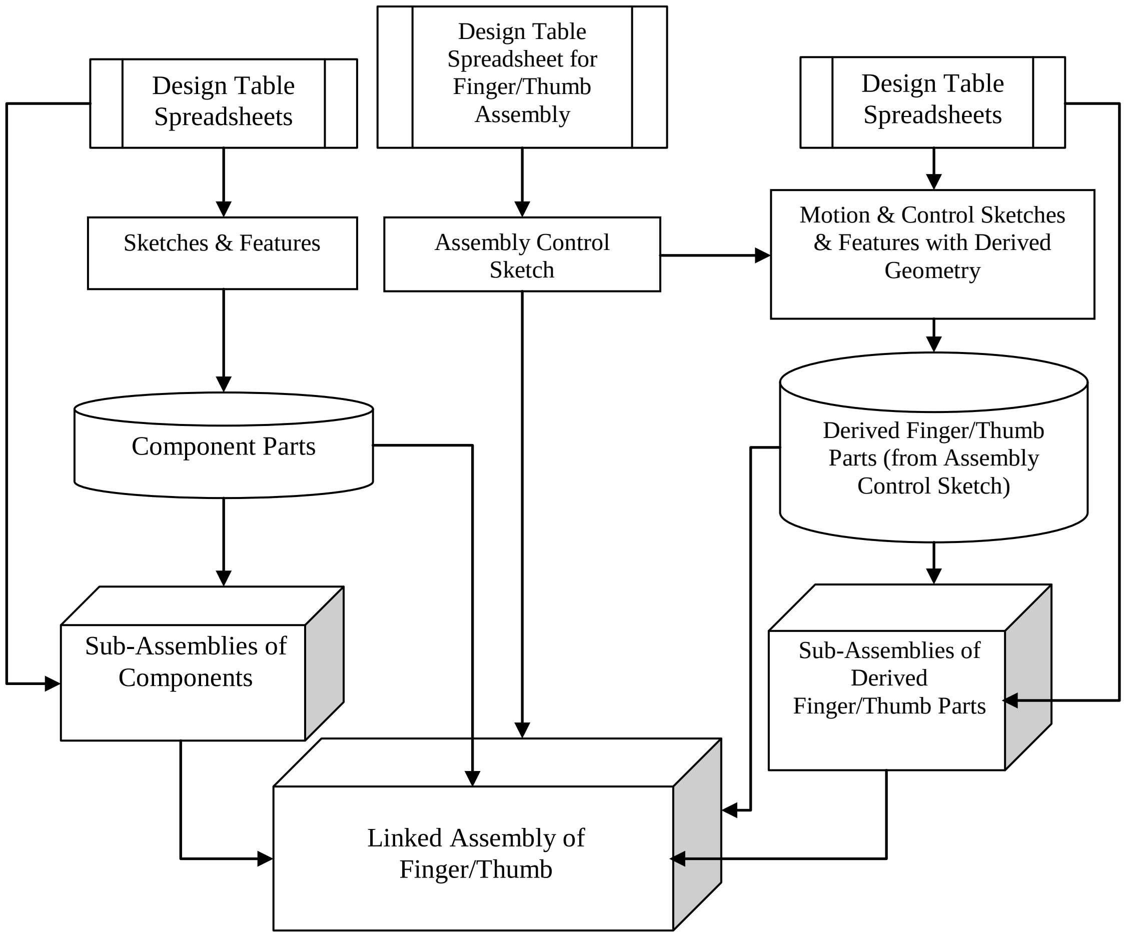

Figure 3.4 Linked finger and thumb CAD structure

These dependent models differ from the finger and thumb models as they use top down design. The finger and thumb models have their motion and control sketches linked to a control sketch in the main assembly. The control sketch is controlled by the design table spreadsheet. Any changes to the geometry of the control sketch will, once the assembly is rebuilt, propagate to the linked parts and subassemblies. Though rebuild time can be a factor in using top down design, it did not impact substantially on the optimisation task. Further justification for using this method was that these particular finger and thumb models were not going to be used in the hand assembly. Thus they did not need to have the potential for simultaneous configurations in a higher assembly.

3.2 Innovative CAD Features

The Canterbury hand's CAD model was shaped by its design objectives. For a complex model it needed to have a robust and manufacturable design. As a test bed for new hand geometries and motors, it needed to have flexibility. For complex CAD modelling it is difficult to reconcile these two viewpoints simultaneously in a design. Thus various innovative features had to be created to suit these goals.

3.2.1 Configurable Model Design

One of the earliest features decided upon was that many of the models within the hand needed to have multiple configurations so as to reduce the number of CAD models in the design. Component models, such as lead screws, have configurations that differ from each other only in dimension value. However other models such as the metacarpal blocks within the fingers would change their appearance and function depending on where they are used in the hand. For example, the middle finger's metacarpal block is fixed in the palm while the other finger blocks rotate within the palm. Both of these different metacarpal blocks would be built similarly but require different features to accomplish these functions.

Instead of using different models for similar functioning parts, such as the finger metacarpal blocks, it was decided to use a single model with multiple configurations. The design tables controlled the configurations by suppressing or unsuppressing features (turned on or off) within the model. For example, a metacarpal block could be configured from one that had a bearing hole to one that had instead a circuit board gap in the same place.

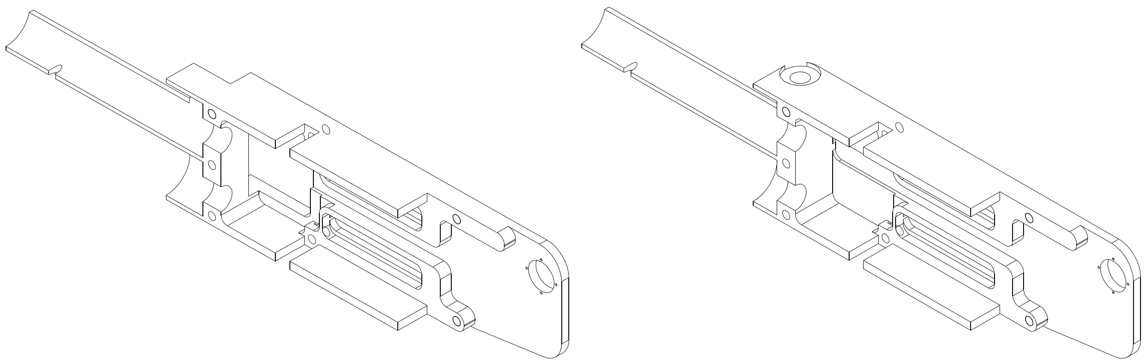

Figure 3.5 Right Metacarpal blocks for Index and Middle (Maxon finger)

Many parts within the linkages have an opposite part which forms the other half of an assembly. Examples of this type of assembly include the metacarpal blocks, and the proximal linkages of the finger and thumb models. Instead of creating two parts with the same geometry, except with opposite direction features, a single part was used. This part would have the same features of a joined part except it would be cut in half at the end to form two opposite parts in two configurations. In the assembly the same part would be added twice but mated to the opposite configuration of itself. Using these modelling techniques makes for a more complicated CAD design but does reduce the number of parts considerably in the assembly.

3.2.2 Motion and Control Sketches

Another problem to address were the singularities within the linkages of the finger and thumb. These singularities limited the motion and created large forces on the linkage bearings. As part of the optimisation these singularities had to first be located within the design. This is explained in detail within the Optimisation section. While some of the singularities were avoided by design, others were chosen as design limitations on the motion of the finger and the thumb models. These limitations were simulated as 'motion position sketches' within the linkage models. These sketches represent the position that the finger or thumb model would take just before they hit the singularity.

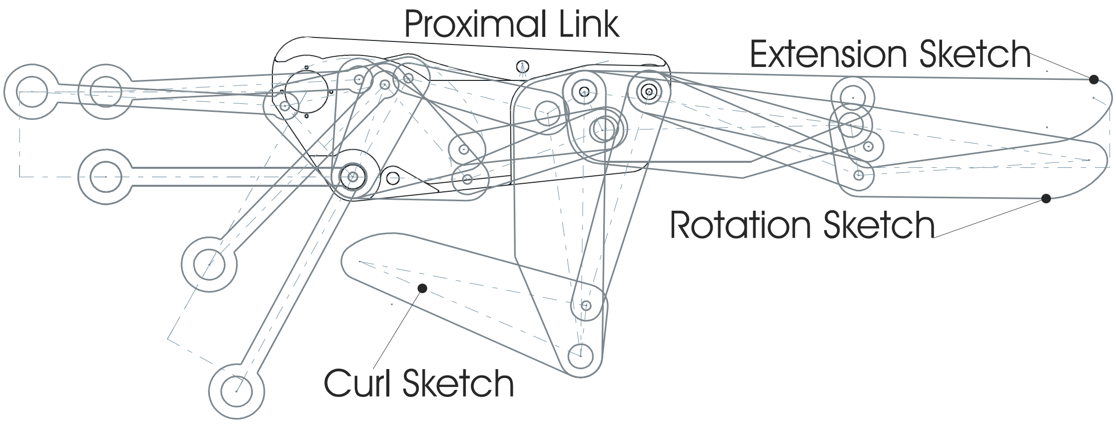

Figure 3.6 Proximal Link with Motion and Control Sketches Visible

Within the finger there were three motion position sketches. The first sketch was of the extended position of the finger at rest. The second sketch was of the curled finger at the singular position. The third was the singularity position of the rotated finger. Within the thumb there was only two motion control sketches. The first was of the thumb in its extended position. The second was of the thumb in its curled state.

The linkage models with this position information could create features that could take into account the dynamic conditions of the finger and thumb assembly. For example the medial link within the finger could remove material where the distal link moved within it. It also uses the curled finger singularity position to create a stop for the distal link. The information could also be used to improve the aesthetic appeal of the models. The metacarpal support bracket at the knuckle for example is shaped to give a smooth look to the extended finger.

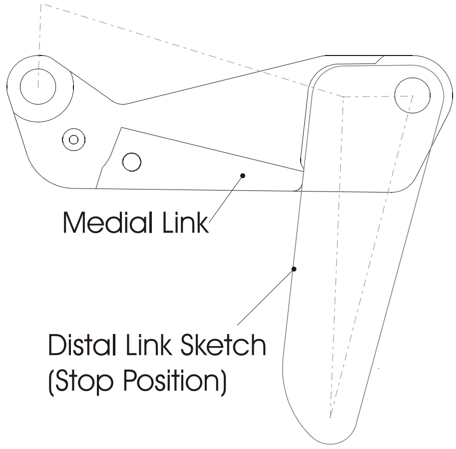

Figure 3.7 Medial link showing Distal links location and stop

3.2.3 Design for Geometry Modification

Another important aspect of the dependent thumb and finger models was making the CAD models flexible for changes in the linkages bearing geometry. Very little was known about the design decisions or choices a person would make when creating an optimised geometry. To help in the CAD design, initial bearing geometries were created and Ward and Bain's geometry schemes were consulted. This helped lay the groundwork for the later optimisation of the hand.

Some basic constraints and observations were found for the bearing geometries of the finger and the thumb models. For example in the finger the motors were separated by as small a distance as possible (1mm) to reduce the height of the metacarpal block. This was for both the Maxon and the Mini motor configurations. Other basic constraints for the CAD models included information on what linkages moved within other linkages. The allowable positioning of the bearings had to be thought out for the optimisation. For example, in the proximal link it is known that the knuckle bearing (at joint B5) will always be attached to the metacarpal block support bracket. It will be positioned as high up from the bottom actuator as possible so as to give the maximum force output to the fingertip from the rigid finger's rotation. Also the bearing B8 will always be at the end of the proximal link instead of the bearing B7 as otherwise the finger could not curl properly and there would be unacceptable interferences within the medial linkage.

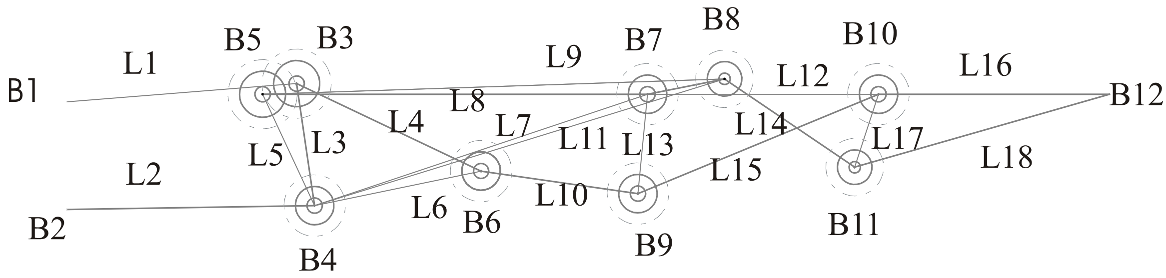

Figure 3.8 Finger Naming scheme

However the linkage models would have to deal with valid bearing geometries (during the optimisation process) that did cause interferences. Innovative CAD design solutions were found for these problems. For example the bearing at the end of the proximal link (at the B8 bearing) may cause interference with the medial linkage depending on its relative position. This interference was incorporated in the design of the medial linkages by adding a cut adjustment feature. The adjustment added a cut feature into the medial link that would provide a space for the B8 bearing shaft if it interfered with the design. If it did not interfere the cut adjustment feature would only cut away a dummy piece out of the design. If the bearing interfered with the finger or not no longer mattered in the design.

The proximal linkage in the finger model also presented a unique problem. It had four bearings (B4, B5, B7 and B8) that formed the shape of the linkage. The linkage would have to be stable for these bearing positions. This caused a problem in modelling the top and bottom surfaces of the link, as it was unknown what the bearing geometry would be. Multiple base features were created for the part. Since the aesthetic look of the proximal linkage was also important these base features were shaped to resemble the proximal phalange of the human finger. This was done by making the slope of the top and bottom sides of the proximal link shaped so that the lines of the finger would seem to line up with the medial and metacarpal phalanges.

The aesthetic appeal of the hand was a big factor in the design of the CAD models. When it did not compromise function or manufacturability it was implemented wherever possible. Examples of this were linkages should appear as solid as possible while allowing space within them for moving linkages. This meant that gaps for moving linkages had to be covered up on the outside as much as possible so as to give the illusion of solidity. This can be seen in the medial linkage of the finger where space for the wires and the distal driving linkage is provided but the curled distal linkage space is covered as much as possibly by two ledges.

However the features and spaces within the model also depend on the bearing geometry. For example the proximal link has various other linkages (the actuator links, the rocker, the medial driving link and the medial linkage) moving within it. To hollow out the proximal linkage the cut features had to each represent the space that these internally moving linkages took. These features also had to occur in a certain order due to possible overlapping of volumes. Larger cuts occurred last as otherwise there would not have been enough material within the proximal link to allow smaller width cut features. If they did not occur in the correct order then errors would appear within the model.

Within the proximal linkage, and indeed within the models for the finger, thumb and the palm, space had to be allowed for circuit boards and electrical wires for the motors and the FSRs. The space allowance for the wiring paths was another design constraint for the kinematic modelling of the motion sketches and cut features of the finger and thumb models.

3.2.4 Palm Base Part for Derived Palm Assembly

The creation of the palm assembly using a base part within them was also innovative. It allowed all the palm parts to be controlled from the single base part using the ‘Configure’ program. By using this method the CAD models for the derived hand parts was simplified, and the number of features within them was reduced. Most of the geometry was already within the base part from which they were derived. The derived palm parts were simplified as much as possible to make them manufacturable. Each part was to be as flat and two dimensional as possible to reduce wastage of material when machining. The hand was separated into sides, rear, palm and top parts. The palm’s internal motor holders and worm gear holding features were in turn separated into simpler internal part.

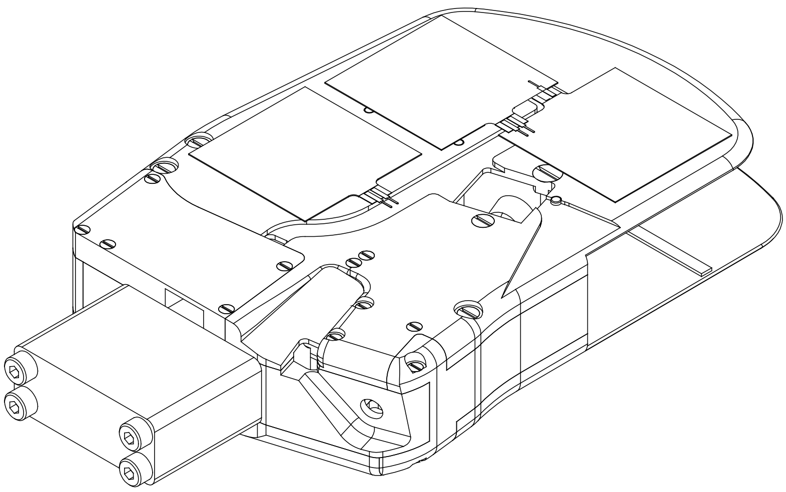

Figure 3.9 Palm Assembly (Maxon Configuration)

One problem in designing the CAD model of the palm base was that it had to shrink when it changed from the Maxon to the Mini Motor configuration. When this occurs the palm base loses and gains new features. The derived parts needed stable features on which to base their sketches and derived geometry. These were found after examination of the changes within the palm base's CAD model.

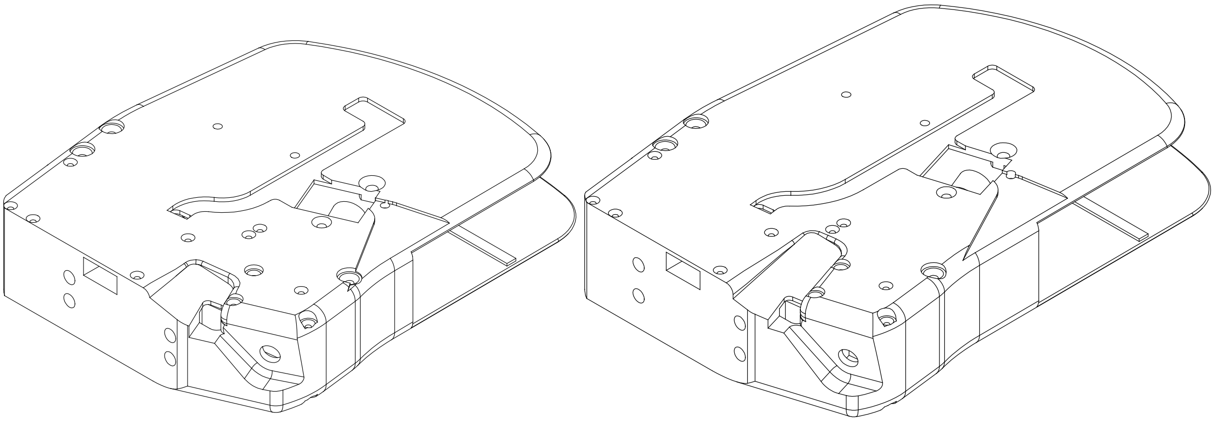

Figure 3.10 Mini and Maxon configurations of the Palm Base part

The features within the palm base part had to hold the internal components of the worm gear and the motors etc, even when the components changed in size and angle. This problem was very similar to that found in fitting the motors to the metacarpal models of the finger and the thumb. The palm as with the metacarpals had to hold at least two types of motors and two sets of components for the configurations. The problem in this was finding a way to hold the smaller motors at different angles within the palm while keeping the derived parts manufacturable. The features would also have to have space above them for the palm's circuit board and the motor wires. A nested series of cuts were designed around the motors and the circuit board to form the motor holder features and the circuit board location. The motor holder feature was designed so that it would be held within the little finger side panel. The motor wires slot feature was added to the motor holder after this. Care was taken to keep enough material to hold the motors within the little finger side panel even with the wire slot.

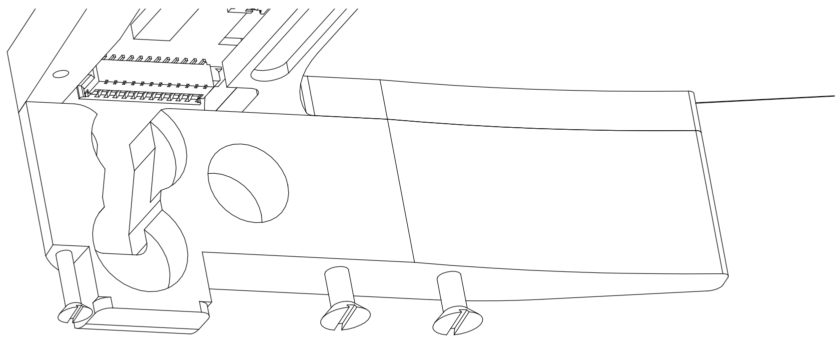

Figure 3.11 Little finger side Panel with Hand PCB above

The palm base part also had an innovative use of the thumb axis for creating the bearing holder. The thumb's axis can be thought of as a vector. That is it has a starting point (defined from X, Y, Z coordinates), and a vector (one horizontal angle, one vertical angle, and a length). The vector was constrained so that the thumb's bearing holder did not protrude very far from the surface of the palm. The bearing holder was constructed within the space between the index and middle metacarpal block. It had to hold the bearings of the front strut of the thumb, and orient it in the angle of the axis. The thumb also had to revolve around the palm and give a motion that approximates that of the human thumb. Thus the axis also had to give the most anthropomorphic angle within the tight space limitations. The CAD model of the bearing holder had to be fastened within the palm of the hand. Also since the finger metacarpal blocks revolved into the space beneath the holder, the base had to be very thin. The CAD model solved this by having a thin shell around the bearing, and a thin tapering base that attached beneath the bearing holder onto the top plate of the palm assembly. The bearing itself was held in place behind and below by screws that fitted neatly into the thin holding material. The part will be complex to manufacture as it will involve a number of machining operations for getting the bearing axis located correctly.

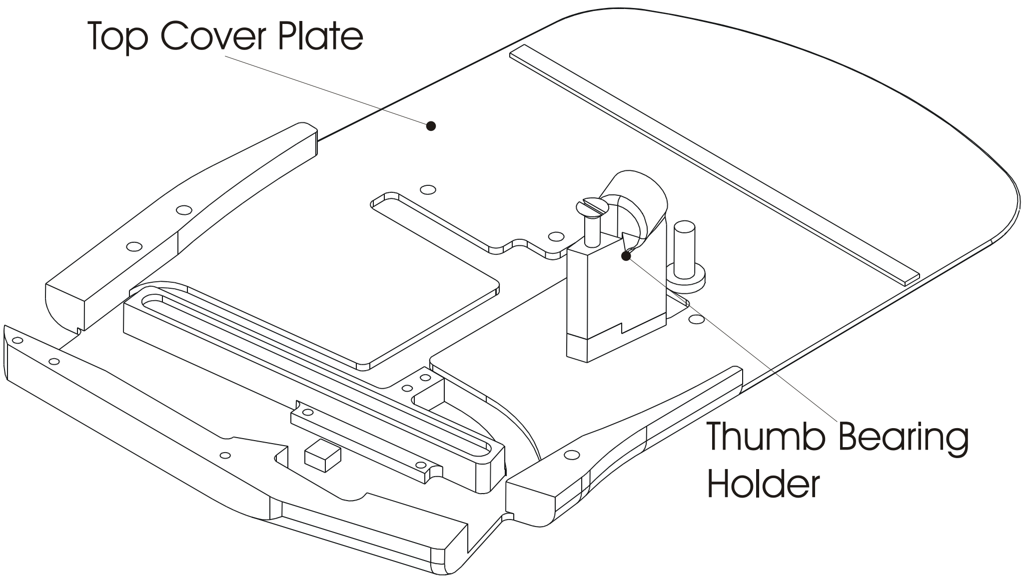

Figure 3.12 Thumb Bearing holder as located on the top cover plate

3.2.5 Hand Assembly Manipulation

Previous assemblies of the fingers within the palm showed that the finger's mating relationships, if left undefined, caused the drive nuts within the metacarpal blocks to lock up at certain finger positions once the hand model was rebuilt. In part this was caused by the finger's spreading motion. This motion freedom meant that the metacarpal base was not fixed in the design. This seemed to cause difficulties for the mating relationships defining the finger drive nuts positions along the drive screws within the metacarpal block. The hand model thus had to have the fingers fully defined for stability of the model. Yet the hand model needed to be able to form grips, so the fingers needed to be manipulated.

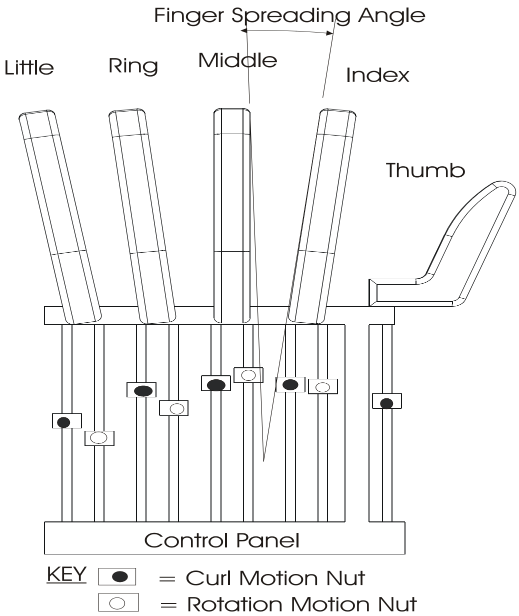

Defining the position of the drive nuts using distance mates solved this problem. A motion control panel was added to the assembly to control the motion of the fingers. It did this by linking the distance mates of the nuts to the reference dimensions of the sliders in the panel. A relationship of three times the distance of the slider gave the distance the drive nut moved. The fingers would form their grip position after the sliders had been moved and the hand model was rebuilt.

Figure 3.13 Motion Control Panel for the Hand

3.3 How to use the Hand Model

The previous sections have dealt with the structure of the finger, thumb and hand models. This section is on how to manipulate the hand's grip position, and how to use the Configure spreadsheet to implement changes to the finger, the thumb's bearing geometry and the thumb's axis geometry. It does not show how to use SolidWorks step by step, as this requires training. It will deal only with basic manipulation.

3.3.1 Hand Geometry Modification with the Configure Program

Before the design table spreadsheet program ('Configure') two methods of implementing optimised geometry were used for the fingers and the thumb. They could change the dimensions from the control sketch, which meant changing the dimension values for each Cartesian coordinate for the bearings and their size. A better way is to change the dimensions from within the embedded design table spreadsheet. Once the changes were made, or when the spreadsheet was closed, the model will need further rebuilding to implement the new geometry. For a number of configurations and parts, the amount of time taken would be substantial. Note that although the hand could have been made with top down design to avoid this repetition, this method would have created a far larger, slower and altogether worse CAD hand model.

The 'configure' spreadsheet can make modifications for various geometries within the hand. It can modify the bearing positions and size for the various configurations within the models of the finger and the thumb. It can also change the axis position and the strut geometry of the thumb model.

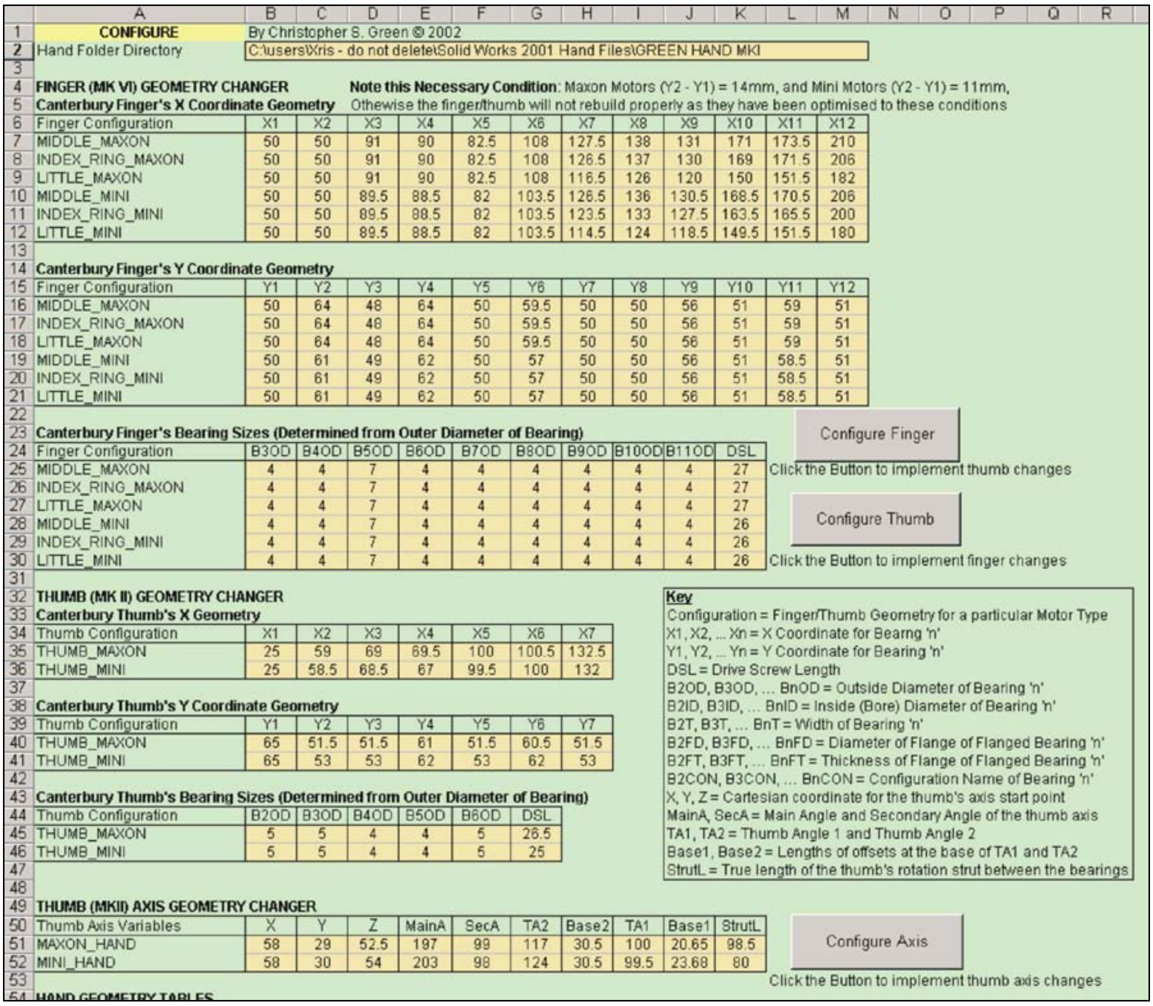

CONFIGURE By Christopher S. Green © 2002

Hand Folder Directory: C:\users\Xris - do not delete\Solid Works 2001 Hand Files\GREEN HAND MKI

FINGER (MK VI) GEOMETRY CHANGER

Note this Necessary Condition: Maxon Motors (Y2 - Y1) = 14mm, and Mini Motors (Y2 - Y1) = 11mm, Othewise the finger/thumb will not rebuild properly as they have been optimised to these conditions

Canterbury Finger's X Coordinate Geometry

Finger Configuration	X1	X2	X3	X4	X5	X6	X7	X8	X9	X10	X11	X12
MIDDLE_MAXON	50	50	91	90	82.5	108	127.5	138	131	171	173.5	210
INDEX_RING_MAXON	50	50	91	90	82.5	108	126.5	137	130	169	171.5	206
LITTLE_MAXON	50	50	91	90	82.5	108	116.5	126	120	150	151.5	182
MIDDLE_MINI	50	50	89.5	88.5	82	103.5	126.5	136	130.5	168.5	170.5	206
INDEX_RING_MINI	50	50	89.5	88.5	82	103.5	123.5	133	127.5	163.5	165.5	200
LITTLE_MINI	50	50	89.5	88.5	82	103.5	114.5	124	118.5	149.5	151.5	180

Canterbury Finger's Y Coordinate Geometry

Finger Configuration	Y1	Y2	Y3	Y4	Y5	Y6	Y7	Y8	Y9	Y10	Y11	Y12
MIDDLE_MAXON	50	64	48	64	50	59.5	50	50	56	51	59	51
INDEX_RING_MAXON	50	64	48	64	50	59.5	50	50	56	51	59	51
LITTLE_MAXON	50	64	48	64	50	59.5	50	50	56	51	59	51
MIDDLE_MINI	50	61	49	62	50	57	50	50	56	51	58.5	51
INDEX_RING_MINI	50	61	49	62	50	57	50	50	56	51	58.5	51
LITTLE_MINI	50	61	49	62	50	57	50	50	56	51	58.5	51

Canterbury Finger's Bearing Sizes (Determined from Outer Diameter of Bearing)

Finger Configuration	B3OD	B4OD	B5OD	B6OD	B7OD	B8OD	B9OD	B10OD	B11OD	DSL
MIDDLE_MAXON	4	4	7	4	4	4	4	4	4	27
INDEX_RING_MAXON	4	4	7	4	4	4	4	4	4	27
LITTLE_MAXON	4	4	7	4	4	4	4	4	4	27
MIDDLE_MINI	4	4	7	4	4	4	4	4	4	26
INDEX_RING_MINI	4	4	7	4	4	4	4	4	4	26
LITTLE_MINI	4	4	7	4	4	4	4	4	4	26

Configure Finger

Click the Button to implement thumb changes

Configure Thumb

Click the Button to implement finger changes

THUMB (MK II) GEOMETRY CHANGER

Canterbury Thumb's X Geometry

Thumb Configuration	X1	X2	X3	X4	X5	X6	X7
THUMB_MAXON	25	59	69	69.5	100	100.5	132.5
THUMB_MINI	25	58.5	68.5	67	99.5	100	132

Canterbury Thumb's Y Coordinate Geometry

Thumb Configuration	Y1	Y2	Y3	Y4	Y5	Y6	Y7
THUMB_MAXON	65	51.5	51.5	61	51.5	60.5	51.5
THUMB_MINI	65	53	53	62	53	62	53

Canterbury Thumb's Bearing Sizes (Determined from Outer Diameter of Bearing)

Thumb Configuration	B2OD	B3OD	B4OD	B5OD	B6OD	DSL
THUMB_MAXON	5	5	4	4	5	26.5
THUMB_MINI	5	5	4	4	5	25

Key
Configuration = Finger/Thumb Geometry for a particular Motor Type
X1, X2, ... Xn = X Coordinate for Bearng 'n'
Y1, Y2, ... Yn = Y Coordinate for Bearing 'n'
DSL = Drive Screw Length
B2OD, B3OD, ... BnOD = Outside Diameter of Bearing 'n'
B2ID, B3ID, ... BnID = Inside (Bore) Diameter of Bearing 'n'
B2T, B3T, ... BnT = Width of Bearing 'n'
B2FD, B3FD, ... BnFD = Diameter of Flange of Flanged Bearing 'n'
B2FT, B3FT, ... BnFT = Thickness of Flange of Flanged Bearing 'n'
B2CON, B3CON, ... BnCON = Configuration Name of Bearing 'n'
X, Y, Z = Cartesian coordinate for the thumb's axis start point
MainA, SecA = Main Angle and Secondary Angle of the thumb axis
TA1, TA2 = Thumb Angle 1 and Thumb Angle 2
Base1, Base2 = Lengths of offsets at the base of TA1 and TA2
StrutL = True length of the thumb's rotation strut between the bearings

THUMB (MKII) AXIS GEOMETRY CHANGER

Thumb Axis Variables	X	Y	Z	MainA	SecA	TA2	Base2	TA1	Base1	StrutL
MAXON_HAND	58	29	52.5	197	99	117	30.5	100	20.65	98.5
MINI_HAND	58	30	54	203	98	124	30.5	99.5	23.68	80

Configure Axis

Click the Button to implement thumb axis changes

Figure 3.14 Interface of Design Table Spreadsheet 'Configure'

For the program to work it needs the path for the hand files set-up properly in the B2 cell of the 'Configure' spreadsheet. For example it might read:
C:\users\Solid Works 2001 Hand Files\GREEN HAND MKI

The path can be created easily by copying and pasting the path from windows explorer’s address bar into the cell. Once the path has been set the hand geometry values may be changed in the clear cells. Since the spreadsheet is protected the only parts that the user can modify are the input cell values.

The extended arrangement of the linkages was the datum position for the Cartesian (X, Y) coordinates for the bearings within the finger and thumb. The outer diameter of the bearings and the drive screw length within the metacarpal block can be specified. The bearing diameter values are selected from the list of bearing sizes. There are six finger configurations and two thumb (Maxon or Mini motor) configurations. The finger configurations can be divided in two for the Maxon of Mini motor configurations, and there are a further three configurations for each of the fingers in the hand assembly model. That is the Little, Middle and Ring (which is the same as the Index) finger configurations. Any modifications that are made to either the finger or the thumb may be implemented by selecting either the ‘Configure Finger’ or the ‘Configure Thumb’ buttons.

The thumb axis and strut geometry values may also be modified using the ‘Configure’ spreadsheet. The thumb axis is made up of the origin point for its vector (X, Y, Z coordinates) and also the vector of the axis (horizontal, vertical angles). The thumb’s strut geometry was specified from a further two angles (horizontal and vertical) and two offset lengths for those angles. The strut length can also be changed once the ‘Configure Thumb’ Button is clicked. When a button is clicked the program will automatically change the design tables within the particular models affected by the changes.

Care should be taken when selecting geometry values. The user should first find their optimised geometry from modification of the linked finger or thumb models. The models will allow small modification of their values without errors within the models. The thumb axis and strut geometry is especially sensitive to modification and great care must be taken that these values are only modified slightly. If a model has been modified and contains error messages it is probably unable to handle the new geometry values. The models may be reset to their default settings by copy and pasting their values from the tabulated optimum geometry values in the Configure worksheet.

3.3.2 Manipulation of the Finger and Thumb Assembly

The finger and thumb models have similar mechanisms for motion. Their linkage mechanisms are both controlled by motion of drive nuts within their metacarpal block.

The finger by itself has two degrees of freedom of motion. That is the linkage mechanism can move within an area. The fingers motion was split into two types of motion: the finger curl and its straight rotation motion about the knuckle. The top motor in the finger actuates the curl, while the bottom motor actuates the finger's straight rotation motion. Both motions are combined.

In the CAD model, the top and bottom drive nuts can only be moved individually with the move command tool. If a model is not fully constrained in an assembly it may be moved by this button by selecting the model either within the feature manager tree or in the Document window and then moving the mouse. However only one object and it's mated dependents can be moved at a time with this tool. This means that in the finger assembly only one drive nut may be moved at a time. The top drive nut when pulled back towards the motors causes the finger to curl. When the bottom drive nut is pulled back it causes the finger to pull downwards as it rotates around the knuckle bearing.

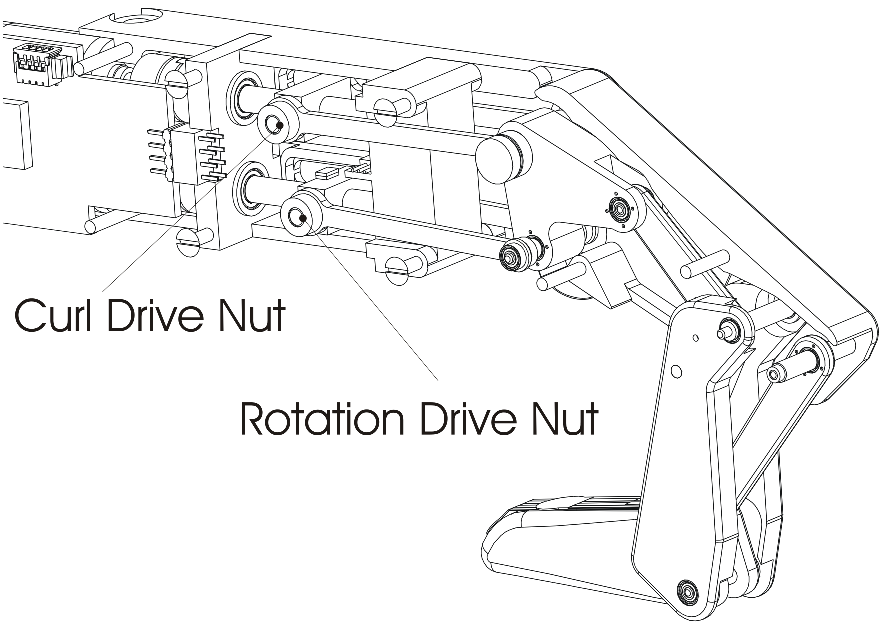

Figure 3.15 Curling Finger showing drive nut positions

Getting to view the drive nuts in the document window may be a problem due to the metacarpal blocking the view. In this case using the hide part command button on one of the metacarpal blocks will allow the drive nuts to be seen. This applies to the thumb model as well.

The thumb model is a very similar mechanism to the finger. It has one degree of freedom of motion so that its linkage mechanism can only move along a curve. In the thumb the motor is directly above the drive screw. The drive screw is rotated by a spur gear attached to the motor. As the drive screw rotates it moves the drive nut and hence moves the thumb linkages that are attached to it. To move the thumb linkages, select the drive screw in the thumb with the move command tool and pull it backwards. This will cause the thumb to curl.

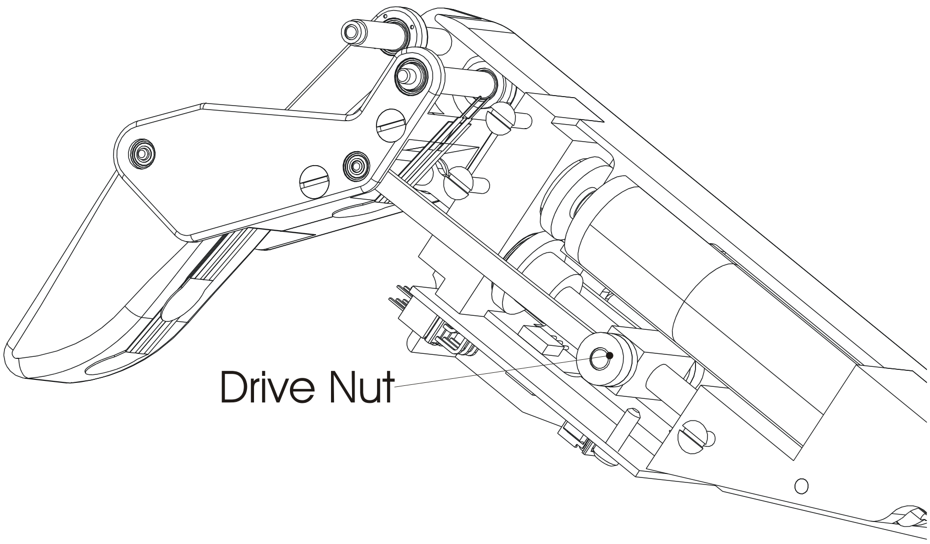

Figure 3.16 Thumb Curled showing drive nut position

When a finger or the thumb reaches a singularity for any of these motions it will not be able to move any further. The singularity occurs when certain linkages reach a point and cannot move any further. Mathematically it is a point that cannot be resolved for a particular motion. This is explained in more detail in the background theory chapter of the Canterbury hand.

3.3.3 Manipulation of the Hand Assembly

The hand assembly has so many components that movement of individual fingers was difficult. A number of parts were added to the hand assembly to be used as the 'Hand Motion Control Board'. They are linked to the model of the hand so that motion of a particular slider on the control board represent three times the motion of a corresponding drive nuts motion. The sliders control all the drive nuts within the finger and thumb models. Moving the 'red' coloured sliders (looking down on the palm of the hand) represents a curling motion for which ever finger or thumb is represented in the panel. Moving the 'blue' coloured slider represents a rotation motion for the finger linkages (about the B5 bearing joint). The effects of the control board's motion are implemented in the hand once the assembly is rebuilt. If errors occur after moving and rebuilding, they are due to the hand having moved the linkages too far so that they after the singularity positions. The hand model will not move and SolidWorks shows errors occurring within the mating relationships. This is because it cannot match the constraining mates to the geometrically impossible linkage position that the user has specified. To remove these error messages the user should move the problem linkages via the control board back to positions that are not within the singularity. The error messages should disappear after the hand is rebuilt.

The control board also controls the spreading motions of the finger. The angles between the finger metacarpal blocks are linked so that there was an equal angle between the fingers as they spread. By rotating one of the finger models on the control board a corresponding angle is given to all the fingers in the hand assembly once the hand is rebuilt.

The thumb rotation around the palm of the hand is not linked to the control board. It can be moved independently and freely with the move control button. Selecting the thumb and moving the mouse can rotate the thumb into any position.

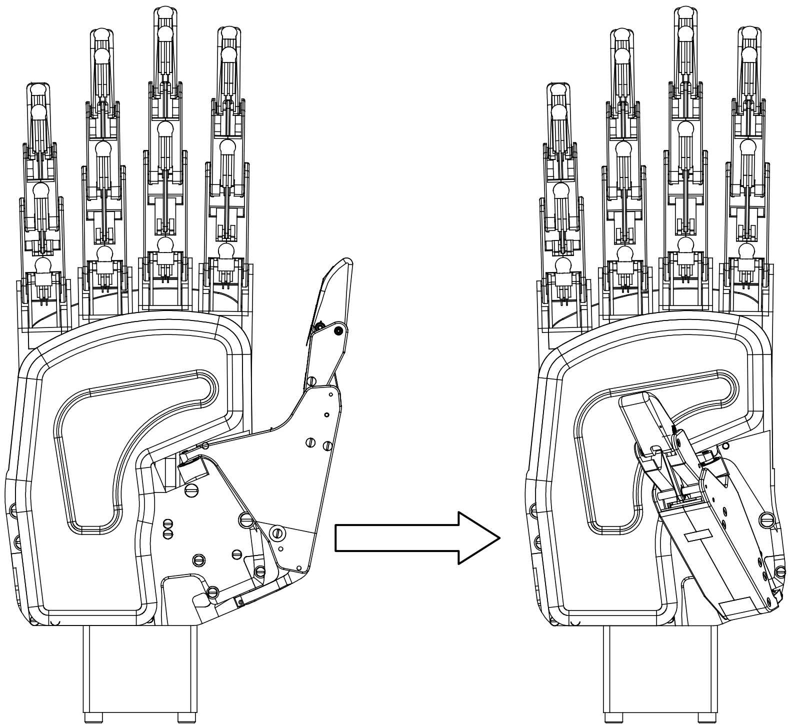

Figure 3.17 Thumb rotation in the Canterbury Hand CAD Assembly

Care has been taken to avoid interferences within the models of the hand. However there are some motions that the hand finger and thumb models cannot reach in real life that SolidWorks allows. Such motions include moving the thumb model's strut through the palm of the hand. To avoid this sort of interference when moving objects, collision detection can be selected from within the feature manager options. If errors occur within the hand model it may be that it needs to be rebuilt. If this does not solve the problem then the error may be due to an unstable geometry for the palm, finger or thumb models.

3.4 CAD Summary

This chapter has given an overview of Computer Aided Design (CAD) and how it is used in design. The CAD program SolidWorks was selected as the CAD program for the modelling of the Canterbury Hand. SolidWorks is a feature-based parametric solid modeller, which is fully associative, able to be constructed with or without constraints, and could utilise relations to implement the users design intent

The Computer Aided design of the Hand has incorporated many innovative CAD features. It is both robust and simple to manipulate within the main hand assembly as well as the individual finger and thumb assemblies. The bottom up assembly method was used principally for the structure of the hand models. Linked models of the finger and thumb using the top down assembly method were also created to aid in the bearing geometry optimisation for the finger and thumb.

The linkage models of the finger, thumb, and thumb axis within the hand can incorporate changes within their geometry. Design table spreadsheets embedded within the SolidWorks models controlled these values. Because bottom up assembly requires that each individual part be modified within the assembly, a spreadsheet program called Configure was created. It was designed to automatically update the design tables and rebuild the models that are affected by geometry changes. Overall the Canterbury Hand model is both a flexible and stable CAD model. This was by proven by creating two hand configurations that incorporated different sized (Maxon and Mini) motors within them. The hand model with heavy modification has the potential to use other motors and components for future redesign.

Chapter 4: Design of the Canterbury Hand

4.1 Introduction to the Design

The concept of the Canterbury Hand led to the development, at the University of Canterbury, of a prototype mechanical finger [Ward 1996]. The Canterbury finger is a two-degree of freedom multi-bar linkage mechanism. Ward had selected two types of motors for the actuation of the finger. The Minimotor 1016 M 006 G DC motor (0.5 Watt, Ø10mm by 39mm long) was selected for use in a prosthetic hand (and the prototype finger) due to its smaller size and weight. The Maxon RE-013-35-10EAB103A DC motor (3 Watt, Ø13mm by 65mm long), motor was intended for use in a larger and stronger robotic hand. The Mechanical Engineering department bought fifteen motors of each type for the use in the Canterbury Hand designs. This purchase acted as a constraint in the design of the current Canterbury Hand design.

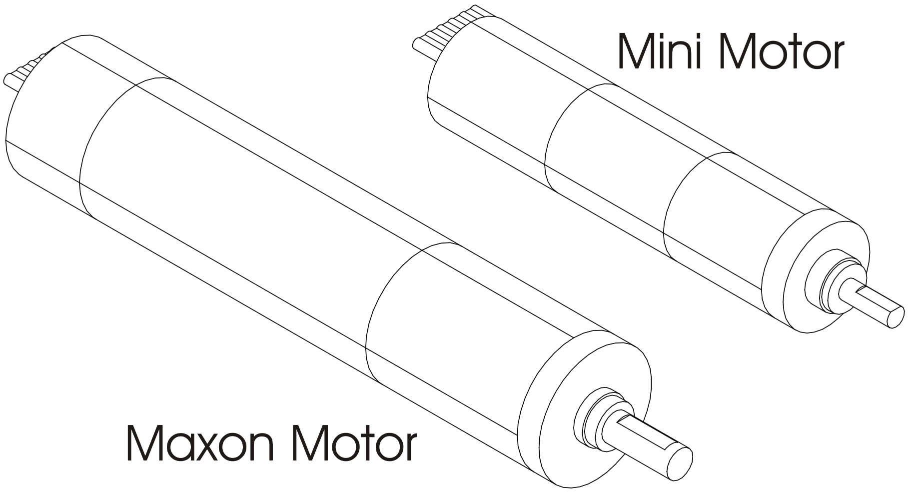

Figure 4.1 Maxon and Mini Motor Size Comparison

Dr Dunlop originally visualised the Canterbury Hand as a six-fingered hand with fifteen degrees of freedom (DOF) [Ward 1996]. The original application for the prototype Canterbury Hand was for a robotic arm. It would have four fingers (4x2DOF), with a finger spreading mechanism (1DOF), and two opposing thumbs (2x2DOF) each of which would have a thumb rotation mechanism (2x1DOF). The fingers and thumbs of the hand would be the Canterbury Finger mechanism. By having two thumbs the hand would provide greater stability when picking up objects.

It was decided for this thesis that a simpler more anthropomorphic hand design would be more useful as a prototype hand device. It would serve as a step closer to the end objective of the Canterbury hand as a prosthetic device. It would also be easer to use as a telerobotic manipulator if it had an anthropomorphic motion and appearance. However while the six-fingered hand has not yet been developed it may still be designed as another project later.

The design objectives for the Canterbury hand are described in the next section. They include such goals as designing for anthropomorphic appearance, minimisation of size, and increasing the hand's prehensile interactivity. The development of the hand had to incorporate many of the design elements of previous designs of the Canterbury Finger and thumb. For example, the finger still had to use the linkage same linkage arrangement, and to have a coupling between the motor and the lead screw. Suggestions for improvements from previous students work and Dr Dunlop also had to be included into the design. Such objectives included having surfaces on the finger for FSRs (force sensing resistors), clamping the motors in the metacarpal blocks and having continuous shafts through the linkage bearings within the finger and the thumb. These particular objectives had to be accomplished while keeping the overall design goals of the hand. For example these general goals included having the actuators, wiring and circuit boards entirely enclosed within the hand. The hand design also had to have an anthropomorphic appearance and a maximised grip force.

At the start of this thesis the method of actuating the hand had already been decided upon. Electrical motors had been decided upon for their compactness and power output. The particular Maxon and Mini motors had even been purchased for the eventual design of the hand. The method of transferring the motors power by certain linkage arrangements had also been decided upon. While linkages are slower than cable operated hands, they are far more compact, efficient and require less maintenance and control complexity.

The hand was modelled in SolidWorks, which is a parametric fully associative 3D solid modeller. The reason CAD was used was that the hand had to have accurate design of a large number of complex components. By using a CAD program a much more complex and useful design could be accomplished in a smaller timeframe. The CAD solid model of the hand involved entirely redesigning the finger and the thumb parts so as to accomplish these objectives. The finger and thumb linkages for example had to be created so that they could still give an optimum design for different bearing joint geometries. New mechanisms such as the finger spreading mechanism and the thumb rotation mechanism also had to be invented. Previous design work by other students, though relevant, had not been designed in the context of the entire hand. Thus results that were not applicable to the current hand design had to be ignored. For example the optimised finger geometry found by Bain had to be disregarded due to the changed size of the current hand designs and the poor anthropomorphic appearance of the geometries.

As stated previously there were two sets of motors bought for two different Canterbury Hands. Since SolidWorks is a parametric and fully associative CAD package it was decided that both hands would be modelled simultaneously within the same CAD model as two different configurations. This in effect meant that there would be two hand designs that incorporated many common design features, but were optimised for different sizes, motions and force outputs. It was decided that the first hand to be manufactured would be the Maxon hand design. Since this hand is larger it would be easier to manufacture and to correct any problems that may be found in the design. The mini motor hand would then be created.

From previous research [Markenscoff, Ni and Papadimitriou, 1990] it has been shown that only three fingers are required for force closure of a two-dimensional (2D) object, and four fingers for grasping a three-dimensional (3D) object. The number of fingers in the hand may be reduced by one finger for known conditions. That is only two fingers for a 2D object, or three fingers for a 3D object. However for maximum dexterity for grasping of a 3D object a redundant finger is best. Since the human hand may be considered evolutions ideal design it was decided that the Canterbury Hand would have five fingers (in particular four fingers and a thumb).

The hand model eventually settled into the current eleven degree of freedom design. It is anthropomorphic with four fingers (of two degrees of freedom each), and a thumb (with a single degree of freedom curling motion). It was decided that the Canterbury hand would be right handed. This is important for Teleoperation, as a person likely to operate the hand would also be right handed. The hand also has (1DOF) finger spreading mechanism and a (1DOF) thumb rotation mechanism, which is actuated from motors enclosed within the rear of the hand. The thumb linkage arrangement was based on the Bain linkage design. For information on the theory behind the hand, fingers, or the thumb, please refer to Chapter 5: 'Background Theory'. After the design was completed the finger, thumb, and thumb axis had to be optimised. The optimisation process and results are discussed within Chapter 6: ‘Optimisation of the Canterbury Hand’.

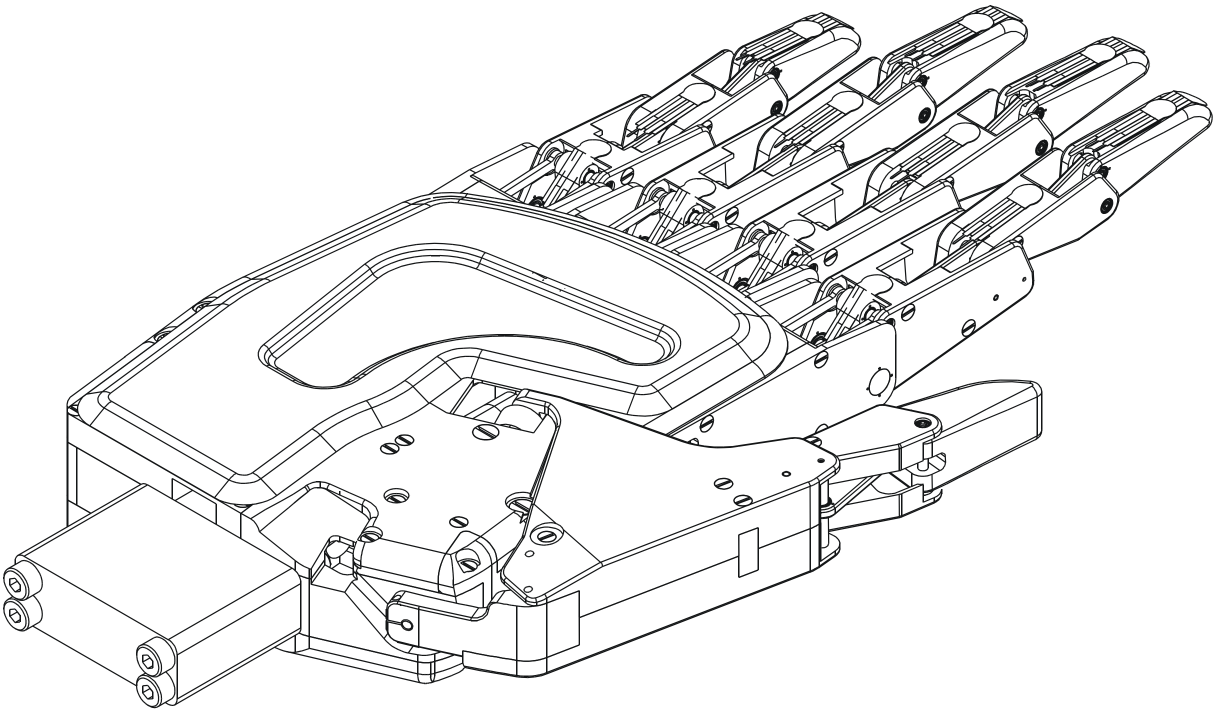

Figure 4.2 Canterbury Hand (Mini Motor Configuration)

It should be noted that while the Maxon and Mini motor Canterbury Hand designs of this thesis are anthropomorphic, and reasonably lightweight, they are still too large and heavy for use as a prosthetic device. Instead both hands would best serve as test beds for research that would eventually lead to the design of the prosthetic Canterbury hand design. A glove may also be used to cover the hand’s robotic looking features to improve its appearance.

This chapter will cover the current design of the Canterbury Hand and the parts that form it. It will start with the objectives for the hand design and how they were implemented in the features of the parts and mechanisms. It will discuss the details of the design, what will be necessary when constructing and assembling the parts of the hand and how they interact within the hand. The implementation of the objectives within the design features and the design decisions will also be evaluated. The hand design will be summarised for its main innovative features at the end of the chapter.

4.2 General Design Goals for the Hand

The creation of the Canterbury Hand had to embody various objectives. These goals were separated into general and individual objectives. The general objectives for the hand design were for:

- Anthropomorphic motion and appearance (using anthropometrics data for scaling).
- Simplified manufacture for low cost using bought in components if possible.
- Ease of assembly and disassembly.
- Maximum prehensile interaction and working volume.
- Surfaces on hand, thumb and fingers for gripping objects and for attaching sensors.
- Maximum grip force and speed of hand closure.
- Wires, FSRs, and circuit board amalgamation.
- Minimal interference/friction of moving parts.
- Stability of design for internal forces.
- Flexible design for multiple geometries and different motors.
- Minimisation of hand size for low weight and efficient use of space.
- Two hands; one using Maxon motors, one using Mini motors (motors from Mini motor).

4.3 Materials for Hand

The hand uses Aluminium (alloy 7075) for its default material. The reason for this is that it is relatively inexpensive, has a good strength to weight ratio (which is important for having a low weight hand) and it is easily machined. Another good reason for choosing aluminium is that is a good conductor of heat. This is important as though the motors are mostly air cooled there will still be considerable heat built up in the hand that needs to be conducted away. Aluminium is also corrosion resistant due to the oxidised layer that forms on its surface. However this can give it an oily feel and appearance after machining. That is why the aluminium parts will be anodised black after manufacture to improve their appearance, to protect them from dirt, and to give an extra coating of protection to the hand. If there is corrosion problems with other parts in the hand electro plating the hand's aluminium parts with zinc may be considered.

The drive screws, and shafts within the hand (i.e. finger linkage shafts, lead screws) will be made of stainless steel (steel grade 430). The reason for this is that the shafts will have a large amount of force applied across them. They should thus be made of a strong material. Stainless steel is also readily machined and is corrosion resistant. It should not have a problem with corroding the aluminium parts of the hand (due to their coating) for most environments. The exception to this is the finger-spreading shaft as it has the largest stresses for loading in the hand. It will use the Aluminium 7075 alloy due to its higher proof stress. If this material is insufficient for the finger spreading shafts some other stronger material will be considered.

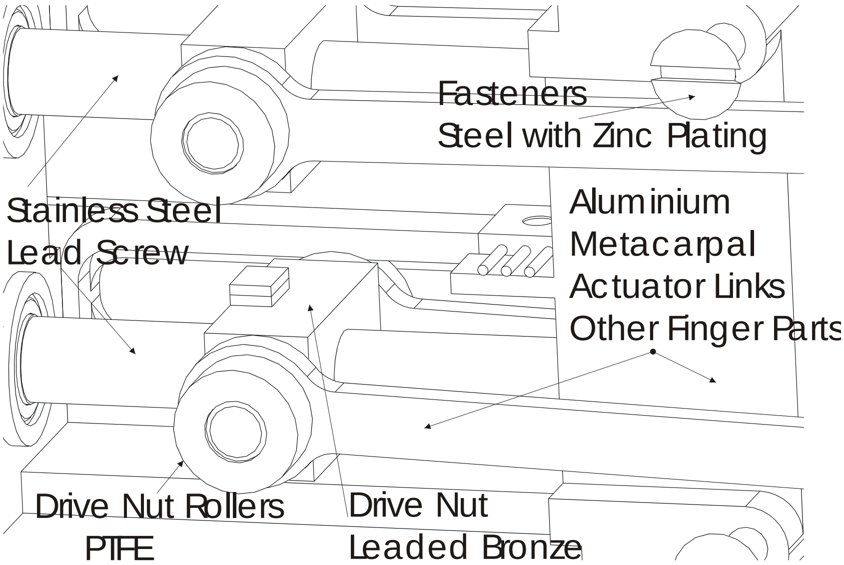

Figure 4.3 Materials used in the Drive Assembly

The fasteners should be made of steel with zinc plating or from Aluminium. The reason for this is to avoid corrosion with the aluminium parts of the hand. Stainless steel fasteners could be used as well however there may be some corrosion in marine or industrial environments.

The drive nuts within the hand, finger and thumb will be made of leaded Bronze. This material is otherwise known as Gunmetal or bronze impregnated with bronze. Leaded bronze is easily machined, is low cost, has good structural properties, and has a high load capacity. The main reason for selecting this material is that it has good lubrication. The lead will wear and help lubricate the motion of the drive nuts for their travel along the lead screws. It is also cheaper to have the lead screws wear, than the more expensive lead screws in the finger. It is also a good intermediate material between the lead screw and the drive nut rollers. An alternative material for the drive nuts is Delrin AF. This material was used in the prototype finger drive nuts [Ward 1996]. Delrin AF is an acetal homopolymer with PTFE uniformly distributed through it. It has improved wear resistance and strength compared to normal PTFE. It has lower friction than normal PTFE.

The rollers on either side of the drive nut are used to hold the nut in the metacarpal (or the palm) so that their motion is linear along the lead screw. The rollers for the hand, it was decided, would be manufactured from PTFE (polytetrafluoroethylene) otherwise known as Teflon. Teflon is well known for having a very low coefficient of friction and has a good chemical resistance, and a wide temperature operating range. It is also well known as a bearing material. The drive nut rollers will not be under pressure or under compressive stress, which would usually cause Teflon problems. The rollers should rotate well within the aluminium housing and on the bronze drive nut. Teflon will also be used in strips on the inside of the palm assembly. It will act as a low friction support material between the fingers and the palm assembly for the finger spreading motion. Acetyl/Delrin AF may be considered as an alternative material for Teflon if there is too much wear.

It should be noted that electrical components within the hand will be made of or coated in plastic (probably ABS) so as to make them nonconductive. It is also important for wear resistance, as there can be considerable motion of the wires in the hand from the curling of the fingers and rotation of the thumb. However the reduction of the wires in the hand should reduce the problems that may occur from this.

Table 4.1 Reasons for Material Choices in Hand Design

Material	*Components*	*Reason*
Aluminium (Anodised)	Hand Parts/Coverings, finger and thumb metacarpals and linkages	Strength, machinable, conductive, light weight,
Steel with zinc plating	Fasteners within the hand	Strength, Good chemical interaction with hand parts
Leaded Bronze (Gunmetal)	Drive Nuts in finger, thumb and palm assembly	Machinable, Strength, Self Lubricating, low cost
Stainless Steel	Shafts and lead screws, (exception being finger spreader shafts)	Strength, Machinable, corrosion resistant
PTFE	Drive nut rollers and palm support strip	Self lubricating, low friction,
Delrin AF	Alternative material for PTFE	Stronger than PTFE, reasonably low friction

4.4 Manufacturing Methods

The design of the Canterbury hand had to be able to be created within the Engineering Workshop of the Mechanical engineering department at the University of Canterbury. The machines available are standard engineering lathes, grinders, drilling and milling machines. There is a CNC lathe, EDM wire cutting machine, and a CNC milling machine available as well.

To reduce the machining time of the workshop as many bought components have been used in the design as possible. When this is not possible parts have been designed so as to reduce cutting and set up time.

The majority of the shafts and spacers in the hand will need to be hand turned on a small toolmakers lathe due to the precise tolerances required for these parts. The lead screws also will require taps and dies. In particular an M4 tap and die with 0.7mm pitch for the finger and thumb lead screws. For the spreader screw M10 with 1.5 pitch, and Right Hand (RH) and Left Hand (LH) M3 taps and dies with 0.5 pitch will be required. Fortunately most of these are already available in the works shop except for the left hand pitch tap and die. All the thread sizes selected use coarse thread sizes for reducing the cost of the taps and dies.

The rest of the components (i.e. Metacarpal blocks, linkages, palm assembly parts) are manufactured using the CNC milling machine. Since the majority of the features for the hand are two dimensional cuts and bosses on a plane there should be a minimum of set-up time for these machines. The electronic data for these machines can be created quickly from 2D drawings of the part in SolidWorks exported in the DXF format.

Some of the components (notably the bearing holder in the palm assembly) may need wire cutting. Though this has been minimised due to the expense involved. Many of the drilled holes in the hand, notably those for holding bearings (i.e. linkage holes, bearing housings), will need to be drilled and then reamed to get the necessary tolerances. After the manufacturing many of the sharp outer edges of the fingers and the palm assembly will need to be ground and deburred to give the required rounded edges. The aluminium parts in the hand will also be anodised to give it a protective oxidised layer. It will also make hand more attractive in appearance and reduce problems related to dirt contamination. Since the bearings within the hand move at relatively low speeds and are shielded they will not require oil baths in the design. Some greasing/lubricant may be required around some parts (i.e. perhaps for lead screws or Teflon rollers) but this will be minimal as most of the materials in these situations are self-lubricating or have low friction. Some parts such as the finger's pivot shafts on the top cover plate will need adhesive for attaching within the hand assembly. The wires in the hand will be held in place by RTV silicone sealant.

4.5 Canterbury Finger

The Canterbury finger is a two-degree of freedom multi-bar linkage. There are eight separate sets of linkages attached to the metacarpal block. These linkages are actuated by two vertically stacked DC electric motors in the metacarpal assembly. Each motor is connected to a lead screw via a coupling. A drive nut moves down the lead screw as it rotates. Attached on opposite sides of each drive nut are a pair of actuator links that transmit the motion to the other finger linkages.

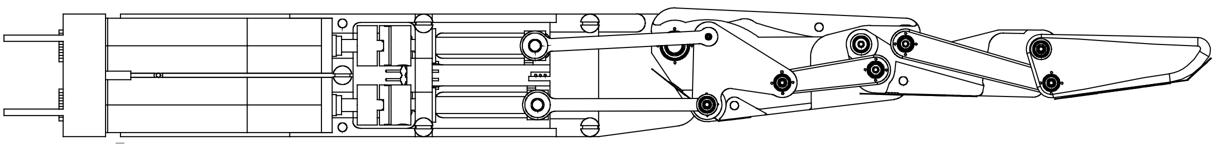

Figure 4.4 Canterbury Finger (showing internal parts)

The finger model had to use both types of motors in the design. The Maxon finger would be stronger (due to the greater torque output of the motor) and heavier due to the larger size of the motor and the finger. The Mini motor finger would be reduced in size due to the smaller size of the motor, and the smaller sized linkage geometry.

There are four types of fingers in the Canterbury Hand. They are the index, middle, ring and little fingers. Each of these fingers has different design properties. For example, the middle finger is attached to the hand by screws, while the other fingers are attached to the finger spreading mechanism. These fingers would require pivot points in the metacarpal blocks and motor end caps that trap the finger spreading nuts for the rotation motion. The middle finger end cap however would only need screw attachment points.

For both the Maxon and Mini finger designs, each finger type would require different linkage bearing joint geometry. This was so the fingers within the hand would look anthropomorphic and have a realistic gripping motion. This would mean that the finger linkage models had to be flexible for different joint geometries.

The design of the hand followed an iterative process. The hand design was modelled at the same time as ideas were embodied into the design. While this eventually gave a better design it unfortunately led to a lot of remodelling. The design also had to follow the general and particular design objectives for the hand. The particular design objectives of the finger are detailed in the next section. After the requirements for the finger were set out the SolidWorks model was started.

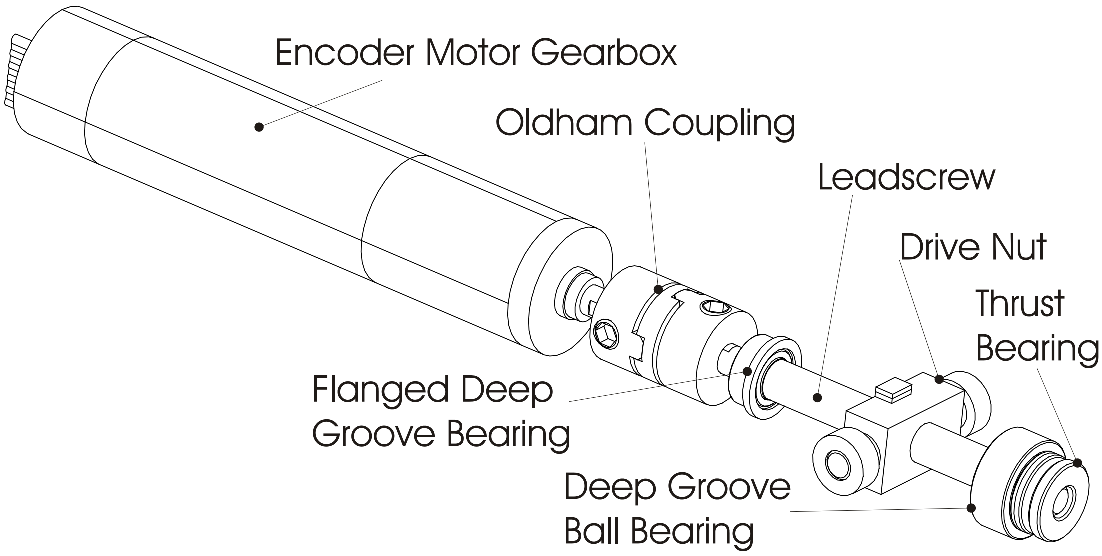

Figure 4.5 Finger Drive Assembly

The design of the drive assembly and how it fit within the metacarpal block assembly was the first design task. The drive assembly had to be made so that the actuator links on the drive nut fit around the support bearings for the screw. The bearings had to be selected so they had a minimum outer diameter while being large enough to support the forces in the lead screw. The metacarpal block was then shaped around the drive assembly. It was designed to be as small a size as possible while keeping the minimum material required for strength, and for fastener attachment. It had to allow for maximum motion of the actuator linkages without interference with the metacarpal block. The metacarpal assembly (and the linkages held within it) was split length ways so that the motors could be clamped in the design. It was decided that Aluminium (Alloy 7070) would be the default material choice for most of the parts within the finger. The reasons for this choice are that Aluminium is easily machinable, conducts heat (from the motors), is reasonably low weight, and has a good strength to weight ratio.

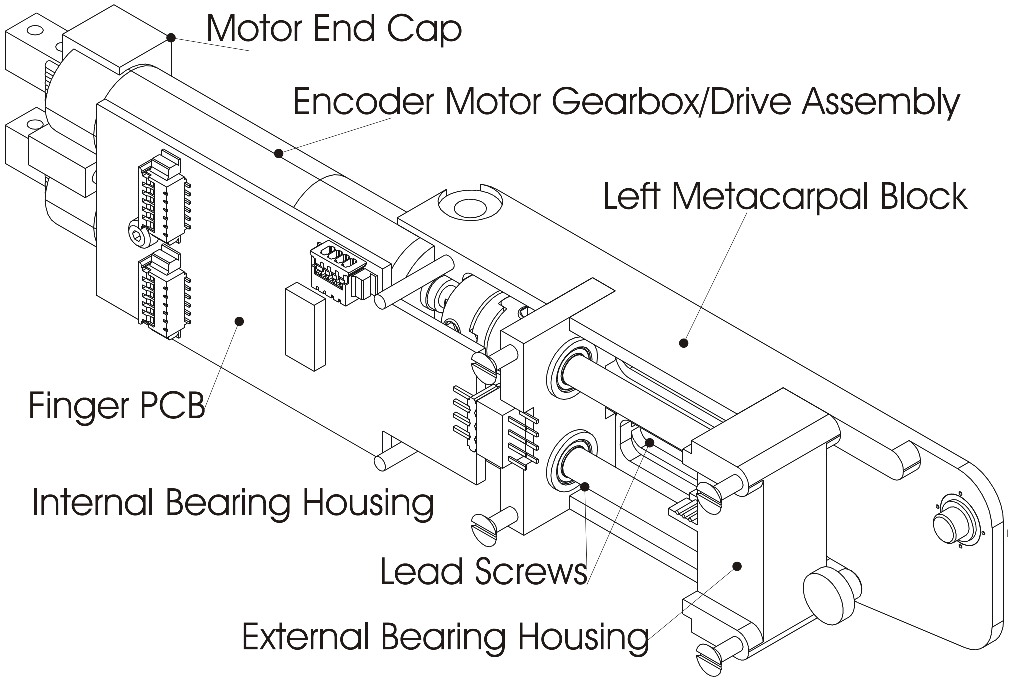

Figure 4.6 Finger Metacarpal Assembly (with Left Metacarpal block removed)

The linkage arrangement was designed next. The linkages had to be assembled within that each linkage phalange in the finger was assembled within the previous linkage. That is the distal link fits within the medial link, which in turn fits within the proximal link. The proximal link in turn assembles within the metacarpal assembly support brackets. The linkages also had to be designed so that the force followed a single path through them. This was to reduce the kind of buckling and misalignment that occurred within the original prototype finger. Certain linkages such as the rocker link for example were reduced to a single part. To help reduce the problems due to misalignment of linkages due to split forces a single common shaft was to be used though the bearing joint positions as much as possible.

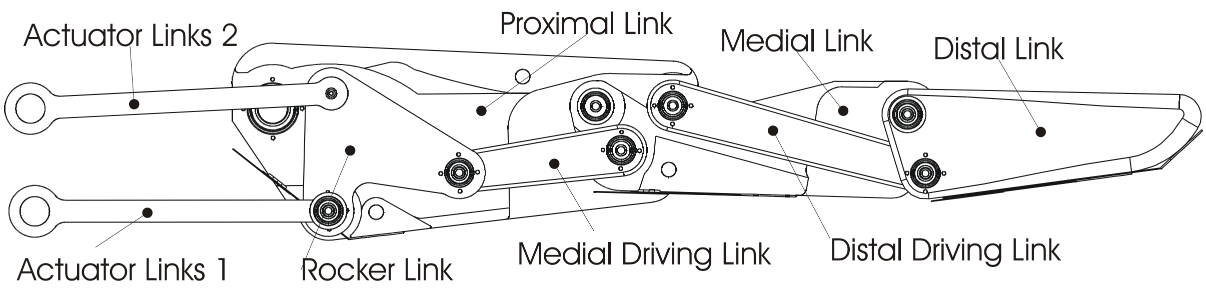

Figure 4.7 Finger Linkages

Once the finger spreading mechanism was designed the metacarpal block had to be remodelled to fit the pivot points for the rotation motion. The end caps also had to be remodelled to locate the spreader mechanism's drive nuts. At this stage the electrical control requirements for the hand had reached a stage that they could be modelled in the design. Force sensing resistors (Part #400 FSRs from Interlink Electronics) were built into the linkage models to measure the grip forces the hand has with an object. For the finger the distal link would have two FSRs while the medial and the proximal link would have a single FSR each. Grip surfaces for mounting the FSRs to the proximal and medial; linkages had to be designed and maximised in size. Circuit boards were designed to fit within the metacarpal blocks to reduce the wires coming into and out of the finger. Without the circuit boards there would have been nineteen wires going out of the finger. With the circuit board this was reduced to only four (possible three) wires. Gaps and travel paths for the wires and connectors between that the sensors and the circuit boards had to be built into the finger model. The wires would have to travel within the finger linkage as much as possible to avoid being pinched between moving parts. The metacarpal block and the internal bearing housing had to be redesigned so that the connector for the circuit board and the FSR and Hall effect wires could be clamped into place.

Finally the finger was redesigned to be as aesthetically pleasing as possible. The gaps between the finger linkages had to be hidden and the finger linkages modified so the shape tapered in appearance. After the design the finger linkage bearing geometry was optimised. This is discussed in detail in the following chapter.

4.5.1 Finger Design Goals

The particular design goals were:

<u>Finger</u>

- Minimise weight & use lightweight materials, but not at expense of weakening design.
- Reduce interferences in motion of hand.
- Aesthetic anthropomorphic design (i.e. reduce gaps visible about linkages).
- Design to be as easily manufacturable as possible (using machines available to the mechanical engineering workshop).
- Finger to be as simple as possible for assembly and disassembly.

- Finger model/design needed to be flexible for different motors and linkage bearing joint geometries.
- Sharp edges to be avoided wherever possible in design.
- Finger should have sufficient grip force of at least 10N.
- Components should be bought in to the design as much as possible to reduce workshop manufacturing time and difficulty.
- The finger should be physically robust to impacts and harsh environments.

Linkages

- Use finger linkage arrangement as originally proposed by Vuskovic and Dunlop.
- Remove circlips from design of finger and thumb linkages. This was due to difficulty in assembly and disassembly of the finger.
- Avoid protruding knuckles in linkage design and in geometry.
- Linkages should be easily assembled. Since the metacarpal block is assembled lengthways so will the linkages.
- Linkages should be assembled within each other so there is a step down effect, i.e. distal linkage within medial linkage. Medial linkage within proximal linkage. Proximal linkage within metacarpal blocks.
- Linkages to be designed so force follows a single path and avoids buckling or misalignment of linkages, i.e. rocker to be a single link unlike original finger prototype.
- A single common shaft to be used for each joint bearings (except bearing joint B5 due to interference of rocker motion and actuator linkages).
- Linkages to be redesigned so they appear more solid. This improves appearance.
- Minimise knuckle widths and heights to improve anthropomorphic appearance.
- Finger linkages to have maximum motion (working area) and output force.
- Surfaces to be designed on finger and thumb for gripping objects and locating FSRs.
- Singularities to be removed from motion of the linkages by the use of stops.
- Since linkages are the most visible part of the finger they should be aesthetically pleasing.
- Linkages should be scaled according to anthropometrics data.
- There should be sufficient width to the proximal, medial and distal linkages to grip objects.

- Bearings for joints should be contained within the finger linkages as much as possible to avoid problems with impact forces and misalignment.
- Joint Bearings should be self-locating in the design (to avoid fiddly assembly/disassembly).
- Bearing joints to be as small as possible to reduce finger size, i.e. miniature ball bearings needed to be sourced from a number of manufacturers.
- Bearings to be shielded to protect them from dirt and other interfering material.
- Fasteners to be flush with side of linkages.
- There should be sufficient clearance between linkages to avoid problems if there is minor buckling. Typically 1mm clearance or greater.

Drive Assembly

- Lead screw in line with a pair of actuator links for linkage motion to avoid jamming.
- Two designs of finger using Maxon and Mini motors within finger in different configurations.
- Lead screw has to be 0.7mm pitch.
- Use a commercial coupling between encoder motor gearbox and lead screw to avoid backlash and forces on motor.
- Coupling size to be minimised for length and diameter.
- Support bearings to be minimised for outer diameter (while still supporting the lead screw forces).
- Drive nut width to be minimised.
- Motor wires to connect to outside circuit board on side of metacarpal block. This is while avoiding having them interfere with the finger spreading mechanism at the motor end cap.
- Low friction between lead screw and drive nut.
- Drive nut and actuator links to be securely located so as to produce linear motion for lead screw.

Metacarpal Block

- Finger spreading pivot points required within finger metacarpals (reduces height).
- Pivot Bearings to be fully within the metacarpal block to reduce height.

- Drive assembly to be fully located so it cannot be pushed out through the rear of the metacarpal block.
- Split design for metacarpal block for clamping drive motors and for easy assembly.
- Minimise size of metacarpal block.
- Metacarpal has most weight in the finger so should be as low weight as possible.
- Fasteners to be flush with side of metacarpal block.
- Actuator linkages to move in metacarpal with minimum interference.
- Metacarpal block one of the most complex parts for finger. It needs to be easily manufactured, i.e. bearing support blocks are added separately to metacarpal assembly.

Electrical Systems, force sensing and finger control

- FSRs to be used in design for measuring grip forces.
- Circuit boards (PSoC chips) and wire routes to be designed into the hand.
- Hall effect switch to be located in metacarpal blocks to locate the drive nut and to zero the encoder.
- Magnets for Hall effect switch to be located on drive nuts.
- Exact clearance required between drive nuts and Hall effect switch without interfering material.
- Wires to be hidden in finger as much as possible, i.e. within metacarpal and finger linkages.
- Wires should avoid being pinched in linkage motion.
- Circuit board to be connected to wires internally in metacarpal block.
- Sufficient area for circuit board in design of metacarpal block.
- Sufficient grip surfaces on bottom of finger linkages for FSRs.
- Output wires to avoid entangling with finger spreading motion.

4.5.2 Metacarpal Assembly

The finger can be broken up into linkage parts and the parts that make up the metacarpal assembly. The metacarpal assembly is defined as the parts that are entirely contained within it. The metacarpal assembly is separated into the drive assembly (encoder motor gearbox, coupling, support bearings lead screw and drive nut), the two metacarpal blocks that hold the drive assembly and the finger linkages in place, and the metacarpal end cap. The electrical and control system (FSRs, connectors, wires, and the finger circuit board) may also be considered as part of the finger metacarpal assembly.

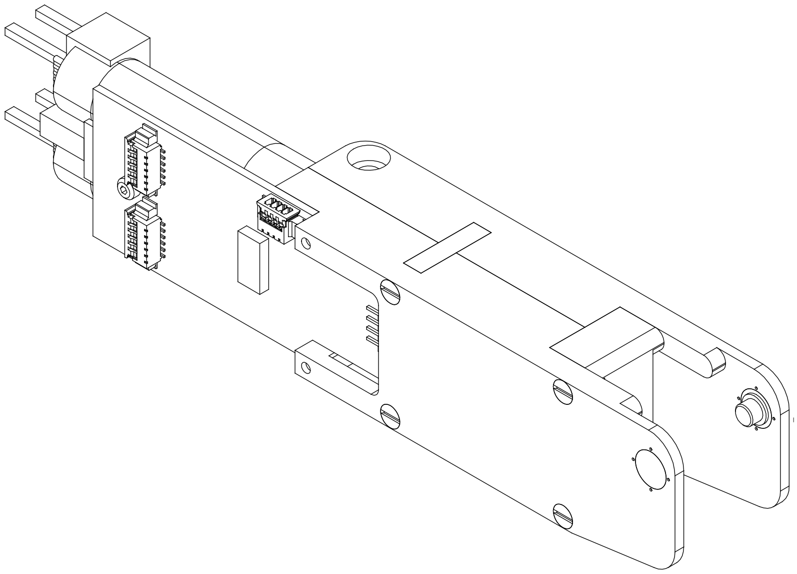

Figure 4.8 Ring Finger's Metacarpal Assembly

The parts of the metacarpal assembly model were designed for simple assembly. The drive assembly is assembled first, with the motor, and the coupling fastened together. The rest of the drive assembly parts (drive nuts, support bearings, and lead screw) are assembled around the internal bearing housing. The wires from the Hall effect switch and the FSRs are positioned around the internal bearing housing. Then the drive assembly and parts are placed within the external bearing block, which is then fastened to the metacarpal block with the circuit board. The two metacarpal blocks are then fastened to either side of the two bearing housings and around the finger linkages

Some design features of the metacarpal assembly are how the motors and the connectors for the circuit board are located. The motors are pinched between the two metacarpal blocks when in assembly. This is to keep them from rotating, and to hold them securely in position. The socket for the motor wires is also trapped within the internal bearing housing and is pressed into place by the metacarpal block. The sides of one of the metacarpal blocks in an assembly are shaped to hold the finger PCB (printed circuit board). The PCB only requires a single screw once it is connected into the socket. The motor end caps that located the motors in place have gaps for the motor output wires to connect to the circuit board's surface mounted 90-degree header.

The finger spreading mechanism can also easily be assembled about the end cap and the pivot point in the metacarpal block. The fingers end cap would first be located about the finger spreading mechanism drive nut. The shaft and the bearings for the pivot point are placed directly in the spaces within the metacarpal block assembly. Then the cover plates would be fastened about the finger trapping the shafts and the finger in place.

4.5.3 Drive Assembly

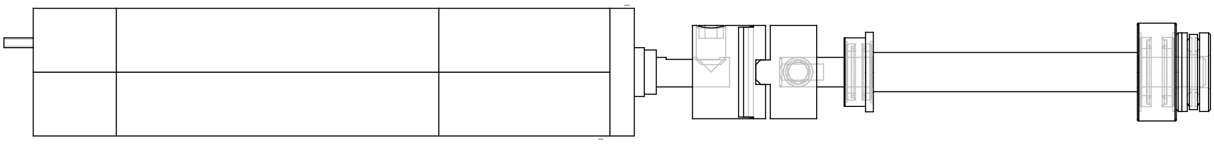

Figure 4.9 Finger Drive Assembly (without Drive Nut)

The drive assembly is made up of the encoder motor gearbox, an Oldham coupling, a drive nut, support bearings and a lead screw. The motor specifications are summarised in the below table.

Table 4.2 Maxon and Mini Encoder Motor Gearbox Specifications

Encoder Motor Gearbox	*Output shaft OD (mm)*	*Size (OD x Length) (mm)*	*Max motor Speed (rpm)*	*Gear Ratio*	*Max (reduced) Torque Out*	*Voltage/ Max. Power*
Mini	2	Ø10x39	18400	16:1	14mNm	6V, 0.46W
Maxon	3	Ø13x65	13300	16.58:1	156mNm	18V 3.86W

The Oldham coupling connects the motor to the lead screw and acts to remove any misalignment between them. It had to be of a diameter smaller than the motor, so it could fit in the metacarpal block. Its length had to be as small as possible so as to reduce the metacarpal length. The bore of the coupling also had to be of the same diameter as the gearbox output shaft. Furthermore the coupling also had to be able to have a torque capacity greater than the maximum output torque from the motor. For the Maxon motor the maximum torque output was 156mNm. For the Minimotor the torque output was 14mNm. The Maximum service torque for the couplings was 100mNm for the Mini coupling, and 450mNm for the Maxon coupling.

Table 4.3 Finger Coupling Data Table

Oldham Coupling Data	*Bore (mm)*	*Size (mm)*	*Max. Torque Service (mNm)*	*Max. Motor Torque (mNm)*
Mini Coupling	2	Ø6.4x12.7length	100	14
Maxon Coupling	3	Ø9.5x12.7length	450	156

The lead screw of each drive assembly is supported on either end by support bearings. The support bearings are located within the bearing housings, which are inserted into the metacarpal block. The motor torque on the lead screw moves the drive nut and the connected actuator links (on either side of the nut) up and down its length. This motion creates axial forces from the interaction of the drive nut on the threaded lead screw, and radial forces from the actuator link, on the bearings. As the finger closes on an object and the motor slows, the axial forces will increase on the front bearings (located closest to the finger). When the finger opens the axial forces will be located on the rear flanged bearing (closest to the motor). Since the motion is unopposed the motor loading will be smaller, and hence the axial forces will be greatly reduced in the flanged bearing. The radial forces on the bearings are the perpendicular reaction forces the actuator links have off the lead screw. This depends on the angle of the actuator link and where it is located. The deep groove bearings in the drive assembly were selected so that there load rating was greater than the worst possible radial loads on the screw for each motor.

Table 4.4 Axial and Radial Force from Lead Screw on Bearings

	Max. Axial Force in Screw (N)	*Thrust Bearing dynamic (N)*	*Approx stall Radial force (N)*	*Deep groove static load rating (N)*	*Flanged bearing dynamic (N)*
Mini	39.5	1790	24.8	630	330
Maxon	440.5	1790	151	630	385

There are greater axial forces on the front support bearing of the drive assembly from the curling and grasping motions of the finger. The front bearings required a thrust ball bearing and a deep groove ball bearing paired together to take the respective axial and radial forces. The reason for this pairing is that they are the only choices available for miniature bearings. The thrust bearing had to have its outside diameter (which is moving) smaller than the outer race diameter (stationary) of the deep groove bearing.

Another factor was the separation of the actuator links and how they had to move past the front deep groove bearing. Their separation determines both the width of the metacarpal assembly and the finger linkages. To make for a smaller finger width and hence a smaller width hand the outer diameter of the deep groove bearing had to be minimised. Since the outer race diameter of this bearing was determined by the thrust-bearing diameter the thrust bearing also had to be minimised in size. The bearings selected for the lead screw can be seen in the below table.

Table 4.5 Finger Lead Screw Bearing Sizes

Bearing size for motor configuration	*Flanged deep groove bearing (Nachi)-mm*	*Thrust bearing (Nachi)- mm*	*Deep Groove bearing (EZO) - mm*
Mini	ID2, OD6, B3	ID3, OD8, B3.5	ID3, OD10, B4
Maxon	ID3, OD7, B3	ID3, OD8, B3.5	ID3, OD10, B4

Key: ID= Shaft Diameter, OD = Outer Diameter, B= Width

The bearings were sized for various factors as well as for their load rating. The rear support bearing was minimised for size to allow fasteners to hold the internal bearing housing within the metacarpal block. It also had to locate the shaft axially so that the rear axial forces from the opening finger were transferred to the bearing housing and not through the coupling to the motor. Due to the space requirements the only bearing that could fulfil these requirements was the flanged deep groove ball bearings from Nachi.

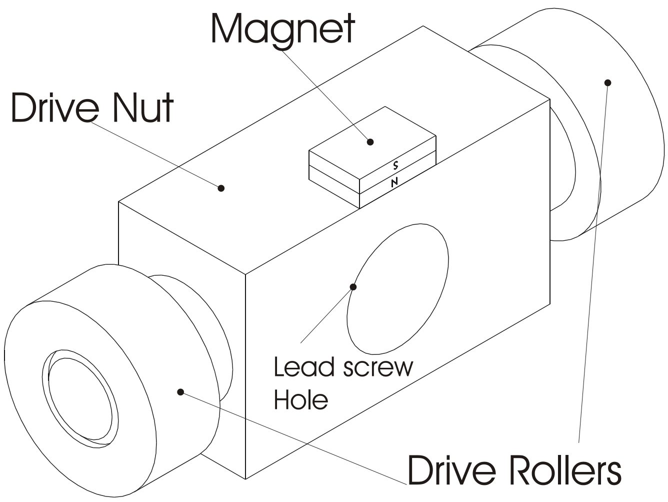

Figure 4.10 Drive Nut Assembly

The bronze drive nut had to be sized so that it was large enough to contain the threaded hole (4mm diameter with 0.7mm pitch) yet minimised in width so that the drive screw length and the metacarpal length could be reduced. The drive nut shape was selected for ease of manufacture and to reduce the number of components for the nut. Its material was selected for its low cost, strength and lubricating properties on the lead screw. The Teflon rollers on either side of the nut were selected because of their low friction between the actuator links, metacarpal and the drive nut. Both drive nut and rollers are easily machined with a minimum number of operations. The drive nut’s height also had to be sized so that the magnet was the correct distance from the Hall effect switch. The Hall effect switch is used for zeroing the encoder for the nuts position. It was found from experiments that the maximum distance for the magnet to take effect was 2mm. However there also had to be enough clearance between the magnet and the Hall effect switch to avoid collision. Thus the magnet was sized for a clearance between 0.75mm and 1.75mm above the Hall effect switch for the Mini and Maxon fingers. A small cut had to be added to the face holding the magnet for Mini motor drive nuts. The reason for this was to keep a minimum clearance for the magnet and the Hall effect switch.

4.5.4 Metacarpal Blocks

The metacarpal block is formed around the drive assembly, the finger linkages and the finger spreading mechanism. It is designed to be simply manufactured and strong enough to handle the forces from the drive assembly and the reaction forces from the finger linkages. However the metacarpal block was previously the heaviest part of the finger its weight had to be minimised. This meant reducing its material to the minimum necessary to locate the parts and to maintain strength. The height and width of the metacarpal block had to be also minimised to reduce the dimensions of the hand assembly. This occasionally meant reducing the clearances about the moving parts (i.e. couplings) to their smallest allowable value. The metacarpal was designed to give minimal material and clearance about the internally moving parts. The size of fasteners was also minimised (to M2 counters sunk screws) to reduce the material and size of the metacarpal block. Since the metacarpal assembly is mostly hidden between the top and palm cover plates of the hand assembly its rearward appearance was not important. However the parts that stuck outside the palm assembly did have to have a pleasing appearance.

The metacarpal block had to hold the two drive assemblies for the finger. The motors were held at the rear of the metacarpal block. The motors are kept from rotating by having a slight interference fit between the metacarpal blocks when they are assembled. Only the first 6.5 mm of the gearbox of the motors are fully gripped between the metacarpal blocks. To the rear of this support the motors are supported only by a thin section of material along their length. The reason for reducing the rear section of the metacarpal block is to reduce its width to improve the finger spread, and to reduce the weight of the metacarpal block. This reduced section for holding the motor is also used for attaching the end cap and the printed circuit board (PCB).

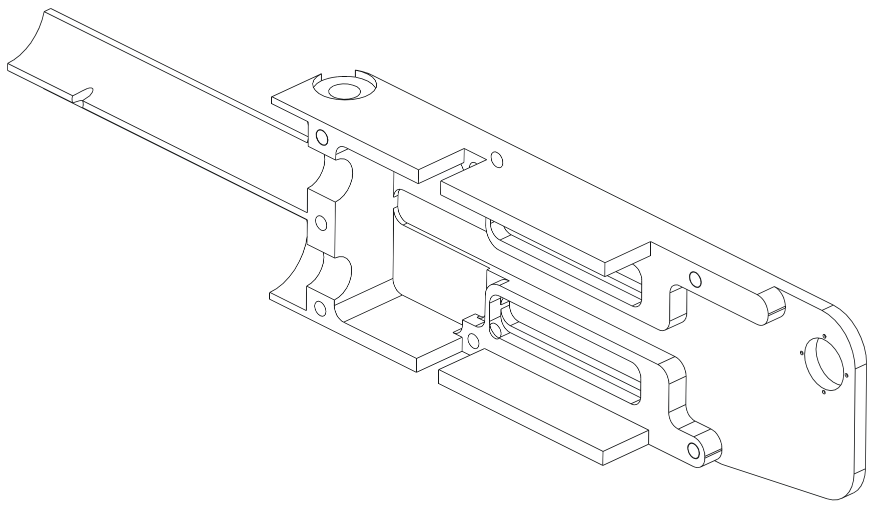

Figure 4.11 Left Metacarpal Block from Ring Finger

As well as gripping the motors there had to be sufficient gap in the metacarpal block to for the couplings to rotate. In the design there is at least 0.75mm clearance between the couplings and the metacarpal block on any particular side. The volume removed around the couplings has been maximised to reduce the weight. The metacarpal block is fastened together through material on either side of the output shaft of the motor. The internal bearing housing that supports the rear flanged deep groove bearings of the lead screw is fastened at the top and bottom of the metacarpal.

On both the left and right hand metacarpal blocks a groove has been machined down the centre of the block in which the wires from the FSRs and the Hall effect block are laid within. This groove enters the metacarpal block from the support bracket and continues through the lead screw volume to open into the coupling space. On either side of this groove behind the couplings is a small shelf that locates the socket (that connects the wires to the PCB). The PCB is attached within a recess on the side of the metacarpal block. The dimensions of this recess has been maximised for the size of the circuit board. It only has the minimum amount of material to locate the fasteners and to hold the socket and the internal bearing housing in place.

The volume surrounding the drive nuts and the lead screw has been hollowed out to provide the maximum clearance for the nuts and to further reduce the weight of the metacarpal block. Beside the drive nuts recesses had been machined into the side of the metacarpal blocks for the rollers of the drive nut to roll within. These were used to keep the drive nuts motion linear down the length of the screw. The recesses also had to have a minimum of material to oppose the torque of the drive screw without yielding.

The support brackets of the metacarpal blocks holds the proximal link of the fingers in place with stub axles at the B5 joint position. There is a large amount of bending stress that can occur at this bearing joint so the support bracket had to have sufficient (2mm) thickness. Since the support bracket lies outside the hand coverings it had to have an aesthetic appearance. The edges were rounded around the external bearing housing to give a softer appearance to the metacarpal block. The support bracket also had to be shaped so that its edges lined up with the extended fingers taper. That is the top edge was parallel to the straight line of the top finger edge, while the bottom edge was linear with the extended finger linkages. A side effect of the shaping of the bracket is that it covers the actuator links coming out of the metacarpal assembly. This gives a degree of protection to the actuator links from side impacts, as well as giving the finger a less robotic appearance. Another aspect of the support bracket was that it had to cover as much of the gap between the proximal link and the external bearing block as possible. The problem with this though was the gap had moving parts within it. A partial solution was to have the top face that supports the external bearing housing extended to act as a shelf covering a portion of the gap between the actuator links and the support bracket.

The pivot shaft location for the finger rotation mechanism had to be added to the metacarpal block. The bearings for this shaft are recessed into the block. The shaft for the rotation axis travels through the metacarpal axis but does not contact the metacarpal directly. Since the motors are located directly down the middle of the metacarpal assembly the bearings had to be recessed to the side of the finger. The location of the pivot point depended on where the finger was located in the hand. The rotation axis for the fingers was located on the side closest to the middle finger. This minimised the offset between the finger spreader drive nuts and the motor end cap guides. The guides for the end caps could be thus have a reduced length and more efficient movement of the finger spreading.

4.5.5 Internal and External Bearing Housings

The housings were designed primarily to hold the support bearings of the drive assembly. Originally the metacarpal block was designed so that it could be manufactured by using drilled holes down its length to hold the bearings. However this would be too difficult to machine due to the accuracy of the tolerance and the excessive length of drill required.

It was easier to manufacture separate inserts that would hold the bearings. These inserts were called the internal and the external bearing housing. The external bearing housing was designed to hold the front deep groove and thrust bearing of the drive assembly. It also had to have enough material (4mm) in front of the bearings to handle the axial force from the lead screws. Spaces on either side were added to allow the actuator links to move past without collision. However the clearance and the distance past the deep groove bearing had to be minimised so as to reduce the width of the metacarpal block. Only 0.5 mm of material around the side of the bearing was allowed for in the design of the external bearing housing. There is only 0.5mm gap for the actuator links to pass by the side of the bearing housing as well.

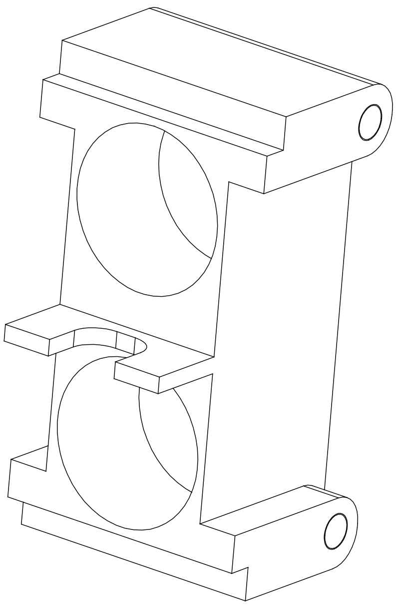

The external bearing housing also had to have a small shelf to locate the Hall effect switch. This shelf had to accurately locate the Hall effect switch under the drive nuts. It also had to have clearance with the drive nuts to avoid collision problems. A gap was machined in the middle of the shelf so that there was no material interference between the magnet and the Hall effect switch. The Hall effect switch is glued on to the housing's shelf for extra stability.

Figure 4.12 External Bearing Housing of the Finger

So that the actuator links had clear motion past the external bearing housing the fasteners had to be located at the top and bottom of the metacarpal block. The fasteners were sized to be as small as possible (M2) so that the metacarpal block's height was minimised. The edges around the fastener (below the actuator links) have been rounded to avoid interference and to improve their appearance. A minimum amount of material was required around the screws so that the holes could securely hold the fasteners. These holes are threaded right through. However since the metacarpal block is made of two halves two sets of two screws are required to hold the block in place on either side within the metacarpal assembly. The screws are sized so that there is no interference between them when they are screwed into a hole on either end of the metacarpal assembly. The bearing housing is further machined to a tolerance on either side so that will fit between the two metacarpal blocks without causing distortion between them.

The internal bearing housing was created to hold the flanged deep groove bearings of the top and bottom drive assemblies. The face that the flange rests against has to be machined flat and perpendicular to the holes. There also had to be a minimum clearance (of 1mm) between it and the rotating coupling.

The internal bearing housing had to have a gap machined in its middle to hold the socket for the FSR and Hall effect switch wires of the finger. This socket would be clamped in place between the housing and the metacarpal block. It shall also securely hold the socket vertically on either side. The pin header (soldered to the finger CB) would fit into the socket to connect the wires to the circuit board. If the clamping effect on the socket is strong enough the act of removing or adding the circuit board to the metacarpal should not dislodge the socket. A gap of the same size is also machined on the other side of the internal bearing housing to the socket. The reason for this is to make the internal bearing housings (like the external bearing block) interchangeable for different fingers, where the socket and the circuit board may be located on the opposite side of the metacarpal assembly.

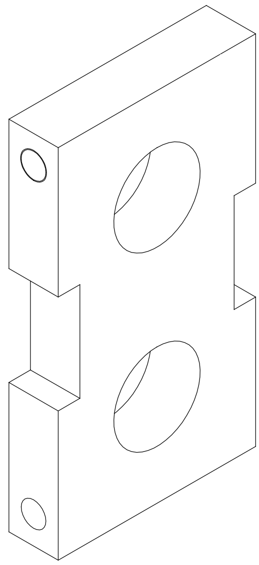

Figure 4.13 Internal Bearing Housing of the Finger

4.5.6 Motor End Cap

The motor end cap is attached to the rear of the finger metacarpal block assembly by two counter sunk machine screws. These go into holes located on either side and between the two finger motors. The main function of the end cap is to hold the motors in place within the metacarpal assembly to prevent them from being pushed out the back. They also have to allow the wires from the motors through them to connect to the finger PCB. Gaps were added to their design that allowed the wires to come out of the side of the block.

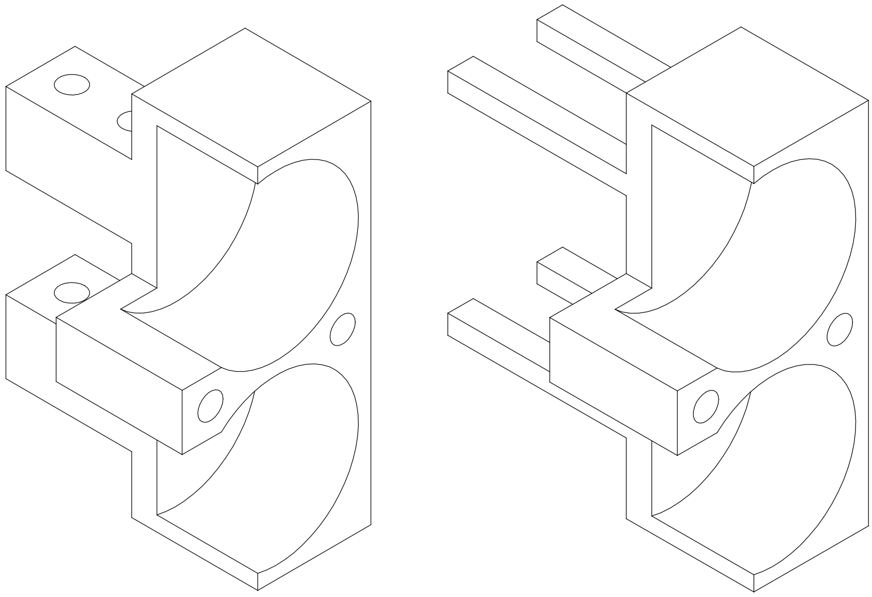

Figure 4.14 Middle and Little Finger End caps

Most of the motor end caps in the hand assembly are different from one another. The index fingers end cap has the wire gaps on the opposite side to the little and ring fingers end cap. The reason for this is that the PCBs are on opposite sides for these fingers and the motors are orientated so the wires come out on the opposite side. The guides on the end caps that trap the finger spreader drive nuts are placed so that the drive nuts are located away from the outer sides of the hand assembly. This choice of placement reduces the hand width.

The middle finger end cap has been designed so that it is fastened in the palm assembly by two pairs of screws behind the motor. One pair of screws attaches the end cap to the palm cover plate, and the other pair connects it to the top cover plate. There is a gap at the rear of end cap between the attachment bosses. This gap prevents collision with the rotating spur gear of the finger spreader mechanism.

All the end caps were sized to give the minimum amount of material around the motors for their height, width and length. The height had to be reduced to at least the height of the metacarpal block for clearance between the palm and top hand cover plates. The width of the end cap is a limitation on how far the fingers can spread before collision occurs between them on their outer rear edges. If the length of the end cap is increased it in effect increases the length of the metacarpal assembly, and hence the hand is lengthened. Another effect of reducing the end cap dimensions is to reduce its weight. The aesthetic appearance was not an issue for the end cap design, as it cannot be seen when it is in the hand assembly. The motor end cap of the finger may need to be made of a stronger material (such as stronger grade of steel) as the spreader guides could possibly break under loading.

4.5.7 Finger Linkages

The finger linkages may be considered as the external moving parts of the finger. The top and bottom actuator are the first links in the finger as they transmit the force from the drive assembly to the linkages. The proximal link, rocker link, medial driving link, medial link, distal driving link and the distal link (at the far end) make up the rest of the finger linkages.

The linkage design had to embody the objectives for the finger. Briefly these were that the fingers actuation forces followed a single path and used a single common shaft at the bearing joints where possible to avoid buckling. The rocker, medial driving, and the distal driving links were all reduced to a single linkage. This meant the forces for the curling motion were not split down the linkages, which could lead to unbalanced motions. However this also meant that they would have to have a single shaft to hold them in place. This was difficult to implement as the shafts often passed through components or had components move through them. Having the distal link located within the medial link, and having the medial link located within the proximal link solved this problem. The shafts for the bearing joints did not interfere with the linkages in this hierarchical arrangement except for bearing joints B5 and B8. The B5 joint located the proximal link on the metacarpal block. The problem with having a common shaft through this position was that the rocker and actuator links would collide with it. The only solution was to split the shaft into two stub axles for this bearing joint. The shaft for the B8 bearing joint’s problem was that for certain geometries it passed through the medial link. These geometries could not be avoided, as they were the only ones that avoided the knuckling effect at the B8 joint. By designing a depression for the B8 bearing’s shaft into the medial link this problem was avoided. The strength of the linkages is another important quality in their design. Since the bearing forces increase as the finger gets closer to the singularity position, there has to be sufficient material to prevent fracture. It was decided that 2mm of material around the bearings would be sufficient for the bearing sizes selected for use in the finger linkages.

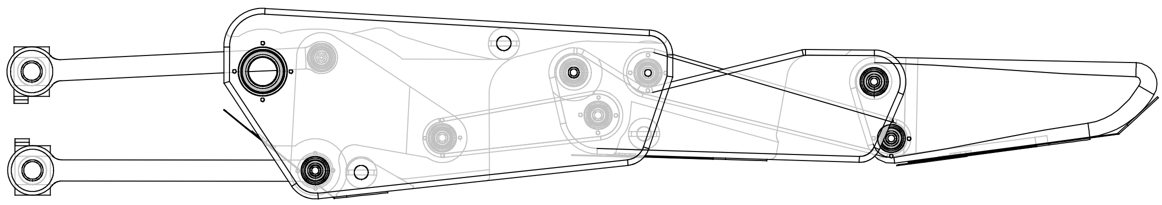

Figure 4.15 Finger Linkages showing hidden internal components

Other objectives that were implemented in the linkage design were the avoidance of interferences and singularities in the motion of the finger linkages. The linkages were designed so that there are gaps within them to allow the motion of internally moving linkages. An example of this is the medial link that has gaps at the B9 bearing joint for the rotation of the distal driving link. It also has a recess for the resting position for the extended distal driving link. The singularities to avoid were the L1 (top actuator) link and L3 (part of the rocker) link singularity in the finger rotation motion, and the L14 (medial driving) link and L17 (part of distal) links in the curling motion. The rotation motion singularity was avoided by adding a stop in the proximal link that halts the rocker link before the singularity can occur. The curling motion singularity was avoided by adding a stop in the medial link that halts the distal link from reaching its singularity. The geometry of the finger had not been fixed during the design process. The spaces for the moving linkages and the position of the singularity stops had to be change with the geometry. The flexibility of the linkage models was implemented within the CAD design of the finger linkages. The results of this can be read in Chapter 6: 'Optimisation of the Canterbury Hand'.

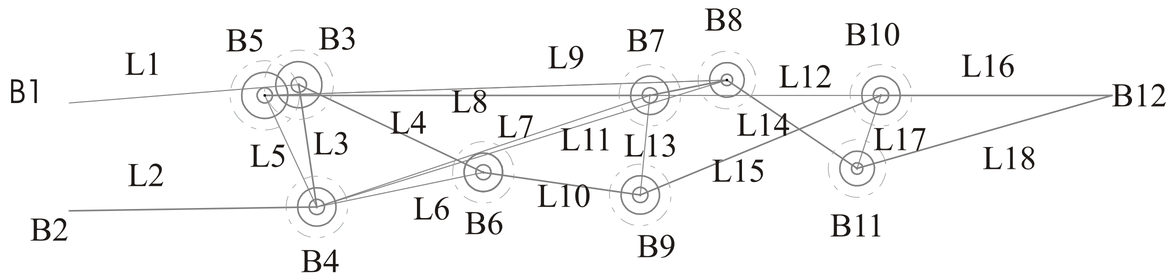

Figure 4.16 Finger Naming Scheme

Clearances were designed into the linkage design to avoid interference between moving joints. The size of the clearances between the metacarpal, and the proximal, and between the medial and the proximal links was minimised to 0.5mm to reduce the width of the finger. The rotation of the rocker through the bottom of the proximal link had a minimal clearance of

1mm between the sides of rocker and the proximal link. The reason for this minimal clearance was so the grip surface under the proximal link was maximised. The clearances within the finger links also had to include space for the wires connected to the FSRs.

One of the more important objectives when designing the finger linkages was to make them as anthropomorphic and solid in appearance as possible. This meant hiding the gaps between the links as much as possible over the fingers motion. The medial and proximal linkages also had the area of their bottom surfaces maximised to give better grip for objects and to hide the internal motions of the linkages. The edges around the linkages will be filleted by grinding to give the finger a softer appearance.

The process of assembling the finger linkages had to be simplified from the prototype design. For that reason finger linkages were designed so that fasteners held the linkages together. They were to take the place of the circlips, which made the prototype fingers' assembly so difficult and time consuming. Locating features were also added to the finger linkages so that assembly would be simplified. An example of this is the raised shoulders on the shafts that are used to locate the joint bearings and the linkages.

The linkages are assembled from the furthest linkage first and then backwards towards the metacarpal block. Due to the manufacture of the components the medial driving link is permanently attached to the rocker link, and the distal driving link is permanently attached to the distal link. The medial link would be fastened first around the distal link and the medial driving link. Then the actuator links would be attached to the rocker link. The top actuator links have an interference fit on the B3 bearing joint shaft in the rocker. Lastly the proximal link assembly would be put together around these links. Finally the metacarpal block would enclose the Proximal link one either side. Connecting the stub axle though the proximal links B5 bearing would complete this enclosure.

4.5.8 Distal link

The distal link is the furthest link away from the metacarpal of the finger and was shaped to resemble the human fingers distal phalange. Its underside in particular was curved to resemble the fingertip. Two force sensing resistors (FSRs) are added to this grip surface for measuring the forces on the fingertip. The distal link would be the principal link used for touching an object directly. That is why it has two FSRs are attached to it instead of only one like the medial and the proximal links. A small recess was added in the distal link to hide the connecting tails and the wires behind the FSR's active area. The wires for these FSRs would go back into the medial link through the distal driving link recess (on either side of the link).

The width of the distal link was considered. Due to the limitations of the available miniature bearings for the drive support the minimum width of the finger was found to be 11mm. This was considered as being sufficient for the hand. If the distal link were to be increased it would also increase the width of the metacarpal block and hence the hand.

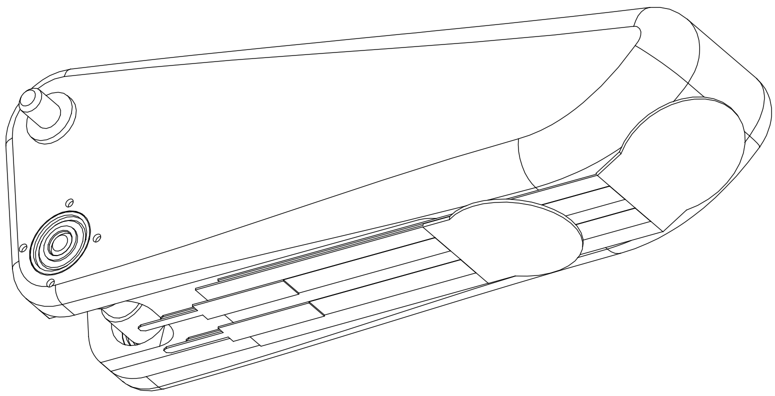

Figure 4.17 Finger Distal Link

The distal link is assembled between the medial links at the B10 joint position. It is gripped at this position on either side by the flanged deep groove bearing located in the medial link. The distal link also contains the B11 joint bearings. These bearings, its shaft, spacers, and the distal driving link are permanently located within the distal link. The reason for this was for ease of manufacture. It is kept in place by deformations of the metal around the bearings outer race. The effect of this is that the deformations cause the metal to form a lip over the bearings, so holding and locating them permanently within the link.

The distal link also contains a gap between B11 and B10 bearings to allow for the motion of the distal driving link through the distal link when the finger curls. The clearance for this gap is small so as to improve the distal links appearance. The outside edges around the distal link are filleted by grinding, to give it a smoother more human appearance. This may make gripping for the hand easier, as it gives more angled faces for the distal link to hold an object against.

4.5.9 Distal driving link

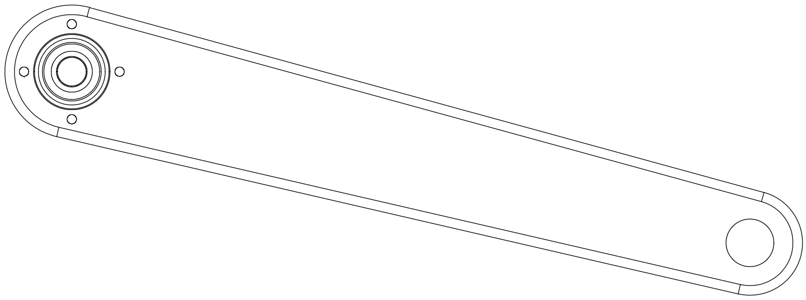

Figure 4.18 Finger's Distal Driving Link

The distal driving link in the Canterbury finger design has been reduced to a single link. This link is located permanently in the distal link to simplify the manufacturing of the finger. The distal link also permanently has located within it a deep groove bearing at the B8 bearing joint position. This joint is used to rotate the distal driving link from the proximal link. The bearing is held in place by deformations on either side of the distal driving link around the bearing's outer race to prevent. This keeps the bearing from sliding out of the link. It also means that the width of the distal driving link is dependent on the width of the selected bearing. The distal driving link's B8 bearing is gripped on either side by spacers that are located in the proximal link assembly. It rotates on a floating shaft that is trapped between the left and right proximal links. The edges of the distal driving link have been filleted to give it a more aesthetic appearance. When the finger is curled and the distal driving link is fully exposed its appearance is more noticeable.

4.5.10 Medial link

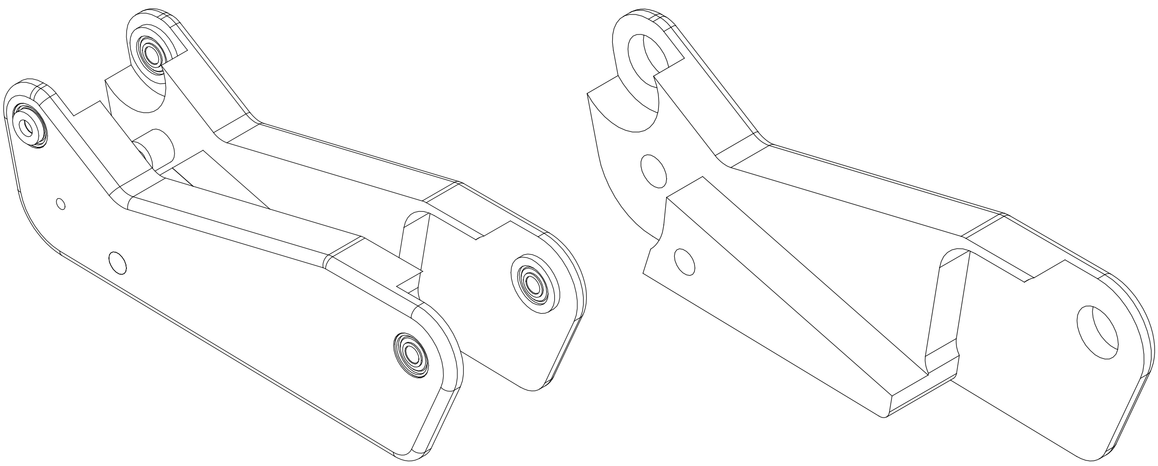

Figure 4.19 Medial Link Assembly and Left Medial Link of Finger

The medial link is the middle linkage between the distal and proximal link. It holds the distal link between a pair of brackets at the B10 bearing joint. It also holds the medial driving link within a recess at the B9 bearing joint position. This same recess contains the shaft, and flanged bearings of the B7 bearing joint. The distal driving link rests within another recess along the top and through the medial link. The two halves of the medial link that form the medial link assembly are located by the shafts of the B7, B9 and B10 bearings. A single counter sunk M2 screw fastens the two halves of the medial link together. The only material available for this screw is located between the two recesses through the bottom middle of the of the medial link assembly.

The B10 bearing is located on the shaft through the distal link by a pair of flanged deep groove bearings. The flange is located on the inside face of the medial link so that the bearings do not slip out. The medial link assembly locates the medial driving link at the B9 joint position by a pair of self-locating spacers. These are held within holes in the medial links. The B9 bearing in the medial driving link rotates on a floating shaft held between the proximal links. The medial link assembly is held between the left and right proximal links at the B7 bearing joint. The rotation occurs on flanged deep groove bearings located on the inside faces within the medial link. The shaft that these bearings rotate upon is held within the medial link assembly. The proximal links grips this shaft on either end when it is assembled.

The medial link assembly has a grip surface on its underside upon which an FSR is mounted. The wires from this run past the medial driving link and join up with the FSR wires from the distal link. The distal link wires run through the distal driving link recess within the medial link assembly. Both sets of wires run past the B7 shaft (which is stationary relative to the proximal link) into the proximal link assembly.

The medial link was tapered so that it lines up with the proximal and the distal link. Its outside edges were filleted to increase its aesthetic appeal. The top outline of the medial link is dependent on the location of the B8 bearing shaft that connects the distal driving link to the proximal link assembly. If the bearing shaft is located outside the medial link it has no effect on the shape of the medial link. In this case it has straight top edge between the B7 and B10 bearings. If however the shaft is located so that it interferes with this line a recess has been designed to occur within the medial link's CAD model (see Chapter 3: 'The Canterbury Hand

CAD Model'). As long as this recess does not occur too far down in the medial link it should not affect the strength of the link.

A gap is visible from above the finger between the medial link assembly and the distal link. It is used to rotate the distal link into when the finger curls. However this gap reduces the solid appearance of the finger. To reduce its size two covers have been added to the top of the medial link over the gap. There is a space between the covers that allows the distal driving link to move past. On the surface facing the gap, a stop has been added. It halts the distal link before it can form the singularity between the L14 (distal driving) link and the L17 (part of the distal) link.

4.5.11 Medial Driving link

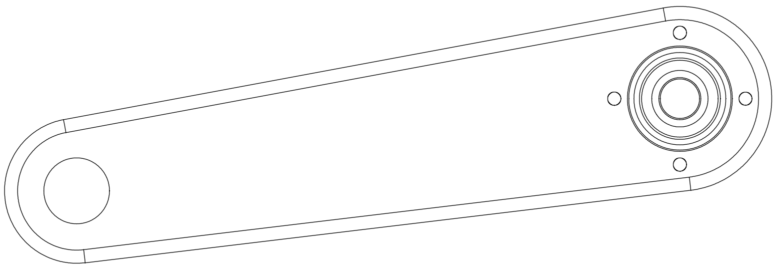

Figure 4.20 Finger's Medial Driving Link

The medial driving link connects the rocker link to the medial link. It has been reduced to a single link (like the distal driving link) to avoid misalignment problems from the splitting of the forces from the rocker. It is held in place within the Rocker link at the B6 bearing joint position. This was accomplished by holding it and its shaft between two deep groove bearings on either side in the rocker link. The bearings (and hence the medial driving link) are held in place by deforming the material around the bearings outer race. The reason for doing this as it simplifies the manufacture of the rocker link. Instead of having the rocker link in two halves, with locating features, and held together with screws it can now be made from a single part.

The B9 bearing is a deep groove bearing located within the medial driving link. It is located permanently within the medial driving link using the deformation method of holding bearings. Since the deformations around the bearings outer race occur on both sides of the medial driving link the width of the link is driven by the width of the specified bearing. This bearing is assembled within the medial driving link by locating it on a shaft between two spacers. The spacers and the shaft are located within the B9 hole features in the right hand and left hand medial links.

The medial driving link though mostly hidden within the proximal link, is visible from the bottom of the finger. Since it is viewable its outer edges have been rounded to give it a softer appearance.

4.5.12 Rocker link

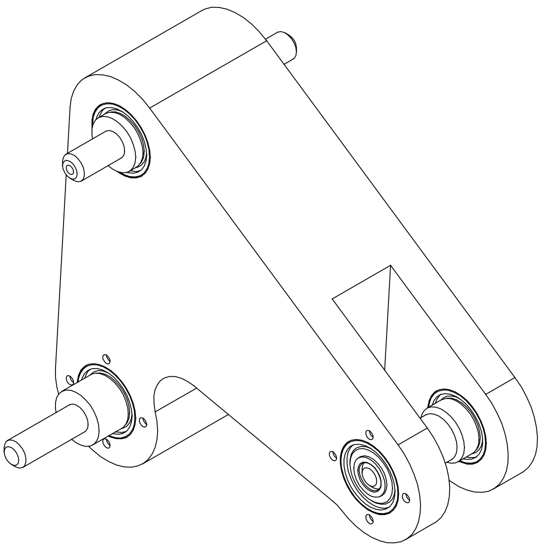

The rocker link is used to transmit the forces and the motions from the actuator links to the rest of the finger linkages. It does this for both the curling and the rotation motions of the finger. It rotates forward and backwards upon the B4 joint bearings connected within the proximal link assembly. Its motion depends on the motion on the within the proximal link assembly.

Figure 4.21 Rocker Link

The rocker link had to have its bearings arranged so that either it or the attached links rotated for the motion. Since the rocker was to be reduced to a single linkage it was simpler to manufacture. The initial design of the rocker was split it in two so that the bearings could be enclosed when it was assembled. This design was far too complicated for the simple link and required a lot of machining to produce the locating surfaces and the threaded holes. It was decided that the rocker would have to be made from only a single piece of material. The placing and retaining of the bearings within the rocker then became the focus of the design. Various ideas for attaching the actuator and the medial driving links to the rocker were looked at. These included using fasteners (screws, grub screws, and pins) through the shafts of the bearings, using circlips, glues/adhesives and even welding. Most of these ideas were impractical or made the rocker unable to be disassembled from the attached links. The use of fasteners had problems due to the severe space constraints the rocker had for motion within the proximal link. If fasteners were added to the shafts they would have to increase the width of the rocker or the bearings holding the shafts would have to be large sized. This would force the proximal link and the rest of the hand wider or it would make the rocker too large to rotate within the proximal link.

Several methods for attaching the links were decided upon. Firstly the bearings for the rocker would be located internally within the rocker link. The reason for this was that they would be protected from external impacts, causing misalignment, and from dirt that fouls the bearings and prevents them from rotating. (It should also be noted that these bearings and the bearings for all the rest of the hand are shielded to protect them from foreign material.) The bearings for the B6 and B4 joints would be permanently located within the rocker by deforming the material around their outer race. A ball peen hammer and a dot punch would create the deformations around the bearing. By doing this, the shafts and the medial driving link would be fully located and trapped within the rocker. For the B4 bearing each of the bottom actuator links would be fitted on the shaft between two spacers so it could not move. Instead of the shaft rotating within the actuator link, it would have the rocker rotate about the shaft.

The B3 joint is manufactured differently. The top actuator links had to attach on either side of the rocker. There was only a 0.5mm clearance between them and the proximal link. To keep this clearance at this minimum it was decided that the actuator links would have a light push fit (H7-k6) on either end of the shaft. The bearings that rotate on the shaft would be positioned within the rocker by a locating edge. For disassembly of this joint all that would be necessary would be to knock the shaft through the bearings (and the clamped rocker link) using a small hammer and a dot punch.

Other design features of the rocker link include space for the proximal links stop and a space for the medial link. A recess between the B6 joint bearings was added to the rocker so that the medial driving link could move within the rocker for its full motion. A clearance of 1mm between the rocker and the medial driving link was added to make sure there is no interference.

A profile cut removed material along the line of the L6 link within the rocker. The reason for this cut was to allow room for the stop that lies between the proximal links. As the rocker rotates forward for the rotation motion of the finger a singularity can occur between the L1 (top actuator) link and the L3 (part of the rocker) link. The rocker is halted by the stop before this position can occur.

Overall the rocker link has been minimised for size and width. It locates all the bearings necessary for its rotation within itself. It can be removed from the finger linkages with only a small amount of difficulty and it is relatively simple to manufacture.

4.5.13 Proximal link

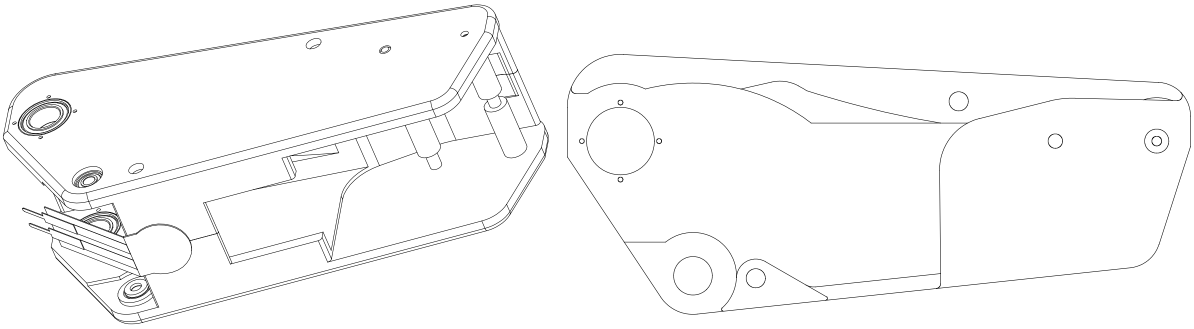

Figure 4.22 Finger's Proximal Link Assembly and Left Hand Proximal Link

The proximal link is the finger linkage closest to the metacarpal block. It is split in two halves lengthwise and is assembled around the other finger linkages. The metacarpal is then assembled around the proximal link.

The proximal link acts as the base that the medial and distal finger linkages rotate upon in the fingers curling motion. The proximal link rotates in the finger rotation motion about the B5 bearing joints. This rotation motion is actuated from the bottom actuator links in the finger. A stub axle that connects the proximal link to the metacarpal block protects the B5 bearing joints from outside interferences. The bearings are located on the other side within the proximal link. They are kept within the proximal links by deformations around their outer race.

The B7 and B8 shafts from the medial and the distal driving links connect directly onto the proximal link. Since the B8 shaft is not fixed it had to have limits placed within the proximal link. Making the diameter of the B9 shaft larger than the proximal link's guide hole did this. The B7 shaft is located within the proximal link by a light push fit (H7-k6). This keeps the shaft stationary allowing the medial link to rotate on the B7 flanged bearings.

The B4 bearing shaft (connecting the rocker to the bottom actuator links) rotates within the proximal link between two flanged deep groove bearings. The flange on these bearings locates and holds the bearings within the two halves of the proximal link assembly. The two halves are held together by two counter sunk screws in the top and the bottom of the proximal link assembly. The reason for using fasteners was to reduce the complexity in putting the proximal linkage assembly together.

The proximal link had to be designed to contain these two fasteners. Unfortunately since the proximal link is the finger link furthest outside it has both the top and the bottom pair of actuator links, the rocker link, the medial driving link, the distal driving link, and the medial link rotating within it. There is not a lot of material left within the proximal to contain any fasteners. Instead it was decided to create space by adding a layer of material above the proximal link. This has the added benefit of covering the top of the proximal link, protecting and hiding the rocker, and the medial/distal driving links and giving the finger a more solid appearance. The best space available above the linkages was between the medial link and the medial driving link at the maximum curl position. At this point there is a small gap that material could be added into. The fastener still has to have a minimum size so an M2 counter sunk machine screw was used. The height of the proximal link had to be kept to a minimum so as to keep it to the same proportions as the other finger linkages. To reduce this effect the top and bottom of the proximal link is tapered inwards toward the distal link. This makes it appear smaller towards the end of the finger giving it an anthropomorphic appearance. To reduce the blocky effect of the proximal link the outside edges have been filleted to soften their appearance.

The second fasteners still had to be added to fully locate the proximal link. To balance the position of the top link it had to be positioned along the bottom surface of the proximal link. The only place available for this was to create a hole within the rocker link for the material for the fastener. Like the top fastener a counter sunk M2 machine screw is used. This material was also useful as a stop for the rocker link to prevent the linkages from forming a singularity between the L1 (top actuator) link and the L3 (part of the rocker) link. The bottom surface of this stop is used to mount the proximal link’s FSR for measuring grip forces. To increase the bottom grip surface of the proximal link assembly the material of the stop was extended around the gaps either side of the rocker link. This material extended to just before the maximum curl position of the medial link within the proximal link.

As mentioned before a number of linkages move within the proximal link. This meant that the material within the proximal link had to be hollowed out to allow for the motion of these linkages. However the gap also serves to allow the wires from the FSRs to travel into the metacarpal block. The wires from the distal and medial FSRs comes out at the B7 linkage position. These wires go through the inside of the proximal link where they join up with the wires from the proximal link's FSR. The proximal links FSR have been curled around the front of the stop so that they go past the rocker link and down the stop. The wires then go out of the back of the proximal link down below the B5 joint. There is some slack in the wires to allow for motion of the finger. A wire groove may be added to the inside face of the support bracket of the metacarpal blocks to allow for the wires to move past the rotating proximal link, or the wires may hang in mid air until they connect to the external bearing block. Whichever method is used the wires will enter the metacarpal block through the wire gap on the inside of the metacarpal block.

4.5.14 Actuator links 1 and 2

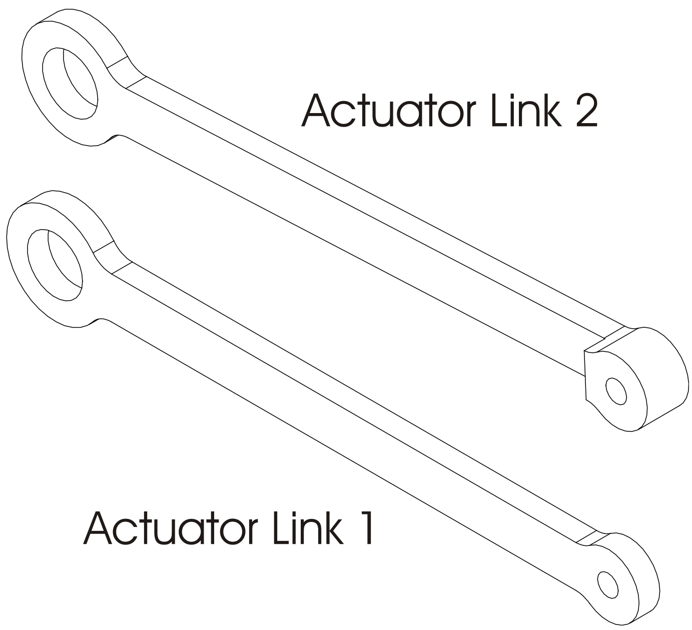

Figure 4.23 Actuator Links 1 and 2 of the Finger

The actuator links transmit the motion/force from the drive nuts in the drive assembly to the rest of the finger linkages. There are two links on either side of each drive nut and these connect to the rocker link. The actuator links are located between the drive nut and the rollers. The actuator links maximum motion for the finger determines the length of the lead screws, and hence the metacarpal block.

There is an easy running fit (H9-e9 hole basis system) between the hole in the rocker link and the shaft of the drive nut. This allows the rocker links to rotate on the drive nut when they move. The actuators are located between the rollers and the drive nut within the drive nut assembly. The rollers are made of Teflon to reduce the friction and the wear and tear on the aluminium actuator links. The drive nut is also made of a wearable bronze material that should reduce the friction in the actuators motion. However since there is only a small clearance of 0.5mm between the actuator links and the surfaces of the external bearing block and the metacarpal block the actuator needs to be located securely and accurately within the drive nut. There should be some small pressure applied across the drive nut from the left hand and right hand metacarpal blocks when they are assembled on either side of the nut. Since there is a large amount of force transmitted to the actuator links the edges between the connection holes and the length of the link is rounded to avoid a stress concentration factor.

After the connection features the length of the actuator link is reduced in height to 3mm. This means that the external bearing block does not have to be so large in height to avoid collision between its top and bottom screw holding features, and the actuator links.

The original width of the actuator links for the prototype finger made by Ward was 1mm. The reason for such a small width was that the linkages are under tension when the finger curls and is under its highest loading. When the finger opens the linkages are under compression, but under a much lower loading, so buckling does not occur. On inspection of the prototype finger it was apparent that some small amount of buckling had already occurred. This probably had occurred either during the assembly and disassembly of the finger, or from the unbalanced forces from the pair of medial driving links at the B6 position in the rocker link. To avoid this potential problem it was decided that for the actuator linkages designed for the hands in this thesis the widths would be increased to 1.5mm. This was a prudent decision due to the larger forces involved within the Maxon actuated hand.

The top actuator links (actuator link 2) are slightly different in how they connect to the rocker link than the bottom actuator links (actuator link 1). The top actuator links has a boss on the end. The reason for this extra material is that a light push fit (H7-k6) is needed to hold the actuator link to the B3 bearing joint’s shaft. This method for attaching the top actuator links was necessary due to size restrictions. The diameter of the B4 bearing shaft could not be enlarged to support a fastener as the rocker had to fit within the proximal link. There was also no room to fit a circlip, pin or a grub screw as there is minimal clearance (of 0.5mm) between the actuator link and the inside surfaces of the proximal link. The only reasonable alternative was either using an adhesive or to fit it onto the rocker. An adhesive would be too difficult to easily disassemble the finger as is wanted in the objectives.

The bottom link does not have a boss for its connection feature to the rocker. Instead it is located on the B4 bearing joint shaft between two spacers. On the B3 and B4 shafts the actuator links are stationary with the shafts. Instead the rocker link rotates about internally located bearings.

To avoid causing stress problems the actuator links are not rounded like the other linkages. They are also less visible behind the metacarpal support bracket and much smaller sized than other linkages. Due to their reduced profile and susceptibility to buckling there aesthetic appearance was judged not to matter.

4.6 Canterbury Thumb

The Canterbury thumb is a one-degree of freedom multi-bar linkage. It is much simpler than the finger linkage in its motion as it only has four sets of linkages connected to the metacarpal assembly.

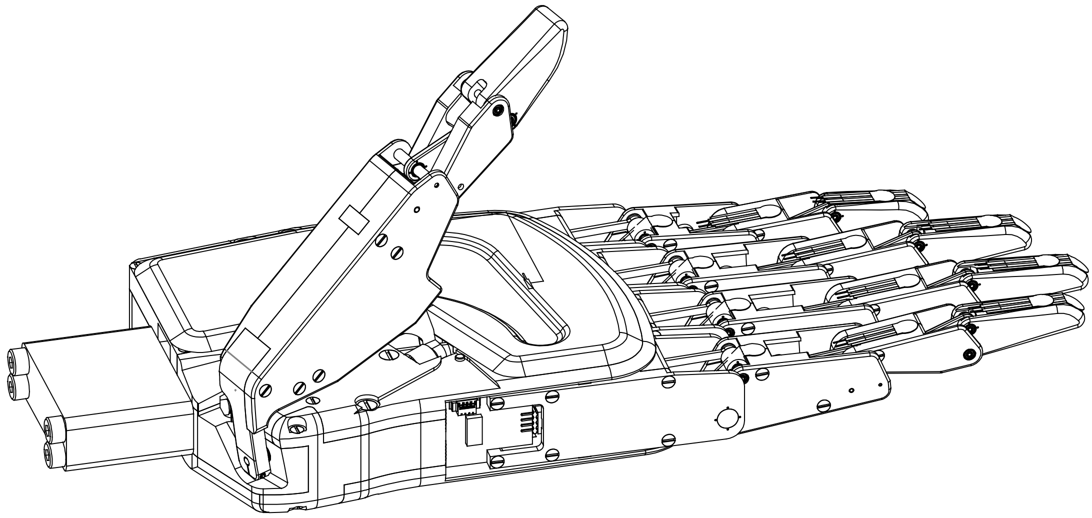

Figure 4.24 Thumb in the Hand design

A single motor actuates the thumb, which is located above the lead screw. The torque from the motor is transmitted to the lead screw by spur gears with a 1:1 ratio. As the lead screw rotates it causes the drive nut to move along it. On either side of the drive nut are the thumb’s actuator links that transmit the motion and the force from the drive assembly to the proximal link. The proximal link rotates on the metacarpal block and is connected to the distal link causing it to rotate as well. The end motion of the thumb is a human like curl.

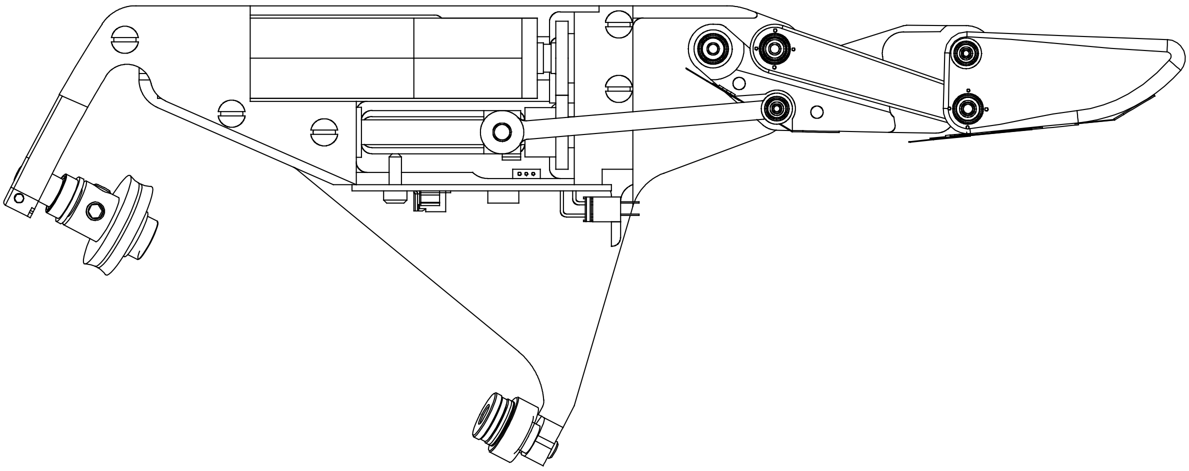

Figure 4.25 Internal Parts within the Canterbury Thumb

The thumb also rotates about the palm. The thumb rotation mechanism is a worm-worm gear mechanism located within the palm of the hand. The rotation axis within the thumb is located in three dimensions. The worm gear is attached to the rear strut of the motor end cap, and it rotated along the axis, with the front support bearings. The font support bearings are located and angled on the front strut of the thumb's metacarpal block. The front support bearings are located within the bearing holder in the hand assembly located between the middle and the index finger's metacarpal blocks.

The original idea for the arrangement of the thumb curl linkages came from Bain [1997]. Bain had used the GA program to create bearing geometries with these linkages. However the thumb had never been previously parametrically modelled. The design of the thumb and its sizing was dependent on the rest of the hand design. Because of this dependence the result of Bain's geometry was no longer applicable.

As part of the brief for this project the CAD model had to use the Mini and the Maxon motors for two different thumb configurations. Since there is only one thumb in each hand only a single bearing geometry for the linkages was necessary for each configuration. Due to the Maxon hand being longer than the Mini motor hand design the thumb linkages had to be longer for the Maxon geometry.

The objectives for the thumb design were less well defined at the beginning of the design than they were for the Canterbury Finger design. This was because the thumb design had not been previously attempted so a lot of the design issues were initially unknown. The design process was iterative and as ideas were found they were modelled in the design. At the beginning of the design for example it was unknown what the thumb rotation mechanism was going to be. It was also unknown how the motor was going to be orientated within the metacarpal assembly so as to give the smallest dimensions. Unfortunately this approach led to a lot of redesign. The design goals for the thumb are listed in the next section.

The thumb metacarpal was designed around the drive assembly and the thumb rotation mechanism. The thumb had size restrictions as to how large and long its metacarpal block could be in the hand. Because of this size restriction the motor had to be positioned above the lead screw. The original hand designs had the motor orientated so that the gearing faced the rear of the thumb. The reason for doing this was that the actuator links would not have to be so far apart to move past (either side of) the spur gears, so reducing the width of the metacarpal assembly. Unfortunately this design had problems with the wires of the thumb coming out the wrong end of the thumb. The lead screw length was unacceptably long as it had to traverse the length of the metacarpal. The thumb ended up being longer and less practical. The decision was made to reverse the motor so the wires came out the rear of the thumb. This also meant the lead screw length was reduced to the minimum necessary for the thumbs curl. Other factors in the design of the metacarpal block was locating the hall effect switch, designing to minimise interference with the actuator links and the positioning of fasteners so as to minimised the thumb size.

The thumb rotation mechanism was designed into the thumb metacarpal later in the design. The reason for this was mostly due to the delay in creating a viable concept for the rotation mechanism. Once the concept was approved it still was difficult to incorporate a thee-dimensional rotation axis into a part that had to be machined two dimensionally. The initial designs for the thumb rotation mechanism included attaching the universal joint to the rear strut and then attaching the universal joint to the worm gear. This arrangement had problems with having the thumb located too high up the palm of the hand to the fingers. Later designs moved the universal joint into the palm of the hand attached to the output shaft of the thumb rotation motor. The initial design of the strut that connected the thumb to the thumb rotation axis was of a separate part. It was very complex and only allowed for a two dimensional axis. The design brief for the thumb rotation axis was changed so that the rotation axis was angled up through the palm of the hand with the front support bearing of the thumb located within the palm of the hand. Instead of having the strut curving in three dimensions it was decided that the strut itself would be separated into two flat parts. One strut would be located on the side of the left metacarpal block. It was used to position the front support bearings. The second strut came off the rear of the thumb off the motor end cap. It holds the shaft for the worm gear and its location bearings. The axis itself would be positioned by machining a three dimensional hole through the struts. This simplified the manufacture of the design considerably and made for a far more aesthetically pleasing design.

The design of the thumb linkages was relatively straightforward and embodied many of the ideas used for the finger linkage design. That is the force transmitted from the actuator links had to traverse down through the linkages along a single force path to avoid misalignment problems with the linkages. This objective was achieved by having each bearing joint within the thumb linkages use a single shaft. The linkages were reduced to a single part when possible to avoid splitting the force path and to reduce machining. Like the finger the linkages of the thumb are assembled within the metacarpal block. The proximal link in turn encloses the distal link. The end effect is more aesthetically pleasing appearance of the thumb tapering inwards towards the distal link.

At the end of the design process the linkages and the metacarpal block had to be modified to hold a printed circuit board (PCB) and FSRs to measure the thumbs grip force. Fortunately this did not require much in the way of modification of the thumb metacarpal block. A cover was created around the base of the metacarpal block that would protect the PCB from impacts. The thumb has three FSRs. One is mounted on the grip surface of the proximal link, while the other two are located on the distal link. The wires for the FSRs wind through the thumb linkages and attach to the PCB below the bearing housing in the metacarpal block. The thumb has also had its outer edges filleted to give it a more rounded appearance. Covers have been created into the design at the top of the metacarpal block and the proximal link to hide the gaps and the internal linkages from view.

Finally after the design the thumb was optimised for the best thumb rotation axis and linkage bearing geometry for the Maxon and Mini motor hands. This is discussed within Chapter 6: ‘Optimisation of the Canterbury Hand’.

4.6.1 Thumb Design Goals

The design goals for the hand are listed here. They were:

Thumb

- Aesthetic anthropomorphic design, i.e. edges, tapering, solid looking.
- Interacted well with fingers in hand assembly.
- Thumb model/design needed to be flexible for different motors and linkage bearing joint geometries.
- Reduce interferences about the palm.
- Thumb to be as simple as possible for assembly and disassembly.
- Simply manufactured using workshop machines.
- Thumb should be physically robust to impacts and harsh environments.
- Thumb strong enough to handle internal forces.

Linkages

- Good force output so that grip force is at least 10N.
- Increased motion so that thumb is roughly 90° between links when in curl.
- Size proportional to anthropometrics data on human thumbs.
- Use thumb linkage arrangement as originally proposed by Bain.
- No circlips to be used in design for ease of assembly.
- Linkages should be assembled simply, i.e. distal within proximal link, proximal link within metacarpal assembly.
- Linkages to be designed so force follows a single path and avoids buckling or misalignment of linkages.
- A single common shaft to be used for each joint bearing.
- Minimise knuckle widths and heights to improve anthropomorphic appearance.
- Singularity to be controlled by the use of a stop in the medial link.
- Joint bearings should be self-locating in the design.
- Linkages should be anthropomorphic in appearance, and anthropometrically scaled.
- Thumb linkages to be wide enough for maximum acceptable grip area.
- Linkage bearings to be protected within linkages as much as possible to avoid impacts.
- Sufficient clearances between linkages (yet minimised to maximise thumb distal width).

- Fasteners to be flush with side of linkages.
- Bearings to be shielded and located internally within the linkages where possible.

Drive Assembly

- Reduced lead screw length.
- Motor is protected and hidden from view (with some air cooling).
- Lead screw in line with a pair of actuator links for linkage motion to avoid jamming.
- Uses either Maxon and Mini motor in two configurations of thumb.
- Motor transmits motion to lead screw.
- Motor placed to minimise length of metacarpal block.
- Lead screw has to be 0.7mm pitch.
- Drive nut width to be minimised but avoids collision with metacarpal or spur gears.
- Support bearings to be minimised for outer diameter (while still supporting the lead screw forces).
- Low friction between lead screw and drive nut.
- Drive nut and actuator links to be securely located so as to produce linear motion for lead screw.

Metacarpal Assembly and Rotation mechanism

- Minimise size of the metacarpal block.
- Drive assembly to be fully located so it does not fall out the rear of the metacarpal block.
- Split design for metacarpal block for clamping drive motors and for easy assembly.
- Metacarpal weight minimised by reducing material yet strong enough for forces.
- Fasteners to be flush with side of metacarpal block.
- Actuator linkages to move in metacarpal with minimum interference.
- Simple manufacture for metacarpal and motor end cap (especially for thumb rotation axis location).
- Thumb rotation axis included in metacarpal assembly for attachment to hand.
- Three-dimensional vector for axis designed into thumb.
- Front support bearings held at end of axis.
- Rear axis connects to worm-worm gear rotation mechanism.

- Minimal clearance between metacarpal block and circuit board for rotation about the palm assembly.
- Minimal length to rear strut on motor end cap (later goal from optimisation).

Electrical Systems, force sensing and finger control

- Motor Wires get to circuit board in shortest distance.
- Wires hidden within thumb.
- FSRs included on thumb linkages.
- PCB to be included in thumb design.
- PCB to be securely fastened to metacarpal.
- FSR wires and motor wires connect to PCB.
- The FSR wires are protected from thumb curl.
- Wires to hand protected from rotation mechanism pinching them.
- Hall effect switch to be located in metacarpal blocks to locate the drive nut and to zero the encoder.
- Magnet for Hall effect switch to be located on drive nut.
- Exact clearance required between drive nuts and hall effect switch without interfering material.

4.6.2 Metacarpal Assembly

The metacarpal assembly may be considered as containing the drive assembly (encoder motor gearbox, spur gears, lead screw and drive nut), motor end cap, and the left and right hand metacarpal blocks. It also holds the Printed Circuit Board (PCB) for the thumb under the metacarpal block. The components of the thumb rotation mechanism that are attached to the thumb axis shafts may also be considered part of this assembly. These components include the front support bearings, the worm gear, and its support bearings.

The thumb was assembled in several stages. First the drive assembly is assembled with the actuator links being attached either side of the drive nut. Then the proximal, distal and distal driving links were assembled around the actuator links. The end cap and its rear strut are attached to the worm gear shaft (via a grub screw) at the rear of the palm. The front support bearings are inserted onto the rotation axis shaft (at the bottom of the left hand metacarpal blocks strut), and then into the thumb-bearing holder in the palm assembly. The right hand metacarpal block, the drive assembly and the thumb linkages are then assembled around the end cap and the left hand metacarpal block. This last assembly is the most difficult in attaching the thumb to the palm assembly. The wires of the motor are located directly from the rear of the thumb to the connectors of the PCB. The metacarpal blocks have a small overhang to protect and hide the wires. The Hall effect wires come out of the metacarpal to attach with the wire bundle from the FSRs (from the linkages) into the socket that connects to the thumb PCB. The output wires from the thumb PCB to the hand circuit board are attached at the same time as the thumb end cap is assembled into the palm assembly.

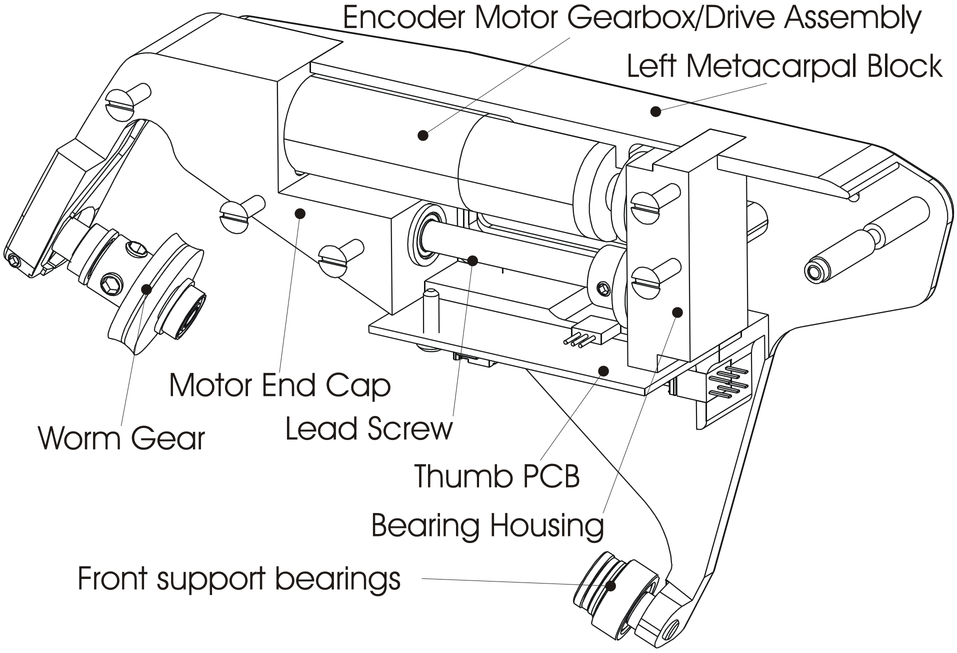

Figure 4.26 Metacarpal Assembly (with Right Metacarpal Block removed)

As with the finger metacarpal assembly location faces within the end cap and the metacarpal block situate the thumb's encoder motor gearbox. The assembly of the left hand and right hand metacarpal blocks pinches the gearbox of the encoder motor gearbox to keep it from rotating. There is also a small air gap between the end cap, and the metacarpal assembly to help air cool the motor. The metacarpal block like the majority of the hand is made of aluminium, which should conduct away the heat from the motor.

Other design features of the metacarpal are the ease of assembly of the thumb within the thumb rotation mechanism. This is surprisingly simple for a three dimensional axis. The manufacture of the thumb for this axis presents some challenges. However with sufficient set up time for setting the line of the axis it should be able to be manufactured by the workshop.

The PCB is also securely fastened to the bottom of the metacarpal blocks with two M2 cap screws. The design of the thumb metacarpal assembly is designed to protect the PCB from impacts and with sufficient clearance for it to avoid collision for rotation around the palm assembly.

4.6.3 Drive Assembly

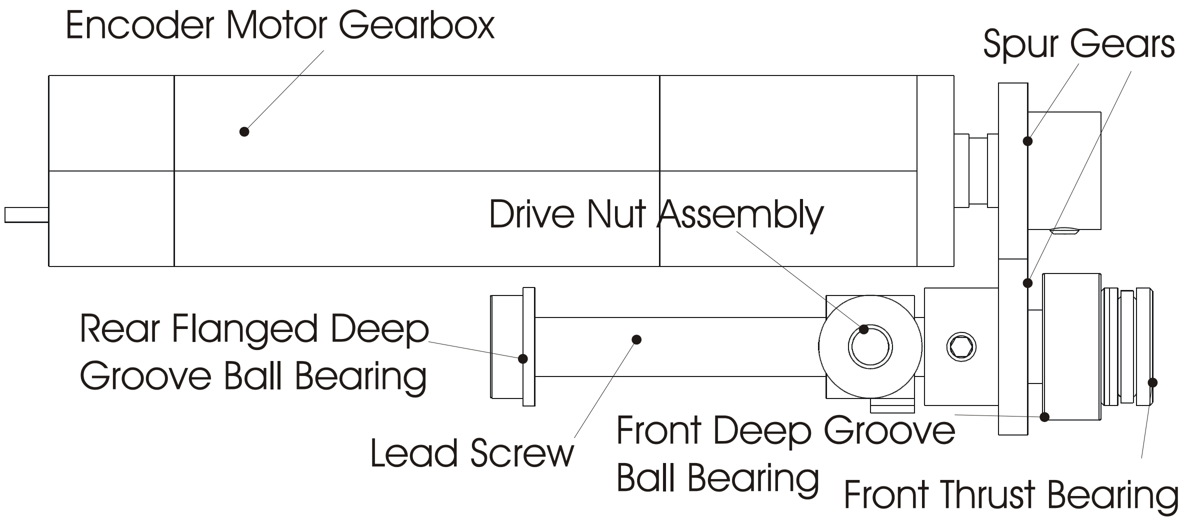

Figure 4.27 Thumb Drive Assembly

The drive assembly of the thumb is comprised of the encoder motor gearbox, spur gears, lead screw and the drive nut. Like the finger assembly the drive assembly had to be designed for both Maxon and Mini motors. The forces on the drive assembly are also very similar. The front bearings required a thrust ball bearing and a deep groove ball bearing paired together to take the axial and radial forces from the lead screw. The motor end bearing has lower radial and reduced axial forces to contend with. That is why a smaller diameter flanged deep groove bearing is used at this location.

The lead screw's front (linkage end) support bearings had to take a large axial force from the curling motion. As the thumb linkages are opposed by an object the motor slows and the torque in the screw increases. The increased torque causes the interaction of the lead screw and the nut to increase the axial force on the front bearings. There is an additional radial force on the front bearings from the spur gears. However the spur gears are located so close to the front deep groove bearing that the effect is reduced and is fully supported. The radial forces the actuator linkages produce as they move down the lead screw are also fully supported between the front and rear lead screw support bearings.

The front and rear bearings were minimised for size. The minimum size thrust bearing also limited the size of the front bearings. The same combination of thrust bearing and deep groove bearing was used. This should also reduce the component cost. The diameter of the rear bearings had to be minimised due to the minimum clearance between the motor and the outer flange of the flanged deep groove bearing.

The drive nut is made of bronze impregnated with lead to lubricate and reduce the friction on the lead screw for the motion of the drive nut. It was sized so that its height was just large enough to hold the threaded hole (4mm diameter with 0.7mm pitch) for the lead screw. The height of the drive screw had to be minimised so that it gave just enough room for the minimum clearance (1.5mm) over the magnet for the Hall effect switch. The Hall effect switch was used for zeroing the encoder for the nuts position.

The drive nut was made using the same design (for easy assembly, and manufacture) as the drive nut used in the fingers. The width of the drive nuts was larger than the finger nuts as it had to have clearance on either side between the actuator links and the spur gears. Since the spur gears are moving it was decided that a clearance of 1mm was necessary between the inner face of an actuator link and the addendum circle of the gear teeth. The drive nut, to keep its motion linear along the length of the lead screw, uses the rollers on either side of the actuator links. The material selected was Teflon, so the friction for the rollers travel within the recess within the metacarpal block was reduced. When the drive nut is enclosed within the metacarpal assembly there is sufficient force to locate the actuator links accurately between the drive nut and the rollers. Yet this force is small enough to allow rotation of the actuator links for the drive nuts travel along the lead screw.

The Maxon and the Mini motor thumbs used different sized 1:1 ratio spur gears so that they both used the minimum distance (equal to the PCD) between the motor and the lead screw. This difference is shown in the below table.

Table 4.6 Thumb drive assembly's 1:1 Spur Gears

	Mod	*Bore (mm)*	*Pitch Circle Diameter (mm)*	*Face Width (mm)*
Maxon	0.5	3	12	2
Mini	0.5	2	10.5	2

4.6.4 Metacarpal Blocks

The metacarpal blocks were designed to enclose the finger linkages and the drive assembly. It had to incorporate the rotation axis into the left hand metacarpal block. It had to fulfil these functions, while meeting the objectives of minimising its size, weight. It also had to still be strong enough to handle the internal motor forces. Unlike the finger the thumb's metacarpal assembly is a very visible part of the hand. Its aesthetic appearance had to be to resemble the shape of the human metacarpal as much as possible.

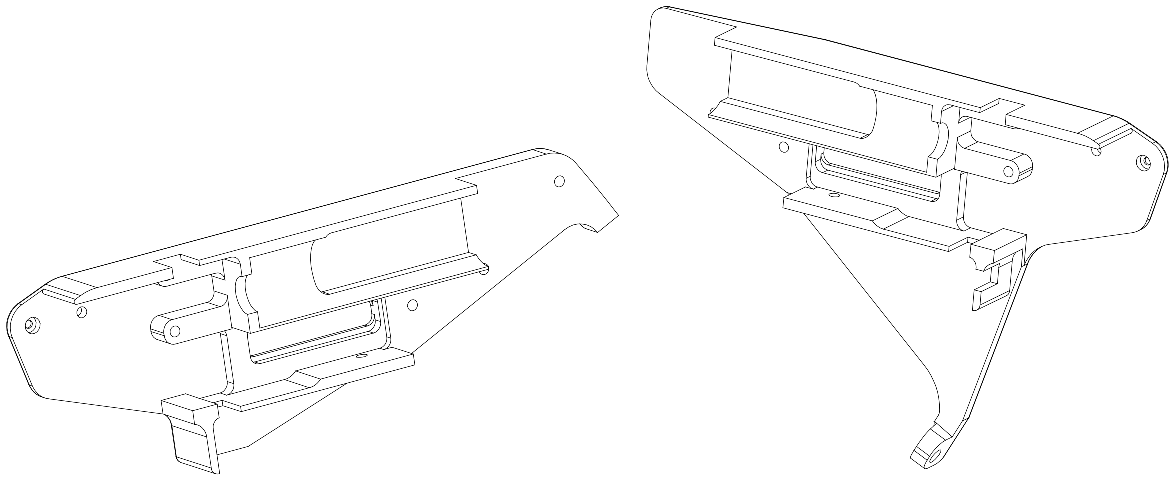

Figure 4.28 Left and Right Thumb Metacarpal Blocks

The metacarpal assembly is split along their length. When assembled they enclose the drive assembly. The main reason for this was for ease of assembly and to pinch the motors together to prevent them from rotating. With this initial design requirement the modelling of the metacarpal assembly was begun. Initially the metacarpal block was designed with the motors reversed. After designing the metacarpal assembly for the finger it was decided that several bearing housings would be required for the thumb. The front bearing housing would hold the motors and the lead screw bearings. The rear bearing housing would hold the rear support bearings and the spur gears. After modelling this it became apparent that the thumb was too long and rectangular. Due to the motor being reversed the drive screw had to be supported across the entire length of the metacarpal block. The motor wires were also coming out the wrong end of the thumb for useful attachment to the circuit board. After the motor was reversed it was easier to reduce the length of the metacarpal block. The lead screw was shortened to the minimum length required for the curl motion of the thumb linkages. This meant that the rear of the metacarpal block could be shaped to the minimum width to support the motor. This also improves the appearance of the thumb as like the human thumb its profile reduces towards its attachment to the palm. The rear bearing housing also had to be modified to support the rear of the motor. To reduce the length of the metacarpal bock the spur gear attached to the front of the motor has to rotate within the front bearing housing. The height of the housing was determined by the clearance between the Hall effect switch and the magnet. Since the actuator links for the thumb were located at the bottom of the metacarpal block there was insufficient material below them for a fastener for the bearing housing. Instead two pairs of M2 screws fastened the external bearing block on either side of the metacarpal assembly. They were located above and below spur gear attached to the motor. The material between the screws was removed to reduce the weight. The bearing housing also had a boss as a locating feature to hold the base of the housing in place within the metacarpal block when forces are acting against it.

The bottom of the metacarpal block had to have a minimum of material beneath the Hall effect switch. To keep the strength of the metacarpal block this material was reduced to the minimum allowed thickness of 1mm beneath the switch. However this material was increased to a larger thickness (2mm) behind the switch to give sufficient material for the PCB cap screws to be screwed into the base of the metacarpal assembly. Above this was the drive screw space in the metacarpal assembly. Within this space a recess for the rollers of the drive nut had to be included. The rollers would be constrained within this recess so forcing the drive nuts to have a linear motion.

The rear bearing supporting the lead screw is located within the motor end cap. The end cap is supported on the metacarpal in three locations. To M2 counter sunk screws are located directly behind the lead screw on both sides of the metacarpal assembly, so that the forces on the screw are directly in shear with the screw. The other two M2 screws locate the end cap onto only the right hand metacarpal block. The reason for this is that the rear of the left hand metacarpal block has been slimmed down to such an extent that there is not enough material to put a thread on it. The reason for this width reduction is to increase the maximum rotation of the thumb. By removing as much of the material that collides with the palm the maximum end point of the rotation is increased. On the opposite side on the right hand metacarpal block the material has been extended to form part of the rear strut. This was to make the lines of the metacarpal and the motor end cap line up and to hide the motor wires curling into the circuit board.

Above the lead screw is the hole within which the encoder motor gearbox is located. Most of the material around the motor in the metacarpal has been removed to provide air-cooling. This should help reduce the heat produced by the motor. However the motor is entirely enclosed within the metacarpal block and the motor end cap some gaps may need to be included to let the air out. The reason for the enclosure was to give the thumb a smooth outer appearance. By hiding the motors the thumb appears less robotic.

When the thumb rotation mechanism was decided upon the metacarpal had to be modified to fit the thumb axis into it. The first iteration of this was to have an attachment part that would be aligned with the axis. This though was unworkable and did not allow the thumb to be located within the palm of the hand. Instead of adding another part the motor end cap and the left hand metacarpal block were modified to hold the thumb rotation axis shafts. The left metacarpal block had a strut extending beneath it that would locate the front support bearings of the axis. This front strut had to be flat along the side of the metacarpal up to the bearings. The reason for this was that this strut would lie flat within a recess within the palm assembly when the thumb was resting alongside. The thumb could have a large axial force located along the rotation axis. Thus there had to be sufficient material around the bearing however for strength. The edges were rounded around the axis hole to reduce the stress concentration factors. The metacarpal strut had to have as much clearance as possible it rotates around the palm of the hand. The more clearance the greater the possible rotation of the thumb before it collided with the palm of the hand. However the strut could not be minimised to a strip of material due to aesthetic concerns. The human hand for example, does not have a gap in the web of skin between the metacarpal and the side of the hand. The strut had to keep the clearance while acting as a web covering the gap between the metacarpal and the hand.

Another design feature is the protection web around the PCB on the metacarpal blocks. This web protects the PCB from knocks and hides the wiring leading into the PCB. This should also improve the aesthetic appearance of the metacarpal block. The aesthetic appearance of the thumb metacarpal block was also improved by putting a fillet around the outer edges of the metacarpal block to soften the appearance. The aesthetic appearance was also improved by adding a cover over the top of the metacarpal. This hides the B2 and B3 bearing joints and their connection to the metacarpal. The support bracket of the metacarpals was tapered so that it aligned with the thumb linkages. The actuator links were thus covered and the thumb looks more streamlined.

4.6.5 Motor End Cap (Rear leg strut)

The motor end cap attaches at the rear of the metacarpal assembly. It locates the rear of the encoder motor gearbox in the assembly and the rear support (flanged deep groove) bearing of the lead screw. It also functions as the rear strut for the thumb rotation axis hole. The height and angle of this strut determines how the thumb rotates about the thumb axis. The worm gear and its support bearings are located on a shaft that is located in this hole. A small depth counter bore has been made into the axis hole so that the worm gear shaft is accurately located. A thin slice has been created through the axis hole so that a setscrew creates a pincer force across the slice to grip the shaft.

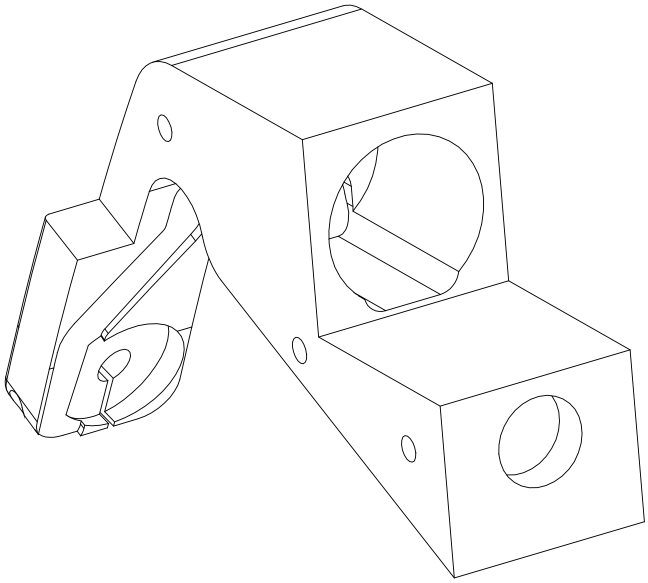

Figure 4.29 Thumb Motor End Cap

The encoder motor gearbox has wires exiting from the encoder. These wires exit through a hole at the rear of the end cap to curve back under its underside to be connected onto the thumbs PCB. The exit wires from the thumb PCB to the hand circuit board also run up the underside of the motor end cap and down a wire groove machined down the strut. The wires will be held in place using RTV silicone sealant.

The top of the strut has a cut into it for a curved cover feature of the right metacarpal block. This feature helps to hide the motor wires from view on the right hand side. The motor end cap is located within the metacarpal block by three screw holes.

4.6.6 Bearing Housing

The thumbs bearing housing was designed to hold the lead screw's front support bearings. To reduce the length of the metacarpal block a hole was added to allow for the rotation of the spur gear within the housing. The bearing housing was minimised in length to reduce the span of the metacarpal block. Only 2mm of material is allowed for in the design to take the axial forces from the thrust bearing housing. There is also a clearance of 0.5mm for the

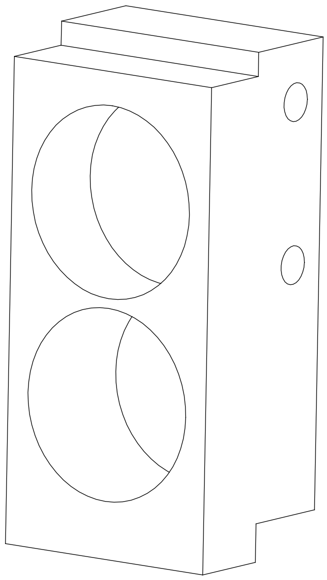

actuator links past the sides of the bearing housing. This clearance could be increased, however it would reduce the strength of the housing.

The bearing housing is secured to the metacarpal block by two pairs of M2 screws on either side of the metacarpal assembly. The screws are located above and below the spur gear attached to the motor. There are no screws attached at the base of the metacarpal, as there is too little material to hold a screw in place. Instead the end cap is positioned within a locating hole at the base of the metacarpal block.

Figure 4.30 Thumb Bearing Housing

4.6.7 Thumb Linkages

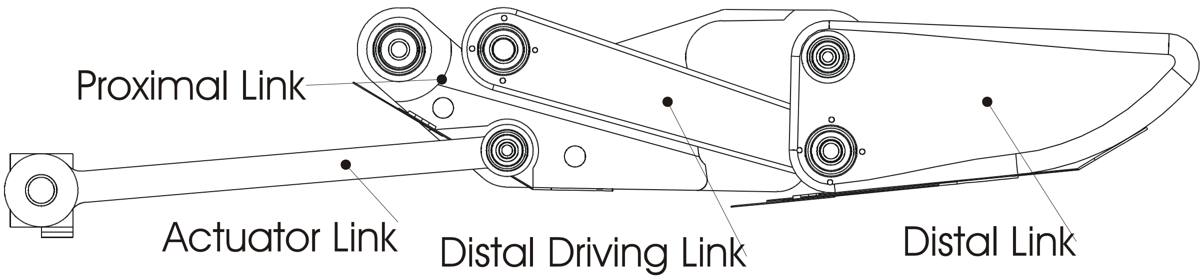

Figure 4.31 Thumb Linkages

The thumb linkages are considered separately to the metacarpal assembly. They are defined as the external moving components attached to the thumb that simulate the thumb digits in the human hand. The linkages are made up of the actuator links, the proximal link, the distal driving link and the distal link.

The function of the thumb linkages was to simulate the curling motion of the thumb. The thumbs end curl position was to have the proximal link 90º to both the metacarpal and the distal link. The singularity between the L4 (distal driving) link and L7 (part of the distal) link was avoided by using a stop within the proximal link to halt the distal links motion before it reached the singularity position.

The objectives of the thumb included optimising its shape to appear anthropomorphic. Part of this was achieved by making the size of the phalangeal linkages scaled according to anthropometrics data. The linkage bearings were minimised in size so that the linkages did not look oversized. Other than sizing other techniques were utilised to reduce the robotic appearance of the links. The thumb links for example have their outer edges filleted to soften their appearance. The gap between the proximal and distal links was covered as best as was possible to hide them from view as well. The proximal and distal links are tapered toward the distal link for the top and bottom surfaces. The bottom surfaces of the proximal and distal links were also used to mount FSRs for measuring the grip surfaces on the thumb.

The assembly of the thumb linkages had to be as simple as possible. Like the finger counter sunk screws (so the ends are flush with the sides) were used to hold the proximal link together. The bearings and shafts had to be self-locating within the design to make the assembly process less difficult. The thumb linkages are assembled starting with the distal link. Due to the manufacture of the distal link the distal driving link is fixed within the B6 bearing joint within the distal link. The proximal link encloses the distal link about the B5 bearing joint. The proximal also encloses the actuator links within itself on the B4 shaft. The proximal link and the distal driving link are then enclosed within the metacarpal assembly by the attachment of the B2 and B3 shafts respectively.

The thumb also had to be optimised to give the best force output over its motion. Part of the solution for this was to make sure that the forces followed only a single path through the linkages. The links of the thumb like those of the finger were designed so that only a single shaft went through each joint bearing and the links were not separated. By utilising this design method the forces would not create the misaligned motions and bending problems that occurred within the original finger design. The forces were also improved by optimising the positioning of the bearings in the linkages to give the maximum moment for the thumb's rotation. The optimisation of the thumb is covered in Chapter 6: 'Optimisation of the Canterbury Hand'.

4.6.8 Distal Link

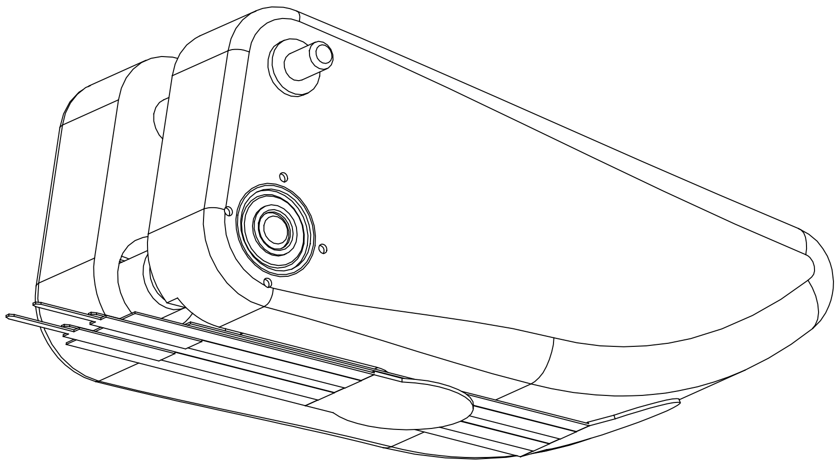

Figure 4.32 Thumb Distal Link

The distal link is the link furthest away from the metacarpal block. It will also be the part with the most interaction with any gripped object. Because of this two FSRs have been added to its bottom surface to measure the grip force. Also the width of the distal link has been maximised for the minimum sized width for the metacarpal block. The clearance between the proximal and the distal link has been reduced to 1mm on each side.

The proximal link grips the distal link on either side through the B5 joint bearings. The outer flanges of the deep groove bearings position the bearings and the B5 shaft between the proximal links support bracket. The B5 shaft is fixed within the distal link using either glue or a light push (H7-k6 size) fit

The distal driving link is connected to the distal link at bearing joint B6. The distal driving link cannot be disassembled from between the two B6 bearings. This was because the metal locating the outer race of the bearings in the distal link has been deformed. This permanently locates the bearings within the distal link (and keeps them from sliding out). The reason for doing this was to reduce the manufacturing complexity of the distal link.

To improve the aesthetic appeal of the distal link its surfaces have been rounded and shaped to resemble the human thumb’s distal phalange as much as possible. Another feature is the gap that has been machined between the bearings. This is to allow the distal driving link to rotate within the distal link. A small recess beneath the tail of the FSR has been machined into the bottom surface. The wires for the FSRs travel from this surface into the proximal link either side of the recess created for the motion of the distal driving link. The wires exit from the proximal link around the outside of the B2 bearings.

4.6.9 Distal Driving Link

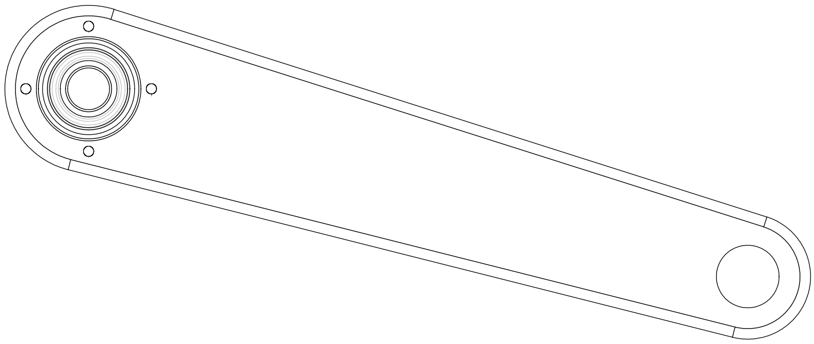

Figure 4.33 Thumb Distal Driving Link

The distal driving link in the thumb is only a single link. As stated above the shaft that is located within it at its B6 joint has been fixed within the distal link. The other bearing joint in the distal driving link is at the B3 joint position. This bearing has been permanently located onto either side of the distal driving link by deformations around its outer race. This also means that the width of the distal driving link is dependent on the width of the bearing specified for this position. The shaft that goes through this bearing is held in place on either side between the proximal links. Two spacers on the shaft locate the bearing accurately midway between the support brackets of the proximal link assembly. The bearings and shafts within the distal driving link have 2mm of material around them to support the forces in this link. The outer edges of the distal driving link have also been rounded to improve its appearance. The distal driving link becomes most apparent at the extreme curl position.

4.6.10 Proximal Link

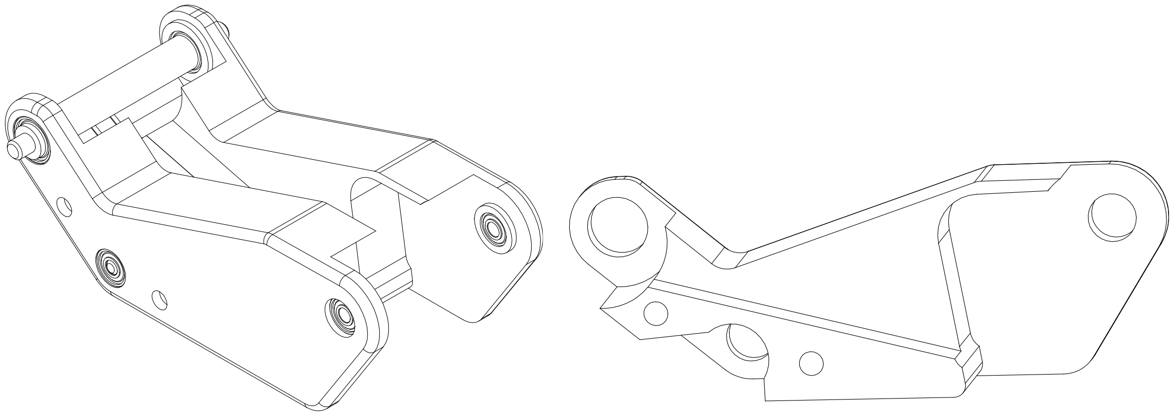

Figure 4.34 Thumb Proximal Link Assembly and Proximal Link

The proximal link of the thumb linkages is the phalange closest to the metacarpal block. It encloses the distal link and is itself assembled within the metacarpal assembly. When compared with the finger links the proximal link of the thumb most resembles the finger's medial link. The reason for this is that the thumb linkage motion was designed after the motion of the finger's medial, distal and distal link motion.

The proximal link was designed for ease of assembly. The best method for this was to use fasteners to hold it, the distal link, and the actuator links together, within the assembly. Two M2 counter sunk screws were used for this. One screw was located along the line of the L3 link (from the thumbs linkage arrangement). This screw had to fit in the material left between the B2 and B4 shaft and bearings spaces. The other screw was located along the bottom surface of the proximal link beneath the recess for the distal driving link. Unlike the finger's proximal link there was sufficient material within these locations to hold the thread for the fasteners.

The proximal link assembly locates between the left and right proximal links the flanged deep groove bearings for the B5, B2 and B4 joint bearings. The bearings are positioned between location faces on their shafts. The shafts are fixed within other linkages or the metacarpal block. The B5 shaft is fixed within the distal link, the B4 shaft is fixed between the actuator links, while the B2 shaft is fixed between the metacarpal blocks.

The reason for this choice of assembly was that the flange on the deep groove bearings makes the bearings self-locating and able to be disassembled later. If the bearings were located permanently in the proximal link by deforming the metal around their outer race the thumb would be disassembled to a far lesser degree.

The proximal link had to embody various design features. The distal link in the curl motion rotates into the proximal link. A space had to be given for this motion. The distal link also had to be halted before it reached its singularity position with the distal driving link. A stop surface was created internally within the distal rotation space for the proximal link. A cover was also created along the top of the proximal link to hide the gap the distal space left within it.

Since the distal driving link was positioned within the proximal link a recess had to be created to allow for it. This recess had to be large enough as well to allow for the distal links FSR wires to be positioned within it. These wires exit from the proximal link past the B2 bearing into the PCB socket that connects at the front of the metacarpal block.

The CAD design for the outline shape of the proximal link also had to cope with the B3 joint shaft interference. When this shaft is above and outside the line between the B7 and B10 bearings the top edge of the proximal link has no interference and appears straight. If however the B3 joint shaft is below this line then it interferes with the proximal link. In this case the CAD model creates a depression in the proximal link around the shaft. (See Chapter 3: ‘The Canterbury Hand CAD Model’ for more information on the modelling of the thumb.) This depression should not interfere with the strength of the proximal link as long as the B3 bearing is not located too far below the B2 bearing joint. The proximal link also has had its outer edges filleted to give it a softer appearance. The top and bottom edges of the proximal link are also tapered so they align with the edges of the distal link when it is in the extended position.

4.6.11 Actuator Links

The function of the actuator links is to transmit the force and motion of the drive nut to the proximal link. It is located on the drive nut at the B1 joint and on the proximal link at the B4 joint. The hole of the actuator link has a an easy running fit (size of H9-e9 using the hole basis system) on the drive nut and a light push fit (H7-k6 size) on the B4 shaft within the proximal link assembly. The B4 shaft has the proximal rotate on its bearings around the shaft instead of having the actuator link rotate on a bearing. This reduces the size of the actuator link connecting to the proximal.

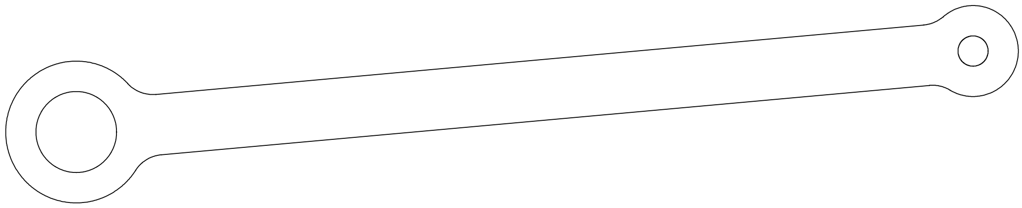

Figure 4.35 Thumb Actuator Link

Each actuator link has been shaped to reduce its profile as it moves through the thumb metacarpal assembly. There are minimum clearances (of 0.5mm) between the actuator links and the bearing housing within the assembly so that the width of the thumb's metacarpal blocks are reduced. The height of the span between the bearings has been reduced so that the actuator link can pass through the metacarpal with the minimum clearance with the fasteners. The link width is also only 1.5mm. Since the largest forces on the actuator link occur in the curling motion where the link is placed under tension the link can have a reduced cross sectional area.

The actuator links are small in comparison with the rest of the linkages and are not very visible from outside the thumb. Because of these reasons the actuator links have not had fillets added to their outer edges. The fillets would also add stress concentration factors to the internal forces within the links that would lead to stress fractures.

4.7 Palm Assembly

The palm assembly for the hand is the outer covering for the hand. It is designed to hold the fingers, the finger spreading mechanism, the thumb and the thumb spreading mechanism. The model of the palm assembly had to be able to use both types of motors to create two configurations for the Maxon and the Mini motor hand.

The palm assembly was modelled using a mixed bottom-up, and top-down assembly method. The palm assembly was modelled in its entirety as a single part. The original creation of the assembly was based on sketches that represented the position of the fingers and the various internal mechanisms of the hand. The objectives of the hand design had to also be applied to the design of the palm assembly. The particular objectives that applied to the palm assembly can be seen in the section below.

As the design matured the volumes that the fingers spread within, and the motors were located within were removed from the part. The features that located and held the motors and mechanisms became more detailed. This included adding cuts for the wiring guide paths and the palms Printed Circuit Board (PCB). The external thumb's rotation also modified how the hand was shaped. For example, material was removed in the middle rear of the palm to maximise the thumb motion by extending its maximum rotation position. At the end of the design process the part was broken up into the components that make up the palm assembly. The parts of the palm assembly have been designed to give the most aesthetic covering for the hand. They had to be shaped to resemble the palm. The holes between moving components such as the finger linkages had to be covered and the wires for the FSRs and the hand PCB had to be hidden.

This design like the rest of the hand took an iterative approach. Much of the time spent on the design was getting the optimum arrangement for the thumb rotation and finger spreading mechanisms in the hand. When the locations of the components of these mechanisms were fixed in the design the rest of the design features that supported them followed.

Part of the design was organising the positions of the FSRs on the palm and how the wires move through the palm assembly. The wires from the thumb's PCB are routed via the end cap strut at the rear of the thumb, and run along side the recess in the wrist connection panel for the rotation of the strut. They pass into the palm assembly through a gap in the angled recess at the rear of the palm, and then pass into the palm PCB connectors through a gap in the wrist motor holder (part of the internal housing). The wires from the fingers run along recessed paths in the top cover plates, pass around the outside of the drive nut recess for the finger spreading mechanism, and straight into the volume under the CB access panel to connect directly up onto the palm PCB. The wires from the finger spreader and thumb rotation motors run through gaps in the little finger side panel, and then loop back and up to connect to the palm PCB that lies above the motors. The wires in the palm assembly are kept within their wire paths by the use of RTV.

The thumb rotation mechanism though needed to have its axis of rotation optimised. This led to the palm assembly having to be part of the 'Configure' optimising program. The results of this optimisation process can be seen within Chapter 6: 'Optimisation of the Canterbury Hand'. This optimisation was very important as the modelling of the palm assembly depends heavily upon getting a workable thumb axis.

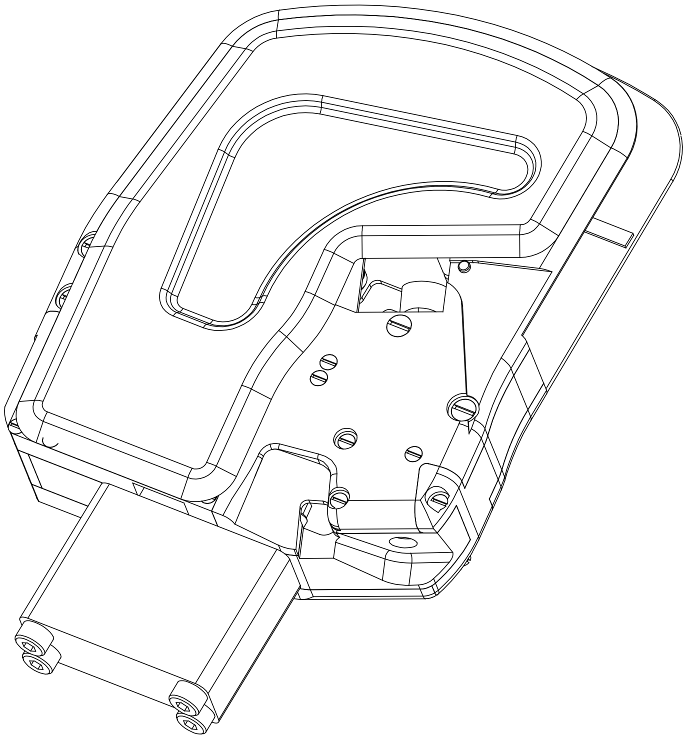

Figure 4.36 Palm Assembly (Mini motor Configuration)

The palm assembly will likely be the most time consuming aspect for the eventual manufacture of the hand. The reason for this is the large amount of geometry that each component is dependent on has resulted in a design that has a number of complex features. For example, by meeting the objective that the palm assembly be as anthropomorphic as possible a large number of curves will need to be ground into the parts. Also the three dimensional axis of the thumb rotation mechanism has added a complexity for the manufacture of the thumb bearing holder, and the features that support the worm gear. While these are likely the most difficult pieces to manufacture they are very necessary if the hand is to produce the expected rotation. In light of these difficulties the hand has been simplified as much as possible. An example of this is that the encoder motor gearboxes of the finger and thumb spreading mechanism have been orientated in the same plane at 7° to the horizontal. This meant that for the little finger side panel all the holes for the finger spreaders support bearings and for the motors are all orientated perpendicular to the panel so that they can be directly drilled. The palm assembly's aluminium parts will be anodised in the manufacturing process to improve the hands appearance. The results of the design for the palm assembly are discussed below.

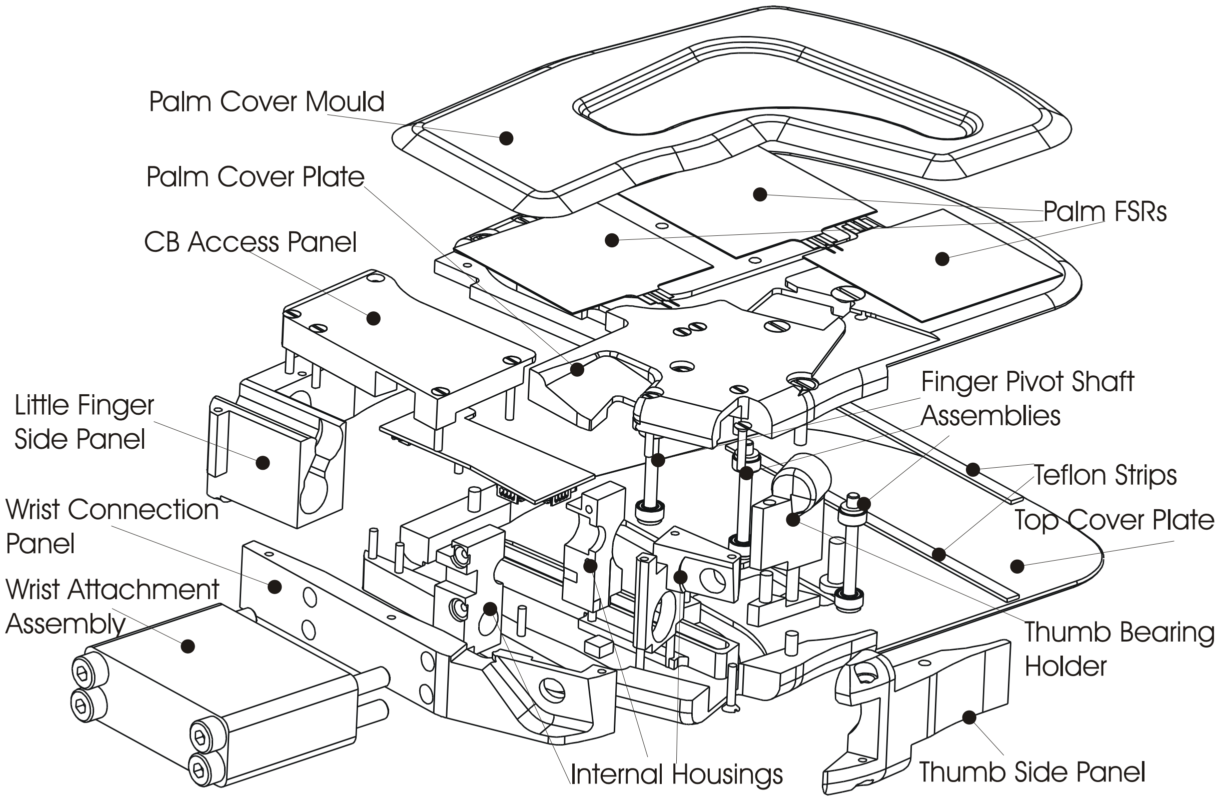

Figure 4.37 Exploded Palm Assembly

4.7.1 Palm Assembly Design Goals

To Locate and Hold:

- Finger spreading mechanism.
- Thumb rotation mechanism and the thumb.
- Little, ring, middle, and index fingers.
- Palm PCB, sensors and wires.
- Attachment feature for the wrist.

Other Objectives:

- Aesthetic anthropomorphic appearance.
- Removal of sharp outer edges.
- Minimum weight and size (length, width).

- Maximum motion for thumb rotation and finger spreading.
- Thumb axis to be angled for maximum anthropomorphic thumb rotation and maximum grip.
- Grip surface on the palm.
- Ease of assembly/disassembly.
- Simple manufacture of palm components.
- Maximum prehensile interaction between fingers and thumb.
- Thumb bearing holder to be hidden within palm.
- Thumb strut to be hidden in palm.
- Sufficient clearance between thumb and finger spreading mechanism.
- Attachment for fixed middle finger.
- Wire path grooves for FSRs, palm PCB, finger, and thumb power/signal wires.
- Exit hole for wires from PCB to computer.
- Protection of internal mechanisms.
- The palm assembly should be physically robust to impacts and harsh environments.
- Minimum size for gaps to minimise dirt effects.
- Teflon strips for reduction of friction effects in finger spreading motion.

4.7.2 Top Cover Plate

The top cover plate function is to act as the top of the Canterbury Hand. It attaches to the little finger side panel, the thumb side panel, the internal housings, the finger spreader shafts and the wrist connection panel.

Some of the features of the top cover plate are the:

- Recess for the rollers of the finger spreader nuts.
- Location surfaces for the internal housings to hold the finger spreading and the thumb rotation motor in place.
- Wire path cuts for the output wires from the finger PCBs to the palm PCB.
- Raised surfaces with internally threaded holes for attaching and fastening other palm parts i.e. the thumb side panel.
- Removal of unnecessary material to reduce mass and allow finger-spreading motion.
- Anthropomorphic outline to mimic human hand outline.
- Holes for the finger spreader pivot shafts (light push fit using hole basis system).

The outside edges of the top cover plate have been curved to give a more rounded appearance. The inner edge surrounding the metacarpal blocks has also been rounded to prevent a slicing effect on any object caught between the metacarpal and the top cover plate. A number of the threaded holes that locate the counter sunk machine screws have been counter bored first. This is due to the outer fillet creating too much a curve in the top covers surface for the screw's chamfer. The material at the end of the palm just behind the fingers has been extended to cover the gap between the metacarpal and the proximal links of the fingers. This improves the appearance of the hand.

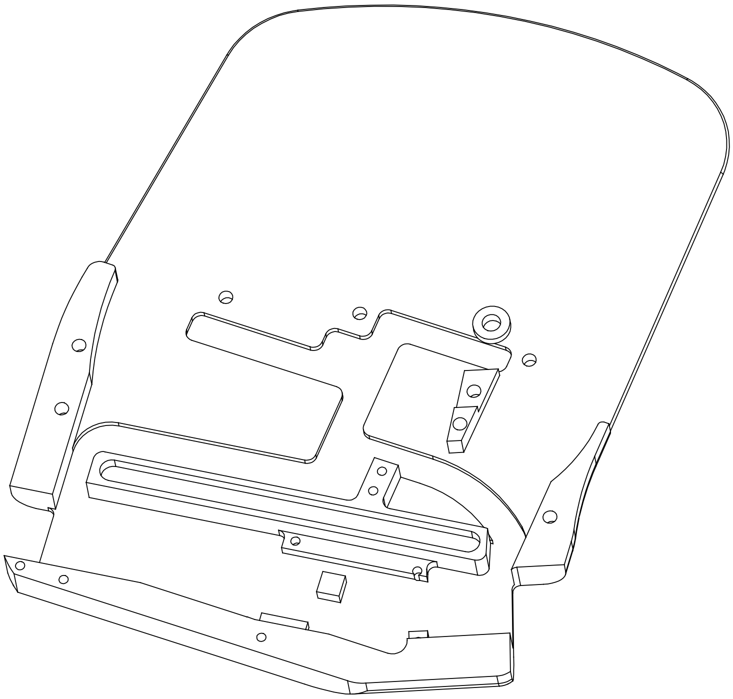

Figure 4.38 Top Cover Plate

The Teflon strip will be attached to the inner surface of the top cover plate with an adhesive such as araldite/glue to locate it on the inner surface. The adhesive should not be so strong as to prevent later removal if the Teflon strip becomes worn. The other parts of the palm assembly shall be attached using counter sunk machine screws.

4.7.3 Palm Cover Plate

The palm cover plate faces opposite the top cover plate. It is possibly the most complex part of the palm assembly. It is attached to the little finger side panel; thumb side panel, wrist connection panel, Circuit Board (CB) access panel, middle finger's metacarpal block/end cap and the finger spreader shaft assemblies. The palm cover plate acts as the palm for the Canterbury hand

The top surface of the palm has several design features. There are wire paths for the palm sensors. These paths traverse the palm and enter the palm circuit board through a recess under the circuit board access panel.

There is also a gap in the middle of the plate for the thumb bearing holder and the front strut of the thumb to be attached. The hole appears wider than it should. The reason for this is that at the maximum rotation position for the thumb, the front strut is angled through the middle of the palm. The gap needs to be quite wide to accommodate the strut at this position. Above and below this gap are fixture holes for the thumb-bearing holder. On the right side of the bearing holder hole is a recess for the thumb strut. This recess is to reduce the profile of the strut when the thumb is alongside the palm in the rest position.

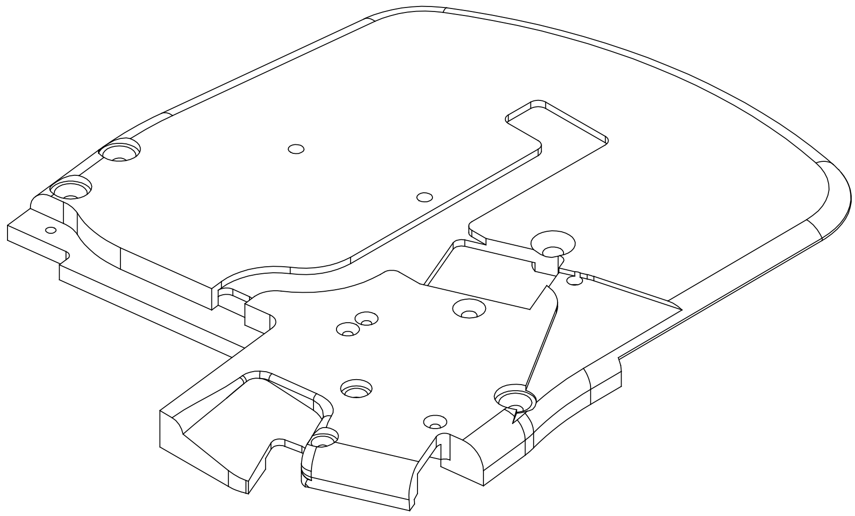

Figure 4.39 Palm Cover Plate

A very large gap has been taken out of the palm below the recess for the finger spreaders drive nuts. This is for the Circuit Board Access Panel. Next to the access panel gap at the rear of the palm is an angled recess. At this position the maximum rotation of the thumb causes a collision with the rear of the thumbs left metacarpal block with the palm. By putting a recess at this point the collision is delayed and the maximum rotation angle of the thumb is increased. Under this recess is a space for the finger spreaders spur gears and the thumb rotation mechanism universal coupling. A gap has been machined in the side of this recess for the wires from the thumb's PCB to the palm circuit board. The thumb side panel is located on the far right of the palm cover plate and is located on the palm surfaces. It is fastened in place on the palm cover plate by a single screw above the thumb side panel gap.

Other design features:

- Screw holes for attaching parts to the palm cover plate.
- Location features on the palm cover plate's underside for the fastening of the middle finger metacarpal block and motor end cap.
- Counter bored holes for attaching a chamfer for the counter sunk machine screws.

- Recess for the rollers of the finger spreader nuts
- Location surfaces for the internal housings to hold the finger spreading and the thumb rotation motor in place
- Raised surfaces with internally threaded holes for attaching and fastening other palm parts i.e. the thumb side panel
- Removal of unnecessary material to reduce mass and allow finger spreading motion
- Anthropomorphic outline to mimic human hand outline
- Holes for the finger spreader pivot shafts (light push fit using hole basis system)
- Rounded outside edges for improving aesthetic appearance of the palm cover plate.

As with the top cover plate the Teflon strip will be attached using adhesives to the inners surface. It is located above the finger's pivot shafts and below the support brackets of the finger metacarpals.

4.7.4 Little Finger Side Panel

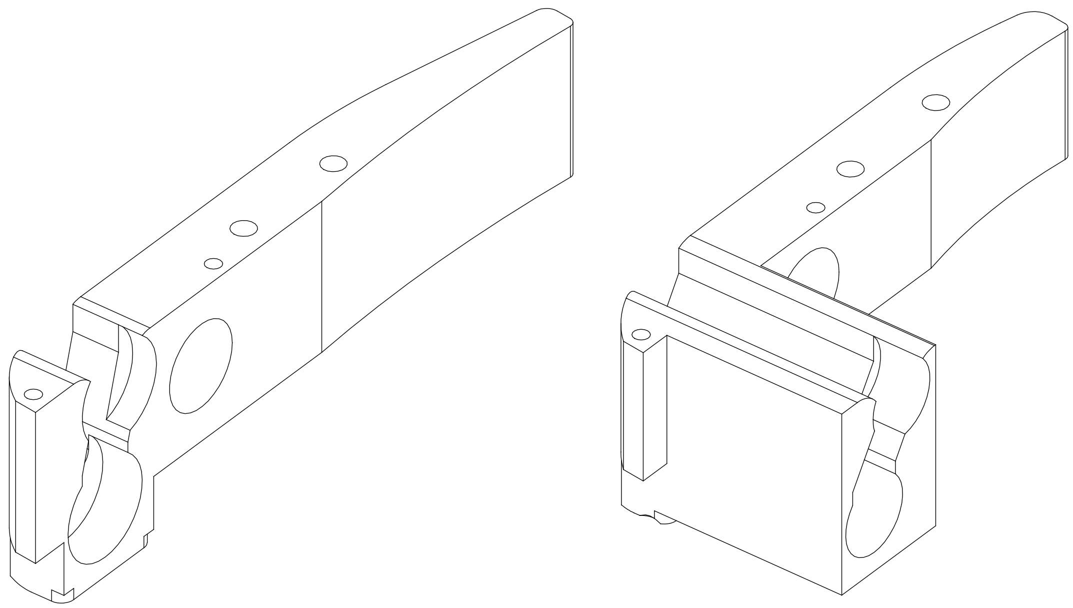

Figure 4.40 Little Finger Side Panel for Mini and Maxon Configuration

The little finger side panel is used to locate the rear of the finger spreading and the thumb rotation motors. It also holds support bearings for the finger spreading lead screw and protects the little fingers PCB from impacts. It assembles between the top and palm cover plates. The wrist connection panel also locates off its rear inner surface. The CB access panel is fastened to its upper surface. The little finger side panel has been reduced in height so that the palm and the top cover plate have sufficient material to have counter sunk machine screws fasten within them. The holes for the screws in the little finger side panel have thus been threaded.

The most noticeable feature in the little finger side panel is the motor holding holes within its inner surface. The bottom of these holes are used to locate the rear of the encoder motor gearboxes of the thumb rotation and finger spreading mechanisms to prevent them sliding out of the internal motor housing. A cut has been machined (wire cut) in the sides to allow the motor wires to exit from the side panel. The motor wires would then loop up to connect to the palms PCB. The PCB is located within the inside of the CB access panel.

The motor holding feature is different between the Maxon and the Minimotor palm assembly. The Maxon configuration of the little finger side panel has the motor holding feature flush with the inner surface that the finger spreading support bearing hole is cut into. The Mini motors though are shorter in length compared with the Maxon motors. The gearbox of the mini motors still had to be connected midway in the palm for the finger spreading mechanism and for attachment to the worm. This meant that the locating surface for the rear of the motors had to be moved into the palm to connect with the smaller Mini motors. The effect of this is the little finger side panel has a large extruded boss for the location holes. However this feature has been largely reduced in weight due to the motor wire gap.

The outer edges of the little finger side panel are located next to the circuit board connected to the metacarpal of the little finger. To give a better clearance of the motion of the finger and to improve the aesthetic appeal of the palm these edges have been filleted.

4.7.5 Thumb Side Panel

The thumb side panel holds support bearings for the worm of the thumb rotation mechanism, and the finger spreading lead screw. It also protects the index finger’s PCB from outside impacts. It is fastened to the top and palm cover plates, and has a gap for the location of the wrist connection panel. These two bearing holes are located at different angles due to the worm bearings having to be angled to be perpendicular to the rotation axis (in the vertical plane). This change in orientation though will make the manufacture of the thumb side panel more difficult as it will require several set ups to get the drilling angles.

Another feature that may be difficult to manufacture is the crescent shaped recess above the bearing hole for the worm. The recess was created as a space to allow for the worm gear's rotation (orientated along the Secondary Axis angle). This recess does not have to be overly accurate since it is only used for clearance. It could be manufactured by a milling cutter in the same set up position that will be used for the worm's support bearing hole.

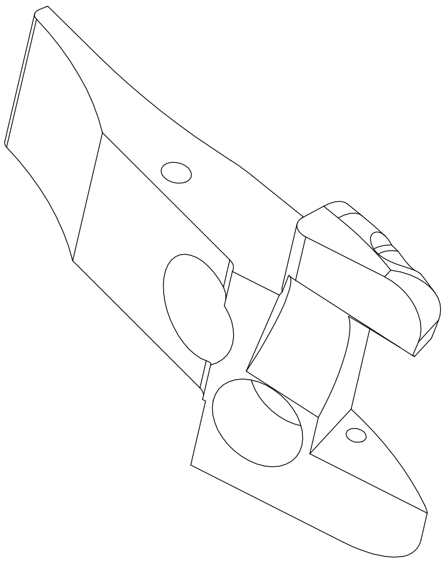

Figure 4.41 Thumb Side Panel

The top and palm cover plates are attached above and below the finger spreader bearing support hole. They are secured to the thumb side panel through a single threaded hole by (M3 counter sunk machine screw) fasteners attached on either side. The edges that locate the top and palm cover plates have been rounded to allow for the milling cutters radius. The gap located at the rear of the thumb side panel is for the wrist connection panel, which is attached to the thumb panel by two (one from above and one from below) M2 machine screws.

The outer surfaces of the thumb side panel are curved for several reasons. Firstly the thumb has to rotate about the panel. By curving the surface the distance needed for the thumb to rotate past the panel is reduced. Secondly the outer surfaces, and the edges closest to the index finger, are curved to improve the aesthetic appearance of the palm assembly.

4.7.6 Thumb Bearing Holder

The thumb bearing holder holds the support bearings connected to the shaft at the base of the thumbs front strut. It is attached with M3 counter sunk machine screws to the top and the palm cover plate.

The shape of the bearing holder is dependent on the space constraints within the hand. The base of the holder had to fit in the space between the index and the middle metacarpal blocks at the maximum finger spread position. Because of this constraint the base had to be thin and rectangular shaped. The top part of the holder that contains the bearing had to hold within itself the circular thrust and deep groove bearings. However it had to have the minimum material around the bearings to reduce its profile in the palm assembly. The top feature had to have minimum size so that it did not stick out of the palm assembly. It also could not be too wide or deep, as this would interfere with the spreading of the fingers. It was decided that the best shape for the minimum material around the bearings was circular. The model of the thumb's bearing holder had to contain both the top and bottom features together so they were attachable to the palm assembly and manufacturable.

This part was fastened to the hand by machine screws. The threaded holes for these screws and the faces used for locating the bearing holder in the palm are located both behind the top bearing holding feature and along the bottom of the base. The base has a stepped face in it to both help locate the holder along the length of the hand, and to balance the forces across it. When the thumb is gripping an object there is considerable force axially through the front bearings towards the rear of the palm. This force can create a large bending moment around the base of the bearing holder. By having a step at the base the bending stress should be distributed across both the bottom locating face and the screws. If the location face did not exist in the design the bending stress would be entirely across the screws. To reduce the stress concentration factors around the outside of the top bearing support the side edges have been filleted. This also allows for the radius of the milling cutter to traverse around this feature. The manufacture of the bearing holder will likely be difficult due to the axis for the bearing holder being radically different to the orientation of the base. It may be that casting this part and then machining it is the best solution. An alternative may be that a central small diameter pilot hole could be drilled right through the bearing support down its axis. This would allow for easier reaming of the hole for the bearing tolerance.

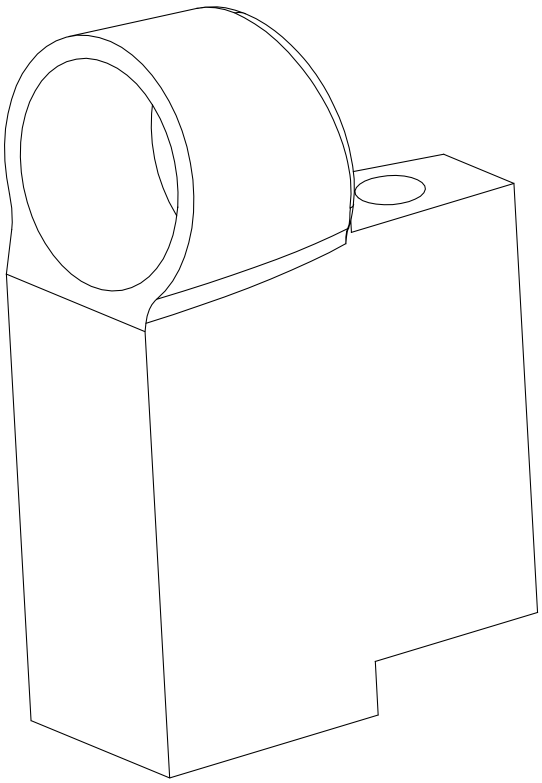

Figure 4.42 Thumb Bearing Holder

4.7.7 Internal Housings

There are three internal housings within the palm assembly of the Canterbury Hand. They are the thumb side support, the wrist side motor holder and the nut side motor holder. The thumb side internal housing was used for supporting the flanged bearing of the worm, and a flanged bearing of the worm gear for the thumb rotation mechanism. It is fastened between the top and palm cover plates. Two M2 counter sunk (CS) machine screws fasten the thumb side housing to the top cover plate. Three M2 CS screws fasten the palm cover plate above it.

The motor holder parts join together to clasp the finger spreader and thumb rotation motors in the rear of the palm. Two screws above and below the finger spreader motor hold the two parts together. The motor holder parts are also fastened between the top and palm cover plates by a single hole that holds two M2 counter sunk screws.

On the base of the internal housings two grooves have been cut. These act as location features that vertically position the internal housings on the top cover plate. A stop on the top cover plate in front of the motor holder housing and the thumb support plate horizontally locate the internal housings within the palm. Since all of the internal parts are within the interior of the hand their aesthetic appearance was not a factor in their design. However some of their outer edges have been filleted to allow for the machining radius within other parts (such as the top cover plate).

Other design features of the internal housings include:

- A groove along the top of the assembled motor holders is used to locate the circuit board access panel along the palm.
- A circular depression across the internal housings as clearance for the drive screw
- Wire space at the top of the thumb side support for the thumb's PCB wires
- Gap around the large diameter hole in the thumb side support. This is for locating the worms flanged support bearing
- Material removed from under the worm gear support-bearing hole in the thumb side support to allow for a possible wire path and to reduce weight.

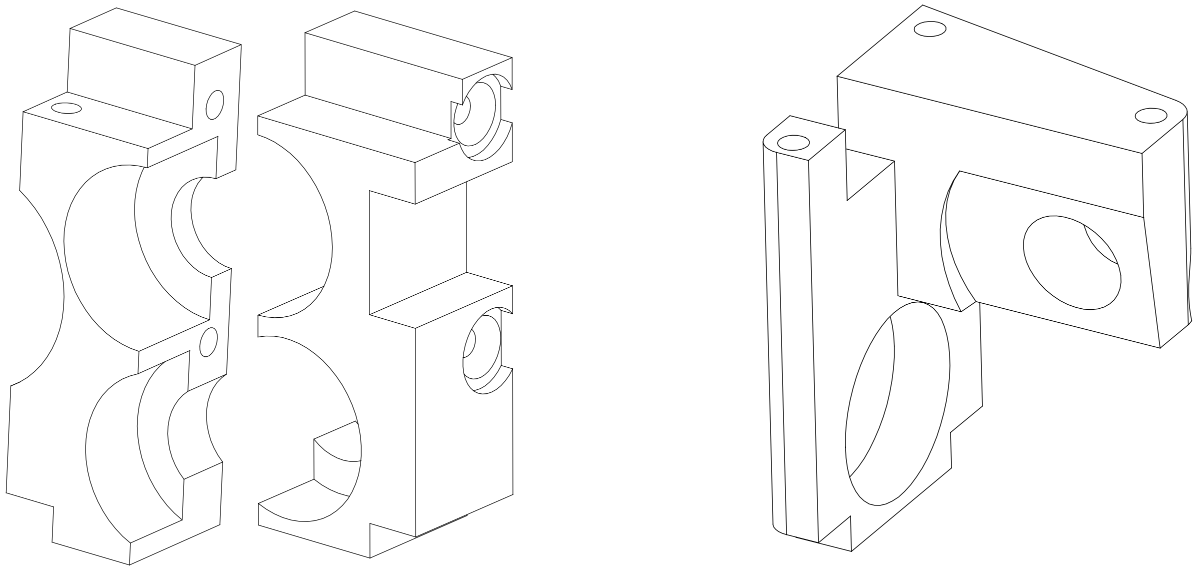

Figure 4.43 Internal Housings (Nut side, wrist side, thumb side)

4.7.8 Circuit board (CB) Access Panel

The circuit board (CB) access panel is used to protect and hold the circuit board within the palm assembly. It is fastened to the wrist connection panel, the little finger side panel and the nut side motor holder (part of the internal housing of the palm). The CB panel however had to have the material within it minimised for the location of the palm PCB. Only features that provided cover or required material to hold the screw holes were not hollowed out. The palm PCB is attached to the inside surface of the access panel. The best means of attaching the PCB to the access panel would be either with cap screws or with a light adhesive.

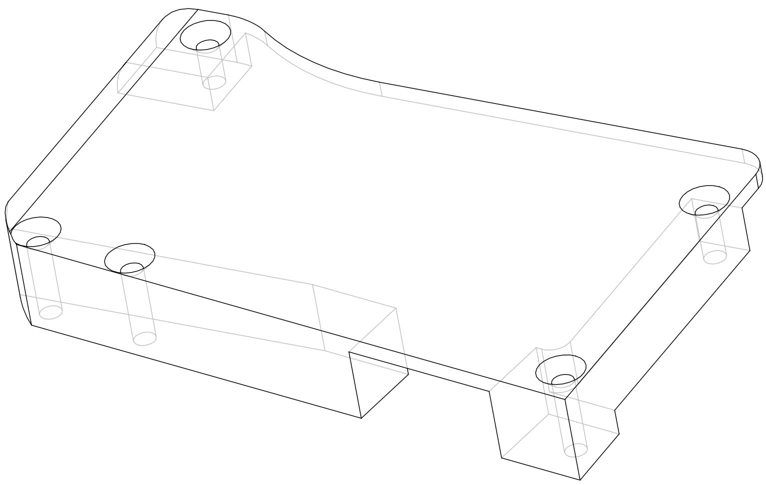

Figure 4.44 CB Access Panel

There are several design features for the CB access panel. There are gaps on the little finger side panel and at the rear of the panel. The hole on the little finger side is for the inlet wires from the palm motors (for the thumb rotation and the finger spreading mechanism). The rear hole is for the wires leaving the palm's PCB, to connect with a computer/power supply. The access panel is located in the palm assembly by two surfaces. The first surface by the motor wire inlet hole locates the panel vertically. The access panel is located horizontally by the second surface facing the palm cover plate by the internal motor housing.

The access panel also has a curved outer edge facing towards the palm. The reason for this curve was to maximise the area of the palm PCB, while avoiding a sharp edge in the design. Since a milling machine will manufacture the palm cover plate the internal cuts require a machining radius. However this would mean either having another surface to locate the access panel horizontally or a small gap. Instead of having a straight edge the curved face was chosen. This face however will not be used for locating the access panel due to the difficulty in putting an accurate tolerance along a curved surface.

4.7.9 Wrist Connection Panel and Wrist Attachment Assembly

The wrist connection panel is used to hold support bearings for the worm gear and to provide a location that the hand can be supported from. It is attached to the palm assembly between the top and palm cover plates by three M2 CS screws. The panel is located for fastening by two surfaces on either end. One surface provides location horizontally by connecting against the little finger side panel. The other provides the vertical location off the thumb side panel.

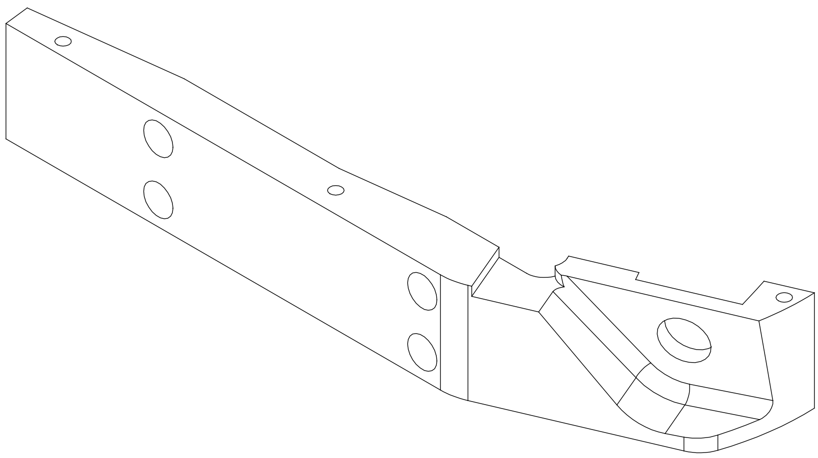

Figure 4.45 Wrist Connection Panel

The worm gear's rear support bearing is located on the inner surface of the wrist connection panel. A counter bore has been cut into this surface to locate the flanges of this bearing. The manufacture of this bearing hole is the most difficult feature in the creation of the wrist panel. This is due to the hole having to lie on the exact thumb rotation axis. A recess also needed to be created around this hole for the rotation of the rear strut of the thumb. At the top of the filleted edge for this recess is a gap for the thumb PCB's wires. In the middle of the wrist connection panel are four M5 threaded holes. These holes allow four cap screws to fasten to the wrist attachment assembly to the wrist panel. They may also be used later for attachment to a wrist rotation mechanism.

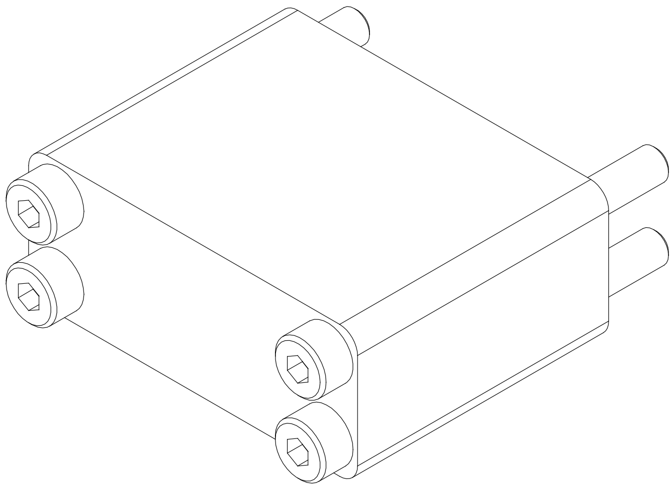

Figure 4.46 Wrist Attachment Assembly

The wrist attachment is a block that attaches (via the cap screws) to the wrist connection panel. It is used as a grip surface for attaching a vice/grasp mechanism to hold the hand at a fixed base. However this attachment part may be temporary, as a wrist mechanism/robotic arm attachment for the hand will one day be created to take its place. The wrist connection panel may also need to be redesigned.

4.7.10 Teflon Strips

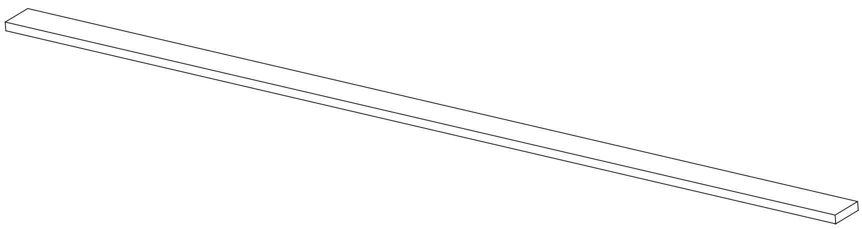

Figure 4.47 Teflon Strip

Two Teflon strips are located within the palm assembly. One is placed on the inside of the top cover plate and one on the inside of the palm cover plates. They are located above the finger pivot shafts close to the support brackets of the fingers metacarpal blocks.

A clearance of 1mm has been designed into the palm assembly between the cover plates and the metacarpal blocks. However when gripping an object the moment about the pivot bearings may cause the metacarpal blocks to bend towards the palm cover plate. The Teflon strips are there to help prevent this situation by keeping a solid connection between the metacarpal blocks and the cover plates. By preserving the clearance between the metacarpal blocks and the hand covers the overall friction and mechanical misalignment problems within the fingers pivot shafts is reduced.

As the fingers spread they rub against the strip. By having the material of the strips made of Teflon the friction of this motion is reduced and the wear is mostly on the strips. If the strips become overly worn they can be easily replaced. The ease of assembling the top and bottom cover plates makes this a simple procedure.

4.7.11 Palm Cover Mould

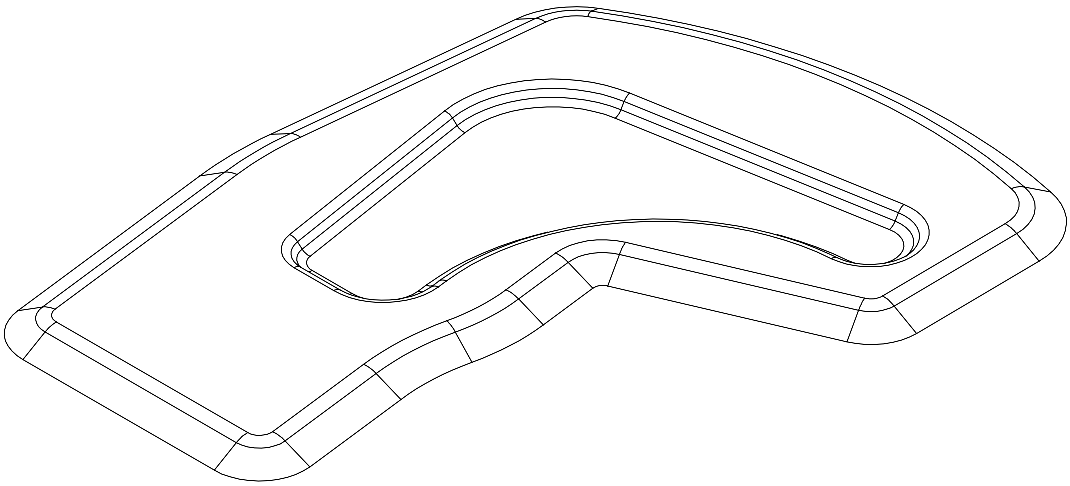

Figure 4.48 Palm Cover Mould

The palm cover mould was designed to cover the palm sensors, wires and to provide a surface for palmar prehensile grips i.e. grasping a screwdriver. The mould will probably be made from rubber, rubber foam or light plastic. The mould would have to be low weight and able to deform and spring back from under a load to increase the grasp friction at the palm. A depression is created in the middle of the mould's surface so that any object grasped against the palm has some small limitation for its motion. If a glove is added it will also look like the palm has a natural depression at its centre. The cover mould would be attached either with Velcro strips or a light adhesive to the palm of the hand. There should be sufficient attachment to avoid it falling off under pressure though.

4.7.12 Palm Actuation

The palm actuation is made up of the finger spreading mechanism and the thumb rotation mechanism. The encoder motor gearboxes and associated components for each mechanism is located in the rear of the palm assembly.

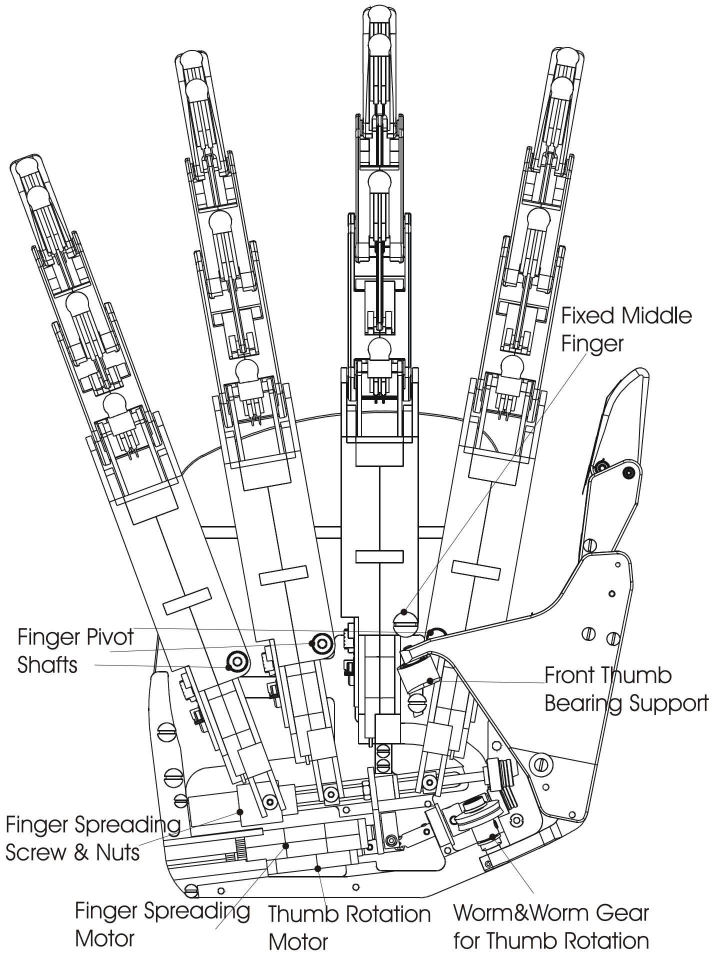

Figure 4.49 Palm Actuation (Fingers partially spread)

The design of the palm actuators had to incorporate the objectives of the hand. One of those objectives is to minimise the width of the hand. That is why the worm gear and the Universal coupling in the thumb rotation assembly will be machined to reduce their size.

The thumb rotation mechanism and the finger spreading mechanism are assembled at the same time. First the worm gear, and the worm are assembled on their shafts. They are assembled perpendicular to each other within holes in the thumb side internal housing and the thumb side panel. These in turn are assembled onto the top cover plate. The universal coupling is then attached to the worm gear shaft and to the output shaft of the encoder motor gearbox that actuates the thumb rotation motion. The encoder motor gearbox that actuates the finger spreading mechanism has its spur gear attached. The nut side and wrist side motor holders are then screwed onto the top cover plate enclosing the finger spreader and the thumb rotation motor between them. The thumb rotation motor is the one closest to the top cover plate, while the spreader motor is the one above it closest to the palm cover plate.

The lead screw of the finger spreader mechanism is then assembled and the drive nuts wound onto it. The support bearings are added to the lead screw. The thumb side support bearings on the finger spreader screw are then placed in their hole in the thumb side panel. The spur gear attached to the centre of the spreader lead screw has to be slid into the spur gear of the finger spreader mechanism. The drive nuts have to be positioned at the same time within the groove along the width of the top cover plate.

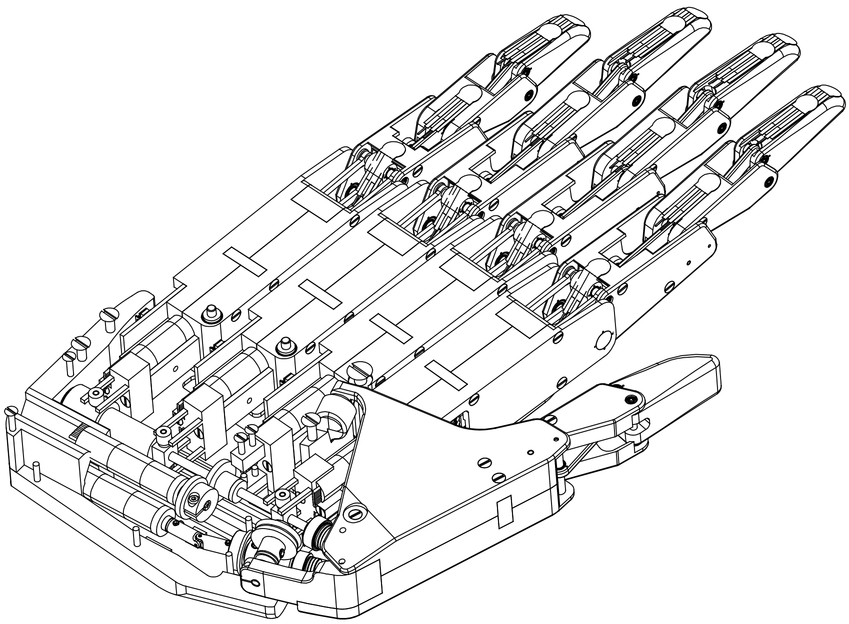

Figure 4.50 Detail of the Palm Actuation (Fingers not spread)

The rear of the motors and the other support bearings for the spreader screw are then placed in their respective holes in the little finger side panel. This panel is subsequently attached to the top cover plate. When doing this operation the motor wires should slide out the hole provided in the little finger side panel. They are connected later to the circuit board located above the motors in the palm.

4.7.13 Thumb Rotation Drive Assembly

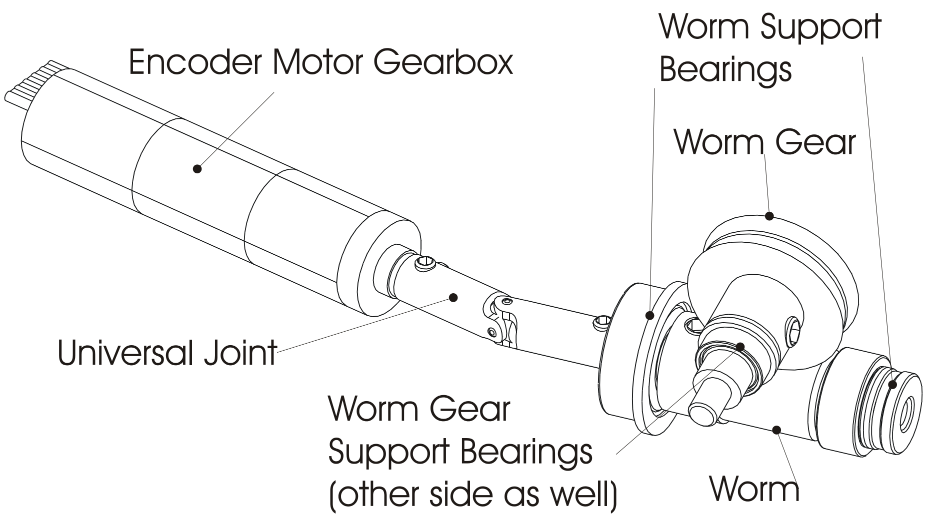

Figure 4.51 Thumb Rotation Drive Assembly

The thumb rotation drive assembly consists of the actuating encoder motor gearbox, universal coupling, worm gear, worm, and the shafts and support bearings that carry these mechanisms. The thumb rotation mechanism uses a 19:1 reduction worm-worm gear arrangement, as this is the smallest mechanism capable of reducing the thumbs rotation speed.

The encoder motor gearbox is located between the internal housing and the little finger side panel. A grub screw secures the output shaft of the motor to the universal coupling. The worm is faced perpendicular to the Main Axis angle of the thumb rotation. The worm gear is angled in line with this Main Axis angle but is tilted up in this plane. This causes the axis to be angled up through the palm and is called the Second Axis angle. The universal coupling is used to change the angle of the motors motion as it enters the worm. Depending on the configuration this means a change of angle of 10º for the Maxon hand and an angle change of 16º for the Mini hand. Both of these angles are less than the maximum recommended angle as can be seen in the below table.

Table 4.7 Thumb Rotation Universal Coupling

	Size (mm)	*Modified Overall Length (mm)*	*Coupling Type from SDPSI*	*Max Angle (º)*	*Motor Torque(N/m)*
Mini	ID2.5xOD4.76xL25.4	24	Miniature Range	25	1.1
Maxon	ID3xOD6xL29	22	Small Series	30	5.1

Key: ID = Bore Diameter, OD = Outer Diameter, L = Overall Length

The couplings can also handle the stall torque of the motors. For the Mini motor the maximum torque it can produce is 14mNm, and for the Maxon motor it is 156mNm. Both of these values are significantly less than the rating torque for the couplings. Thus the selected couplings should be sufficient for the motor torques. To fit the coupling into the width of the hand assembly the length of the universal coupling was reduced.

The universal joint transmits its motion and the motor torque to the worm shaft. As the table below shows the worm has a large axial force component and the worm gear has a high radial load.

Table 4.8 Forces in Thumb Rotation Mechanism

	Max. Axial Force (N)	*Max. Radial Force (N)*
Worm	209	139
Worm Gear	34.6	181.2

The support bearings for the worm shaft were selected for their axial force rating. On this shaft within the thumb side panel the support bearings are a thrust bearing and a deep groove bearing paired together (like the drive assembly for the finger and the thumb). The bearings selected were the same as for the finger and the thumb drive assemblies due to their minimum size, and their load ratings. The worm shaft also had to be supported within the internal housing. However due to space restrictions for the width of the bearing the only alternative that could be used was a flanged (ID4mm, OD13mm, and Breadth 5mm Nachi) deep groove bearing. The selected bearing has a larger diameter to compensate for the axial forces along its smaller width.

Table 4.9 Support bearings in Thumb Rotation Mechanism

Location	*Type*	*Size (mm)*	*Running Load Rating (N)*
Worm - internal housing	Flanged deep groove bearing	ID4 OD13B4Nachi	1300
Worm - thumb side	Deep groove bearing	ID3 OD10 B4 EZO	627
Worm - thumb side	Thrust bearing (axial only)	ID3 OD8 B3 Nachi	1790
Worm Gear - either side	Flanged deep groove bearing	ID3 OD7 B3 Nachi	385

The other bearings for the worm gear had to take a larger radial load but a smaller axial force. Since these bearings also had to locate the worm gear along its axis flanged (ID3mm, OD7mm, and Breadth 3mm Nachi) deep groove bearings were selected. As can be seen in the above table (Table 4.9) all the bearings were sized to handle the loadings. Please note that the actual load on a bearing is dependent on various factors that need to be applied for calculating whether the Running Load Rating is sufficient. However it makes for a good rough comparison.

The sizing of the worm and the worm gear for the thumb rotation mechanism are given in the below table (Table 4.10). As can be seen the worm length has been reduced to 16mm to reduce the width of the hand.

Table 4.10 Thumb Rotation's 0.4 Mod Worm Gear and Worm

	No. of Teeth	*Size (mm)*	*Modified Length (mm)*
Worm (bored)	2	ID4 x PCD9 x L25	16
Worm Gear (M)	38	Bore 3 x Boss 8 x PCD15.2 x L10	~

Note: PCD = Pitch Circle Diameter, ID = Inside Diameter, L = Length

The angle of the encoder motor gearbox was aligned at 7º to the horizontal so that it was perpendicular to the little finger side panel and parallel with the finger spreader motor. Thus manufacture for the hand assembly parts that hold the motors is simplified.

The thumbs rear strut (part of the thumbs motor end cap) is attached to the rear of the worm gear shaft. The thumb's front strut support bearings (part of the left metacarpal block) are attached within the thumb bearing housing on the top cover plate (between the middle and the index finger's metacarpal blocks). The orientation of the worm gear and the thumb bearing housing is collinear. These two components form the three-dimensional thumb rotation axis that passes through the hand. The end result of this rotation mechanism is the thumb rotating about the axis around the palm of the hand. The placement of the axis and the worm gear was crucial for this motion and the anthropomorphic appearance of the thumb.

4.7.14 Finger Spreading Drive Assembly

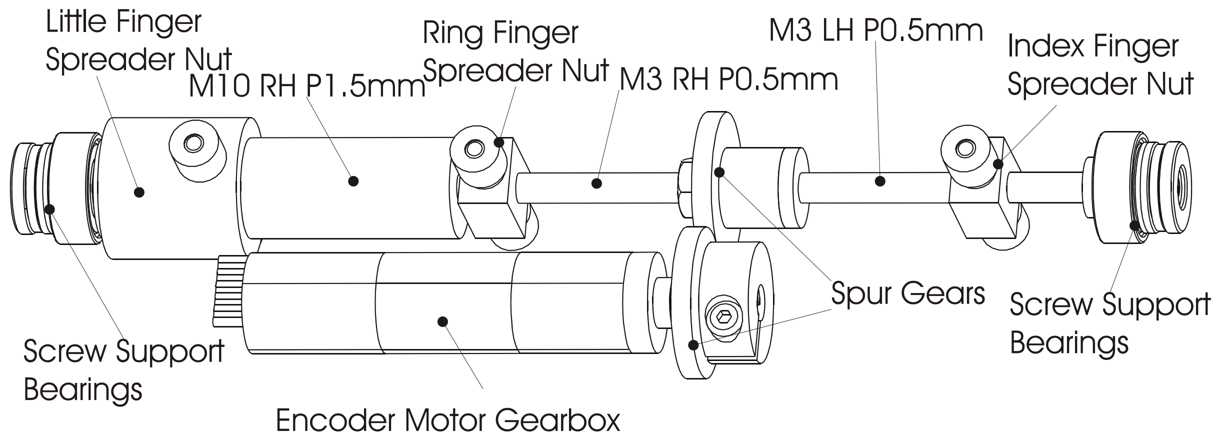

Figure 4.52 Finger Spreading Drive Assembly

The finger spreading mechanism is a one-degree of freedom mechanism. The middle finger is fixed within the Canterbury hand. The finger spreading mechanism acts to spread the little finger and ring finger away from each other and the middle finger. On the other side the finger spreading mechanism rotates the index finger away from the middle finger about its pivot point.

An encoder motor gearbox located in the rear of the hand actuates the finger spreading mechanism. It transmits its torque via 1:1 spur gears (0.5 Mod, Ø of Bore 4mm, PCD 15mm and face width of 2mm) to the spreader lead screw assembly. The spur gear is located on the lead screw by a flange feature and a hexagon nut that fixes it against the flange. On either side of the spur gear the lead screw has been threaded. On the index finger side of the spur gear the lead screw has an M3 left hand (LH) threaded pitch of 0.5mm. On the ring finger side the M3 lead screw has a right hand (RH) pitch of 0.5 mm. On these screws the index and ring finger spreader nuts move. Beneath the little finger the lead screw has a sleeve inserted over it. This sleeve has an M10 RH thread with a pitch of 1.5mm. The little fingers circular spreader drive nut moves down this sleeve. As the motor rotates it causes the spreader nuts to move along the lead screw. The spreader nuts have rollers located on either end of them. These rollers are trapped within grooves within the top and palm cover plates. This forces the drive nuts to have in a linear motion along the lead screw. The motor end caps for the index, ring and little finger metacarpal blocks have guides. Each of these guides traps the drive nuts about their top and palm cover rollers. As the lead screw rotates, the drive nuts along it force the metacarpal blocks to rotate about their pivot bearings. The rollers moving along the open-ended guides compensate for the vertical component of the metacarpal's spreading motion.

The 3:1 ratio between the pitch on for the little finger drive nut and the ring finger drive nut causes the little finger metacarpal to rotate along the lead screw twice as fast as the ring finger metacarpal. (See Chapter 5: 'Background Theory' for more information on this mechanism). The left hand thread for the index fingers drive nut causes it to move down the lead screw in the opposite direction to the other drive nuts. Since most screws are machined with a right hand thread it was decided that the majority of the screw threads (i.e. the little finger and the ring finger drive nuts) would be right handed to reduce the costs. This is important as the lead screws thread will be one of the more costly parts to be manufactured even with the use of common (coarse) thread pitches.

Table 4.11 Spreader Drive Nut Threaded Hole Specifications

	Index finger drive nut	*Ring finger drive nut*	*Little finger drive nut*
Thread	M3 Pitch0.5mm LH thread	M3 Pitch0.5mm RH thread	M10 Pitch1.5mm RH thread

The lead screw is supported on each end by a deep groove (ID4 OD11 B4 EZO) bearing paired with a thrust (ID4 OD9 B4 Nachi) bearing. These bearings are supported on either end within the little finger side panel and the thumb side panel. The reason for the thrust bearing is due to the axial forces that the leads screw/drive nut motion produces. The motor will also be under a fairly large load due to the large number of friction surfaces within this mechanism so a large torque input through the spur gears is expected.

The guides on the motor end caps are located on the side of the pivot point (which is the side closest to the middle metacarpal block). The reason for this is so that when the fingers spread the guides have a minimum of vertical motion. Which reduces the guides length and hence the size of the metacarpal block. It also means that the drive nuts rest position is closer to the middle of the hand. That means the spreader screws support bearings are also closer to the centre of the hand. Because they are supported closer in the width of the palm is reduced.

The lead screw and sleeves of the spreader screw mechanism will be made of stainless steel, while the drive nuts are made of leaded bronze for its lubricating properties for reducing friction along the lead screw. Another design feature for the spreader screw assembly was the reason for the location of the spur gear in the middle of the palm. Normally the spur gear would be located next to one of the spreader screws support bearings to reduce the radial load on the screw. This was decided against in the design in favour of having the finger spreader motor being located in the same internal location blocks as the thumb rotation mechanism. This will reduce the manufacturing complexity and will make for a simpler palm assembly. The radial force from the location of the spur gear is fully supported by the deep groove bearings on either side of the spreader screw. Another design feature is the location of the finger spreading motor above the thumb rotation motor (so it is closer to the palm cover plate).

The placement of the fingers pivot point in the palm assembly was crucial for both the finger spreading motion and for the aesthetic appearance of the fingers. The pivot points were aligned along a line of approximately 13º degrees to the horizontal. This alignment was meant to mimic the 15º line the knuckles take within the human hand.

4.7.15 Finger Pivot Shaft Assemblies

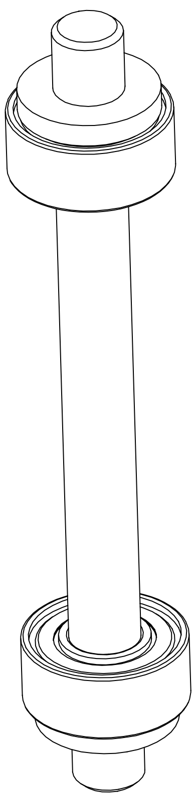

The finger shaft assemblies are used as the metacarpal pivots for the finger spreading motion. The pivot shaft assemblies have been designed so that the metacarpal blocks of the fingers rotated on the bearings located within them while the shaft is kept stationary between the palm assemblies cover plates.

The shafts have considerable bending stress across them from the finger gripping forces. The shaft material decided upon was Aluminium 7075. This is because its 0.2% proof stress of 480MPa was theoretically large enough to handle the finger loadings. However the factor of safety (FOS) for this material is a little low. Other materials/hardening techniques will be considered if this material after testing is found to be insufficiently strong. Steel grade 430 was also considered as a shaft material yet its yield stress of 410MPa was found to be too low.

Figure 4.53 Finger Pivot Shaft Assembly

The finger pivot shafts are assembled through the pivot holes in the thumb metacarpal block and then located between the palm and top cover plates. For each finger the pivot shaft is placed in the accompanying hole in the metacarpal block. Then the (OD7mm ID3mm B3mm EZO shielded) deep groove bearings are slid onto each end of the shaft until they are located flush with the top and of the bottom of the metacarpal. The bottom bearing should also be located on a flange on the shaft. The end of this shaft is then placed into the accompanying hole. The flange on the shaft is a design feature. If the shaft did not have a flange it is possible it could slide out of the palm. The flanges bottom surface may have an adhesive (Araldite or Loctite) added to keep the shaft located permanently in place on the top cover plate. An OD6mm, ID3mm and Breadth 1mm spacer is then added to the shaft end. The palm cover plate is then located on the rest of this shaft. There is a light push fit (H7-k6 size fit) between the shafts and the holes in the top and palm cover plates to keep the shafts accurately located and to prevent them from rotating.

4.8 Circuit Board, Wires and Sensors

This section is an overview of the electrical components within the hand. While this thesis did not involve designing the chip layout or the internal structure of the Printed Circuit Boards (PCB) it did have to incorporate the electrical components into the hand. However the components used in the circuit boards depended on the motor requirements. The basic properties for the motors used in the two hands are given in the below Table 4.12.

Table 4.12 Motor Data

	Max. Power (W)	*Voltage (V)*
Mini	0.46	6
Maxon	3.86	18

Each DC motor is fitted with a magnetic encoder. For the Maxon motor the encoder gives 16 quadrature (square wave) pulses per revolution digital output. The mini motor gave 10 quadrature pulses per revolution. The six wires out of the motor and encoder include; two motor wires (positive, and negative), a voltage supply wire, the ground wire, and the two channel wires.

Table 4.13 Motor and Encoder Data

	No. of Channels	*Lines per revolution*	*Wires Out*
Mini	2	10	6
Maxon	2	16	6

The initial idea for the electrical control of the hand was a single PCB located within the top cover plate of the palm assembly. The circuit board included connectors at the front of the PCB for connecting the wires from the motors to the circuit board. At this time the L6204 DMOS Dual Full Bridge Driver from SGS-Thomson Micro electronics was selected for the Pulse Width Modulation (PWM) control of the motors.

The motor control would be position dependent from the encoder data. The Force Sensing Resistors (FSRs) and the Hall effect switches would connect to connectors at the rear of the circuit board. The signals would then go through A/D conversion (since the resistors give an analogue output signal) and noise filtering op amps. All the signals and power control wires for the sensors and motors connect into a single Field Programmable Gate Array (FPGA) microprocessor. Due to the large number of wires that would connect into the FPGA its size would take a considerable portion of the board. The FPGA would then reduce the control wires for the hand to five wires that would connect out the side of the PCB to a computer. The five wires would have been two (twinned) serial links for the positional control, two voltage wires and one clock signal wire.

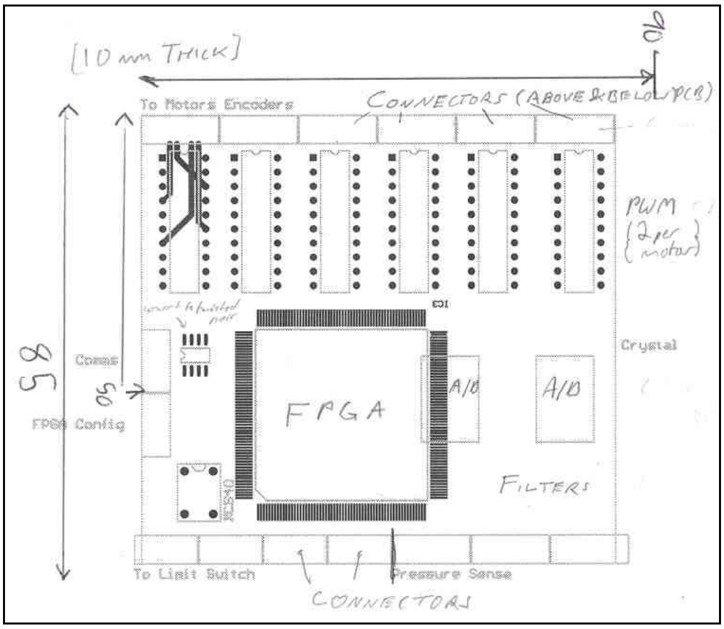

Figure 4.54 Original PCB Layout for a single PCB for the entire hand

There were several problems with the design for this circuit board. Firstly the PCB size was so large as to give an unsightly appearance to the hand. It was estimated the size would measure approximately 90mm wide by 85mm long. Secondly there would be so many wires coming out of the fingers that its spreading motion would be hampered. Each motor has six wires coming out of the motor and encoder for both the Maxon and the Mini motors. Multiplying this by two for the other motor and adding it to the wires from the Hall effect sensor (three wires) and the FSRs (five wires) and there are twenty wires exiting each finger. Even bundled together the wires would have poor flexion and high resistance to motion. The thumb also would have this problem with the wire stiffness interfering with the thumb rotation motion. With this PCB arrangement the thumb would have thirteen wires (six encoder wires, six FSR/Hall effect wires) exiting from itself into the hands PCB. The motor and the FSR wires since they connect to different locations on the PCB would also have to loop awkwardly through the hand. Overall this PCB design would be difficult to incorporate within the palm due to the large number of wires in the hand and the size of the board.

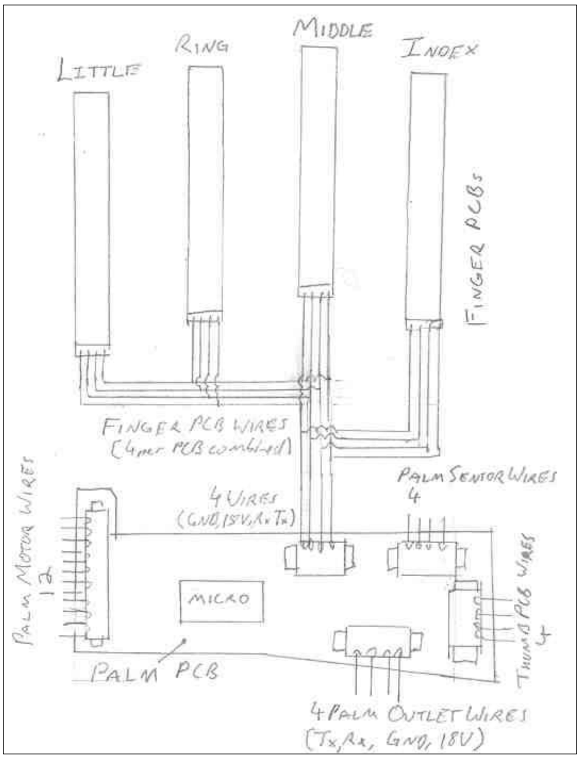

It was decided that for the hand to function with all its degrees of freedom the number of wires moving through the palm had to be reduced. Instead of a single large PCB in the palm that would have all the wires entering into it there would be a number of smaller boards. There would be a PCB within the metacarpal blocks for the each finger, a PCB attached to the thumb and a PCB located within the palm of the hand. The numbers of wires within the hand are reduced considerably. With this design there are only four wires exiting each PCB.

Figure 4.55 Approximate Diagram for the Wiring in the Canterbury Hand

The sensors used in the final hand design are varied, but can be divided into two types. The first type is for position measurement. These include measuring the angular position of the motors using the digital encoders on the motor. Also Hall effect switches are used for zeroing the digital encoders when the finger/thumb drive nuts are at their maximum forward position along the leadscrew. The other type of sensor was used for force measurement. These included the FSRs on the finger and thumb linkages as well as the larger palm FSRs. The current to the motors will also be measured to give an indication of motor torque. If the motor stalls due to too large a load then the control program for the hand will turn off the motors to prevent overheating. Temperature sensors may later be added as another level of control to prevent overheating.

4.8.1 Design Objectives

The design objectives for the electrical components for the hand were:

- To create locations within the fingers, thumb and palm assembly for PCBs
- To maximise area and volume available in the hand for locating PCBs
- Reduce the length of the motor wires to the PCB (to reduce noise)
- Integration of Hall effect switches with magnets in the finger and the thumb metacarpal blocks.
- Testing of Hall effect switches for finding optimal clearances with magnet
- Selection and location of FSRs for fingers, thumb and palm assembly
- To design wire paths through the hands to the circuit boards
- Select connectors for connecting PCBs to wires
- To Locate Connectors on PCBs and within components

4.8.2 Circuit Boards for fingers, thumb and palm

Each circuit board in the new PCB layout design of the hand is controlled by a single microchip; the 28 lead PSoC (Programmable System on a Chip) from Cyprus Microsystems.

The original design requirements for the PCBs were for multiple chips. That is they would have held a driver chip for the PWM, A/D conversion chips, Op amps for filtering the signals, a DC voltage converter and a micro. The new PSoC microchip is versatile as it does both PWM for the motors, and the A/D conversion for the FSRs and the Hall effect switch.

The overall size of the chip is small. It measures 10mm long by 5mm wide, and is 2mm thick and is surface mounted on the PCB. The small size means that there is considerably more surface area on the PCB available. The dimensions of the PCB however are driven by the size of the connectors. The microchip reduces the wires exiting the PCB to four wires. These wires are for the +18V voltage supply, Ground (GND), and the Transmit (Tx) and Receive (Rx) serial wires.

The size of the PCB is dependent on the surrounding geometry. The thickness of the PCB is expected to be 1mm to 1.5mm. The wires in the hand will be held in place within the wire path recesses by RTV.

Finger Circuit Board

The finger circuit board has eight wires entering into the front connector and twelve motor wires entering in the rear connectors. The wires on the PCB connect them to the PSoC microchip.

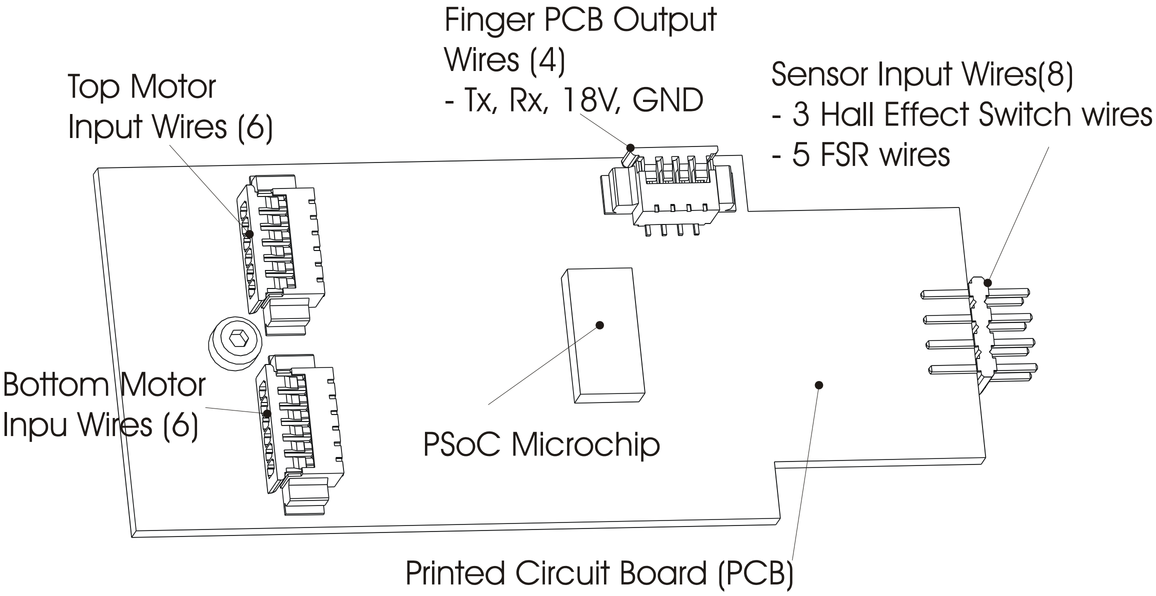

Figure 4.56 Finger (CB) Circuit Board

The eight wires entering the connector have five wires from the FSRs and three wires from the Hall effect switch. The Hall effect switch's three wires are comprised of the signal output, voltage supply and the ground. Each finger has four Force Sensing Resistors (FSRs) along its linkages. There are two FSRs on the distal link, one on the medial link and one on the proximal link.

FSRs are a polymer thick film device that has a decrease in resistance when force is applied across its active area. This results in a greater voltage for the return signal. FSRs do not give precise measurements of the force however due to their non-linear output. The FSRs selected for the finger were Part #400 from Interlink Electronics. They have an active area diameter of 5mm and a thickness of 0.3mm and a tail length of 38.1mm.

Each FSR has two wires. This would mean a potential of eight wires for the FSRs. This total can be reduced by combining the input voltage wire for each of the FSRs along the length of the finger. This reduces the wires to five; four return signal wires plus the supply (as the input). If these are added to the Hall effect switches wires the number of wires entering the finger's PCB connector has been reduced to eight total.

The front connector is a 2mm pitch, 4 ways, double-row, top entry socket, and straight pin header from Harwin Inc. The straight pin header is soldered onto the end of the circuit board. This connector holds and locates the PCB on the side of the metacarpal. The PCB is fixed in place by a single M2 cap screw. The socket for the wires is gripped within the metacarpal assembly between the inside face of a metacarpal block and the side of the internal bearing housing. The PCB when the cap screw is unscrewed can be levered out of the socket easily.

Each motor has six wires in a strip that exit the motor through the end cap. They then loop back along the side of the metacarpal block past the motors to connect to the PCB. Each strip of wires has a connector. Since the wire strip is parallel with the surface of the board the connector needed to have a 90º header for the receptacle. The pitch of the wires was needed to get the correctly sized connector. The pitch is defined as the diameter of the wire, or the distance between wires in a flat cable. The pitch for both the Maxon and the Mini motor wires was found to be 1.25mm. This was calculated from the width of the wire strip, which had six wires over 7.5mm. The connector for the wires also needed to be surface mounted onto the PCB to reduce how far the components stuck outside the finger. The selected connector was chosen for it being the smallest size for these parameters. It is a surface mounted (SMT) 6 way 90º header, with a crimp terminal housing receptacle from Molex. While the department does not have a crimp tool the crimps may still be attached to the wires with needle nose pliers.

The four wires exit from the PSoC microchip through a surface mounted connector along the topside of the PCB. The connector selected was a 1.25mm pitch 4-way 90º header and crimp terminal housing receptacle from Molex. The pitch was selected to be small so that the wires moving through the palm assembly would have a lesser profile. The wires loop over the motors and down the metacarpal alongside the finger's pivot shaft to the wire groove in the top cover plate. From there they go to the palm assembly's PCB.

Thumb Circuit Board

The thumb circuit board has 6 wires entering the circuit board from the motors and 6 wires from the Hall effect switch and the FSRs. The thumb circuit board functions similarly to the finger circuit board. That is the wires on the PCB connect then to the PSoC microchip.

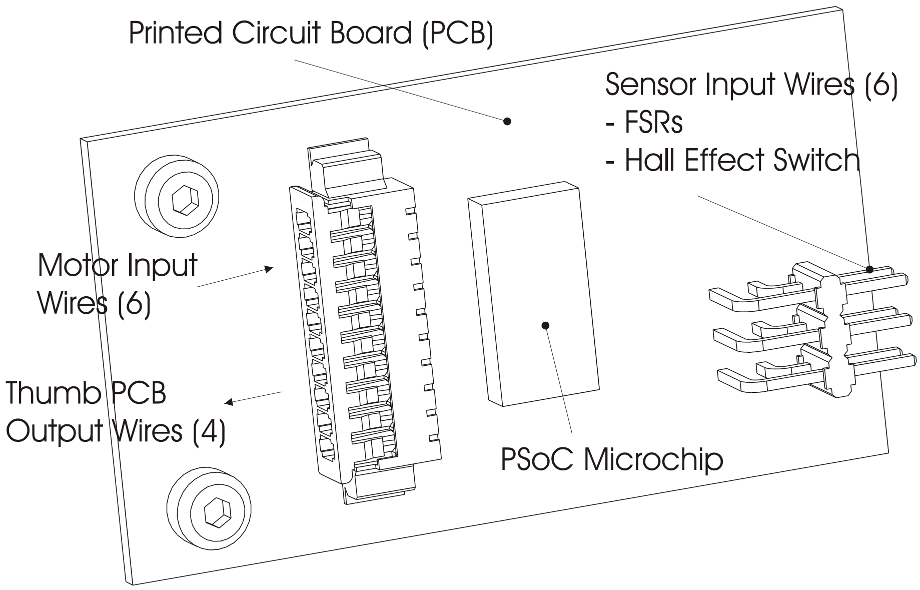

Figure 4.57 Thumb (CB) Circuit Board

Within the thumb there are three FSRs on the thumb linkages (two on the distal, one on the proximal) and a Hall effect switch within the metacarpal block. The 6 wires entering the PCB from the sensors may be broken up into the three signals from the FSRs, the signal wire from the Hall effect switch, the ground and the common (to Hall effect switch and FSRs) supply voltage wire. The FSR wires travel through the thumb to exit outside the B2 bearing joint of the proximal link. The Hall effect switch wires exit from within the metacarpal assembly through one of the front actuator link holes. The FSR and Hall effect wires are soldered onto the PCB socket that connects at the front of the metacarpal block.

The wires are soldered onto a socket located between the metacarpal blocks under the thumb bearing housing. The socket is a 2mm pitch, 3-way, double row socket from Harwin Inc. The thumb PCB plugs into the socket with a 3 ways, double-row, 90º-pin header from Harwin Inc.

The header needs to be 90º so that the socket has its tail prongs facing outside the metacarpal block so that the sensor wires may be soldered onto it.
The motor wires and the exit wires are located within the same connector. That is a 10-way single row, 1.25mm pitch, 90º header, and crimp terminal receptacle from Molex. The reason for using a single connector was that there was not enough width across the thumb circuit board to fit two connectors across.

The thumb wires leave from the thumb's encoder motor gearbox through a hole within the rear of the motor end cap under the rear strut. The wires loop back underneath the thumb metacarpal block to connect with the rear of the PCB. The six thumb wires enter the receptacle on one side of the housing.

The four exit wires from the microchip leave the PCB from the other side of the connector. The exit wires travel under the metacarpal and the motor end cap and down a wire groove on the inside of the rear strut of the motor end cap. The wires then travel past the rear thumb rotation shaft, and into the palm assembly through a hole in the palm cover plate. They then connect to the palm assemblies PCB.

Palm Circuit Board

The wires entering the palm PCB are from the finger PCBs, the thumb PCB, the palm motors, and the FSRs on the palm. The GND, Tx, Rx and 18V supply voltage wires from each fingers PCB are combined (soldered together) within the inner surface of the top cover plate. This reduces the number of wires travelling through the palm assembly and connecting to the palm PCB to four wires. These four wires travel along the wire groove in the top cover plate, around the side of the finger spreader drive nut recess and into the palm motor space.

The two palm motors are the encoder motor gearboxes for the finger spreading and thumb rotation mechanisms. The rear of the motors is kept within the little finger side panel. Six wires in a strip exit from the rear of each motor's encoder and pass through the exit slot. The twelve wires loop up and back to connect into the palm circuit board. The connector for these wires is a single row 12-way, 1.25mm pitch, 90º header, and crimp terminal receptacle from Molex. The reason that a single row connector was selected was to reduce the height of the circuit board.

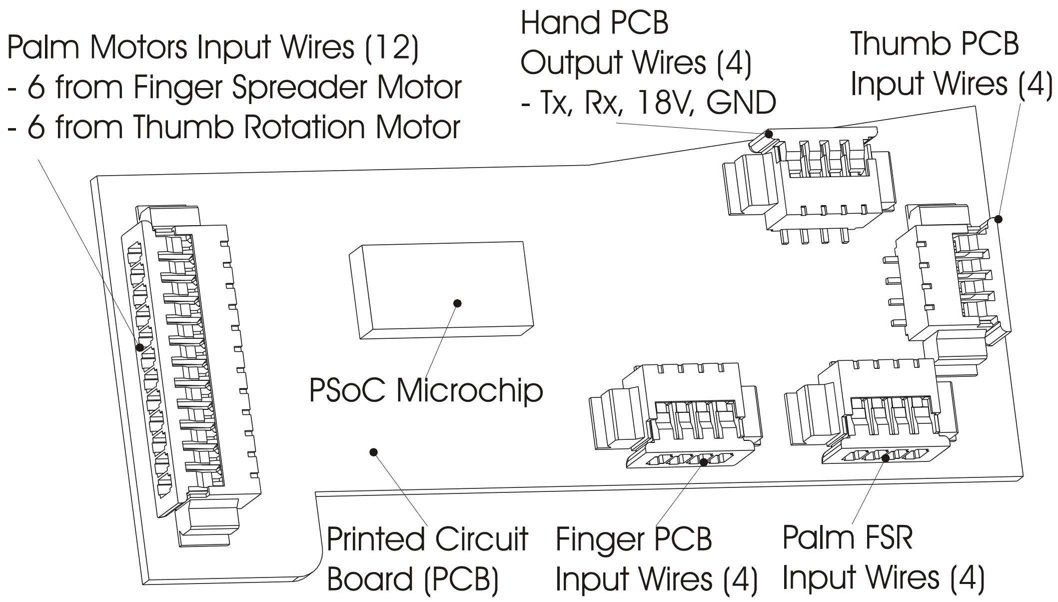

Figure 4.58 Palm (CB) Circuit Board

There are three large FSRs on the palm of the hand. The FSRs selected are Part #406 from Interlink Electronics. The active area is rectangular, unlike the smaller FSRs, and is 38mm by 38mm. The thickness of the FSR is 0.46mm and a length (with tail) of 83.8mm. There are four FSR wires that connect to the palm PCB; three return signal wires, and one common voltage supply wire. The wires connect to a 4-way single row, 1.25mm pitch, 90º header, and crimp terminal receptacle from Molex. The wires have a wire recess down the length of the palm. The wires enter the palm PCB through a gap between the palm and the CB access panel.

The four wires from the thumb PCB exit the rear thumb strut and enter the palm assembly through a gap in the palm cove plate. The wires then pass through a gap in the wrist side motor holder and into the palm assembly PCB. They then connect into a 4-way single row, 1.25mm pitch, 90º header, and crimp terminal receptacle (from Molex). This connector is orientated facing the thumb on the far right hand side of the palms PCB.

The wires from these various features all enter the PSoC microchip located on the PCB. The exit wires exit the hand via another 4-way single row, 1.25mm pitch, 90º header, and crimp terminal receptacle at the rear of the PCB. They exit from the palm through a gap in the CB access panel.

The exit signal wires will then travel from the PCB to a computer via an ISA bus slot. The computer will control the hand via the motor position (from the encoders) and force feedback control (from the FSRs, Hall effect switch). The computer will also control the constant current control and power supply for the hand. Eventually a prosthetic Canterbury Hand device will be developed. The hand in this case will need to control the hands by a combined 18 V battery pack with a control board using a Digital Signal Processor (DSP).

4.8.3 Hall Effect Switch and Magnet Test

The Hall effect switch is used within the metacarpal blocks of the finger and the thumb. They are used as a position control for the finger by zeroing the encoder when the drive nut magnet interrupts the current passing through the switch. The Hall effect switch is positioned so that the magnet interrupts the current at the extended linkage position. This occurs when the drive nuts are at their furthest position to the front of the finger.

The original concept for the positioning of the Hall effect switches within the finger metacarpal assembly came from Judith Taylor's thesis [1998]. Taylor proposed two arrangements using the Hall effect for zeroing the encoders within the motor. The first proposed method was to have a magnet and a Hall effect switch per drive nut. The magnet would be attached to the moving drive nuts while the switches would be kept stationary on one side of the metacarpal assembly. The second solution used a common Hall effect switch between the two magnets and drive nuts. This solution only required three wires within the metacarpal block unlike the six wires of the previous arrangement. It also reduces the number of components from four to three. It also fulfilled the original function of indicating when a drive nut reached the end of the lead screw. The software controlling the hand would be able to tell which nut from the encoder's position data. This idea was incorporated into the current Canterbury finger design and is shown in Figure 4.59.

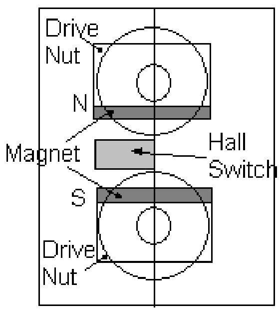

Figure 4.59 Hall effect switch placement in the Canterbury Finger

The Hall Effect IC Switch as quoted by the RS Catalogue [RS Components p.967] as a "miniature semiconductor proximity switch utilising the Hall effect to give 'bounce free' switching when influenced by a magnetic field." That means as soon as the magnetic field of the magnet is in range the Hall effect the switches state will change. The catalogue goes on to state that switching occurs at distances of typically 2mm. (Since the Hall effect switch is not mounted on a ferromagnetic surface the distance will not be increased.) This distance needed to be verified experimentally, as the encoder requires exact positioning of the switch.

The switch is magnetically unipolar i.e. each face on the switch is dependent on a single particular magnetic pole for the switching effect. On the Hall effect switch is a round mark indicating the face that should face the southern pole of the magnet. The other side of the switch (with the dimple) will switch with the northern pole of the magnet. The polarity of the switch had to match the opposite pole of the magnet in the metacarpal assembly.

The magnets were measured to have dimensions of 3mm length x 2mm wide x1mm high. They were supplied from Dr Dunlop and some unknown supplier. The Hall effect switch is 4.7mm long x 4.5mm wide x 1.5mm high. Three wire legs protrude from the base width of the Hall effect switch. These wire legs are for the switch's signal output, voltage supply and ground. Wires are soldered onto the legs, and these wires are eventually connected to the PCB. Hall effect switches are available from many common electrical suppliers, such as Farnell or RS Components.

The aim of the testing of the Hall effect switch was to find and verify the positions and distances at which the magnet caused the switch to change. Also the minimum safe distance between the magnets needed to be found for the positioning of the drive nuts in the finger metacarpal assembly. If they were too close together (on either side of the hall effect switch) their magnetic attraction could cause problems with the lead screw motion or even fracture of the magnets.

The minimum safe distance was found by subjectively measuring the attractive force of the magnets over distance. The method of the test was to have a single magnet attached to a heavy piece of ferrous metal to keep it in place. A small piece of steel (a paperclip) was held at a distance above the magnet. A ruler was held against the side of the metal to measure the vertical distance of the paper clip to the magnet. The paperclip is approximately 30mm long and is held quite firmly at one end throughout he experiment. As the paperclip was brought closer to the magnet it could be seen to be dipping below the horizontal towards the magnet. As the effects became stronger the strength at the height was noted. There is a small but noticeable tug at around 5mm above the magnet. This effect has quite a strong tug at about 3mm. At 2mm the attractive effect is so strong that the paper clip connects with the magnet.

The experiment was conducted again with an additional magnet that is magnetically connected to the paperclip. The magnet was secured to the paper clip with a piece of sellotape. Using this method an attraction was felt at 6mm. This was far stronger at around 3mm to 4mm. At 2mm there was a very strong attraction that caused at 1mm the magnets to touch.

Overall it was recommended that the magnets should be separated from other magnets and ferromagnetic materials by at least 2mm. The design of the metacarpal assembly of the finger has a separation of 5mm for the Maxon configurations and 3mm for the Mini motor configurations. This separation should be sufficient if the magnets are glued with a sufficiently strong adhesive (araldite) to the drive nuts.

The second stage of testing was the testing of the magnets switching distance for the Hall effect switch. A small test board was set up where the Hall effect switch was in series with a resistor and a Light Emitting Diode (LED). The board was powered by a DC power supply. When the magnet was not acting on the test board the LED remained lit. Finding the correct poles on the magnets to use with the switch was reasonably simple. The large cross sectional face (pole) of the magnet was tested over the Hall effect switch across the circularly marked face. When a compatible pole was found the LED turned off, indicating the Hall effect switch had switched. A ruler was set up perpendicular to the large flat face of the Hall effect switch. The magnet was stuck to either a paperclip or a piece of plastic depending on the test. The magnet was then moved over the Hall effect switch to see at what point the LED turned off and at what position the magnet was over the switch.

The magnet switches the LED and hence the Hall effect switch off at distances of approximately 2mm or less. The effect occurs when half the magnet crosses the outer edge of the Hall effect switch. It was found that the material (paperclip or plastic) that supported the magnet did not affect the effect distance. Materials around the Hall effect switch like wise had little effect as long as there was no material between the magnet and the switch. Thus the holding of the Hall effect switch on the external bearing block shelf (with the gap for the magnets travel) in the finger would have no effect on the effective distance of the magnet.

It was also found that the Hall effect would occur in the switch without problems if it had Aluminium material around it. However the design of the external bearing block has only a small amount of material around the ledge that the Hall effect switch attaches to. This should not cause any interference with the Hall effect switch's operation.

The results of these tests were implemented in the Canterbury Hand. The first application was in the Canterbury fingers. The positioning of the Hall effect switch had to have its leg wires facing directly across the width of the metacarpal assembly towards the wire gap between the drive nut recesses. The reason for this was to reduce the interference the wires may have with the motion of the drive nuts as they connect to the legs of the switch. The manufacture of the external bearing housing within the finger required that the Hall effect switch be positioned directly down the centre plane of the finger. Thus the Hall effect switch was positioned from these requirements. This meant that only the positioning of the magnets was needed.

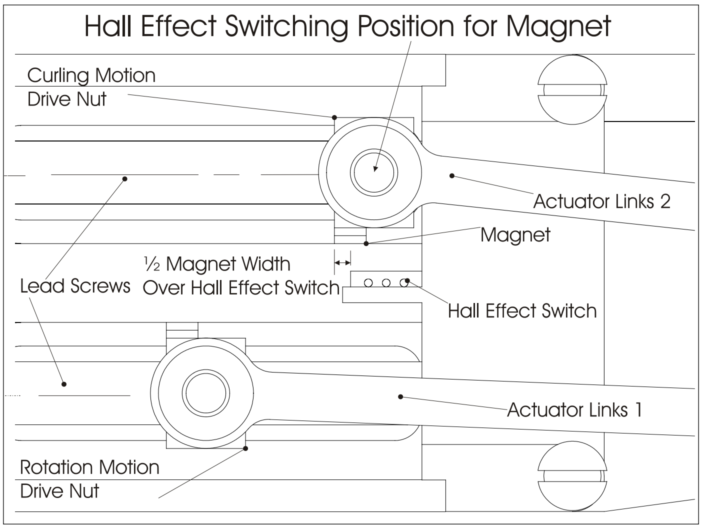

Figure 4.60 Finger Nut Hall effect Switching Position

Due to the Hall effect switch overhanging the lead screw the magnet needed to be a certain distance back on the drive screw. The magnets were placed so their long side were collinear with the length of the drive nut alongside its rear face. This reduced the distance the lead screw had to travel to activate the Hall effect switch, and with it the width of the drive nut. The clearances for the Hall effect switch and the magnet was set to 1.75mm for the Maxon motor configurations and 0.75mm for the Mini motor configurations of the fingers. The clearance between the magnet and the Hall effect switch was set to 1.5mm for the Maxon motor and 1mm for the Mini motor designs. The reason for this decrease was due to the

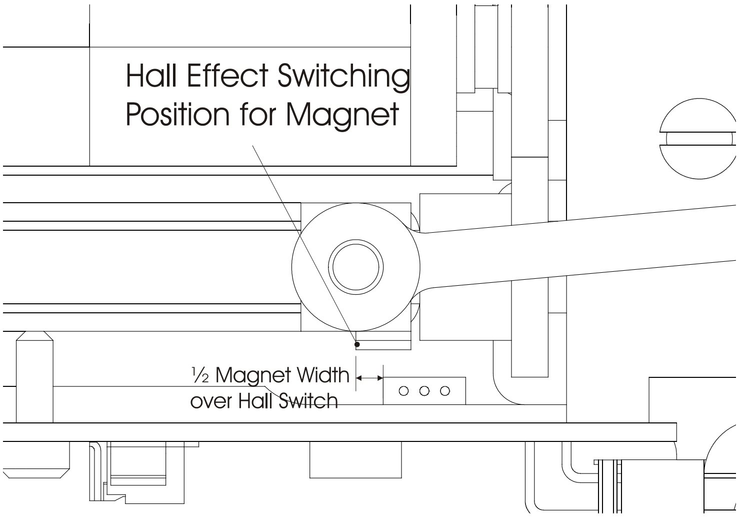

separation distance of the lead screws and the manufacturing constraints for the drive nuts. However it was deemed that a separation of at least 0.5mm was sufficient for minimum clearance. If the clearance was between this minimum value and 2mm it was deemed acceptable.

Figure 4.61 Thumb Drive Nut Hall effect Switching Position

4.9 Expected Results

There were a number of objectives for the Canterbury hand design. They included designing the hand to be anthropomorphic using the linkage designs found from previous theses for the finger and thumb models. The Canterbury Hand design of this thesis will be a prototype robotic hand that will serve as a test bed for the eventual development of a prosthetic hand. Two different types of motors (Maxon and Mini motors) had been bought by the University before this thesis for use in the Canterbury Hand designs. These were the Maxon motor and the Mini motor. Both motors had to be incorporated into the design of the hand. Thus two hand designs were modelled within the same CAD model by this thesis as two different configurations. The larger, heavier and stronger gripping hand design uses the Maxon encoder motor gearboxes. The smaller, lighter hand uses the Mini encoder motor gearboxes. However both hand designs are have similar motions.

The Canterbury Hand design of this thesis is a robotic end effector of 11 degrees of freedom. Both the Maxon and Mini motor hand designs are right handed and anthropomorphic. Each hand has four fingers, and a thumb. Each of the fingers is a multi-bar linkage that has two degrees of freedom. The thumb is a single degree of freedom multi-bar linkage. Within the palm assembly of the hand are motors for the finger spreading and thumb rotation mechanisms. The one-degree of freedom fingers spreading mechanism gives a maximum of 13.5º spread between the fingers. The one-degree of freedom thumb rotation mechanism gives a maximum thumb rotation of 114.5º for the Maxon hand and 115.5º for the Mini hand. The motions of the fingers and the thumb have been designed to mimic the human hand.

The SolidWorks CAD model of the hand was used to give values for the expected size and eventual weight of the hand. The masses, for example, are calculated automatically by the CAD program for a given density for each part in the model. However the values given can only be considered as close approximations to the eventual size and weight of the manufactured hand. Many smaller parts and materials, such as the wiring and adhesives have not been added to the model (due to complexity), which will add weight to the design. The manufactured hand will also have material removed from certain parts where strength or appearance is not an issue so as to minimise weight.

4.9.1 Finger Characteristics

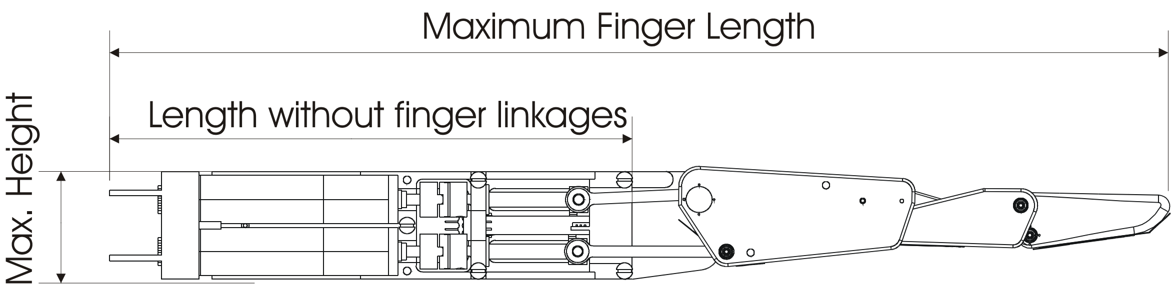

Figure 4.62 Finger Dimensions

Table 4.14 Middle Finger Mass and Dimensions

Middle Finger	*Finger Mass (g)*	*Max. Length (mm)*	*Max. Height (mm)*	*Max. Width (mm)*
Maxon	306 (224.7)	286 (136.5)	29	26
Mini	227.6 (151.7)	258.7 (113.2)	26	26

Note: (#) refers to a measurement without the finger linkages

The table above (Table 4.14) gives the values for the mass and dimensions for the Middle fingers of the Maxon and Mini motor hands. The Mini motor finger has a lighter weight and smaller length and height. The height is reduced due to the smaller separation and motor diameter between the drive screws of the Mini motor configurations (11mm separation) with the Maxon motor configurations (14mm separation). The length is reduced because the Mini motors have a smaller length (of 41mm) than the Maxon motors (of 61.5mm). The drive screw and finger length is very similar for both motor types so it does not contribute to the length of the fingers.

The Maxon finger is as expected heavier than the Mini motor finger. The mass of the finger is largely dependent on the motor sizes. The finger weighs 218.8g without the motors for the Maxon configuration and 192.8g for the Mini configuration. This shows that the metacarpal and finger linkages weigh very similarly without the motors. The prototype finger made by Ward has a mass of 207.5g using the Mini motors. This finger on comparison with the Middle Mini finger (which weighs 227g) seems to weigh slightly less. What this comparison does not show is that the Ward finger length is only 117mm (without the metacarpal) and has been machined from thin panels that have large weight saving holes along their length. The Mini motor design of this thesis has a finger length of 145.5mm, which is considerably longer. The manufacture of the fingers is also far more solid and has not had weight saving holes machined down its length. The reason for this was that the fingers were to be as anthropomorphic as possible. Having large holes along its length would defeat this purpose. From the Table 4.14 it can be seen that the mass of the fingers is approximately thirty percent of the total mass of the finger using the design of this thesis. The Ward prototype finger has a far smaller mass percentage for its finger linkages. Its metacarpal block on the other hand is far less efficient for weight saving than the current finger design.

The width of the fingers is dependent on the separation of the actuator links. This in turn is dependent on the diameter of the front support bearings (deep groove and thrust bearing) within the external bearing housing. The size of these bearings is the same for both the Maxon and the Mini fingers. This is because the bearings are already at their smallest compatible available sizes. Thus the fingers have the same width.

4.9.2 Thumb Characteristics

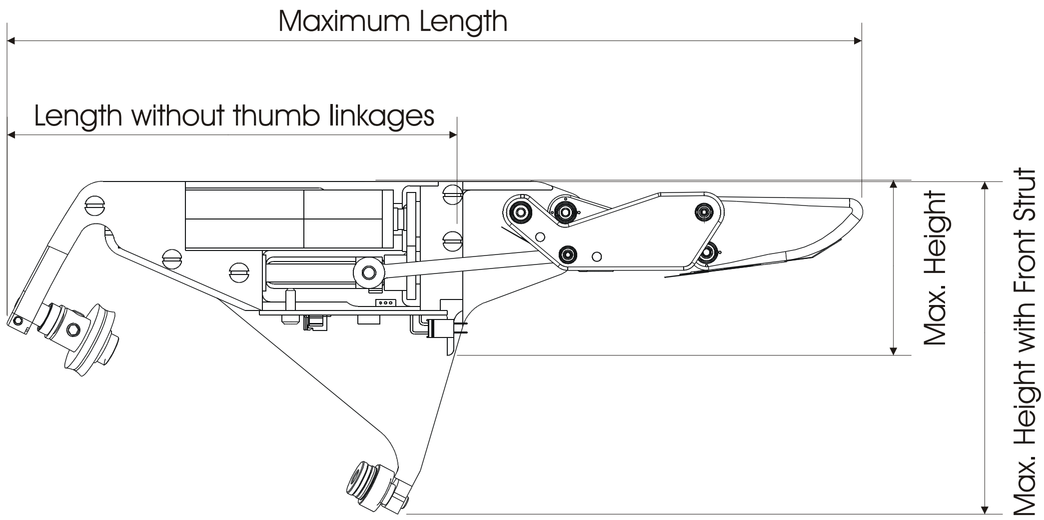

Figure 4.63 Thumb Dimensions

Table 4.15 Thumb Mass and Dimension

Thumb	*Thumb Mass (g)*	*Max. Length (mm)*	*Max. Height (mm)*	*Max. Width (mm)*
Maxon	274.4 (219.8)	192.5 (102.2)	39.4 or 75 with struts	28
Mini	214.5 (164.1)	176.8 (87.6)	27.3 or 72.9 with struts	26.5

Note: (#) refers to a measurement without the thumb linkages

The thumb mass and dimensions are given in the above table (Table 4.15). From the table it can be seen that the thumb mass is heavier for the Maxon motor design than it is for the Mini motor design. Without the motors the thumb weighs 197g for the Mini configuration and 230g for the Maxon configuration. Thus the extra mass is partly due to the weight of the motor. However unlike the middle finger the motors in the thumb are completely enclosed within the metacarpal block. The thumb is also considerably larger in the Maxon configuration for length, height and width, which adds to the mass.

Unlike the finger the width of the thumb is less in the Mini configuration. Like the finger the width between the actuator links determine the width of the thumb. The actuator link width though is dependent on the diameter of the spur gears (addendum circle plus 1mm clearance). The spur gears pitch circle diameter (PCD) is equal to the minimum clearance between the lead screw and the motor. This clearance is greater in the Maxon configuration due to the larger diameter of the motor.

The length and height of the thumb is dependent on the size of the motor. Since the Maxon motor has a longer length the metacarpal assembly that holds it is longer. The height is dependent on the diameter of the spur gears, which is in turn dependent on the size of the motor and the drive nut. The size of the rear strut from the motor end cap and the front strut on the left metacarpal block are dependent on the angle of the thumb rotation axis.

4.9.3 Palm Assembly Characteristics

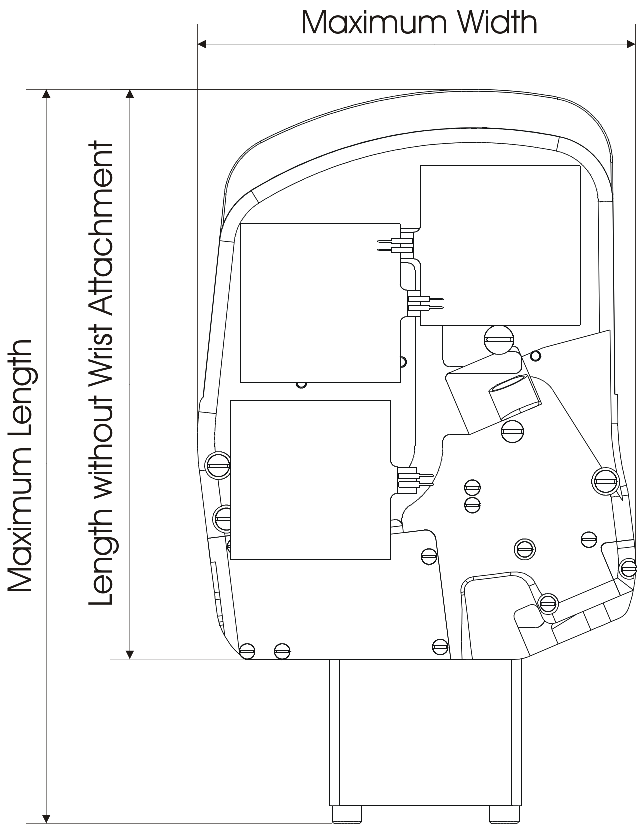

Figure 4.64 Palm Assembly Dimensions

Table 4.16 Palm Assembly Mass and Dimensions

Palm	*Mass (g)*	*Max. Width (mm)*	*Max. Length (mm)*
Maxon	748.8 (577.5)	126	234 (176)
Mini	660.7 (508.7)	126	210.5 (152.5)

Note: (#) refers to a measurement without the wrist attachment.

The palm assembly's mass and size is described in the above table (Table 4.16). The masses of the palm assembly do not include the masses of the finger spreading and thumb rotation mechanisms, nor any of the finger or thumb parts. Without the wrist attachment assembly at the base of the hand, which is solid aluminium, the mass of the Maxon palm assembly is very similar to the mass of the Mini palm assembly. The difference is from the extra length and depth the Maxon configuration gives to the palm assembly's mass.

The depth of the palm assembly is dependent on the height of the finger. The Maxon fingers are 29mm high and the Mini motor fingers are 26mm high. This 3mm difference also led to the 3mm difference in height between the Maxon palm assembly and the Mini palm assembly. Each cover plate for the palm was 3mm thick with 1mm clearance between the finger and the plate. (Note that the depth of the palm assembly is the same as for the hand assembly. The values for this are given in Table 4.17.)

The length of the Maxon palm assembly is longer than the Mini motor configuration. This is due to the extra length of the finger metacarpal blocks. The cover plates were designed to cover as much of the metacarpal blocks as possible, which translated to extra length. This also leads to a longer hand (see Table 4.17 values for length without the wrist attachment).

From the dimensions in this table it can be seen that the width of the palm (126mm) is the same for the Maxon and the Mini motor hands. The reason for this is that the width of the hand is dependent on the combined width of the fingers. From Table 4.14 the width of the Middle finger was shown to be the same for both the Maxon and Mini motor configurations at 26mm. This width is the same for the Index, Ring, and Little fingers as well. Given that the clearances and the material needed to support the fingers is the same the width of the hand is the same for both the Mini and Maxon configurations.

4.9.4 Hand Characteristics

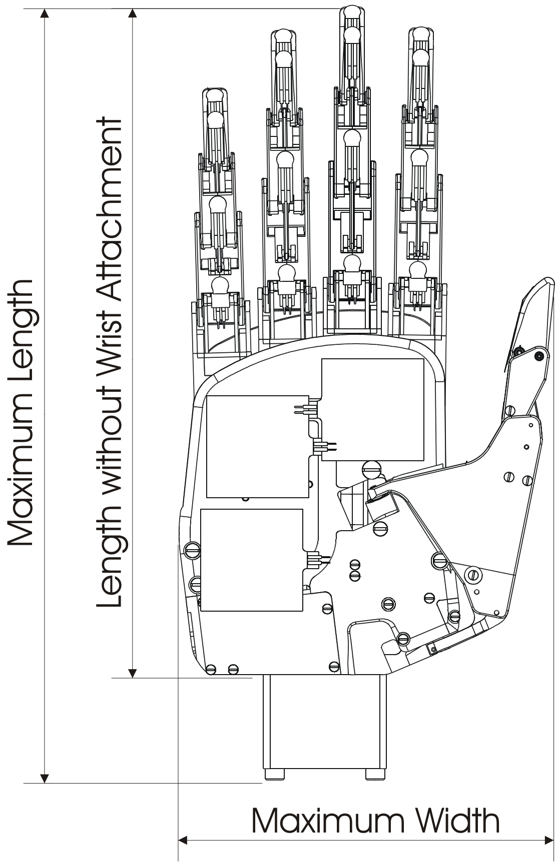

Figure 4.65 Hand Dimensions

Table 4.17 Hand Mass and Dimensions

Hand	*Mass (kg)*	*Max. Width (mm)*	*Max. Length (mm)*	*Depth (mm)*
Maxon	2.48 (2.3)	166.5	373.8 (326.5)	40.5 (37)
Mini	1.92 (1.8)	169	347 (300)	37.5 (34)

Note: (#) refers to a measurement without the wrist attachment or the Palm Cover Mould

This table (Table 4.17) gives the masses and dimensions for the Maxon and Mini hand designs. It can be seen that both hands are very similarly sized. There is only 2.5mm difference between the widths and 3mm in difference between the depths of the two hands. The palm assembly width is the same for both the Maxon and Mini motor hand configurations. Thus the difference is dependent on how far the thumb sticks out the side of the hand when it is in the rest position. The Mini motor configuration has the thumb sticking further out the side of the hand. This was due to the shape of the palm assembly having to require the thumb to have a larger (Main Axis angle and Angle2) angle for clearance when rotating.

The Maxon hand is 2.48kg in total weight, while the Mini motor hand is 1.92 kg. The reason for the difference is that the combined extra masses of the Maxon fingers thumb and palm assembly sum up to create a heavier hand than the Mini configuration. Both hands are still far too heavy for a prosthetic device, which would require a hand to weigh less than 400 to 500g.. However both hands are still lighter than the majority of other similar sized, and functional experimental robotic hand designs. A lot of these experimental designs unlike this hand do not include the weight of their actuator devices. Some of the smallest weight designs are the Anthrobot-2 and Hitachi robotic hands, which weigh around 4 to 5kg. The weight of these Canterbury hand designs is also larger than Wards original estimate of 1037.5g for the weight of the hand. However this estimate was based on a simple hand of five fingers, with no palm assembly or finger spreading or thumb rotation mechanism.

4.9.5 Hand Grasp Types

The Canterbury hand can make a large number of the grasp types that a human hand is capable of making. In particular the hand can form (with both the Maxon and Mini motor hand designs) the six generic grasps that have been described in section 2.2.4.2. That is Fingertip Prehension, Lateral Prehension, Palmar Prehension, Spherical Grasp, Cylindrical Grasp, and Hook Grasp. These grasps are illustrated using the Canterbury Hand in the below figures.

Fingertip Prehension and Spherical Grip

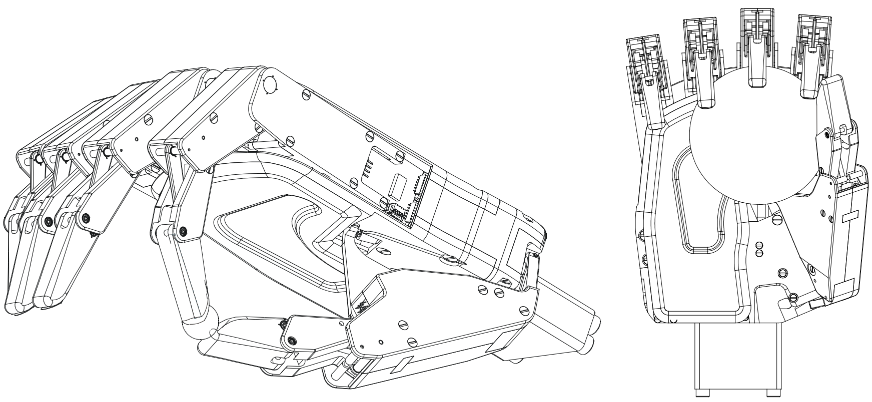

Figure 4.66 Fingertip Prehension and Spherical Grip

The Canterbury Hand can form fingertip prehension over limited ranges with both the index and middle fingers. It can even oppose the thumb with the ring finger. However the size of the fingers is such that it can only handle a minimum size of object. From viewing the parametric model it seems that a minimum size of 10mm diameter for a sphere will be possible for basic grasping. If a fingernail projection was used on the finger and thumb tips the size of the minimum sized object may be decreased. For a large spherical grasp the fingers of the hand have to be abducted. It is estimated that the hand may hold a sphere of approximately 110mm. However both these grips depend on the surface smoothness of the objects held.

Lateral and Palmar Prehension

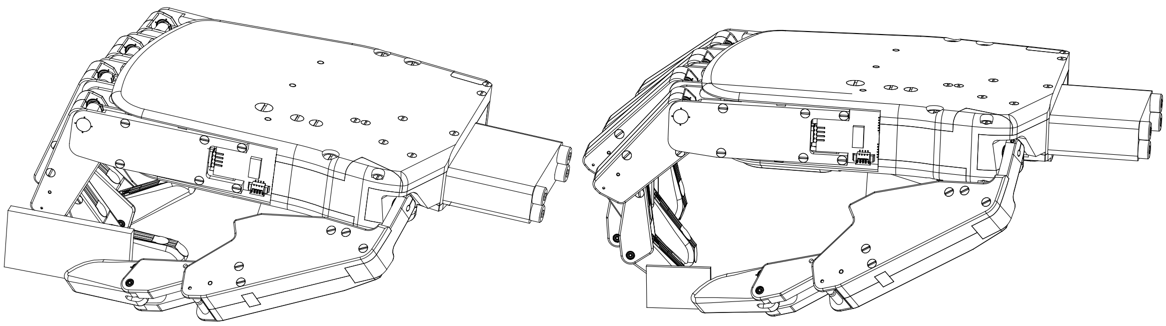

Figure 4.67 Lateral and Palmar Prehension

The Canterbury hand can make both lateral and palmar prehension between the index finger and the thumb for varying sized flat objects. Overall there is a wide range of positions along the index finger that the thumb can grasp against.

Cylindrical and Hook Grasp

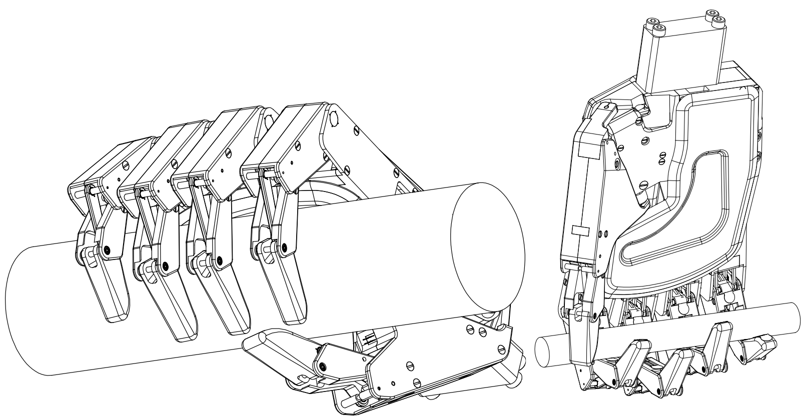

Figure 4.68 Cylindrical and Hook Grasp

The hand can also grasp cylindrical objects in both a cylindrical grasp and a hook grasp. The minimum size of the cylindrical object for gripping on the palm is approximately Ø20mm and the largest size is approximately Ø70mm. Hook grasps are possible for cylindrical objects of around a minimum size of Ø10-15mm up to approximately Ø60mm. The length of the gripped objects is independent of the grasping type.

In addition to these generic grasp types, the hand can make a large number of the various other grasp types as specified in the Cutkosky and Howe classification [Iberall & MacKenzie, 1990], as well as the MacKenzie and Iberall [1994] system. Later improvements to the hand design will include deformable grip surfaces to increase the friction and stability of gripping.

Further information on the capabilities of the motion of the fingers can be found in Chapter 6: 'Optimisation of the Canterbury Hand'. The output forces for the finger, and the thumb have an example calculation in the compendium [Green, 2002]. At the time of writing this thesis the Canterbury Hand has not yet been manufactured. The main reason for this was the lack of time at the end of the parametric design. Creating the engineering drawings can be quite time consuming between the drafting, getting the drawings accepted, buying in (and waiting for) components and creating DXF files of the parts that would be CNC machined. The times available for manufacturing the hand is dependent on the workshops job load. The most likely period available for manufacture is in the Christmas holiday break and the first term of the next year. The time period for manufacturing the hand is unknown and is job dependent but was estimated as being over a month.

While the next stage of creating the engineering drawings is relatively straightforward (as the CAD model's design has been completed) it has not yet been started. The reason for this is that the geometry of the hand is still being optimised by other student's projects. In particular Marlene Helfert's work on the gripping forces in the hand will lead to improvements that will be incorporated into the CAD model's geometry. Once these improvements have been made the process of creating the drawings and getting the hand manufactured will be begun. The first hand to be manufactured will be the smaller Mini motor hand. The reason for choosing this particular configuration for creation is that it is the most anthropomorphic looking of the two hand designs. It will also have smaller internal forces due to the smaller motors and will be less likely to be plagued by failure problems. Even though both hands were designed to avoid these types of problems it could possibly occur due to the complexity of the hand design. Since both hand designs are for most respects similarly sized, it will be just as easy to manufacture as the hand driven by the Maxon motors.

4.10 Design Summary

In conclusion the parametric design for the Maxon and the Mini motor Canterbury Hand has been completed. This chapter has summarised the objectives, development and design of the hand. In particular what parts make up the hand, what their design features are, and how they relate to the design objectives. It has also given an overview of the electrical wiring paths, FSR, and PCB layouts. It has described how the hand is assembled and the material and manufacture requirements involved. Finally it has summarised the expected results for the grasp types, sizing and weight for the two hand designs.

Chapter 5: Background Theory

This chapter describes the linkage theory for the finger and thumb actuators. It summarises how the fingers, thumb and hand move, where the singularities are, and how the forces are transmitted. The detailed calculations made for the design of the Canterbury Hand, are contained within the compendium [Green, 2002].

The finger and thumb linkages contain singularities that can limit their motion. A singularity is a geometrical location of the linkages that cannot be resolved. Mathematically the two solutions for the linkage position collapse to a single point (repeated root) of the singularity (b) as shown in Figure 5.1. Reversing the action of the control input (angle between the L1 and L4 links) may lead to an indeterminate position i.e. it is uncertain which of the two possible solution positions (a) or (c) shown in Figure 5.1 the linkages will move towards. Note that other singularities can occur in the four-bar linkage when the links cross.

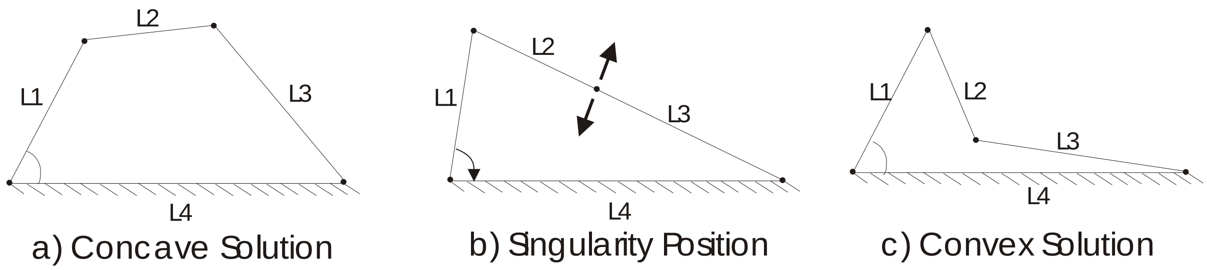

Figure 5.1 Four-bar linkage moved from singularity position

The finger and thumb linkages may be considered as connected systems of four bar linkages and thus are at risk of approaching singularity positions. When the coupled linkages approach singularity positions, the bearing forces can increase substantially. To prevent access to the singularity positions, mechanical stops were used in the linkages so that only one position is physically possible at any point in the finger/thumb motion. The singularity positions that were prevented using stops were called the controlled singularities. The remaining uncontrolled singularity positions were blocked by designing the linkage geometry so that they occurred after the controlled singularity positions.

5.1 Finger

The Canterbury Finger is a two-degree of freedom multi-bar linkage. Two motors stacked vertically within the metacarpal block drive the finger. The multi-bar linkage was made up of eight separate sets of linkages. These linkages move from the metacarpal block, which could be said to form the base or the ninth fixed linkage. Each motor drives a screw that causes a drive nut to move linearly along it. A pair of actuator links is attached on either side of each drive nut. These transfer the drive nuts motion to the finger linkages.

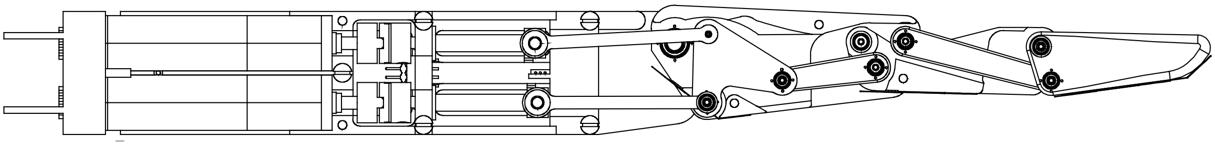

Figure 5.2 Canterbury Finger

The finger can produce two kinds of motion. The top motor causes a curling motion, while the bottom motor makes the finger to rotate around the knuckle bearing at joint B5 (see Figure 5.3). These actions (separately or combined) give the kinds of anthropomorphic motions that a human finger can produce.

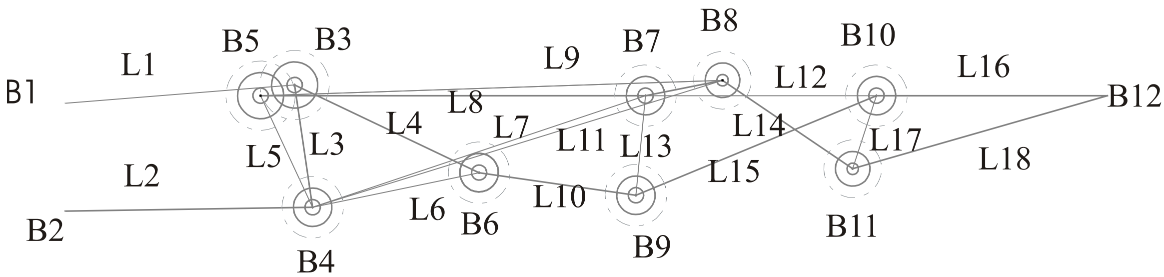

Figure 5.3 Finger Bearing and Linkage Naming Scheme

5.1.1 Curling Motion

The first motion to be described is the finger curl. It is produced by three linkage systems: the rocker five-bar system, the medial linkage four-bar system, and the distal linkage four bar system. These three systems are connected together at various joints.

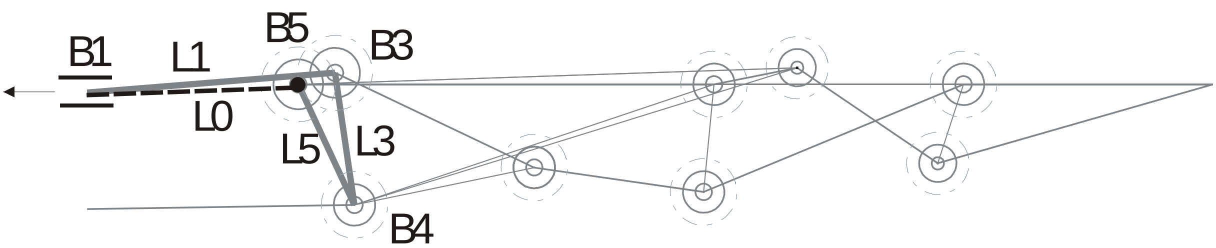

Figure 5.4 Rocker five-bar linkage system

The rocker five-bar linkage system is made up of the drive/nut sliding motion, the top actuator link 2 (link L1), the rocker link (link L3), the proximal link (link L5) and the metacarpal block (link L0). The metacarpal block makes up the fifth linkage as it is the base upon which the curling motion occurs upon.

It is known that a five-bar linkage system, such as the one described above, is inherently unstable and uncontrollable. The finger would not curl if it relied only upon this system. However once the rotation motion is fixed the curl motion becomes controllable. The reason for this is that when the rotation motion, through actuator link L2, is fixed the bearing joints B2 and B4 become fixed. This fixes the proximal link L5 in place and the system reduces to the rocker four-bar linkage system (as can be seen in Figure 5.5).

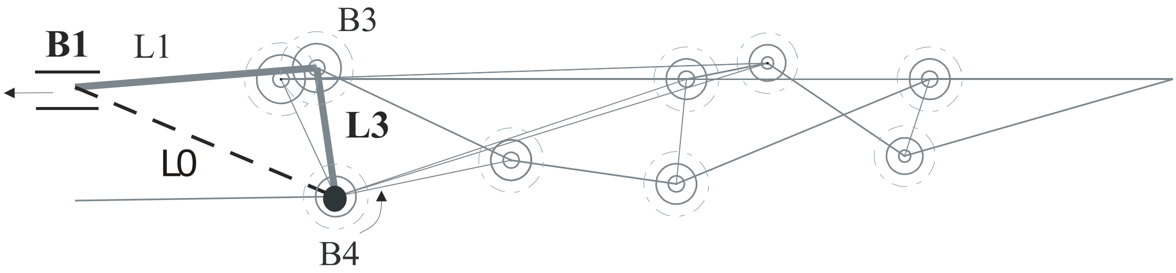

Figure 5.5 Rocker four-bar linkage system

The rocker's four-bar linkage's motion is driven from the top motor. As the motor rotates the drive screw it pulls back the drive nut connected to the actuator linkages (link L1). As the actuator link pulls back, the rocker link rotates backward about bearing joint B4 within the proximal linkage.

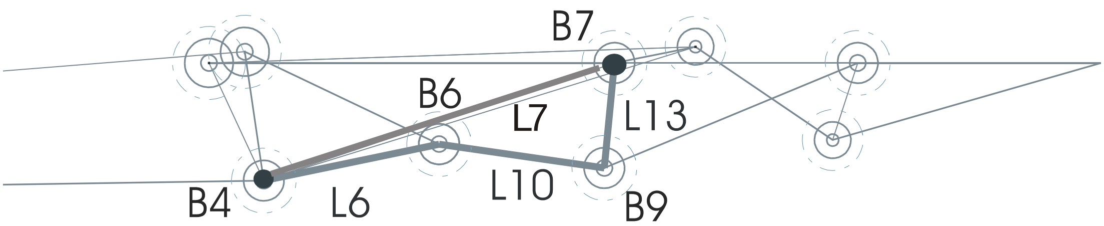

Figure 5.6 Medial four-bar linkage system

The second four-bar linkage system is the medial linkage system. It is made up of the rocker link (link L6), the medial driving link (link L10) and the medial link (L13). The proximal link (link L7) is stationary with the metacarpal block in the curl motion (when there is no rotation motion) and forms the fourth base link.

The motion originates from the rocker link's rotation from about bearing joint B4. As the rocker rotates it causes the finger to curl, and pull on the medial driving link. The medial driving link in turn causes the medial linkage to rotate about bearing joint B7. The rotation of the B7 and B4 joint bearings is upon the stationary proximal link.

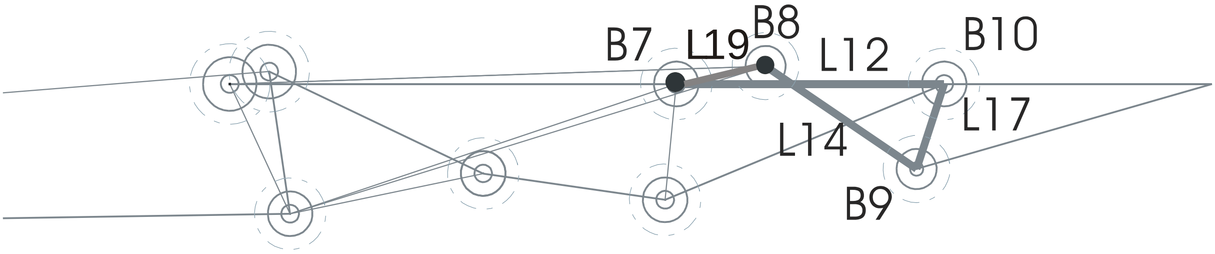

Figure 5.7 Distal four-bar linkage system

The third and final four-bar linkage system that forms the finger curl is the distal link system. It is comprised of the medial link (link L12), the distal link (L17), and the distal driving link (link L14). The distal driving link and the medial link are respectively connected to the proximal link via bearing joints B7 and B8. The proximal link (L19) acts as the fourth link in this system and is the base upon which the other linkages rotate.

The motion of the medial link (from the previous system) is connected at bearing joint B10 to the distal link. As the medial link rotates downwards (about bearing joint B7) it pushes down on the distal link. The distal link rotates around the joint bearing B11. This joint in turn is within the distal driving linkage, which is rotating around the proximal link joint at the bearing B8. Near the end of the distal curl motion the distal driving link is hardly rotating about the B8 bearing. This causes the final curl motion for the distal link to occur around the B11 joint bearing. The overall motion of these systems causes the medial and the distal links to curl around the proximal link.

5.1.2 Rotation Motion

The Canterbury finger's rotation motion about the knuckle shall be described. The finger rotation motion is formed by three systems: the proximal four bar link system, the rocker five-bar linkage system and the medial four-bar linkage system.

The finger rotation starts with the proximal four-bar linkage system motion. This system is formed between the bottom drive nut/screw sliding motion, the actuator 1 linkages (link L2), the proximal link (L5) and the metacarpal block (link L0). The metacarpal block acts as the fixed frame of reference for the moving linkages.

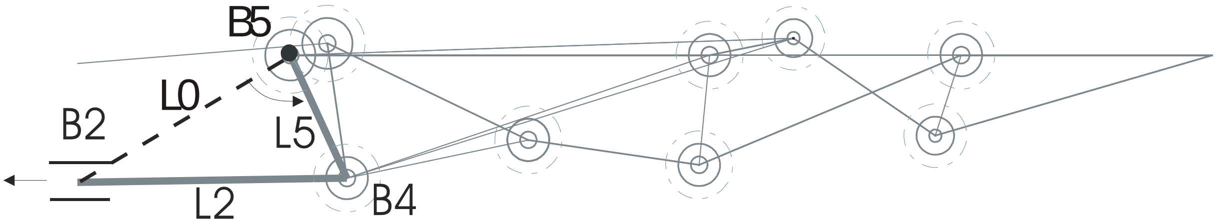

Figure 5.8 Proximal four-bar linkage system

As the bottom motor rotates the drive screw it pulls back the drive nut connected to the actuator linkages (link L2). The actuator linkages in turn pull back the proximal link causing it to rotate about the knuckle bearing joint (B5). This motion accounts for all of the rotated finger motion and a small amount of the curl.

While the proximal link rotates there is a corresponding motion produced within the rocker five-bar linkage system. The reason for this is that the two systems are linked together as they both utilise the L5 link in the proximal link for their movement. The rocker five-bar linkage system (see Figure 5.4) is the same linkage system as described in the previous curling motion section. As before this five-bar linkage system is unstable and uncontrollable. If however the curling motion is fixed the finger rotation becomes controllable. The reason for this is that the B1 bearing joint can now be considered as a fixed joint. This reduces the rocker five-bar linkage system to the proximal/rocker four-bar linkage system (see Figure 5.9). The proximal/rocker system is formed between the top actuator link 2 (the L2 link), the rocker link (link L3), the proximal link (link L5) and the metacarpal block (link L0). In this system the metacarpal block again forms the fixed frame of reference.

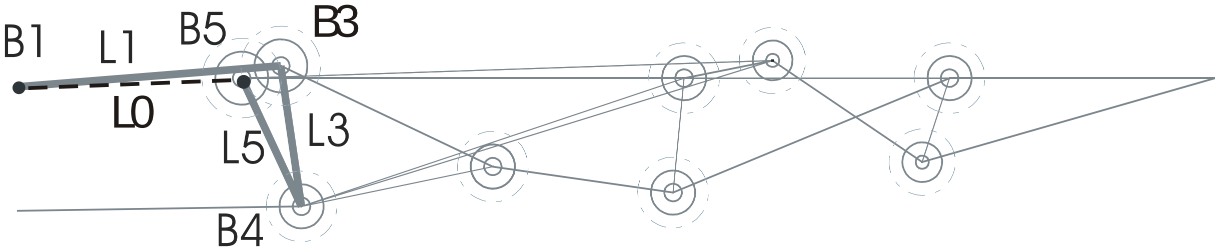

Figure 5.9 Proximal/Rocker four bar linkage System

As the proximal link is pulled back (about bearing joint B5) it causes the rocker link to rotate forward about joint B4, and about joint B1. The reason for this is that the rocker link is constrained in its motion by its attachment to the top actuator link (link L1). If the top actuator link does not move then the rocker link will rotate forward because of the linkage motion. Between the two motions of the proximal four-bar linkage system, and the linked proximal/rocker four-bar linkage system, the other finger linkages rotate at roughly the same rotational angular amount. Although there is some coupling, for most of the rotation movement of the finger these motions are congruent.

However there is some difference with further rotation. The proximal/rocker four-bar linkage system rotates the rocker link further along than the relative rotation motion of the proximal link. The rocker link furthermore is attached to the medial four-bar link system. As already described for the finger's curling motion, the medial four-bar linkage system is comprised of the rocker (link L6), the medial driving link (link L10), the medial link (link L13) and the proximal link as the fixed base link. The relative angular motion between the proximal link and the rocker creates a motion that reverses the motion of the medial driving link (opposite to it's curling motion). The medial driving link is pulled down with the rocker link so that it rotates around the medial link attachment joint B9. This rotation eventually rotates the medial link upon its bearing joint B7 about the proximal link. This motion causes the finger's medial link to curl. (The distal three bar linkage system also begins to curl slightly, but this is for a negligible amount of motion.) It must be noted however that the rotation motion of the finger has caused the L10 and L6 links to travel through the cusp (recoverable singularity) position. The manufactured fingers would not be allowed to travel through this position due to the large bearing forces it would provoke.

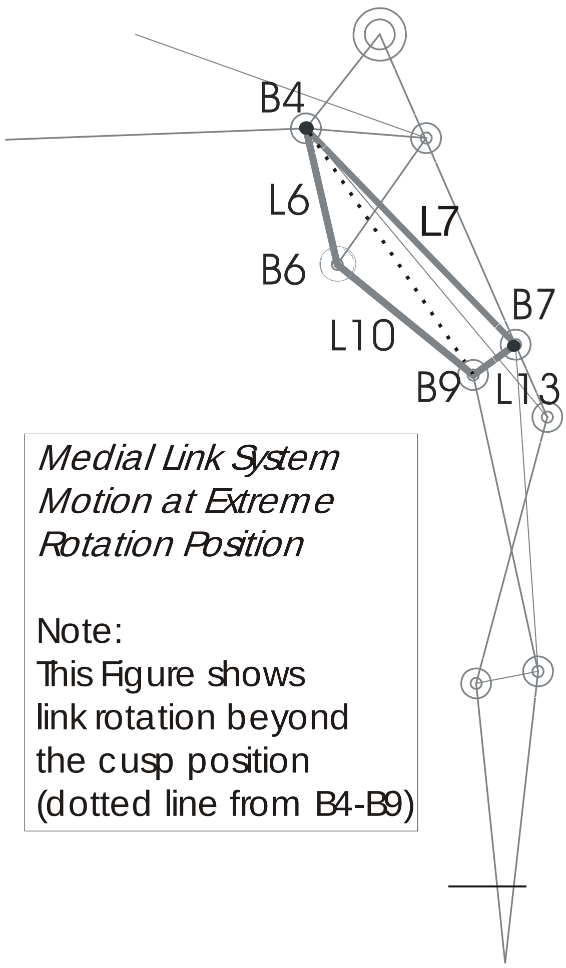

Figure 5.10 Extreme Rotation Position System

5.1.3 Output Force

This subsection explains the processes behind the calculation of the forces within the finger linkages. The linkages in the finger may be considered as being fixed for the analysis due to the linkages being fully located by the position of the drive nuts. It should be noted that the location of the external force on the finger could occur at any position on the finger linkages. The usage of a mechanical hand like a human hand would generally have the grasp forces located on the underside of the finger beginning at the distal link.

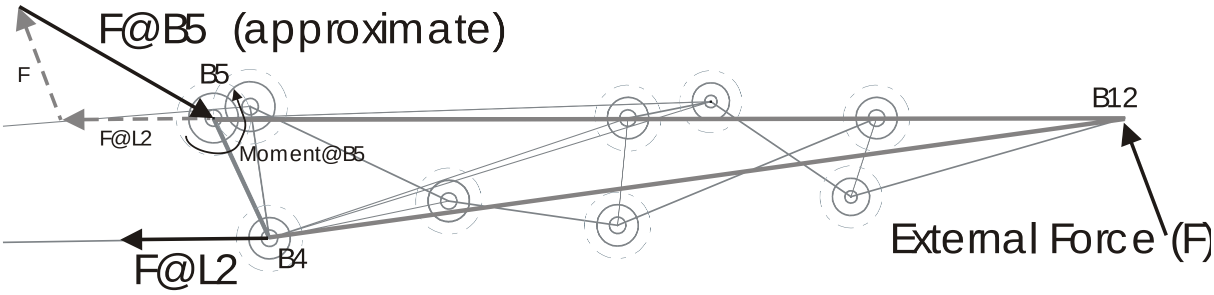

Figure 5.11 Approximation of Finger Forces

For this analysis the worst-case external force location on the finger is assumed to be at the tip of the distal link, as it would give the greatest moment about bearing joint B5. This is illustrated in the above diagram (Figure 5.11), which shows an approximation of the forces of the finger if it were treated as a single linkage. This approximation though is only useful for a quick estimate of the forces on the B5 bearing joint. The rest of this subsection gives a more detailed consideration of the forces in the finger.

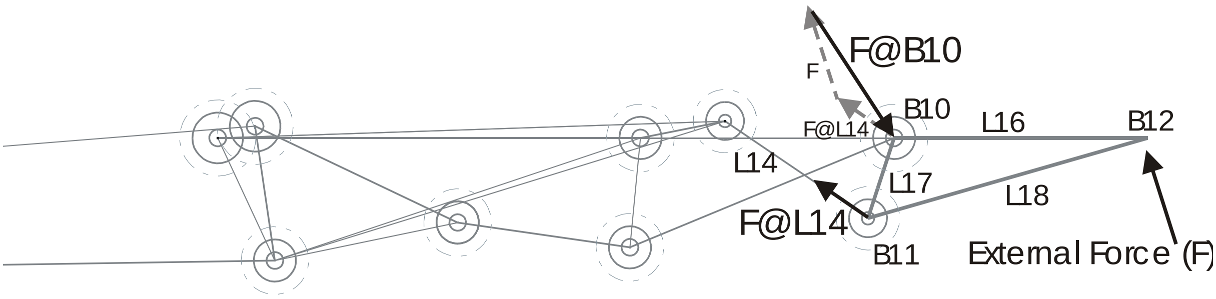

Figure 5.12 Distal Link Forces in the Finger

The free body diagram of the distal link (Figure 5.12) is the first link analysed, as this is where the external force is applied. The external force (F) creates a torque about the B10 bearing joint in the distal link. The moment at bearing joint B10 is balanced by the force in the distal driving link (F@L14). The external force and the force in link L14 create a reaction force (F@B10) at the bearing joint B10.

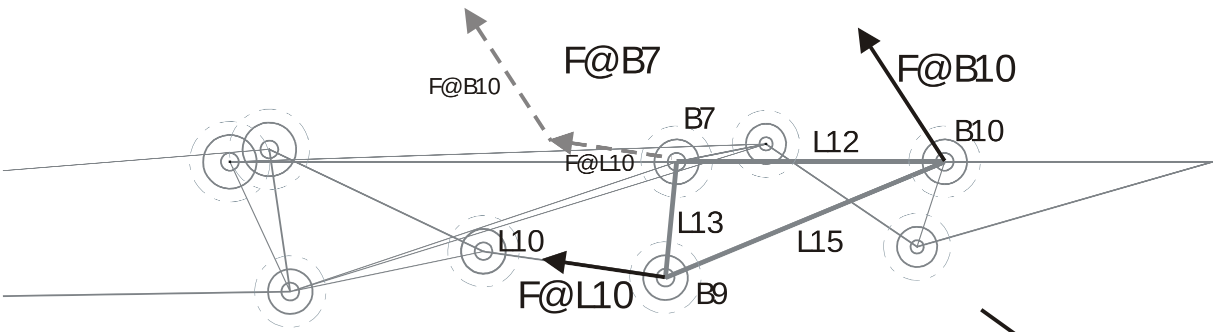

Figure 5.13 Medial Link Forces in the Finger

The force at B10 is then transmitted to the medial link (see Figure 5.13) where it creates a torque about the B7 bearing joint. This torque is balanced by the countering force (F@L10) in the medial driving link (L10). The reaction force at bearing joint B7 (F@B7) balances the forces on the medial link.

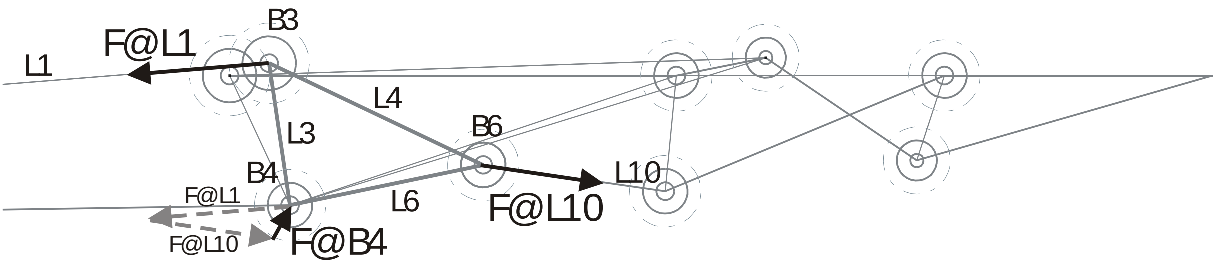

Figure 5.14 Rocker Link Forces in the Finger

The tension force (F@L10) in link L10 pulls on the rocker link (see Figure 5.14) and creates a moment about the bearing joint B4. This moment is balanced by the force in the top actuator link (F@L1). These forces create a reaction force in the B4 bearing joint (F@B4).

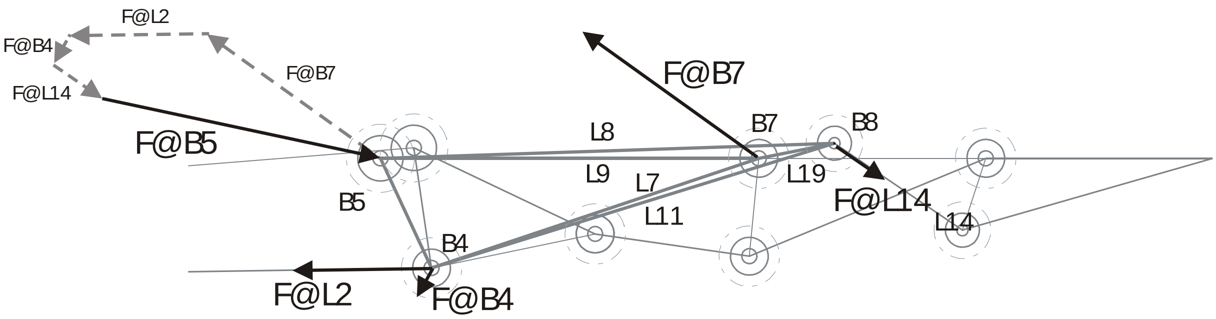

Figure 5.15 Proximal Link Forces in the Finger

The forces in the previous linkages are calculable and known and are added to the proximal link free body diagram (see Figure 5.15). The reaction forces from B4 (F@B4) and B7 (F@B7) are added to the proximal link along with the forces from the linkages L14 (F@L14) and L2 (F@L2). These unbalanced forces create a torque around bearing joint B5 that is balanced by a force through link L2 (F@L2). The forces in the proximal link create a reaction force in the bearing joint B5 (F@B5). Overall from the above free body diagrams it can be seen that the greatest bearing forces are located at bearing joints B10, B7 and B5. The approximations above also show that the greatest bearing force is at bearing joint B5. The worst case for the B5 bearing force occurs when the forces in linkages L10 (F@L10) and L1 (F@L1) cancel each other out to give the least reaction force at bearing joint B4 (F@B4). Thus maximising the reaction force at bearing joint B5.

5.1.4 Singularities

There are four singularities within the linkages of the Canterbury Finger. They occur when the following linkages attempted to either cross each other or extend straight within the motion of the finger.

The problem linkages alignments are:

1) Links L1 and L3
2) Links L2 and L5
3) Links L10 and L13
4) Links L14 and L17

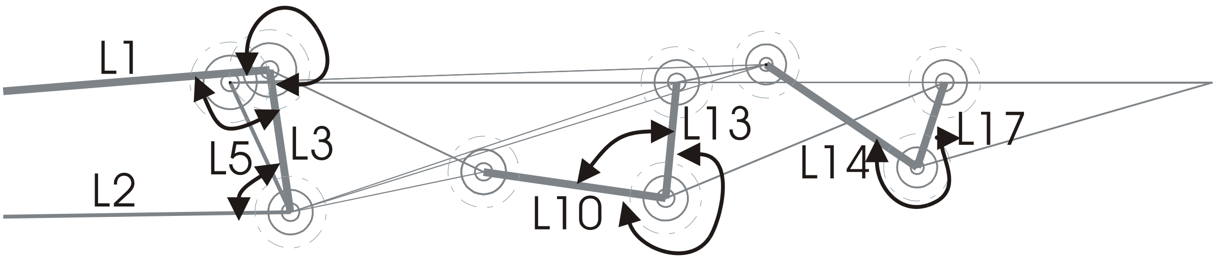

Figure 5.16 Location of Linkages that can give Singularities in Finger Motions

Most of the above singularities are avoided in the finger’s motions. Linkage geometry was chosen that had a controlled singularity for each motion of the finger. For the curling motion the singularity between L14, and L17 was chosen as the one that would occur first. This is controlled by a stop within the distal link that halts motion of the finger before this singularity can occur.

For the rotation motion of the finger the singularity within the four-bar linkage system between L1 and L3 was chosen. This singularity is avoided by placing a stop within the proximal link. The stop halts the rocker before it can approach this singularity position. This stop also prevents the cusp position from occurring.

The other singularities are placed so that they occur only after the controlled singularity positions are reached by the finger motion. These uncontrolled singularities occur in non-optimum geometries, so there are few disadvantages to these choices. The following sections detail examples of the singularities that can occur with the curling and rotation motions of the finger. (It should be noted that the finger bearing geometry is taken from the extended finger position, and changes to the geometry were made at this position in the optimisation process.)

There is one additional singularity position that should be mentioned called the cusp position, which is a recoverable singularity. That is the linkages can be recovered from this position even though there are large bearing forces. The cusp position occurs when the L6 and L10 links extend them selves straight. This can be prevented from stopping the B6 bearing joint from crossing the line between the B4 and B9 bearing joints. It can occur in either the rotation or curl motions of the finger depending on the initial geometry of the bearing joints B4, B6 and B9.

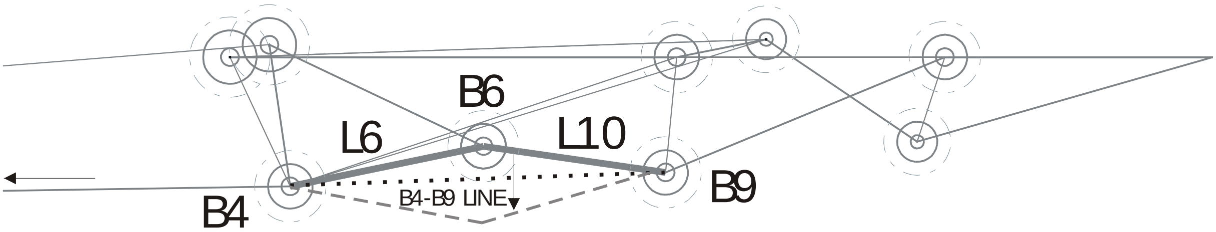

Figure 5.17 Location of Cusp/Recoverable singularity position

5.1.5 Singularities within the Curling Motion

This section describes the singularities that can occur within the curling motion of the finger. When the curling motion occurs in the rocker for-bar link system a singularity can occur between links L1 (the Actuator link 2), and L3 (within the Rocker link) when the two linkages align.

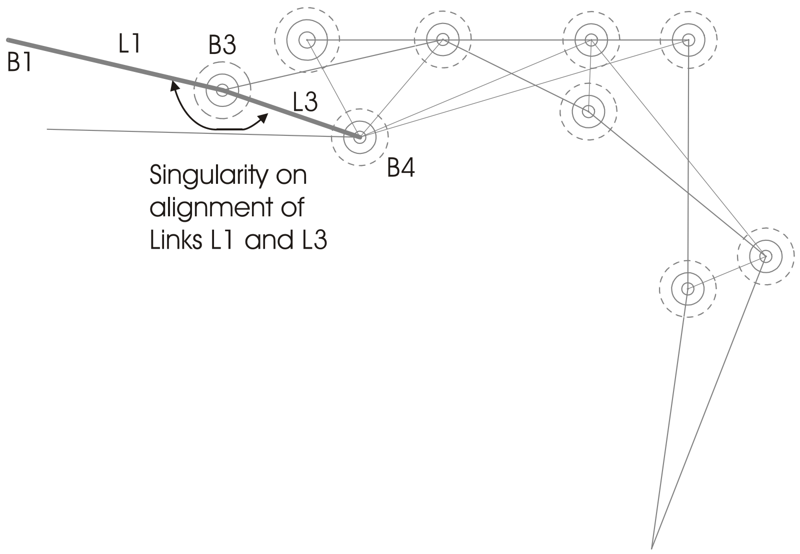

Figure 5.18 Example Singularity Position for L1 and L3 Links in Finger curl

Another example of a singularity in the curling motion of the finger occurs between L10 (the medial driving link), and L13 (within medial link). As the finger curls, these two linkages can attempt to pass through each other and form a singularity.

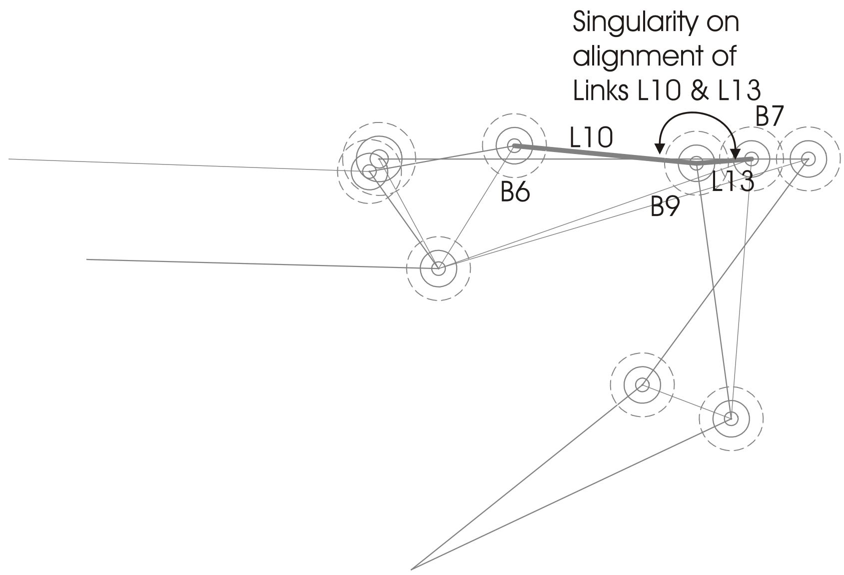

Figure 5.19 Example Singularity Position for L10 and L13 Links in Finger curl

The final singularity that can occur within the curling motion is between links L17 (within distal link) and L14 (the distal driving link). It occurs at the end of the curling motion when the two linkages align themselves. This is a controlled singularity as a block in the linkages prevents it from occurring. Its time of occurrence can be modified by the starting angle between the two links (defined in the finger geometry). The singularity position is also dependent on the arrangement of the distal four-bar link system.

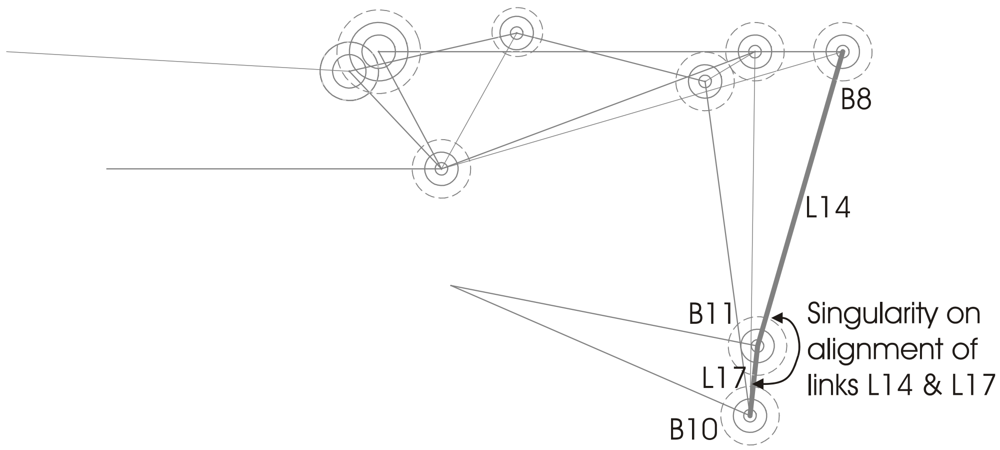

Figure 5.20 Example Singularity Position for L17 and L14 Links in Finger curl

5.1.6 Singularities within the Rotated Motion

This section describes the singularities that can occur within the rotation motion of the finger. It should be noted that the examples given here show singularities that occur after the cusp position has been crossed. As the medial four-bar link system rotates with the rocker, the medial driving link (L10) rotates with respect to link L13 (part of the medial link). The singularity occurs when the L10 and L13 linkages attempt to align themselves.

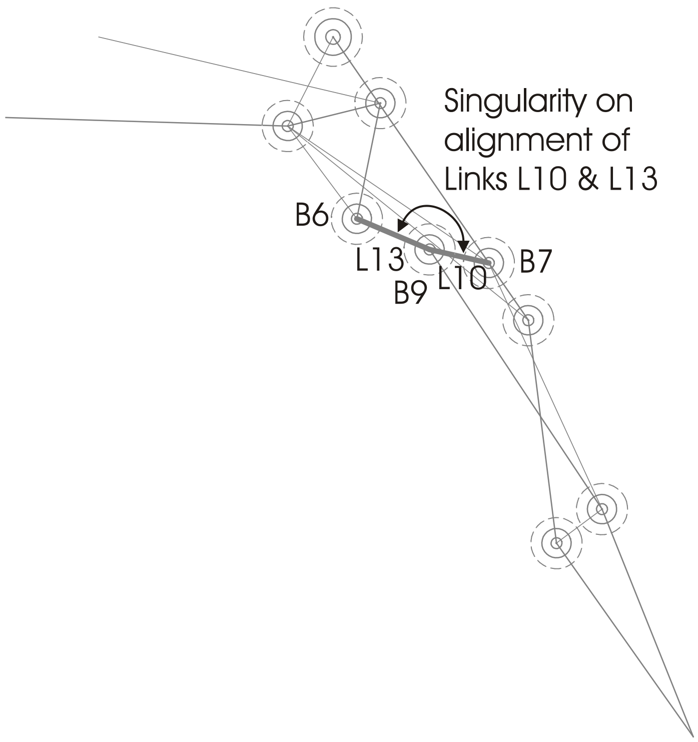

Figure 5.21 Example Singularity Position for L10 and L13 Links in Finger Rotation

A singularity can occur in the proximal four-bar linkage system. This singularity occurs when the L2 (actuator link 1) and L5 (part of the proximal) links are aligned.

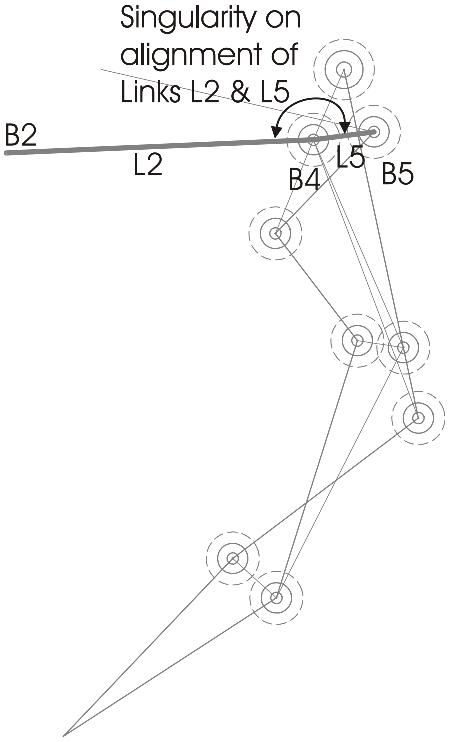

Figure 5.22 Example Singularity Position for L2 and L5 Links in Finger Rotation

There is a singularity that can occur within the rocker/proximal four-bar linkage system. This singularity was between the L1 (actuator link 2) and L3 (part of the rocker) links when the motion of the rocker tries to align them by crossing them over each other. This is a problem singularity as it is opposite the curling motion singularity, (between the same two links). To avoid one singularity would be to make the other more likely to occur. This controlled singularity was prevented from occurring by a stop in the proximal link.

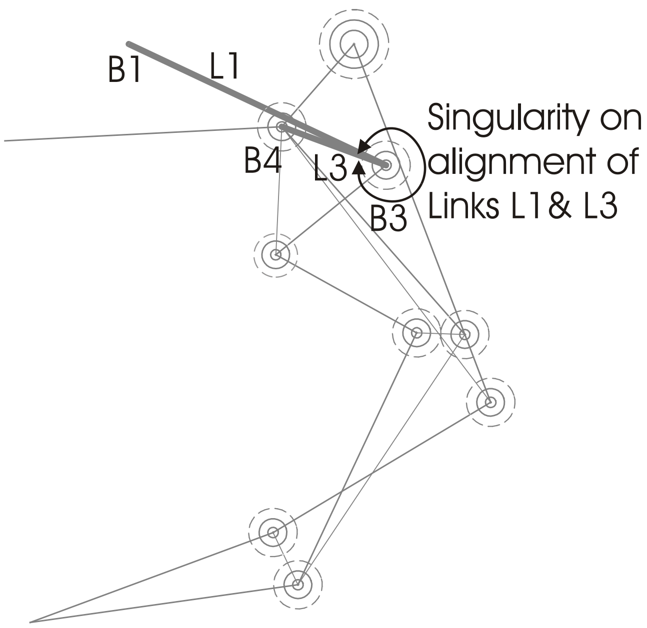

Figure 5.23 Example Singularity Position for L1 and L3 Links in Finger Rotation

5.2 Thumb

The thumb is a single degree of freedom linkage mechanism. A single motor lies above the drive screw and nut in the metacarpal block. The motor's torque is conveyed to the drive screw by 1:1 spur gears. This moves the drive nut linearly up and down the screw. Actuator links on either side of the nut transmit the motion of the nut to the thumb linkages. The thumb's single motion is a curl. It is made up of two systems of four-bar linkages connected together. There are two singularities that can occur within the motion of the thumb's linkages.

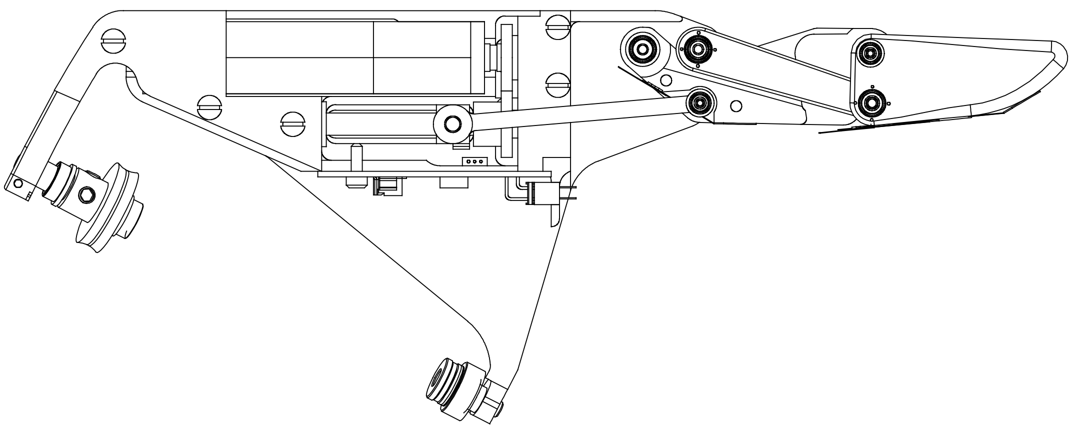

Figure 5.24 Thumb with internal parts visible

5.2.1 Curling Motion

Since the thumb is a single degree of freedom mechanism the curl motion is a curve. The linkages are made of two systems of four-bar linkages. The first system was the proximal four-bar link system. The second system was the distal four-bar link system.

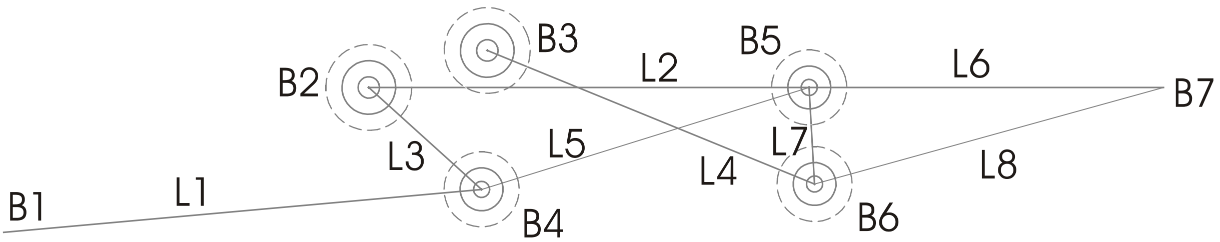

Figure 5.25 Thumb Bearing and Linkage Naming Scheme

The proximal four-bar link system is made up of the drive nut/screw sliding motion, the actuator link (L1 link), the proximal link (L3 link) and the metacarpal block (L0 link) that acts as the fixed reference link. When the thumb curls the drive nut moves to the rear of the metacarpal block. This pulls back the actuator link, which in turn causes the proximal link to rotate downwards. The proximal link rotates about bearing joint B2, which is connected to the metacarpal block.

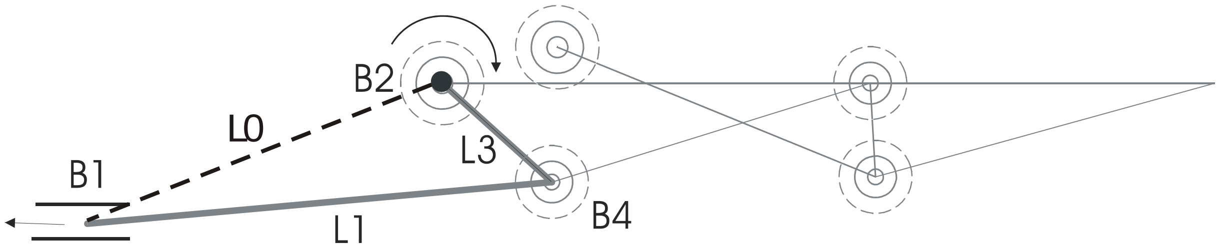

Figure 5.26 Proximal Four-Bar Link System

The second part of the curling motion comes from the distal four-bar link system. This system was made up of the proximal link (L2), the distal link (L7 link), the distal driving link (L4 link), and the metacarpal block (L0). The metacarpal block again acts as the fixed reference link. The distal link system is linked via the proximal link (L2) to the motion of the proximal link system.

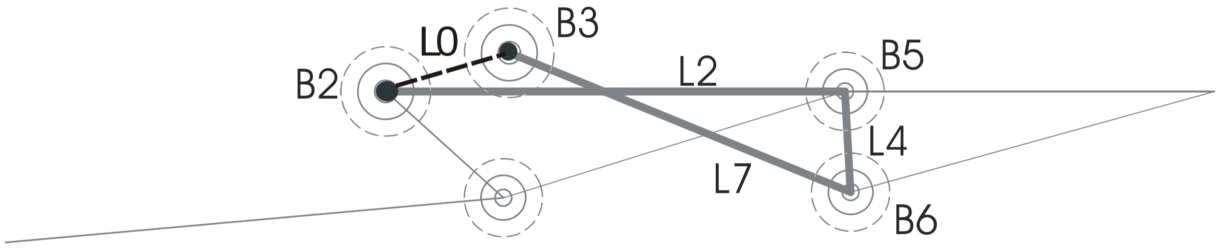

Figure 5.27 Distal Four-Bar Link System

The proximal link downwards curling rotation causes the distal link to rotate down and towards the metacarpal. The distal link rotates about the bearing joint B6, which is connected to the distal driving link. The distal driving link and the distal link also rotate about bearing joint B3, which is connected to the metacarpal block. The motion of these linkages mimics the human thumb motion.

5.2.2 Force Output

This section describes the forces within the thumb linkages. Numerical values are not given, as these are highly dependent on the geometry of the linkages and the external force. The thumb linkages may be considered as being fixed for the analysis as they are fully determined by the position of the drive nut. The external force will also assumed to be applied at the bearing joint B7 in the distal link. The reason for this is that this location gives the maximum reaction force to the B2 bearing joint, which makes it useful for a worst-case analysis. An approximation for the forces in the distal link such as in the finger force analysis (see Figure 5.11) could be made, but will be ignored since the thumb is much less complex.

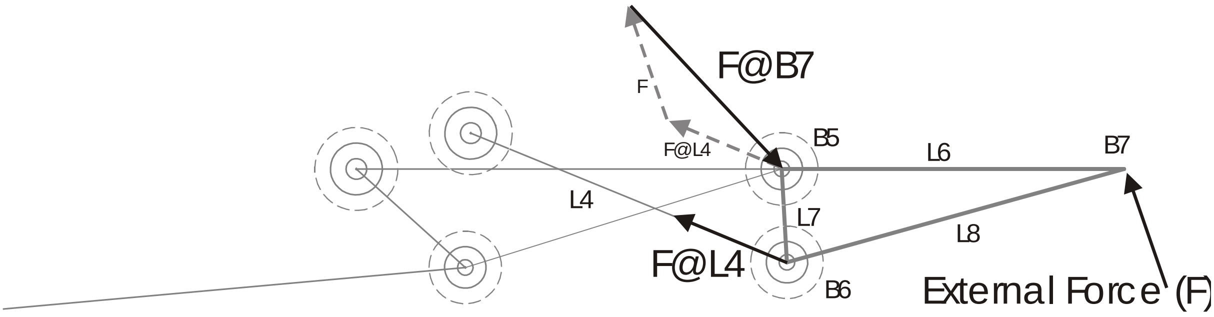

Figure 5.28 Forces in the Thumb's Distal Link System

The free body diagram above (Figure 5.28) shows the forces in the distal link. The external force (F) is applied at the B7 bearing joint, which creates a moment about the B7 bearing joint. This moment is balanced by the force in the distal driving link L4 (F@L4). Both these forces create a reaction force in the B5 bearing joint (F@B7).

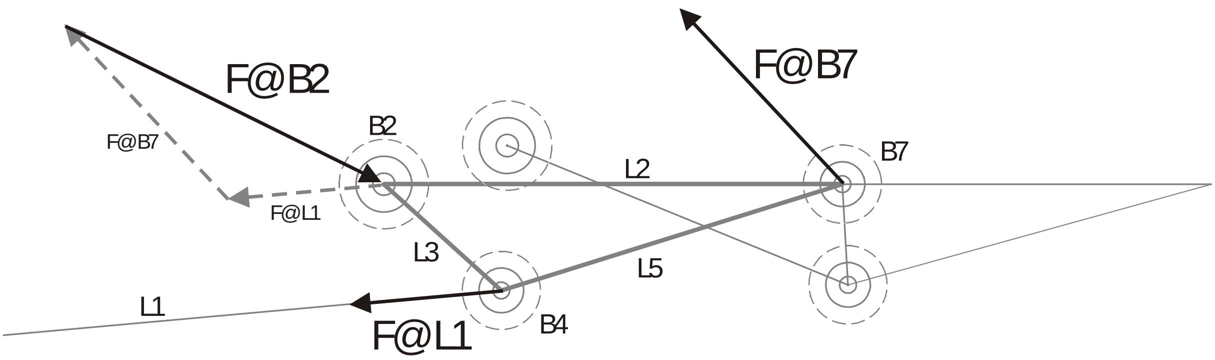

Figure 5.29 Forces in the Thumb's Proximal Link System

The reaction force at B7 (F@B7) is then transmitted to the proximal link where it creates a moment about bearing joint B2. The moment at B2 is balanced by the force (F@L1) in the actuator link (L1). The forces in the proximal link give a reaction force (F@B2) at bearing joint B2. From these diagrams it can be seen that the reaction force at B2 will be the largest expected bearing joint force in the thumb.

5.2.3 Singularities

There are two singularities that can occur within the curling motion of the Canterbury thumb linkages. They occur when the following linkages become aligned within the thumb. The problem linkages are:

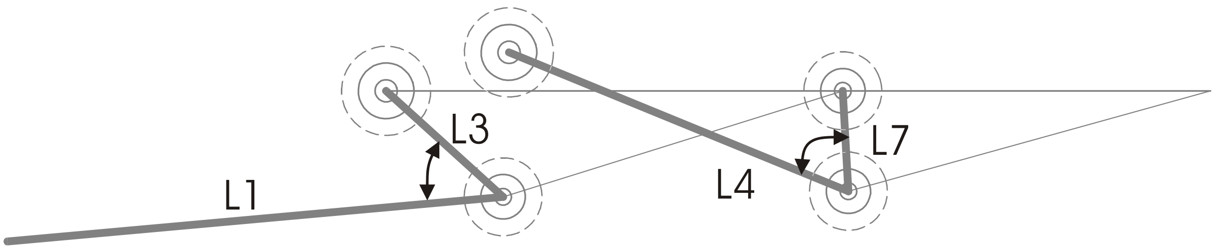

Figure 5.30 Location of Linkages that can give Singularities in Thumb Motion

1) Links L1 and L3
2) Links L4 and L7

The thumb curl is defined by which of the singularities occurs first in the motion. The singularity that aligns the L1 (actuator) link and the L3 (part of the proximal) link was avoided in the optimisation of the thumb, as it gave the worst force output. At this singularity the actuator (L1) link aligns with the B2 bearing joint. This greatly reduces the moment about this joint (and increases the direct force on the bearing). If an object opposes the thumb the smaller moment at the B2 bearing joint reduces the balancing output force.

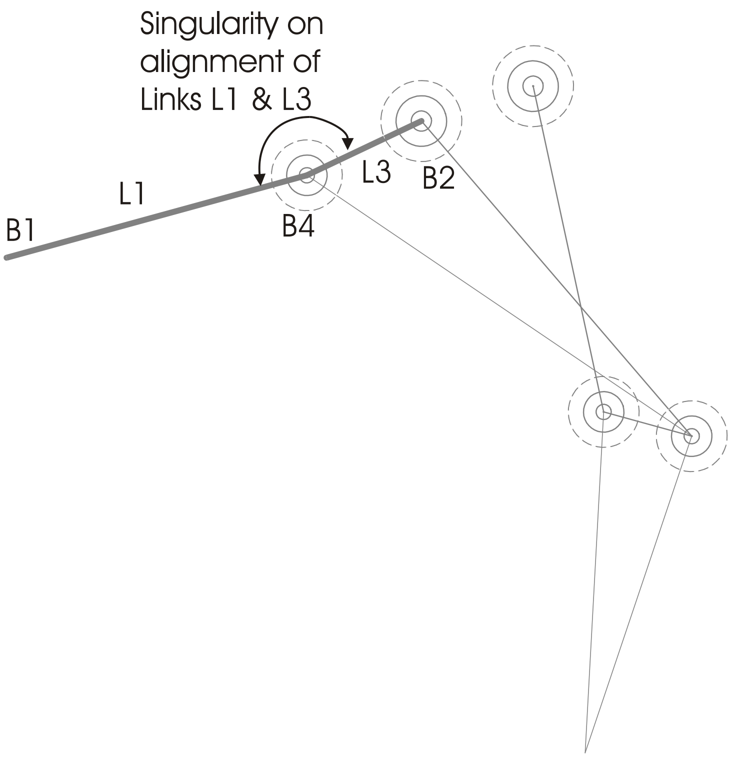

Figure 5.31 Example Singularity Position for L1 and L3 Links in Thumb Curl

The singularity between the L4 (distal driving) link and L7 (within the distal) links occur when the curl motion extends the angle between them so that the linkages align. This was the controlled singularity. A stop within the distal link was used to halt the thumb linkages before this position could occur. The other singularity between the L1 and L3 links is avoided by making it occur after the controlled L4/L7 singularity. The thumb's final curl position between the L4 and L7 links is determined by a number of factors including the initial angle between them, and the distal link four-bar system arrangement.

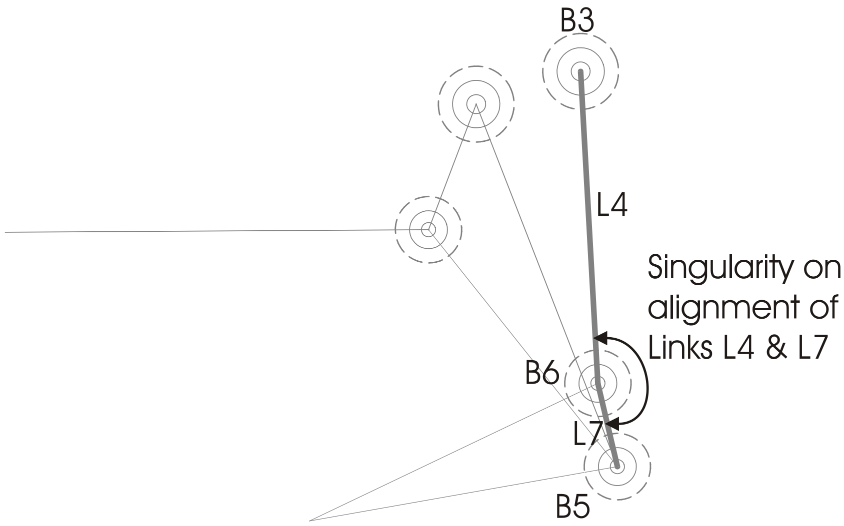

Figure 5.32 Example Singularity Position for L4 and L7 Links in Thumb Motion

5.3 Hand

The hand has two motions actuated within the palm assembly. They are the spreading mechanism for the fingers, and the rotation mechanism for the thumb. This section will deal with the theory behind these mechanisms. The detailed description of them can be found in Chapter 5,'Design of the Canterbury Hand'.

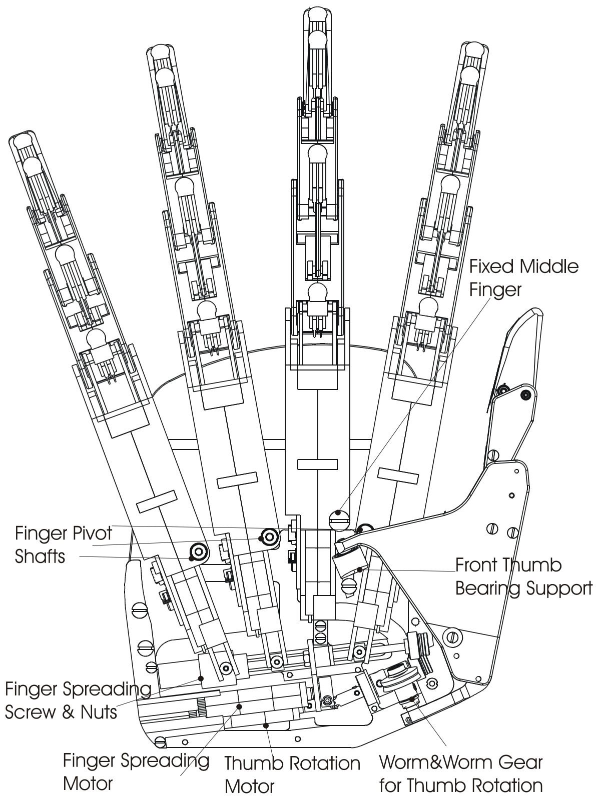

Figure 5.33 Finger spreading and Thumb rotation mechanisms in the hand design

5.3.1 Finger's Spreading Motion

The finger spreading mechanism has to spread the metacarpal blocks of the fingers away from each other. This replicates the human finger spreading motion. For the Canterbury Hand the middle finger is fixed in the palm. The index finger and the ring finger spread apart on opposites sides and in opposite directions from it. The little finger spreads apart from the ring finger by keeping the same angle between them as was kept between the ring and the middle fingers.

The mechanism for this motion is a motor driving a lead screw via spur gears in the palm assembly. Three nuts rotate on three sections of the drive screw. Each nut traps the motion of a metacarpal end cap of a finger. As the nuts move on the lead screw they cause the trapped finger metacarpals to rotate in the spreading motion.

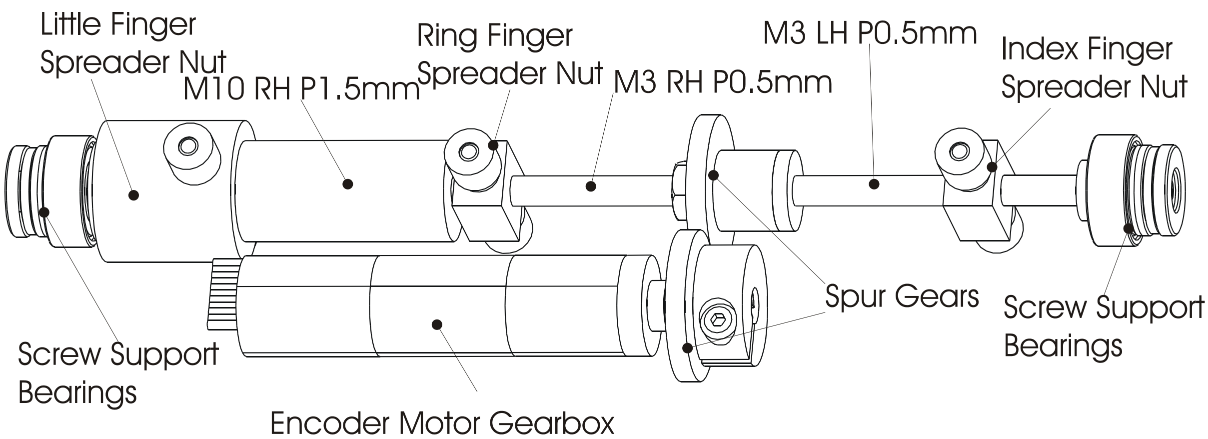

Figure 5.34 Finger Spreading Mechanism

Each of the three sections of the drive screw has different thread pitches. The ring finger and the index finger spread at the same speed but in opposite directions. This meant that the screw thread had to be the same pitch but with the thread in the opposite direction. The Right Hand (RH) screw thread is the standard thread direction. However while it is still possible to machine Left Hand (LH) screws it will be more expensive. Left hand screw threads require less commonly used and therefore more expensive machining taps and cutting dies. It was decided that the thread pitch on the index finger's drive screw section was to use a left hand thread. The reason for this was that the little finger and the ring fingers would each require different pitches with the same thread direction. It was cheaper to have two right hand threaded pitches on these two fingers in the rotation mechanism than to have two left handed screws.

To keep the same angle between the little, ring, and middle fingers the little finger has to rotate twice as fast as the ring finger in the spreading motion. However the drive nuts on both fingers travel on the same screw. For each revolution of the screw the drive nuts move their pitch distance down their particular threaded section. To have the little finger drive nut move twice the speed of the ring finger drive nut it needs to have three times the pitch distance for it's thread. That is it would move three times the pitch distance in one revolution of the screw compared with the other nut.

The rule for a drive nut having to move X times faster than another nut (on the same drive screw) is that it needs to have (X+1) times the pitch size as the other nut. For example, if the little finger's drive nut needed to go six times faster than the ring finger's drive nut it would need seven times the pitch size.

It was decided that the ring finger would have a right-handed screw thread of pitch 0.5mm for an M3 diameter screw. The index finger would have the same pitch and screw diameter but use a left-handed screw thread. The little finger would have a drive nut of M10 screw diameter with a right-handed pitch of 1.5mm.

Another aspect of importance for the finger spreading mechanism is the location of the rotation bearings within the finger's metacarpal block. Because the metacarpal blocks have motors in the way, there was no material left over for the rotation bearings down the centre of the metacarpal block. That meant there was a choice of having the bearings on either the side closest to the middle metacarpal block or the side furthest away. Based on the way the metacarpal blocks rotates it was decided that an inside bearing position would be best. The reason for this is that the metacarpal block swings away the least distance from the drive nut. This meant that it was easier to keep the drive nut located between the prongs in the metacarpal block.

The drive nuts for the spreading motion are located down the side of the inside bearing of the metacarpal block. This gives the most efficient use of space within the palm, as the lead screw's support bearings on either end are closer into the hand. This reduces the width of the palm.

5.3.2 Thumb Rotation Motion

A single motor located in the palm assembly of the hand actuates the thumb rotation mechanism. The motor connects to a universal coupling, to allow for the horizontal angular offset between it and the worm. The reason a worm gear system was chosen was that it was the smallest mechanical system that would step down the speed of the motor that fitted within the palm of the hand. A 21:1 gear reduction was used to slow down the thumb rotation mechanism to an acceptable rate. No other gearing arrangement of that size and simplicity was available. By gearing down the motor speed, the torque output from the motor is increased by a factor of over 13 for the thumb rotation mechanism.

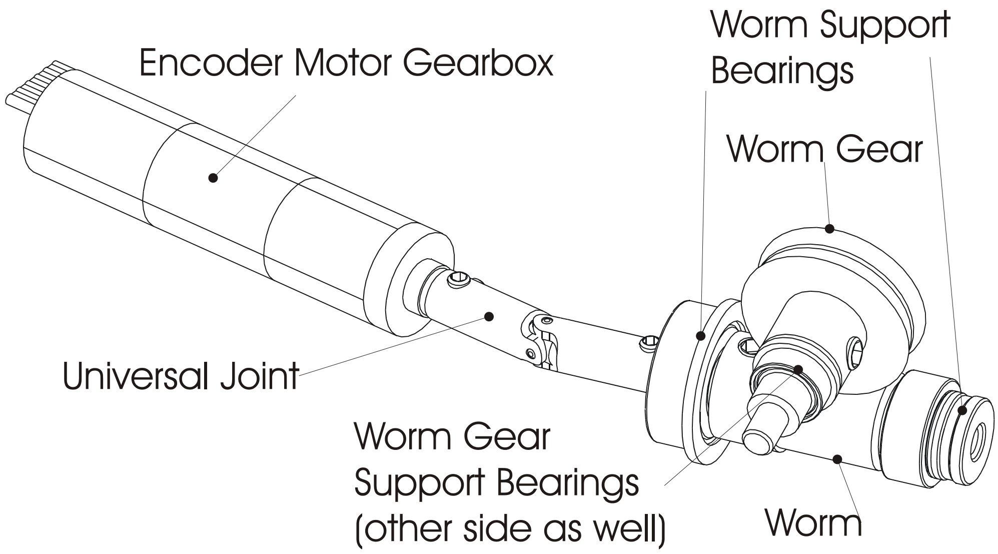

Figure 5.35 Thumb Rotation Mechanism

The worm wheel has its shaft attached to the rear strut of the thumb rotation mechanism. Whatever the angular position of the thumb axis, the thumb rotation mechanism is still a one-degree of freedom mechanism. The thumb rotation motion is along a curve, and by changing the angles of the thumb axis in the hand assembly this curve can be modified. For example, to get the maximum grip volume under the thumb's rotation curve, the axis was angled up through the palm of the hand.

The axis location within the thumb can also be modified so that the thumb's orientation along this rotation curve can be changed. An example of this is that for a pinch grip the thumb needed to be orientated to oppose the index and middle fingers. The positioning of the thumb and the orientation of the axis was optimised so as to give the most anthropomorphic motion for the thumb's rotation.

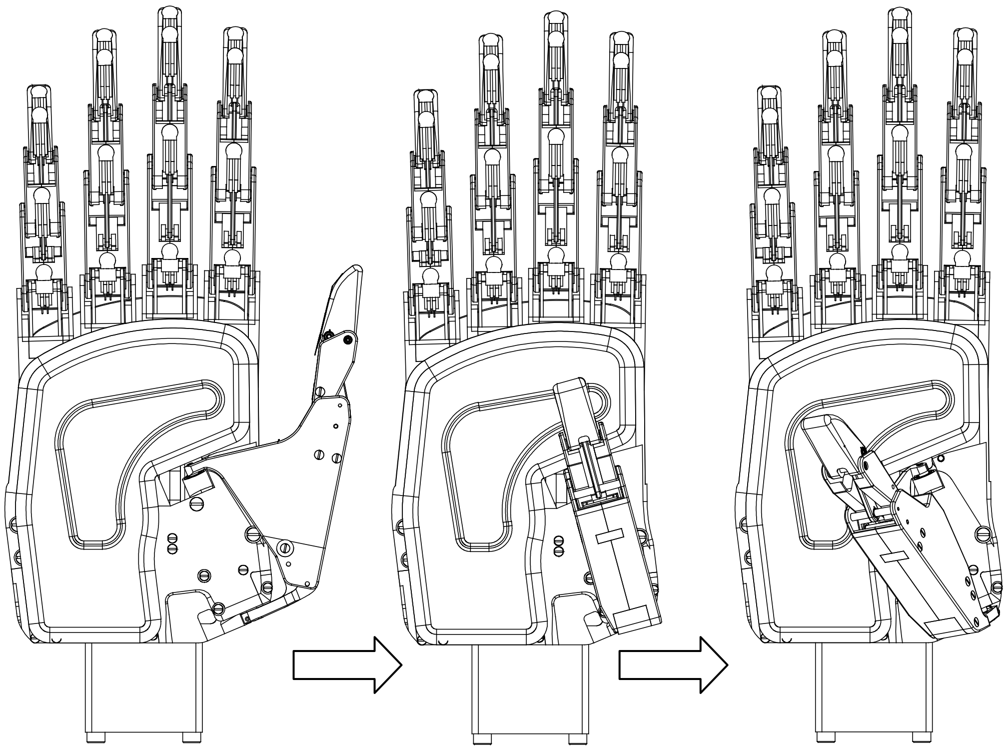

Figure 5.36 Thumb (rest, opposing, extreme) Positions in thumb rotation motion

The limitations of the motion of the thumb's rotation of the hand are the resting position at the side of palm, and the maximum rotation position. The resting position limits the rotation, as the thumb's front rotation strut cannot rotate further than the groove in the palm of the hand. The maximum rotation position occurs when the bottom rear side of the thumb's left metacarpal block collides with the middle rear of the palm of the hand. A depression has been fashioned in the palm at this position to increase the maximum rotation of the hand by a few degrees.

5.3.3 Hand Grip Force

The grip force of the hand is dependent on how many fingers are gripping the object with the thumb, where the object is being gripped, and what the linkage positions are for the grip. Thus it is difficult to comment on the probable output force from the hand. For a stable grip on the object the limiting force upon it would be the maximum output force from its weakest gripper (finger or thumb) mechanism.

To have a stable grip on an object a force balance is required in the gripping mechanisms. As force on the object is increased a point will be reached where a mechanism's force output reaches a maximum. If the limiting force is exceeded the grasp will no longer be stable i.e.

the grasp is unstable and the object begins to move out of position within the hand as more force is applied to it. An equilibrium position may be reached however where the linkages of the gripper lock into a position that allows greater force to be applied across the object. The grip force for the hand needs to either be simulated or experimentally found. This may only apply for specific grips and objects.

Chapter 6: Optimisation of the Canterbury Hand

6.1 Introduction

A prototype design is seldom completely optimised when it is first created. Most engineering products require a degree of iterative redesign to better fulfil their objectives. The objectives are usually numerous, and could include such things as market forces, design lead times, advertising and various design factors. Design factors directly influence the engineering design and creation of the product. These may include such things as the product's cost, weight, lifetime, or improvement of strength. They may also include less measurable qualities such as aesthetic appeal, recyclables, or ease of use. To achieve the designer's ideal solution the design factors usually require optimisation.

The process of optimisation is seldom straightforward. Designs often require compromises between the various design factors. Factors like cost versus quality are frequently incompatible with each other. Often compromise decisions of choosing one factor over another needs to be made by the designer. Designs can have problems with so many variables that they need to be solved numerically. This can take a very long time computationally, and there is no guarantee that a solution found using numerical methods is optimal.

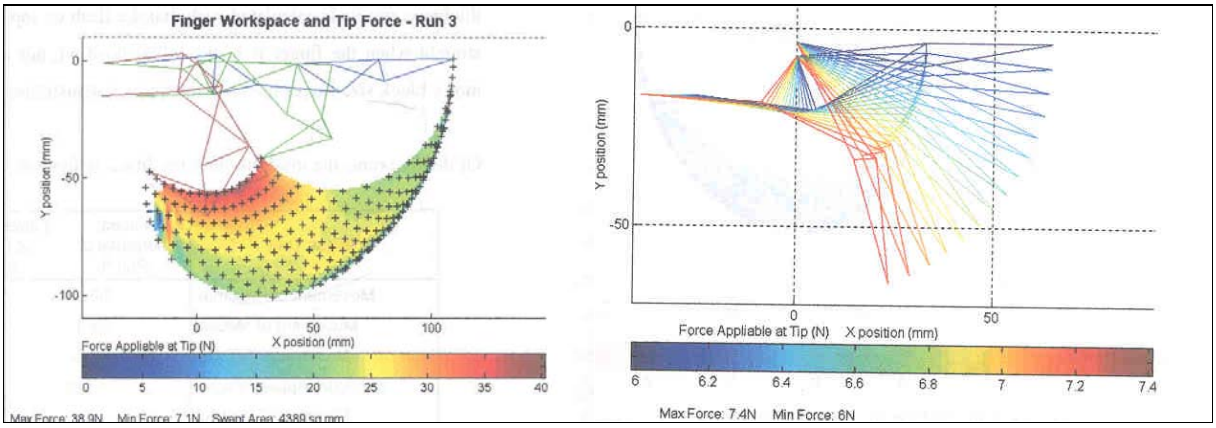

Figure 6.1 Bain's Optimum Finger and Thumb performance

The optimisation of the finger linkages has been an ongoing topic ever since the Canterbury Hand project began in the early 1990's. The first attempt at the finger optimisation was made by Magnier and Monier [1993]. They used measurements of their own fingers to give them the sizes of the linkages. Ward [1996] made a computer program that would evaluate the forces and motions of the finger. Dietmar Traub [1996] also attempted an optimisation of the finger model with a Genetic Algorithm (GA) program. However the geometries that resulted were not the best. Bain [1997] for his thesis created a GA that used Darwinian evolutionary processes to optimise the finger's motion and fingertip force. A thumb linkage design known as the Canterbury Thumb was also designed and optimised by Bain.

These designs have all had reasonable success. However none had the advantage of working with the entire hand design. The results have either not been applicable to the current Canterbury Hand design model or have been non-optimal. While the previous work may not have developed usable geometries it has contributed largely to the background knowledge, and optimisation processes that this thesis has used. This chapter will not be introducing any new numerical techniques, but it will attempt to explain the optimisation procedures that were used to create the final design geometries for the Canterbury Hand. The areas in the hand design in particular that required optimisation were the finger and thumb's linkage bearing geometries, and the thumb's rotation axis geometry.

6.2 Variables to be optimised

6.2.1 Finger Geometry Variables

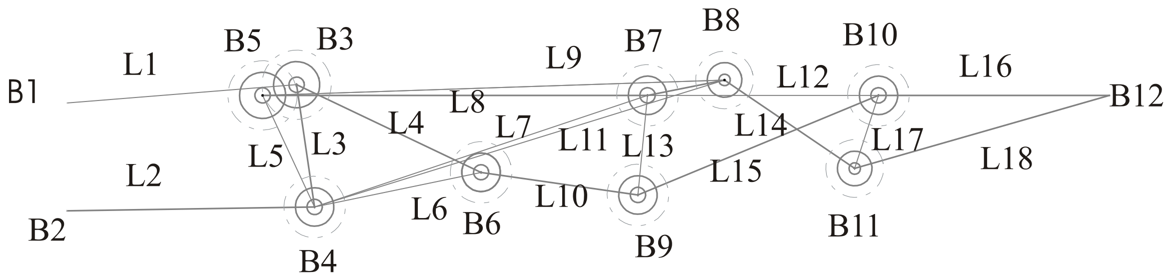

Figure 6.2 Linkage and Bearing geometry of the Canterbury Finger

The linkage geometry was taken from the extended finger state. This is represented two dimensionally in Figure 6.2. The variables that need to be optimised are the coordinates of the linkage joints, the outside diameter of the bearings at these joints and the minimum length of the drive screw.

Cartesian Coordinates (X, Y) locate the position of the linkage joints and the bearings within them. The coordinate system was taken from the extended position of the finger. The origin for the coordinates was taken from a point above and behind the metacarpal block of the finger. By positioning the origin far enough away only positive values are given for the joint coordinates. The reason for this is that the SolidWorks sketches cannot use negative values for dimensions. The outside diameter for the bearings was chosen because a range of possible bearings had already been selected for the optimisation process. The bearings chosen had the largest internal diameter to outside diameter so that the finger linkage forces were less likely to deform the shaft. The design of the finger was such that most finger joint bearings did not contribute to its width. The minimum drive screw length is determined from the extreme curled position of the finger. This is determined in the optimisation process and is dependent on the joint coordinates of the linkages.

6.2.2 Thumb Geometry Variables

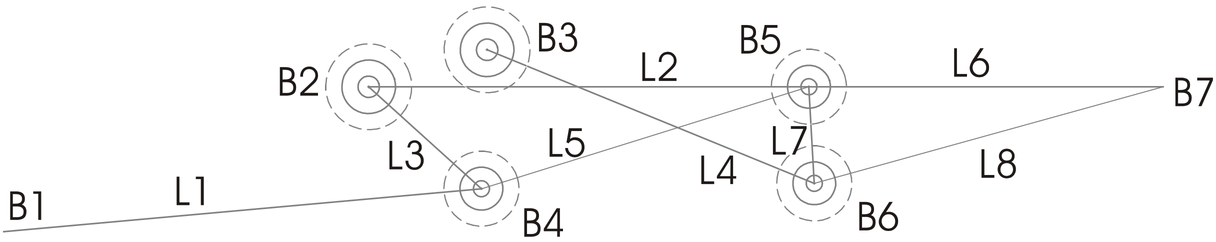

Figure 6.3 Thumb linkages at extended position

The coordinate system was taken from the extended position of the thumb. The two dimensional representation of the thumb linkages can be seen in the diagram. The variables that need to be optimised are the joint coordinates of the thumb, the outside bearing diameter of the joint bearing, and the drive screw length within the metacarpal block.

Like the finger the linkage joint geometry is given with Cartesian (X, Y) Coordinates taken from an origin position above and behind the metacarpal block of the thumb. The bearing diameter is chosen from a pre-selected range of bearings. The drive screw length is determined from the curled position of the thumb as it is just about to reach its singularity position.

6.2.3 Thumb Rotation Axis Variables

The thumb's rotation axis is defined within the hand assembly and the thumb assembly. Both locate the axis away from each other using different variables that had to be optimised. The thumb's rotation axis in the hand assembly is located using a starting point and a heading. The starting point was located using Cartesian (X, Y, Z) coordinates from the origin of the assembly. The heading of the rotation axis was found from a horizontal angle (main axis angle) and a vertical angle (second axis angle) from the starting point. Thus the axis of rotation is defined within the hand assembly.

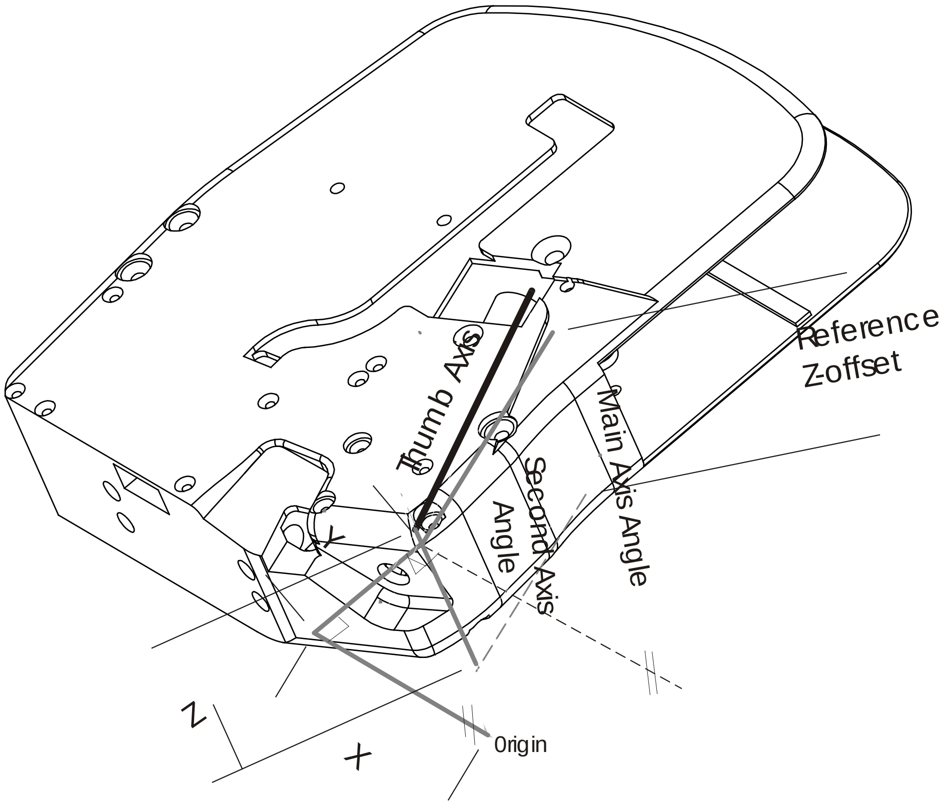

Figure 6.4 Thumb Rotation Axis Variables in Palm

The thumb’s rotation axis in the thumb assembly was created as a vector. This vector was defined by five variables. The first two variables locate the horizontal projected axis line of the thumb axis. This is created from an angle (angle 1) and an offset distance (base 1) from a reference line, in the plane at the top of the metacarpal block on that plane. The vertical location of the rotation axis is located by two other variables. In the vertical plane created beneath the horizontal projected axis line a vertical angle (angle 2) and a second offset distance from the rear of the metacarpal block (base 2) forms the axis of rotation for the thumb. The final variable, the ‘strut separation distance’ from the thumb’s rear strut to the front strut, defines the magnitude of the vector.

The axis variables in the hand and thumb assembly have been defined. However the point at which the thumb assembly is fixed to the hand assembly needs to be described. Otherwise the thumb could be located at any distance along the axis of rotation within the hand. The starting point for the thumb axis in the hand assembly is also at the centre of the worm gear, in the plane of the worm-worm gear rotation. The worm gear is held within the motor end cap, which forms the rear strut of the thumb metacarpal assembly.

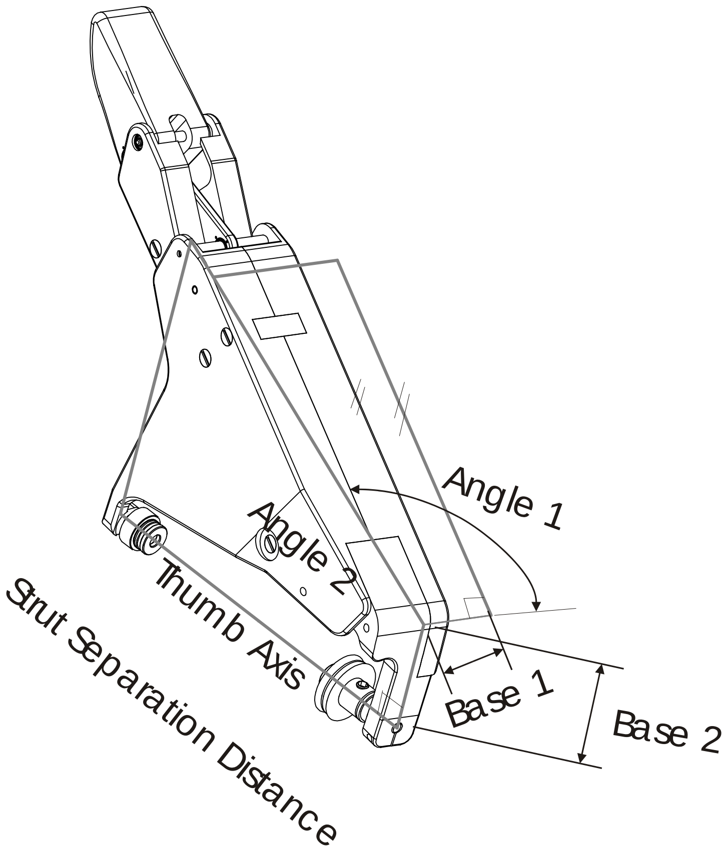

Figure 6.5 Thumb rotation axis variables in the Thumb

6.3 Design Goals

As was mentioned above there are three main areas that require optimisation. They are the linkage geometry for the finger and the thumb, and the thumb's rotation axis.

Briefly the design goals for the optimisation were:

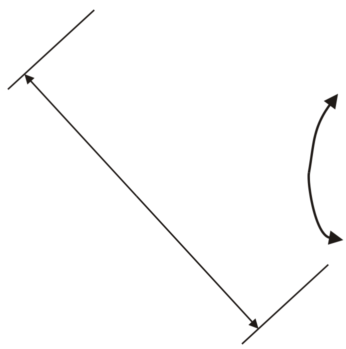

- Reduction of singularity effects on motion.
- Maximum working area.
- Anthropomorphic motion.
- Maximum grip force.
- Aesthetic anthropomorphic appearance.
- Reduction or negation of interferences.
- Maximum prehension for hand.

6.3.1 Reduction of Singularity Effects on Motion

Singularities occur within the within the finger and thumb linkages. When they occur they can radically increase the bearing forces. This can cause stress fractures within the linkages and plastic deformation of the bearing shafts. Since the linkages cannot reach beyond a singularity they can also reduce the working motion. The objective was to create geometries of the finger and thumb linkages that removed singularities from occurring from as much of the working motion as possible.

6.3.2 Maximum Working Area/Volume

The motion of the moving models of the fingers and the thumb needs to be as large as possible so as to have maximum prehension of the hand. The greater the prehension of the hand the larger number of grips at different positions it could make. By having more possibilities for a hand grip the user would not need to think so hard before attempting a grip. The hand would thus be easier to operate and have greater flexibility. These are important qualities if the hand is to be used in a wide range of applications.

For the finger assembly this meant that the proximal, medial and distal linkages needed to move as far about each other and the metacarpal block as possible so as to have the maximum range of motion. The limitations for these motions occur when the linkages come close to their singularity positions. These motions needed to be anthropomorphic in appearance. They had to be balanced so that linkages did not go too far in some motions or too little in others.

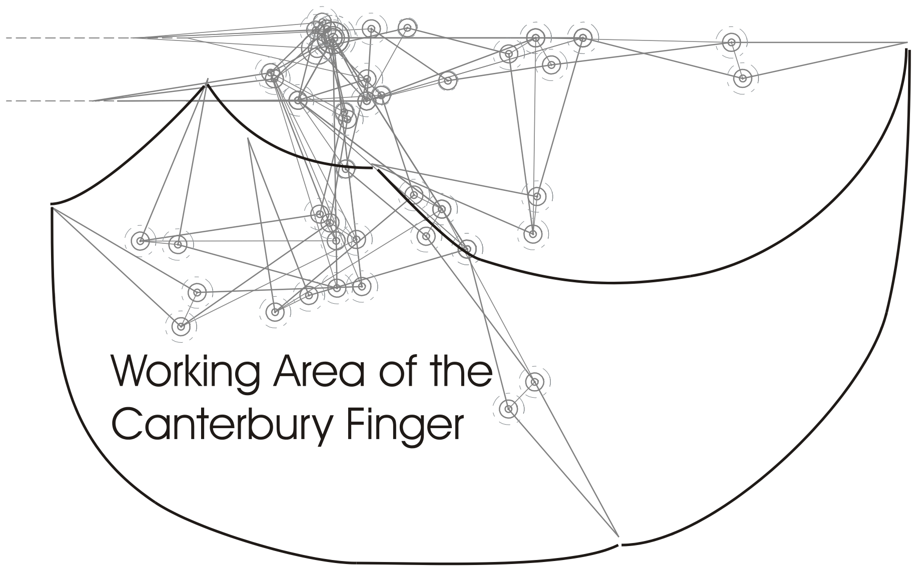

Figure 6.6 Working Area of the Middle Finger (Maxon)

For the thumb assembly this meant that the maximum curl position of the thumb had to occur before it collided with the palm of the hand. It also had to avoid colliding with the circuit board held at the bottom of the thumb's metacarpal block. The singularity position had to occur far enough in the motion so as to not hinder the thumb's curl as well. The movement of the thumb linkages should be smooth and resemble the curling motion of a human thumb.

The thumb's rotation in the hand assembly needed to have the maximum volume so that it could grasp large shaped objects. It had to rotate out of the palm far enough so that objects of a large size could be grasped under the thumb linkages. Yet when doing this it had to have as small a length for the rear of the thumb (base 2) as possible so that the thumb did not look unnaturally detached. The thumb also had to rotate as far around the hand as possible before its metacarpal block collided with the palm. The larger this rotation angle was, the more grasp positions the hand could make.

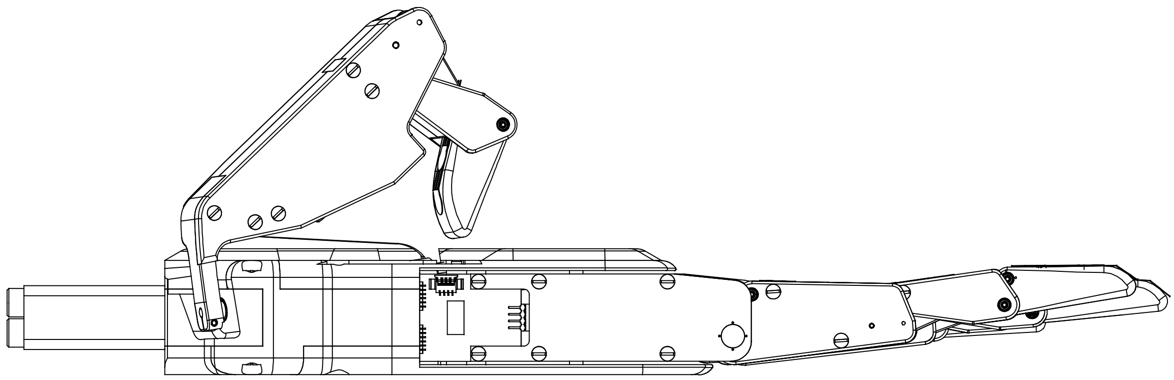

Figure 6.7 Curled Thumb in Hand Assembly

6.3.3 Anthropomorphic motion

The motions of the hand should be as human like as possible. If the hand is to one day be used as a telerobotic device, or eventually a prosthetic device, then it would be far more intuitive to use if it replicates a human hand's motion. A natural human like motion would also be more acceptable for a user of a prosthetic device.

In particular the finger linkage motions needed to reach the same angles as the human finger when it curled or when it moved around the knuckle. When curled the distal link of the finger should come close to the rear of the proximal linkage for example. The thumb linkage motion had the potential to move further past the back of the knuckle than the human thumb. However if it did this it would still hit the thumb's metacarpal block. It needed to be limited so that its final curl occurred before this collision. Also the thumb has the potential to hit the palm of the hand if its length is too long.

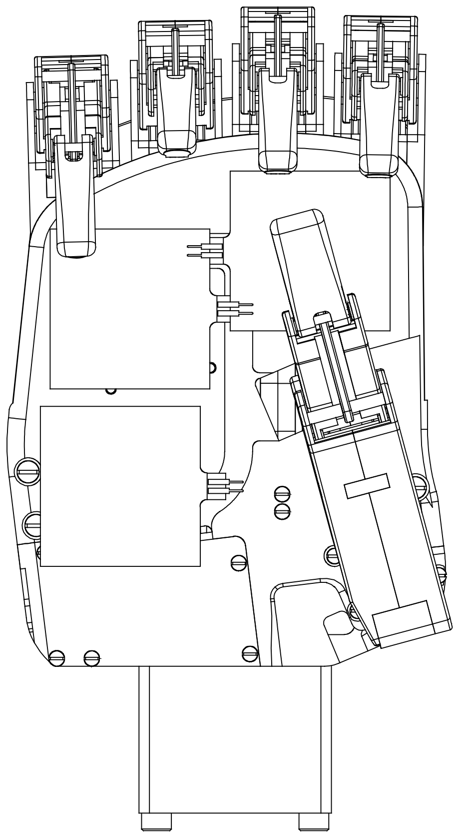

It was very important that the thumb axis in the hand gave an anthropomorphic rotation of the thumb. It needed to have the thumb opposite the Index and Middle fingers at the height of its rotation like the human hand. It also needed to move as far around the hand as possible so that it did not look artificially limited. The thumb needed to start its motion from a natural looking resting position next to the side of the hand. It had to rest so that the thumb's rear strut did not protrude out of the surface of the palm or at an angle out of the hand when in the resting position. Further there needed to be enough space between it and the hand so that the fingers could spread without collision with the thumb.

Figure 6.8 Thumb Opposition Position in the Hand

6.3.4 Aesthetic Appearance

The goal of this project is the creation of a multi-degree of freedom hand prototype that will one day be developed into a prosthetic device. It is better if the anthropomorphism of the human hand is introduced into the design as early as possible. This will reduce later redesign. If the hand were eventually to be used as a prosthetic device it would be far more acceptable to others if the hand has a human like appearance. Even if it is not used as a prosthetic an anthropomorphic dexterous robot hand has many more applications than a non-anthropomorphic one.

The finger and thumb models had to have their linkages arranged so that they had relatively human sized phalanges. For the finger this would mean that the proximal, medial, and distal links had to be proportioned like a human finger. They could not be human sized as this would make the hand was so large that the fingers would look mis-proportioned. They should also look human in appearance at different positions in the fingers motion. When the finger and thumb curls, the linkages move into each other making them smaller in size. Therefore slightly longer phalanges were needed to keep an anthropomorphic appearance when the finger and thumb are curled.

The thumb's axis location and the thumb's appearance within the hand were very important. The front thumb strut had to line up within the recess within palm so the thumb was tidily placed when in the resting position. It also had to be aligned as close along the side of the palm like the thumb. Also the thumb had to have its rear strut (base 2) as close to the palm as possible so the thumb did not look like it hung unnaturally from the hand.

6.3.5 Maximum Grip Force

The output force from the thumb and the finger should be as large as possible. The reason for this is to have an adequate grip of objects within the hand's grasp. By having a more efficient grasp smaller motors can be used in the hand design. This would reduce the mass of the hand. Whatever device holding the hand would also have less dead weight to move around.

Knowledge of how the force output was calculated for the finger and thumb linkages was necessary when maximising the grip force. The idea was to have the maximum moment and output force for a given input for each of the linkages. The force output was constrained by the limits to the geometry of the linkages. There was a maximum width to the finger and thumb linkages, and the longer the finger or thumb was the less force output was possible. The position of the actuator links determines to a large extent the force output. The closer the actuator links got to lining up with the rotation joint the smaller the moment output force. An example of this motion was the finger curl motion with Actuator link 2 about bearing joint B4.

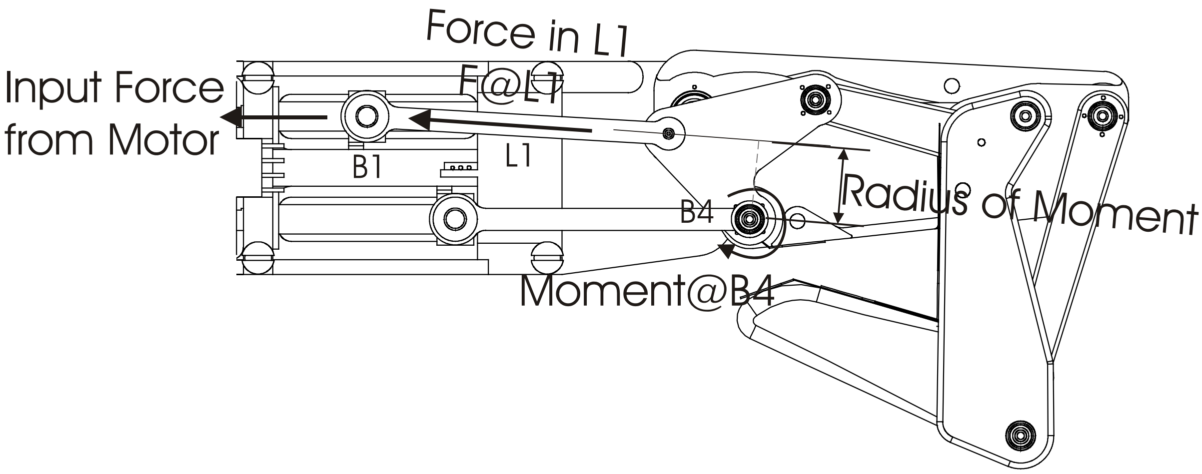

Figure 6.9 Moment about Bearing Joint B4 at the Fingers Maximum Curl Position

For the rotation of the thumb within the hand assembly the leg length from the worm to the metacarpal block (base 2 length) needed to be minimised so that the hand had the maximum moment from the worm gear. This would mean a higher grip force on an object between the thumb and the palm of the hand.

6.3.6 Reduction or Negation of Interferences

In the human hand there are no linkages that cross into each other that limit it's motion. It is therefore a good idea to create the linkage design so it doesn't do it either. A good example of a possible interference is the proximal link curling and hitting the metacarpal block at the limit of its travel. It would be best if this only occurred after the extreme curl position. Other interferences to avoid would be within the finger and thumb linkages. Bearings within the linkages are located on shafts that travel through the width of the finger. As linkages travel within the finger during its motion it is best that they avoid hitting the bearing shafts.

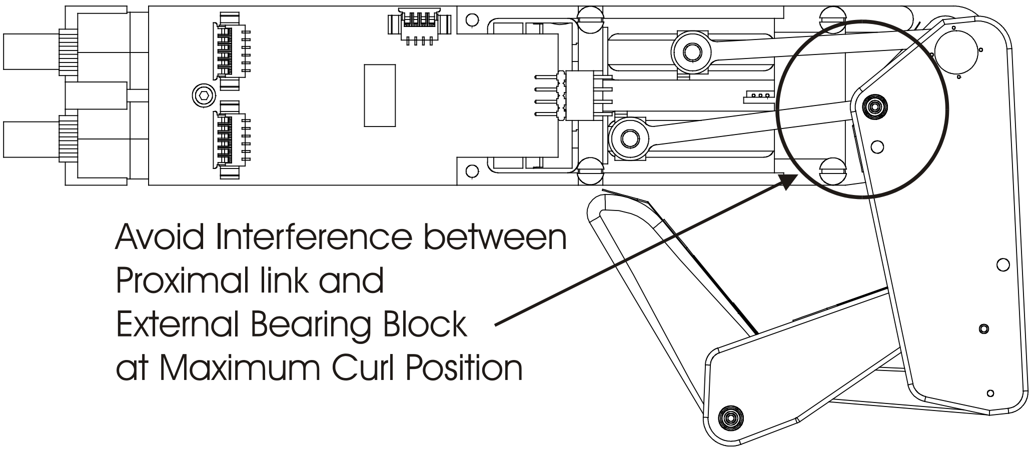

Figure 6.10 Clearance between Rotated Proximal Link and External Bearing Housing

The bearings in the linkages need a minimum amount of material around them to support them. It is therefore best to avoid getting the bearings too close to each other. Another interference to avoid is between the curl of the thumb and the palm of the hand. It would do not good to grip an object if the thumb cannot reach past the palm to get to it. When the thumb is in repose along the side of the hand it should be at an angle that does not interfere with the spreading of the fingers.

6.3.7 Maximum Prehension for Hand

To have as dextrous a hand as possible there needs to be maximum interaction between the fingers and the thumb. The prehension of the hand is dependent on the relative locations of the fingers and the thumb in the hand. It is also dependent on the sizes and volumes of the linkages motion. For example, the thumb has to be able to make pinch grips with the fingers for a number of positions. The linkages and thumb have limitations to their length, otherwise they appear overly long. As the linkages move into each other when the finger and thumb curl the interaction volume is therefore limited.

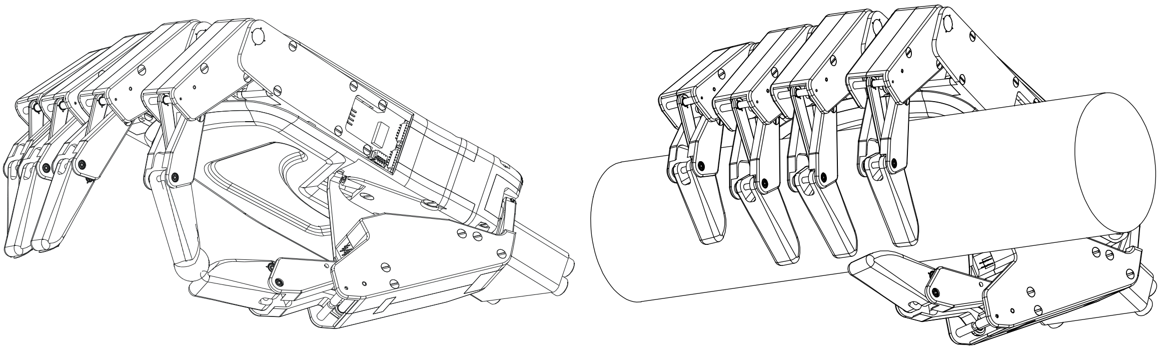

Figure 6.11 Examples of Canterbury Hand's Prehension

By having maximum prehension more grips for different sized objects can be achieved. Thus smaller objects can be grasped and manipulated more easily. The thumb's position in the hand, and the degree of motion it possessed was critical for the number of possible grips.

6.4 Method

This section is a brief description of the methods used for the optimisation of the finger, thumb and thumb axis within the Canterbury Hand. Though the methods were similar with each other, they had different optimisation goals for their variables. The overall goal of these methods was to find the optimum geometries for the Maxon and Mini motor hands. That is why each of these methods included evaluating the geometries within the context of the Canterbury Hand model. It should also be mentioned that the optimisation processes occurred after the design of the finger, thumb and hand CAD models. The models were flexible enough to allow changes from the optimising process to be made automatically. Implementation of the new geometries was made by changes to the affected models design table spreadsheets. These spreadsheets were embedded within the models, and used logic equations to make limited design decisions based on changes in the geometry. Such design characteristics as bearing configurations, or spacer widths and diameters could be automatically changed with the new geometry. The process of updating the embedded spreadsheets with the optimised geometry was automated using a design table spreadsheet.

This spreadsheet utilised Visual Basic Application (VBA) language in Excel in a file called ‘Configure’.

The thumb axis was the first geometry that was optimised for the Mini and Maxon hands. The reason for this was that prehension between the thumb and the fingers depended on getting this optimised first. The thumb and then the finger geometry were then optimised and their geometries recorded. The results of the optimisation process for the thumb axis, thumb linkage geometry and finger linkage geometry are given at the end of this chapter.

6.4.1 Finger Linkage Bearing Geometry

The creation of the initial CAD models of the Canterbury finger required that bearing geometries separate from those created by previous students needed to be made. By doing this the CAD model stability could be tested for different positions and the inherent limitations of the bearing geometry positions could be found. The geometries were made within 2D sketches of the finger linkages. The elements that represented the links in the finger were defined so they could be moved. The motion of the finger and the affects that changes had on this motion were explored and recorded. While the geometries from this initial process could not be used for the final hand model they were useful. It helped locate the singularity positions within the finger linkages. It defined general guidelines and constraints for optimising the finger geometry. This information was put to good use when the optimisation of the final finger geometries was required.

The later optimisation of the finger was made within the linked SolidWorks model of the Canterbury finger. The reason for this was that the top down design of the linked finger allowed for immediate changes of the finger linkage models. If changes were made to the control sketch, (or the embedded design table spreadsheet that controlled it) all the linkage models would change to fit this new geometry. This was useful for immediately finding whether the CAD models could stably handle the new geometry. Since it was the solid model that was updated, interferences in the motion could be checked, and the effects of the geometry could be visually evaluated.

The optimisation process within the linked finger model began by evaluating geometry within test sketches. These test sketches were independent of the control sketch so they did not affect the linkage models. Each 2D sketch was made of elements that represented the linkages within the finger model. The sketch elements had the bearings represented as circles at the various joint coordinates. Each of the sketches served different functions.

Test Sketch: This sketch was the first step in the optimisation process. It was used to set out the variable finger linkage geometry. The elements that made up the sketch's links were not dimensioned or defined to any external feature. Instead the joint coordinates were defined from the Property Manage using Cartesian coordinates from the origin. Changes could be made to the linkage geometry by modifying the position of the joint coordinates. The origin was positioned above and behind the sketches so that the bearing coordinates could be recorded as positive values above zero. This is important when the coordinates are dimensioned in the control sketch, as a dimension can never be below zero. This sketch was also used to show the limitations of the fingers size and motions. Within it is represented the boundaries of the palm cover plate and the face of the metacarpal block's external bearing housing.

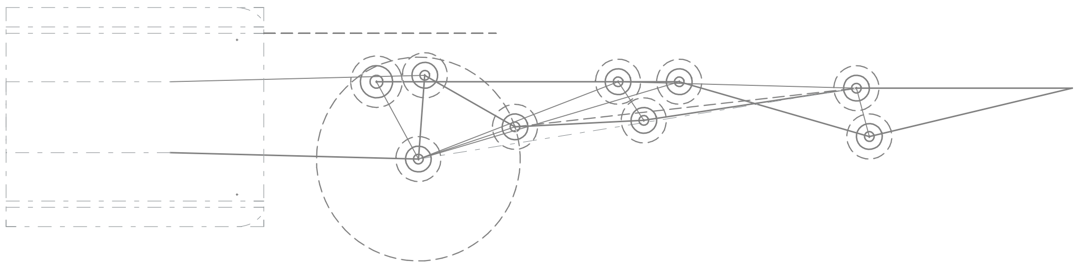

Figure 6.12 Finger Test Sketch

Mobile Test Sketch: This sketch is freely movable. The geometry of the line elements is constrained by relations with the Test Sketch. These constraints include the fixed position of joint B5 and the line of actions of both the bottom and top actuator linkages. Dragging an actuator link sketch element creates the motion of the linkages (although for the rotated motion the bottom link needs to be fixed). The motion is the same as the solid models and was used as a verification of the finger motion.

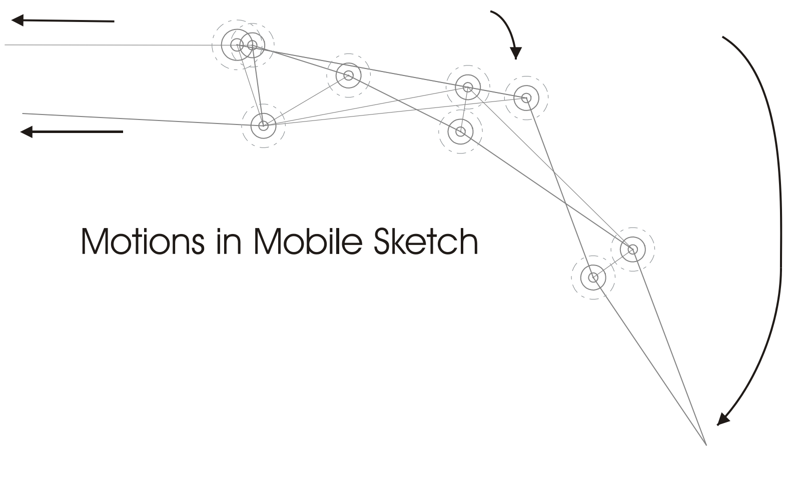

Figure 6.13 Finger Mobile Test Sketch

Curled Test Sketch: This sketch represents the finger at its singularity position in the curled motion. It is used as a visual guide to see instantly what the curled finger position is with a given geometry. It is constrained exactly the same way as the Mobile Test Sketch. However it is fixed in place by a dimension that sets the angle between the linkages that form the singularity position. This sketch is defined by the controlled singularity position between the L17 and L14 linkages. The angle between them was set at 170º, which is just before the singularity. A problem can occur with this when geometry is created that has one of the other two singularities occur before this position. When this occurs the finger sketch would have an over defined error. To fix this either a dimension driving the sketch from the new singularity would need to be created, or the geometry would have to be modified in the Test Sketch.

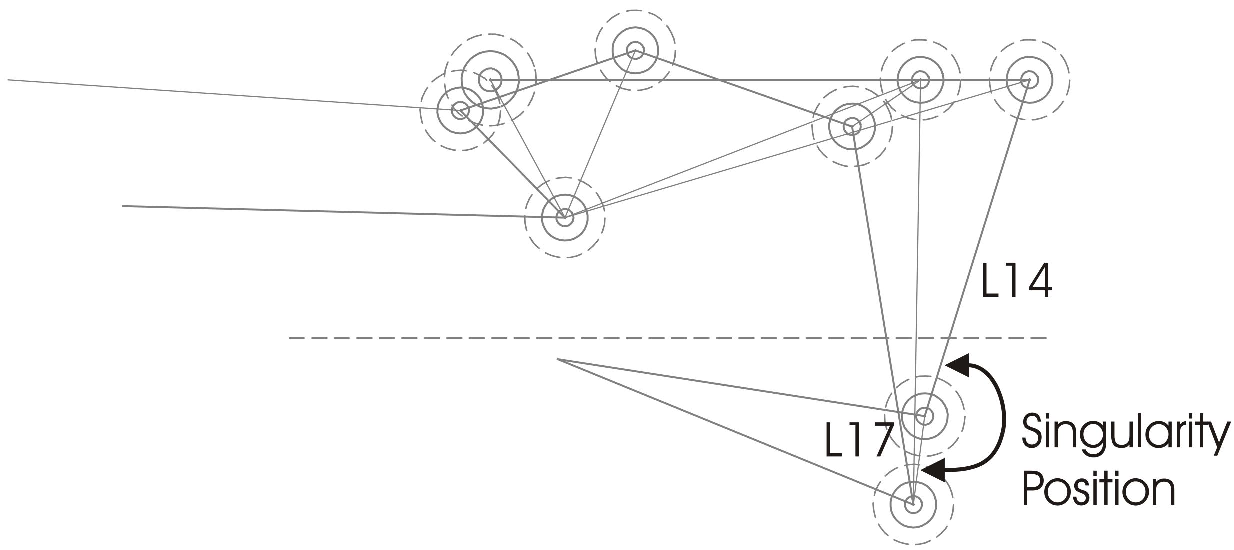

Figure 6.14 Curled Test Sketch of Finger

Rotated Test Sketch: This sketch shows the finger at its singularity position for its rotated motion. Like the other sketches it was derived from the Test Sketch and was constrained by an angular dimension at the controlled singularity. In the case of the Rotated motion the controlled singularity was between links L3 and L5. The angle between these two links was chosen to be 160º. This was because at any further distance there would be a collision between Actuator links 2 and the bearing joint B4. Like the curled sketch this sketch was used as a visual guide for the rotated position of the finger.

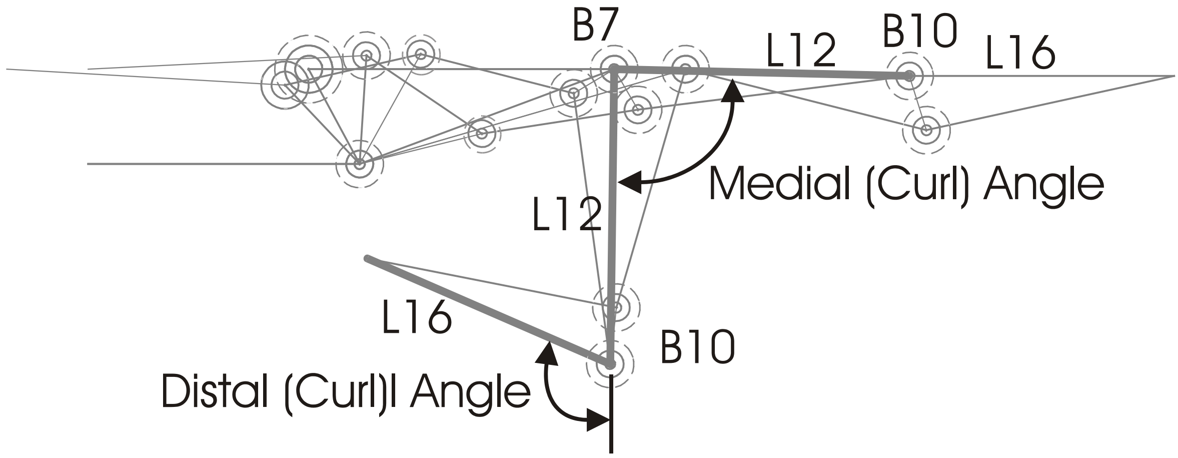

Figure 6.15 Rotated Test Sketch of Finger

Rotated and Curled Test Sketch: This sketch shows the position the finger would take when the finger linkages are curled from the rotated test sketch. It is used as a visual guide as a kind of halfway point between the curled sketch and the extreme position sketch. The linkages are controlled at the singularity location between links L14 and L17 (with an angle of 170º).

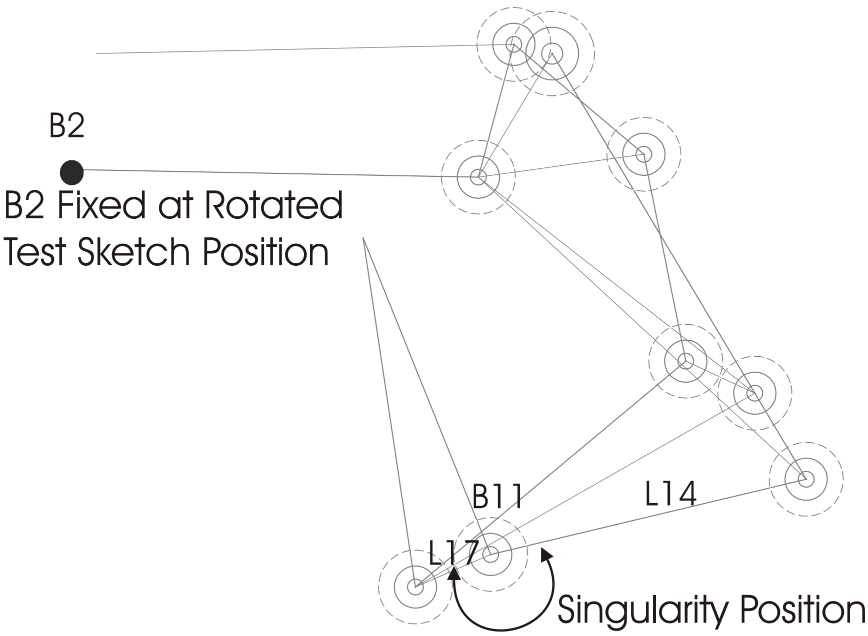

Figure 6.16 Rotated and Curled Test Sketch of Finger

Extreme Position Sketch: The extreme position sketch represents a visual limitation of the extreme motion that the finger linkages can reach. It can be thought of as the curled finger rotated around the knuckle as far back as possible. It does not take into account interferences that the finger might make with the solid models. It is located between two controlled singularities, which represent the limitations of both actuators. The curl is fixed by an angle (170º) between the L14 and L17 links. The rotated motion is fixed by an angle (160º) between the L2 and L5 links.

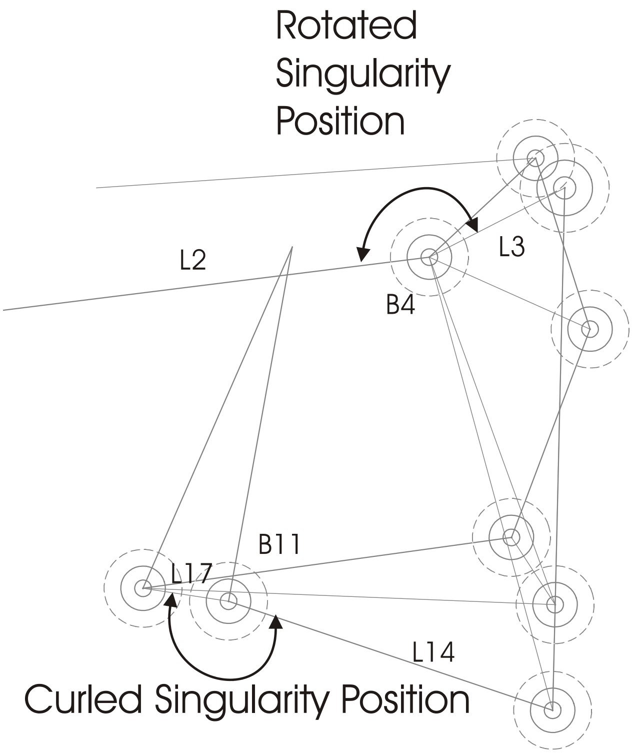

Within the linked finger model were also sketches that showed the motion of the solid model. These sketches are separate from the test sketches, although they showed the same functional detail. They are controlled (like the solid model) from the control sketch and show the positions/motions of the current geometry finger linkages. These motions could be verified by moving the solid model.

Figure 6.17 Extreme Position Sketch of Finger

The optimisation process was begun in the test sketch by making joint position changes. The geometry changes were always rounded to the nearest 0.5mm, so that the geometry was easier to manufacture. One of the problems with previous finger geometry from Bain and Ward was the unnecessary precision that was used. This made it harder for the finger to be manufactured.

Since the motion sketches (as described above) were derived from this sketch they updated automatically to reflect these changes. By having the two sets of sketches superimposed upon each other (one set for the current geometry and one set for the modified geometry) the comparison of the effects could be made. The comparison of the changed and non-changed geometries can straight away be used to see if a finger's motion has been improved. It can also show whether the new geometry fits within the motion and sizing constraints. The changes in the sketches curl and rotation motions were verified by using the 'Measure' tool within SolidWorks. When evaluating whether a bearing geometry was improved or not the design goals had to be looked at. These were:

a) Reduction of Singularity Effects and Maximum Motion: These two design goals were almost congruent. They were easiest to evaluate as well. The finger geometry was created so that the singularities within it always occurred after the two controlled singularities. The motions before these two singularities could then be maximised.

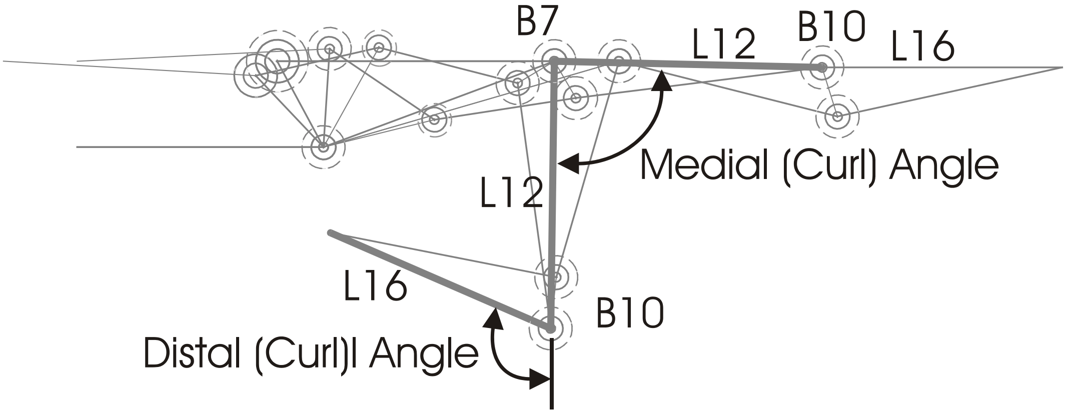

Figure 6.18 Motion Measurements for Maximum Curled Finger

The rotation motion of the finger around the knuckle bearing was measured from the rotation of Link 9 between the test sketch and the rotated test sketch. The curl of the finger was measured from the medial and distal motions. The medial rotation was measured as the rotation of either link L14 or link L12 from the extended finger position to the curled test sketch. The distal link rotation was measured from several locations. It could be measured as the rotation of the L16 link from its original extended position in the test sketch to its position within the curled sketch. The L16 link could alternatively be measured as a relative rotation between it and the L12 (or L15) link in the curled sketch. These measurements and the visual comparisons between geometries were used for evaluating the motion of the finger's linkages. To achieve the best motion the most efficient curl of the finger had to be accomplished. The guidelines towards optimising the finger were useful in helping to create this.

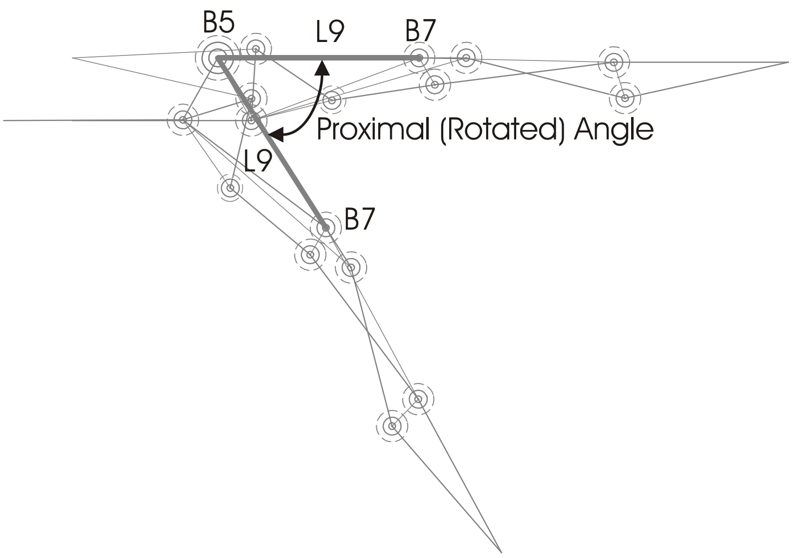

Figure 6.19 Motion Measurement for the Maximum Rotated Finger

b) Maximum Force Output: This was not quantitatively measured in the optimisation process. However it could be maximised by having the maximum input moment in each given linkage motion so as to increase the output force. An example of this was to maximise the input force going into the finger curl. The force going into the finger curl depends on the angle of the top actuator (L1) link to the rocker link (L3). As the finger curls the angle between the two links increases and the perpendicular distance between them decreases. Since the moment is equal to the force (which is constant) multiplied by the perpendicular distance (which is decreasing with the curl) the end angle between L1 and L3 is crucial to the force output of the end finger curl. The end curl angle between these two links was just one indicator that was used when maximising the finger force output.

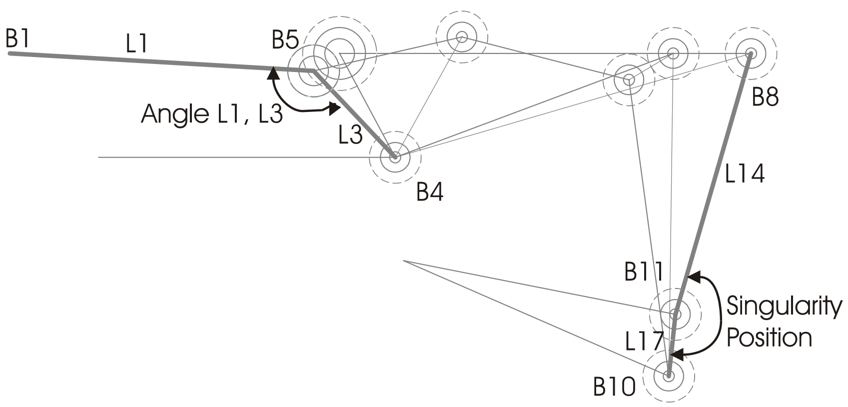

Figure 6.20 Finger Force Output Indicator

c) Aesthetic Appeal: The aesthetic appeal was the hardest to evaluate for the finger. Mostly it was a case of keeping the sizing of the linkages within human proportions and within the constraints given within the test sketch. The motions of the linkages was also important as they had to follow human like motion and not be stuck on a singularity half way through the curl. The motions also had to be constrained to avoid interferences with the hand model such as with the palm base. Also the finger linkages could not move with motions unnatural and greater than a human finger. The appearance of the finger also had to remain anthropomorphic even though the relative positioning of the linkages changed when the finger moves. While the finger had to have the maximum motion it simultaneously also had to have the drive nuts travel the minimum distance. This was because a longer travel distance required a longer drive screw and hence a longer metacarpal block. This would make the fingers appear too long for the rest of the hand design. Therefore the travel of the actuator links and on the drive nut had to be decreased as much as possible.

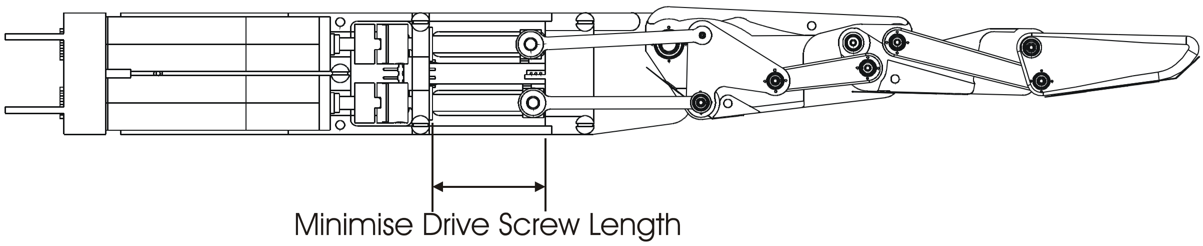

Figure 6.21 Minimised Drive Screw Length in Finger

d) Prehension: The prehension of the finger in the hand was a very important quality that had to be evaluated. That is there had to be sufficient interactions between the fingers and the thumb when grasping an object in the hand. To test this the fingers were curled in the hand and their interaction with the thumb was observed. Test objects were placed in the hand assembly to simulate how well the hand could grip them.

The prehension of the hand had to be balanced with the length of the fingers. When the finger curls the linkages move within each other. The end effect of this motion was to make the finger smaller once curled. The fingers could be made longer to compensate for this so as to increase the prehension. However this had the disadvantage of making the extended fingers look out of proportion to the rest of the hand. The other alternative was to move the thumb closer to the fingers. This however had it's own disadvantages which will be discussed in the section below.

Since the grip of the fingers on the object and their anthropomorphic sizing was so important to the hand, the length of the fingers was the first optimisation constraint to be set before the optimisation of a finger. This constraint was set from the maximum anthropomorphic sizing of the finger for prehension in the hand. The position the finger had in the hand was the biggest factor toward its sizing. The middle finger would be considerably longer than the little finger. The relative sizing of the finger lengths was taken from the hand assembly and proportional to hand morphology data. The particular distance was set as being the distance from the knuckle bearing B5 to the fingertip joint position B12.

Once the finger length was set it was divided up into phalanges in distances proportional to hand morphology. These lengths formed rough constraints as to how long the linkages could be within the finger without making the phalanges unnaturally long or short. The proximal phalange length was taken as being the distance from the rear limit of the knuckle bearing joint at B5 to the front limit of the B8 joint. The distal link was taken as the fingertip distance from the B12 joint (with material added) at the fingertip to the rear material position outside the B10 link. The medial link distance was taken as the difference between these two constraint systems. That is the medial link was the distance between the outer rear distance of bearing joint B8 and the front outer distance of joint B10.

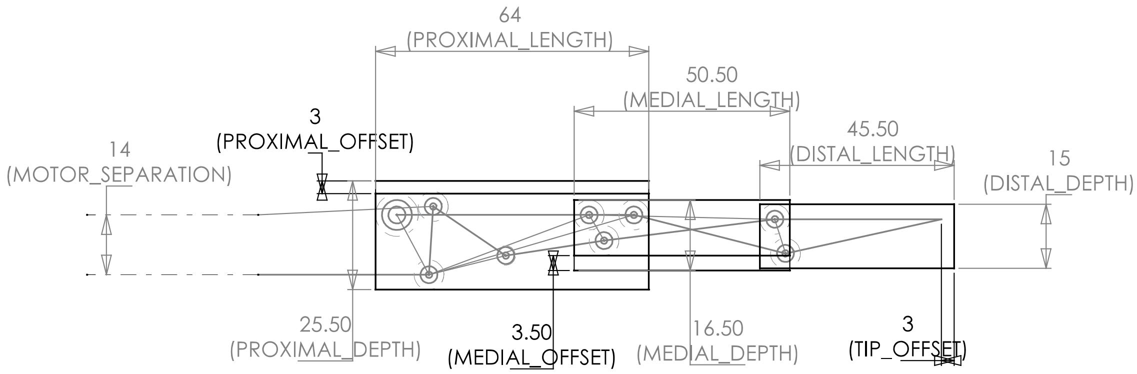

Figure 6.22 Finger Size Measurements for the Middle Maxon Finger

The motors within the metacarpal block determined the vertical separation distance between the actuator linkages L1 and L2. This meant that for the Maxon motor finger configurations the separation distance was 14mm, and the Mini motor configurations the separation distance was set to 11mm. Due to the model of the finger the height of the finger metacarpal block had been determined as being 26mm for the Maxon motor and 29mm for the Mini motor. The height of the metacarpal block served as a maximum height for the finger linkages. There was meant to be a taper from the knuckle joint of the proximal link to the distal link so as to give an anthropomorphic appearance to the finger.

Once the bearings within the linkages were set out within the phalange areas as determined by these rough constraints the optimisation process was begun. As stated above changes were made in the test sketches and implemented and compared against with the solid model of the linked finger. If the geometry was an improvement it was recorded within both the design table of the linked finger assembly and within an archive spreadsheet. This process also used guidelines that helped speed up the optimisation process and to create an optimised geometry. These amounted to suggestions for the bearing placement, etc. The guidelines can be summarised as modifying the bearing joint positions for; reduction of singularity, maximising curl/rotation efficiency, increasing aesthetic appearance and increasing the force output from the finger. The descriptions of the linkage positioning for the bearing geometry optimisation was done within the Test Sketch. The finger linkages of the test sketch are arranged at the extended finger arrangement of the linkages so all the guidelines are written from that position.

The linked model is limited to a single bearing geometry at a time and was unsuitable for use within the hand model. Due to the use of multiple configurations of components in the Canterbury Hand, a separate finger model using configurations of different geometries was necessary. After an optimised geometry was found using the linked finger it was implemented in the hand model using the configure program.

6.4.2 Guidelines for Finger Optimisation

The following guidelines were used for helping to quicken the optimisation process.

6.4.2.1 Quick Optimisation by modification of an existing geometry

To create a new geometry while making the minimum changes to the existing one a technique was created that kept the relative positions of bearings within a group. By moving the groups of these bearing joints the geometry could be improved more quickly.

There were three bearing groups for the finger. They have been named the Proximal, Medial and Distal Bearing groups. The B10, B11 joint bearings formed the distal group. The B7, B8 and B9 joint bearings formed the second medial group. The bearing joint positions of B3, B4, B5, and B6 formed the proximal group. The constraints of the length, and width of the finger determined the prior positioning of the B1, B2 and B12 joint positions. After the constraints and the positions of these three joints were found the bearing groups were moved about and the finger's performance was evaluated.

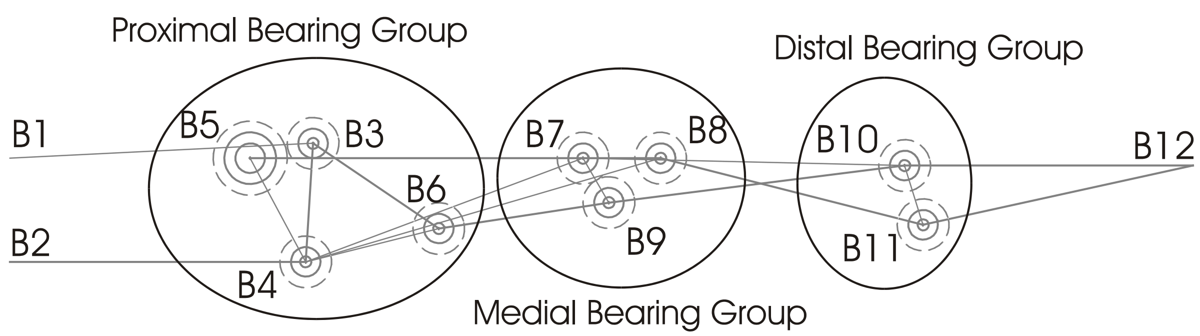

Figure 6.23 Bearing Groupings for Quick Optimisation of the Canterbury Finger

6.4.2.2 Singularity Reduction:

This section has been discussed briefly within the Background theory. The fingers were controlled from two singularities, one for each motion of the finger. The two control singularities were between links L14 and L17 for the curl motion, and between links L1 and L3 for the rotation motion. These singularities had to occur first before any others in the finger motion.

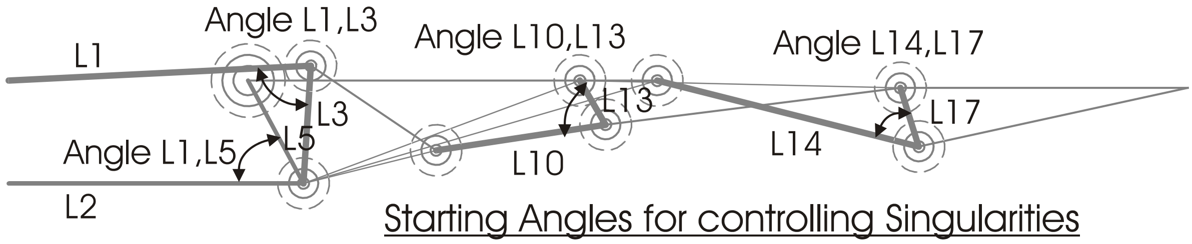

Figure 6.24 Starting Angles for Singularity Control within the Finger

Curl Motion Singularity Guidelines:

- Links L1 and L3

The singularity occurs when the two linkages attempt to align themselves. The singularity is controlled by the starting angle between them in the extended finger sketch. The smaller the starting angle between the links the further the finger linkages can move before it encounters this singularity. This singularity in particular is a problem as there are no mechanical stops to prevent it from occurring. Another reason for this singularity not to happen (beside the large bearing forces produced from it) is that the moment produced in the rocker (about B4) is reduced to negligible when the singularity occurs. The output force would therefore also be reduced to nearly zero.

- Links L10 and L13

The next possible singularity in this motion occurs when these two linkages attempt to cross over each other. The singularity between the two links only occurs if there is too small an angle between them when the finger curls. It can be avoided if the angle between them is sufficient. Care should be taken that the angle is not too large as it also causes a singularity within the rotation motion of the finger about the knuckle bearing.

- Links L14 and L17

This was the controlled singularity. It occurs when links L14 (the distal driving linkage) and L17 (in the distal link) attempt to align themselves. The stop in the distal link prevents this from occurring. The positioning of this singularity should be just beyond the maximum wanted position of the finger curl. It can be controlled by the starting angle between the two links. If this angle is reduced the singularity occurs later in the finger curl. The positioning of the distal and the distal driving link on the proximal also controls the singularity occurrence within the curl. The motions of the medial linkage system also lead the motion of the distal link. The rotation of the medial and distal linkage systems should occur so that they are roughly perpendicular to each other before the singularity occurs in the motion.

Rotation motion Singularity Guidelines:

- Links L2 and L5

The singularity between these two linkages in the rotation motion can be avoided by keeping a large enough angle between them. When the bottom actuator is pulled back the angle between them increases. If a singularity does occur it gives high bearing forces. The perpendicular distance between the line of the actuator and the knuckle bearing B5 is negligible. This reduces the moment into the proximal link system and hence the force output to a negligible amount.

- Links L10 and L13

Another singularity for these two linkages occurs in the curling motion of the finger. However in the rotation motion the two linkages are rotating in the opposite direction. The singularity in this case happens when they attempt to align themselves. The larger the angle between L10 and L13 the more quickly the singularity occurs within the rotation motion. There is a balance however for the starting angle between these two linkages due to the curling motion singularity in the other direction. If the angle is too large it will make the curling motion singularity occur early. This kind of singularity is a standard problem in four-bar linkages.

- Links L1 and L3

The singularity occurs when these two linkages attempt to cross over each other. This singularity was the controlled singularity in the rotation motion. The stop in the proximal link prevents this singularity from occurring by halting the rocker. To maximise the rotational output moment of the finger the initial angle (at the extended finger position) between links L1 and L3 should be maximised. This angle has to be balanced though with the finger curl's motion and force output. In particular the force output of the finger curl is determined by the angle between these two links.

6.4.2.3 Maximising Finger Motion Efficiency

The finger motion efficiency is increased by various techniques. One technique to increase efficiency is to remove the slack between linkages so that motions occur earlier. Increasing the coupling between the linkages can also increase the efficiency. By coupling it is meant the motion of an output linkage is increased with the same input motion of the connected linkage. An example of this could be the medial link system. As link L13 (part of the medial link) is decreased the coupling between it and the input motion from the L6 link (part of the rocker) is increased.

The motion guidelines that were used are summarised briefly below. Not all the guidelines given though were followed in the optimisation. Other guidelines such as aesthetic appearance or force output requirements were just as important. Often compromises and choices of one guideline over another had to be made.

Motion Guidelines:

- The diameter of swing of the rocker is the length of link L6. It determines how far the rocker sticks up when the finger is at full curl. The rocker should not stick out of the proximal link. The length of L3 should be sized with the same constraint in mind.

- The rocker should not have to rotate too far for the curl motion. If the rocker is moving further than necessary it is giving a worse force and motion output and is probably due to inefficiencies in the finger linkage arrangements.

- The medial four bar link system is dependent on the coupling between links L6 and L13. By increasing L6 and decreasing the length of L13 the medial link will rotate more quickly about bearing joint B7. Yet L13 must not be so short as to make the singularity at L10 and L13 occur. Also the length of L13 is related to the force output of the finger.

- The links of L6 and L13 are connected by link L10. For the optimisation it was best to keep L10 short so that when the rocker link (L6) rotated it doesn't need to swing back so far before motion in the L13 link (part of medial link) occurred. If L10 is long the effect of the rocker rotating out of the bottom of the proximal link, in the finger rotation motion, will be accentuated. That is L10 (medial driving) link will be more exposed and the mechanical nature of the finger will be further enhanced.

- A general rule for increasing the coupling within the medial link (between L6 and L13) was to have B6, B9 and B10 on a straight line with each other. By doing this slack in the system is reduced as well. That is the rocker travels less far before significant motion in the medial link. If there is slack in this line between the bearings then the finger's rocker linkage will have to rotate further to give the same equivalent curl.

- As the medial link rotates the length of L13 should not be so long or offset too far vertically away from B7. When the finger curls it will cover the distal link and can limit how objects are gripped.

- Joint bearing B8 needs to be closer to the distal link than joint bearing B7 for the distal curl motion to occur. It is best if B8 is horizontal to B7. If it is too far below B7 the medial link looks deformed from the B7 shaft recess.

- The ratio of the lengths of links L14 (distal driving link) and L12 (part of medial link) give the coupling within the distal linkage system. For a smaller L14 link the coupling increases resulting in a larger rotation of the distal link for a given rotation of the medial link. Also the length L14 (or it's ratio to L12) determines how much actuator travel is needed for the rocker link/medial link system to rotate for a full distal curl motion. If L14 is long it will take more of a medial rotation to produce the singularity at L14 and L17. The L17 link should also be reduced if the input motion from L12 is to accentuate the distal curl motion. However the bearings should still have a minimum amount of material about them. This will limit how much the link can be reduced.

- Bearings at the joints within the finger should be small enough that finger size is minimised. However they should be large enough so that they can handle the forces within the finger.

- The curling of the finger was chosen to be a slightly more important motion than the rotation of the finger. That is why L3 is tilted towards the distal direction instead of being vertically above bearing joint B4. It means better force output for the finger curl motion if the actuator travels more evenly above bearing joint B4. It should not be tilted too far as it means that there is less motion for the finger rotation before the singularity between links L1 and L3. The larger the angle between links L3 and L1 the more the finger can rotate (about joint B5). The L3 link should also not have too much of an angle as this has an impact (though less important) on the finger straight motion. This angle depends on the singularity of L3 and L1.

- On the finger straight motion the B4 bearing will rotate backwards about the B5 bearing. As it rotates the B4 bearing may collide with the external bearing block of the finger metacarpal assembly. This can be avoided by minimising the L5 link length. However this would mean that the finger has less force output in the finger rotation motion. Alternatively when the finger goes into the extreme curl position the length of L5 determines how far up the B3 bearing sticks out of the gap between the proximal link and the external bearing block. The alternative would be to have the B5 bearing (and with it the B4 bearing) offset further away from the external bearing block towards the distal link. This however creates a bigger gap between the proximal link and the metacarpal block, which is aesthetically unpleasant. It also makes the actuator links longer, and hence the length of the drive screw within the metacarpal length is increased. The increased length of the metacarpal block makes the hand appear longer. A balance therefore between aesthetics and force output needs to be made for the finger geometry optimisation of the position of the B4 bearing location.

- A situation to avoid when placing the rocker link is geometry where the rocker rotates to a point where any further rotation has no affect on the medial links motion. In this situation the rocker would then rotate further back until L1 and L3 are nearly aligned and only just before this singularity takes place would further positive motion of the medial driving link occur.

Note: These guidelines should come with a warning. If the user is only working with the wire frame sketch of the finger they should be aware that the model is a solid formed about this. That is, there is material that surrounds and holds the joint bearings. For example, at the B12 end joint position of the distal link there is an extra 3mm radius of material extending beyond it. Therefore the finger is larger than the wire-frame and its motion and interferences with surrounding models will be affected by changes in the model.

6.4.2.4 Improving Aesthetic Appearance

The aesthetic appearance of the finger is formed by the placement of the joint bearing constraints. However the aesthetic appearance of the finger diverges once the fingers moves from the extended finger position from which the geometry is set. The guidelines for the dynamic aesthetic appearance for the finger optimisation are summarised below.

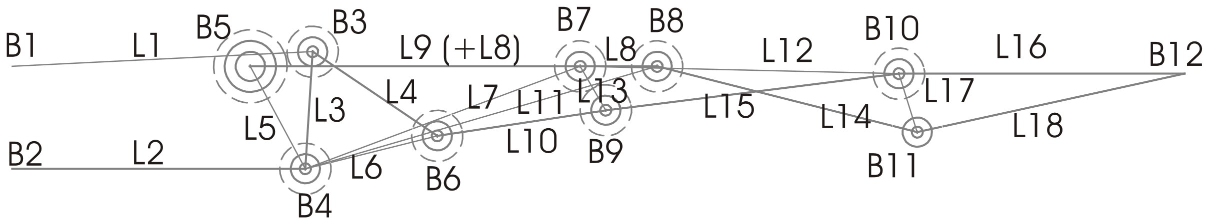

Figure 6.25 Finger Linkage and Bearing Naming Scheme

- The B8 and B7 bearing joints should be horizontal to each other and not too far apart. This is to avoid the knuckle affect as can be seen in Ward’s geometry. Also when the finger is fully curled the L14 link will not stick out as far without any gaps around it. If they are too far apart the links may not allow the medial to fully rotate about B7.

- Minimise the length of L10. As the finger rotates it will not stick out the bottom of the proximal link so far when the finger gets close to the singularity between links L1 and L3.

- The motion of the finger should be natural. Therefore the finger should not curl too far towards the metacarpal nor curl unnaturally away from it. The distal link curl should be fully developed and not halt prematurely near a singularity. The motion should be maximised so that the finger has maximum grip for both curl and rotation motions.

- The finger should be tapered along its bottom edge upwards toward the distal link. The top line should be as horizontal as possible. This is to imitate the appearance of the extended human finger.

- The B5 joint bearing should not be too far to the top of the metacarpal block as it can give an ugly shape to the metacarpal block's phalange support bracket. Also as the finger assumes the extreme curl position the length of link L5 and the vertical placement of the B5 bearing will determine how far the B3 bearing will stick out above the proximal link. The placement of the B5 bearing should allow full rotation motion of the finger without collision of the B4 bearing with the metacarpal's external bearing block.

- The B9 bearing should be kept not too far beneath the B7 joint bearing when optimising the geometry. The reason for this is that as the finger curls the distance between the bearings will cross over the distal linkage. This is aesthetically unpleasant and is a potential source of interference for making a good grip. It also makes the distal link look smaller when the finger is curled.

- The rocker link should be sized so that it does not require a gap in to the top of the proximal linkage for rotation. In particular this means sizing B3 joint to a small enough bearing. It also means having an appropriate length for the L3 and L6 links.

- For the largest area motion of the finger it was best to have a slightly longer proximal and distal link. This is so the finger can go further and higher back to grasp objects in the palm of the hand. As the finger curls the proximal link and the distal link will rotate into the metacarpal and the medial links respectively. This makes them appear smaller and reduces their grasp area.

6.4.2.5 Maximising Finger Output Force

To maximise the finger's force output for each of the finger motions (curling and rotating the finger) the moment should be maximised about the rotation bearing joints. The section below gives some methods on how this was done for the optimisation of the finger. While several of these guidelines may maximise force output they should also be used only if they do not limit motion of the finger.

Curling Motion Guidelines for Maximising Force output

Maximise Moment about Rotation Points:

- Bearing Joint B4
    - Maximise perpendicular distance from joint to actuator link 2 (link L1) for the range of motion.
    - Angle between links L1 and L3 to be kept close to perpendicular over the range of motion.
    - Maximise the length of link L3 (part of rocker link).
    - Minimise the distance actuator link 2 travels.

- Bearing Joint B7
    - Maximise perpendicular distance from joint to medial driving (L10) link.
    - Maximise the length of the L13 link (part of medial link).
    - Minimise length of link L6 (part of rocker link).

- Bearing Joint B8
    - Maximise distance from this joint to bearing joint B10.
    - Minimise length of link L12 (part of the medial link).

- Bearing Joint B11
    - Maximise length of link L17 (part of distal link).

Maximise Output Force:

- Minimise distance from joint B12 (in the distal link) to the B8 bearing joint.
- Minimise length of link L18 (part of distal link).

Rotation Motion Guidelines for Maximising Force output

Maximise Moment about Rotation Points:

- Bearing Joint B5
  - Maximise perpendicular distance from actuator link 1 (link L2) to bearing joint B5.
  - Maximise length of link L5 (part of Proximal Link).
  - Angle between links L5 and actuator link 1 to be kept close to perpendicular.
  - Minimise the distance actuator link 1 travels.

- Bearing Joint B7
  - The same guidelines as those applied for the bearing joint B7 in curling motion apply here.

6.4.2.6 Constraints

The finger constraints are:

- The finger curling motion should avoid the palm of the hand.
- The rotation motion should avoid collision with the external bearing block within the metacarpal block.
- Joint bearing constraints. These constraints fix the lengths of the phalange links so the finger is properly proportioned.
- Rocker link should not rotate out of the proximal link (they should be enclosed).
- The solid model of the finger should not be higher than the top of the metacarpal block. This requires careful placement of the bearings (B5, B7, B8, B9 and B10) along the line of the finger.
- The bearing order in the geometry is fixed to a degree. This is necessary if the finger is to curl properly. That does not mean that coordinate positions of each individual bearing cannot be modified by large amounts.
- The motor size sets the separation distance between the actuator links.

6.4.3 Thumb Linkage Bearings Geometry

The optimisation procedure for the thumb geometry was very similar to that of the finger optimisation. The very first attempt at the optimisation of the thumb used sketches of the thumb linkages. These were modified and the changes to the thumb motion and force output were observed. A basic geometry for the thumb was found using this initial process, and this was used for the building of the thumb solid model in SolidWorks. The creation process also located the singularities within the thumb linkages and various guidelines that would help in future optimisation of the thumb geometry.

After the thumb model was completed it was split in two. One of the thumb models was used within the hand as the ‘configured’ thumb. It used multiple geometries for both a Maxon and Mini motor configuration and was used in the hand model. The other thumb model called the ‘linked’ thumb was used in the optimising process. The linked thumb model used a control sketch that controlled the geometry of all the linkage parts. The linked model had the advantage that by modifying the control sketch the rest of the model would automatically update to reflect the new geometry. However unlike the configured thumb only a single geometry could be used in the model at a time. This limited it from being used in the hand assembly.

Within the linked model were three test sketches that were used for optimising the geometry. Each sketch had elements that represent the thumb linkages. They are independent of the model. That is any changes made here would not modify any of the models in the thumb assembly.

Test Sketch: The test sketch is a 2D representation of the extended thumb’s linkages. The mobile test sketch and the curled test sketch both take their geometry off this sketch. If changes were to be made in the test sketch the other sketches would automatically change to reflect this change. Small changes were made to the test sketch as part of the optimising process and the results to the curling motion were observed in the other sketches.

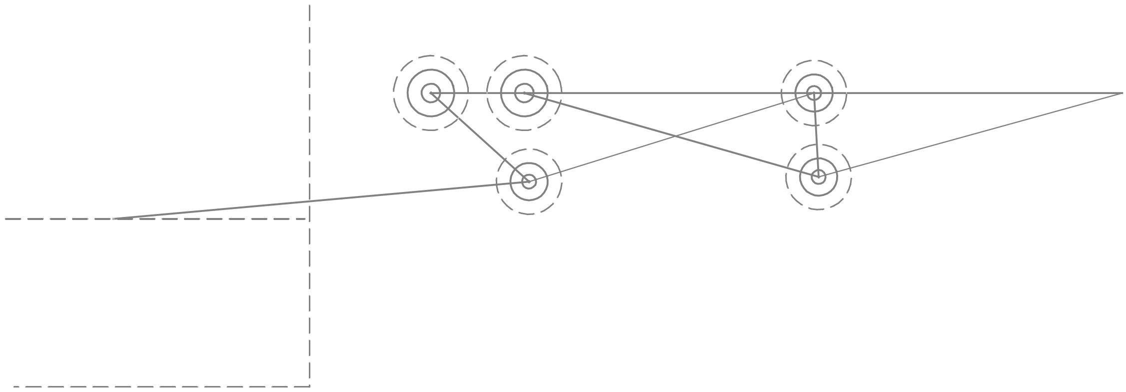

Figure 6.26 Thumb Test Sketch

Mobile Test Sketch: The mobile sketch was used to look at the motions of the thumb linkages. It is linked to the test sketch for the sizing of its geometry. The actuator link was constrained to the line of its action in the sketch. It could be dragged to give the curl motion of the thumb.

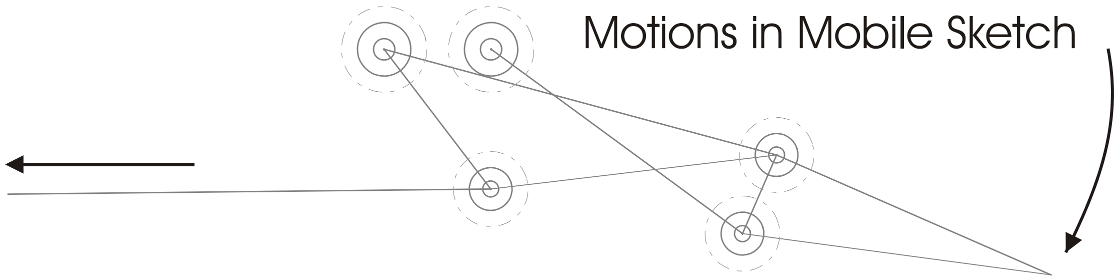

Figure 6.27 Mobile Thumb Test Sketch

Curled Test Sketch: The curled test sketch was used to see what position the thumb linkages would form at the controlled singularity position. It was linked to the test sketch for it's linkage sizing. The controlled singularity angle (170º) was between links L4 and L7 as the links attempt to extend themselves straight at the end of the thumb's curl. This position was the end limitation of the curl motion.

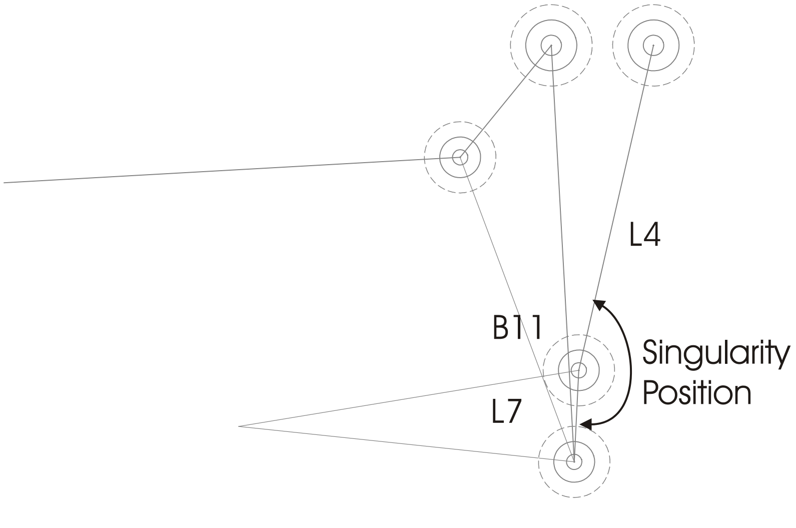

Figure 6.28 Curled Test Sketch of the Thumb

Within the linked thumb model were three other sketches that showed the motion of the solid model. These three sketches were the control sketch, the mobile sketch and the curled (thumb) sketch. These last two sketches have their geometry derived from the control sketch instead of the test sketch. They are all functionally the same as the test sketches as described above. These sketches were used for comparison with the test sketches when evaluating whether the test geometry was better or not than the current model geometry.

The optimisation process began by determining the ideal prehensile position and length of the thumb within the hand assembly model. It had to have the longest length for maximum prehension, yet not be so long as to appear unnatural. When the thumb was in the rest position alongside the hand the thumb tip was taken to be collinear with the B5 rotation bearing of the index finger. This approximated the maximum acceptable aesthetic length of the thumb. It also was a close approximation of where the thumb is placed in the human hand.

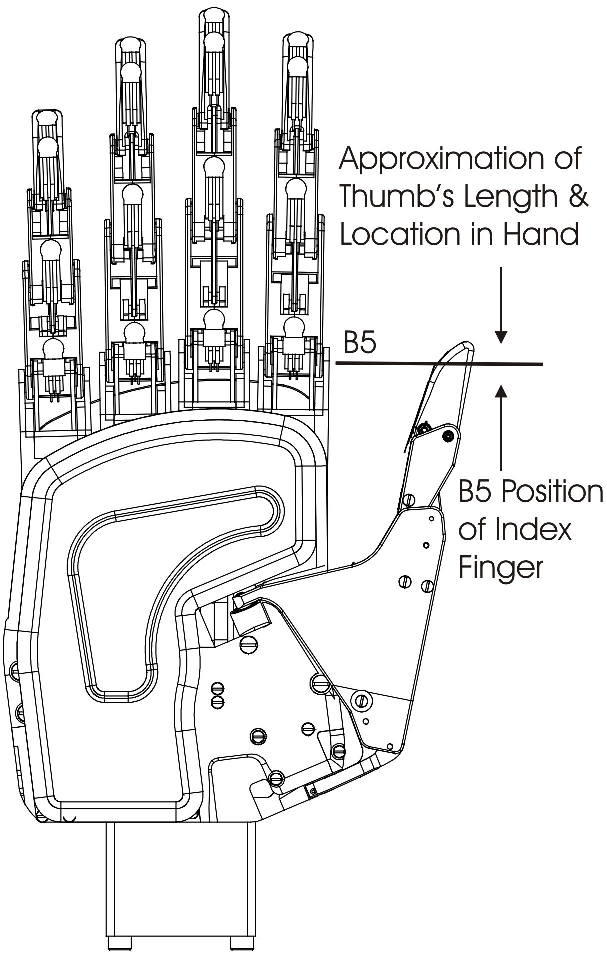

Figure 6.29 Thumb Location with

Once the length of the thumb was defined it was split into half to determine the length of the distal and proximal links. The test geometry of the thumb is then created around this constraint. Since the motor size of the thumb has been selected for a particular optimisation the location of the drive screw and the actuator link can be defined. The rotation bearing (B2) of the proximal link was then defined as well as the location of the other bearings in the thumb. The height of the thumb (in the Y axis) was mostly an aesthetic choice.

An approximate geometry for the thumb would be found and used by the solid model and the control sketch. A new geometry would then be created within the test sketch by modifying the joint coordinates. The joint geometry for each change was always rounded to the closest 0.5mm for ease of location and manufacture. The modifications were made using the guidelines to create an optimised geometry more quickly. The new geometry would then be compared against the one in the control sketch and the solid model. If it successfully fulfilled the evaluating criteria the geometry was recorded, and implemented in the linked thumb solid model. This was achieved by modifying the control sketch geometry. Then the process was either further refined or stopped if the geometry was considered satisfactory.

<u>The evaluation criteria were:</u>

Reduction of Singularity Effects and Maximum Motion:

The thumb had to curl fully before the controlled singularity (between links L4 and L7) could take effect. The curl had to be fully formed and anthropomorphic. That is it had to have the proximal link curl ninety degrees to the metacarpal block and have the distal link curl ninety degrees to the proximal link. The thumb linkages curling motion also had to avoid interferences such as collision with the thumb's circuit board, external bearing housing and collision with the palm of the hand.

The motion was measured for the thumbs two main linkages: the proximal link and the distal link. The proximal link was measured for the change in angle its L2 link made between its extended and curled state. The distal link's performance was measured as the change in angle it's L6 link made with the L2 link in the proximal link when it is at full curl.

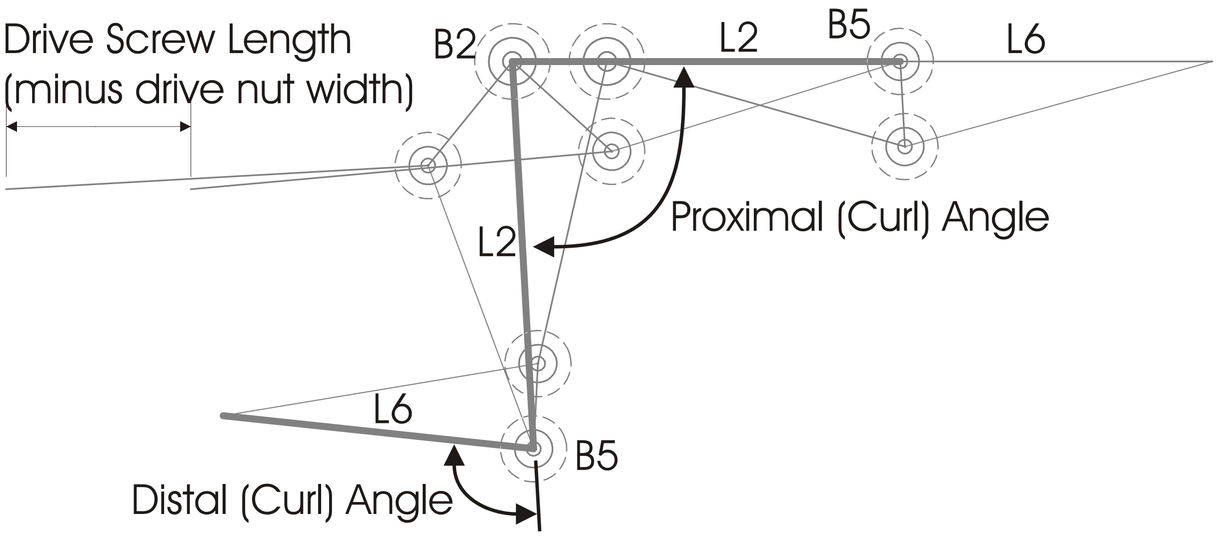

Figure 6.30 Measurement of Motions of the Thumb

Maximum Force Output:

The thumb needed to have the maximum force output at the thumb tip. While this was not quantitatively measured it could be inferred from the linkages. The object was to have the maximum moment for the proximal and distal linkages. For the proximal linkage this meant having the maximum moment about the B2 joint bearing. For the distal link this meant having the maximum moment about bearing joint B3 (and later in the curl motion bearing joint B6).

Aesthetic Appeal:

The thumb's aesthetic appeal could not be directly evaluated. The thumb should be human proportioned and move in an anthropomorphic motion. The end curl position should be fully formed (like the human thumb) and not be under or overdeveloped. That is each link should form roughly ninety degrees with each other. The proximal link should be slightly below ninety degrees with the metacarpal block.

Prehension

There should be maximum interaction with the fingers in the hand. That is why any optimised thumb geometry also had to be evaluated for prehension by evaluating its grip for different sized objects in the hand assembly. This was a subjective comparison of geometries and no actual measurements were taken. Generally the better the interaction the hand had the smaller the object it could grip.

Once a final geometry was selected it was implemented in the 'configured' thumb model. This process was automated using the 'Configure' program. The new geometry was then evaluated for prehension in the hand assembly. If there was sufficient interaction with the objects and the fingers in the hand model the geometry was accepted. If it was not acceptable new requirements (such as a changed thumb length) were decided upon for the new geometry. The optimisation process in this case was begun again.

It should be noted that the thumb's prehension in the hand was dependent on the thumb axis geometry. That is why the thumb axis geometry was optimised and defined before the optimisation process for the thumb linkages geometry was begun.

6.4.4 Guidelines for Thumb Optimisation

6.4.4.1 Singularity Reduction

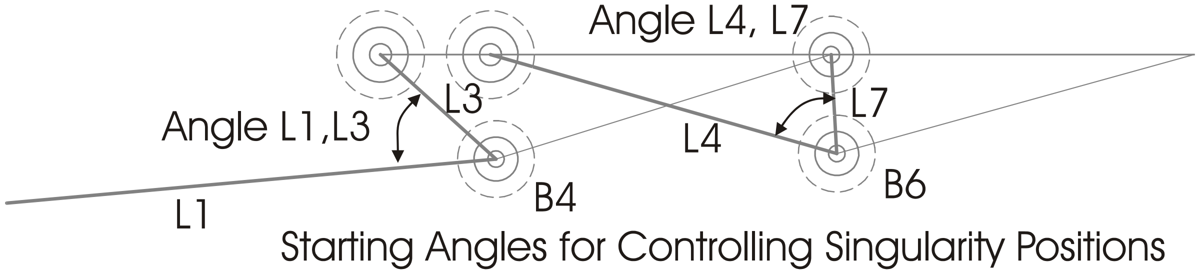

Figure 6.31 Starting Angles for Singularity Control within the Thumb

- Links L1 and L3

The singularity between links L1 (actuator link) and L3 (in the proximal link) happens when they attempt to extend themselves straight in the curl motion. The singularity's location in the thumb curl is dependent on the starting angle between them (from the extended linkage diagram). The smaller the starting angle is the longer the delay the linkages have before singularity. If the singularity were to occur it would mean that the thumb has a negligible force output. At the singularity the actuator link would be nearly aligned with the B2 bearing that the proximal link swivels around. This would mean that the moment about the bearing B2 would be negligible. Therefore the best way to delay this is to keep as small a starting angle as possible between the L1 and L3 links. The thumb linkage design attempted to keep the angle at approximately ninety degrees between the L1 and L3 links during the motion so as to maximise the moment about bearing B2 and hence the force output from the thumb.

- Links L4 and L7

The singularity that occurs between these two links occurs when they attempt to extend themselves straight. It was avoided from occurring in the thumb by designing a stop in the proximal link that physically halts the distal link before the singularity position can occur. While the singularity is avoided the location of the thumb at the curl needs to be positioned. By modifying the starting angle between links L4 (distal driving link), and L7 (part of the distal link), the final curl position can be controlled. If this angle is reduced the singularity occurs later in the thumb curl. The coupling between the proximal and the distal links also controls what position the thumb will take before the singularity.

6.4.4.2 Maximising Thumb Output Force

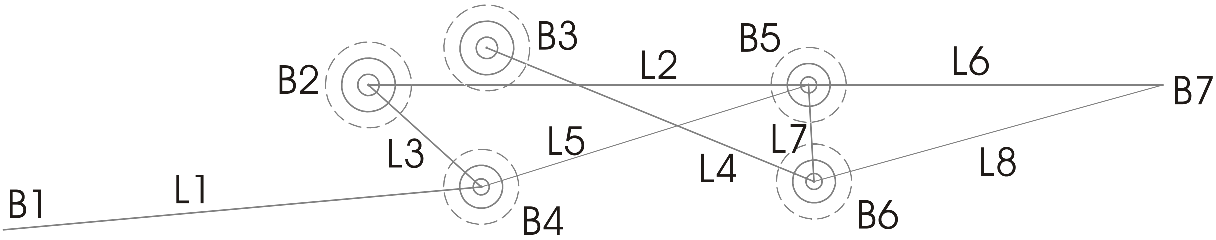

Figure 6.32 Thumb Bearing and Linkage Numbering Scheme

Maximise moment about rotation points:

- Bearing Joint B2
  - Maximise perpendicular distance from joint to actuator link (link L1) over the range of motion.
  - Angle between links L1 and L3 (part of proximal link) to be kept close to perpendicular over the range of motion.
  - Maximise the length of link L3.
  - Minimise the distance the actuator link travels.

- Bearing Joint B3
  - Maximise distance from this joint to bearing joint B5.
  - Minimise length of link L2 (part of proximal link).

- Bearing Joint B6
  - Maximise length of link L7 (part of distal link).

Output Force:

- Minimise length of L8 (part of distal link).
- Minimise distance from bearing joint B3 to the joint B7.

6.4.4.3 Maximising Thumb Motion Efficiency

There were several techniques to improve the motion of the thumb linkages. One method was to increase the coupling between the proximal and the distal links. Other methods increased the control on the curling motion and the aesthetic look of the moving thumb.

- The B2 and B3 bearings should be close together. For the best aesthetic appearance it was best if these two joint bearings were kept horizontal to each other. For the curl of the thumb it was best if it occurred directly underneath the position between these two bearings. This best approximated the ninety-degree curl between the proximal link and the metacarpal block.

- The lengths of links L2, L4 and L7 can control the coupling between the proximal and the distal links. By decreasing the length of L4 (distal driving link) to the length of L2 (part of the proximal link) the coupling is increased. That means that for a given rotation of the proximal link the distal link will rotate even further. The length of L7 (in the distal link) can determine when the singularity curl position can occur. By making it shorter the final distal curl will happen more quickly.

- The position of the B2 bearing joint on the metacarpal phalange support bracket is important for the curling motion of the proximal link. As the proximal link curls the L3 link (in the proximal link) and the B4 bearing rotate about the B2 bearing joint. There is a possible collision problem that can occur between the proximal link and the external bearing block of the metacarpal assembly. The L3 link should be long enough to give the maximum rotation and moment about the B2 bearing. It should be short enough that collision does not result.

- The length of the links should be sufficient to give the maximum curl. For example the link L2 should be long enough that the distal link can curl underneath the metacarpal block of the thumb without impacting the circuit board or the metacarpal assembly.

6.4.4.4 Improving Aesthetic Appearance:

The B2 and the B3 bearing joints should be close together on the metacarpal support bracket. The reason for this is that when the thumb curls the distal driving link becomes more visible at the end of the curl motion. If there is a large gap between the two bearings then it appears as if the distal driving link has separated from the proximal link entirely. This can look unattractive, especially if there is a gap visible around the distal driving link. There should also be sufficient room between the top of the thumb's metacarpal block and the B2 and B3 bearings for a cover. The cover helps hide these two bearings and gives a more pleasing appearance to the thumb.

To control the thumb's anthropomorphic appearance the best way is to keep it within the sizing constraints for the bearing location. To reduce the height of the thumb the joint bearings should have a small outer diameter. However they should be chosen to be large enough to handle the internal forces. The (extended) thumb geometry should also be shaped so that the thumb is flat along its top length. It should also be tapering upward along its bottom length to the distal thumb tip. The end curl motion should have the proximal link roughly perpendicular to the metacarpal block. The distal link when curled should be perpendicular to the proximal link.

6.4.4.5 Constraints

When the thumb curls it should avoid collision with:

- The thumb circuit board at the bottom of the metacarpal block.
- External bearing block of the metacarpal assembly with the B4 bearing of the proximal link.
- The palm cover plate of the hand assembly.
- The screw holding external bearing block to the metacarpal block with the actuator links.

Size Constraints:

- The thumb should fit within the constraints given for the thumb length.
- The thumb linkages should not exceed the height of the thumb metacarpal block.
- The bearing order in the geometry is fixed to their approximate positions. This is necessary if the thumb is to curl properly. That does not mean that positions of each individual bearing cannot be modified by small amounts.
- The B2 and B3 bearings should not be separated too far from each other. This is to increase the aesthetic appearance of the thumb.
- The B2 and B3 joint bearings should have sufficient room above them for a cover on the metacarpal block.

6.4.5 Thumb Axis

As described in the variables section of this chapter the thumb axis was a three dimensional vector shared between both the palm assembly and the thumb assembly. This section will describe the method of optimisation for finding the best geometry of the thumb axis.

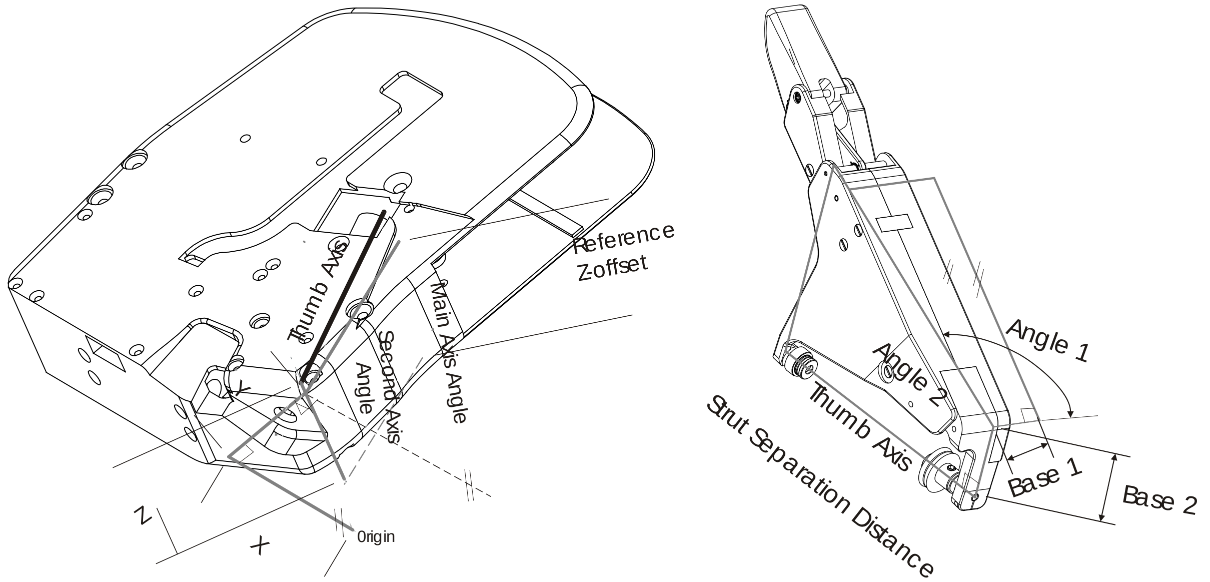

Figure 6.33 Thumb Axis Variables

Briefly the goals for the optimisation of the thumb axis were:

- *Maximum Grip Volume*: The thumb would be able to grip large objects between it and the palm of the hand. That means having the maximum angle for variable 'thumb angle 2' (see 6.2.3 Thumb Rotation Axis Variables) for the optimised geometry. Also it means having the maximum second axis angle so the thumb is angled up as much as possible.

- *Maximum Rotation of the thumb*: The thumb could rotate as far around the palm as possible so as to achieve the maximum number of grips with the thumb. This can be measured as the maximum rotation of the thumb from the resting position about the thumb axis.

- *Anthropomorphic resting and grip positions*: This goal is a little more difficult to evaluate. It means that when the thumb is in its resting position that it does not stick out too far from the side of the hand (so thumb angle 2 is minimised). However there still needs to be enough room for the fingers to spread without collision. Also the front thumb strut has to rest in the recessed space within the palm cover plate. This means that the thumb has to lie exactly parallel with the side of the hand. This can be verified using the sketches in the palm base part. The hand needs to also have its maximum grip position to occur so that it opposes the index and middle fingers. This opposition was critical if the hand was to mimic the grasp types of the human hand.

- *Anthropomorphic Thumb Rotation Motion*: The rotation of the thumb has to be anthropomorphic in appearance. That is, it has to be as human like as possible. Also the thumb's rear strut should not hang too far from the base of the palm cover plate as this accentuates the thumbs rotation mechanism.

- *Minimisation of Collisions*: The extended thumb linkages should not collide with the fingers when they spread. When the thumb rotates past the thumb side panel its circuit board should not collide with the palm assembly. Lastly the thumb should have the maximum rotation about the palm cover plate. It should avoid collision with the palm cover plate for as long as possible for its maximum rotation position. A depression in the middle of the palm was created so as to maximise this rotation.

The optimisation began with the modification of the axis within the palm base part. Changes were made to the thumb axis geometry and the results were observed in the model. Due to the constraints of available volumes for the thumb rotation bearings only very small changes could be made at any single time. And they had to be made so that the axis kept within the constraints of the model. If larger variations were created the model would create errors and would not rebuild properly. Once axis geometry modifications in the palm base part gave a tolerable geometry the Configure program was used to implement it within the hand models.

To help in the visualisation of the optimisation of the thumb axis several sketches were created in the palm base part. They showed how the thumb was positioned as it rotated about the palm of the hand. These sketches were the:

- *Finger Spread sketch*: This sketch showed the positions the finger metacarpal blocks and their motors took when the fingers were spread to their maximum angle of 13.5 degrees. This sketch was useful in positioning the thumb axis so that the front thumb bearings lay between the middle metacarpal block and the spread index metacarpal block.

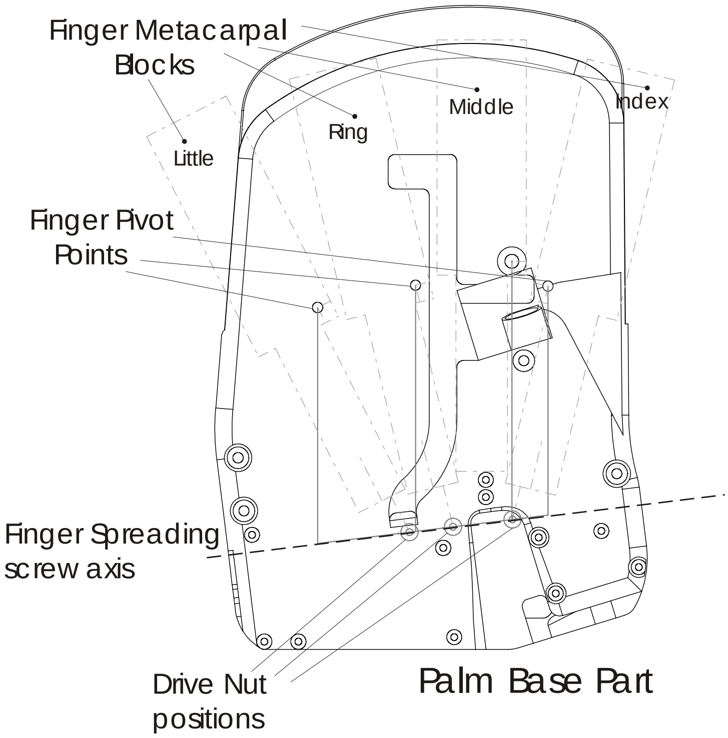

Figure 6.34 Finger Spread Sketch

- *Main Thumb Axis & Thumb Rest Position*: This sketch shows how the thumb axis is positioned for the X, and Y coordinates for the worm gear, and how the axis is angled with the main thumb axis angle. It also shows the top down view of the thumb in its rest position next to the side of the palm (base 2 length and thumb angle 2).

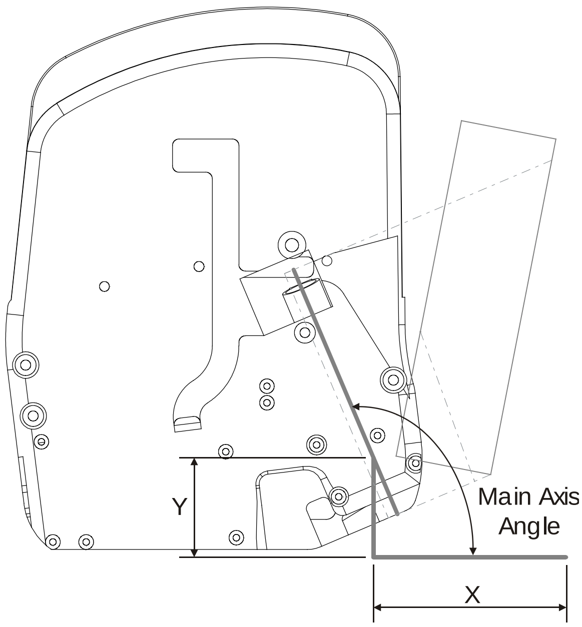

Figure 6.35 Main Thumb Axis Sketch

- *Second Thumb Axis Sketch (And Side View Grip 6)*: This shows the thumb at its maximum grip position directly over the axis (in the vertical plane). It shows how the 'Z' variable offset for the worm gear positions the thumb axis as well as how the 'second axis angle' when combined with the 'base 2 length' and the 'thumb angle 2' give the thumb metacarpal's grip position.

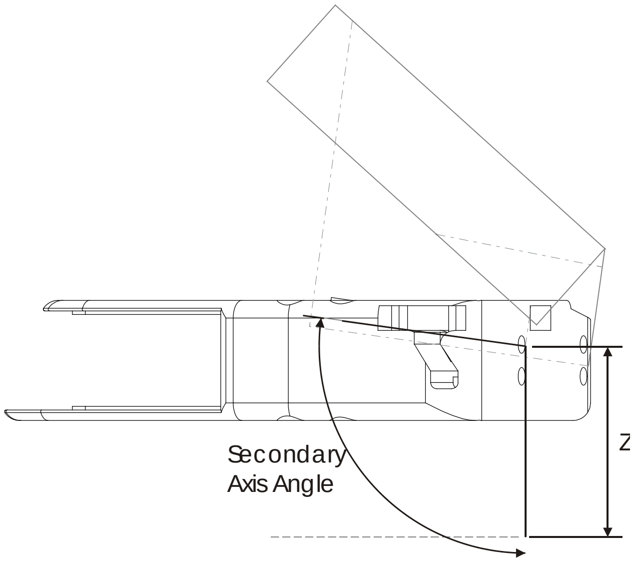

Figure 6.36 Second Thumb Axis Sketch

- *Worm Gear Sketch*: This sketch showed how the worm gear, and the front thumb bearings were vertically positioned within the palm base part. It is in the same vertical plane as the second thumb axis sketch above.

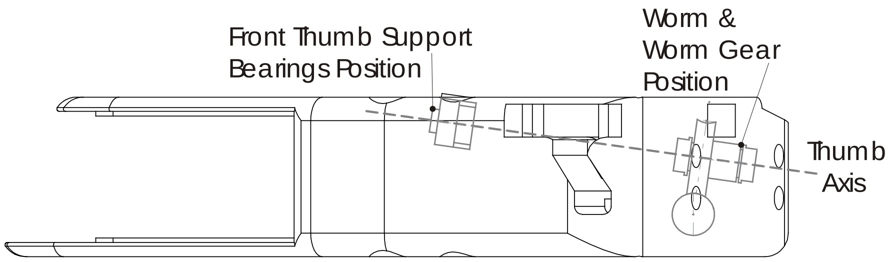

Figure 6.37 Worm Gear Sketch

- *Top View Of Thumb At Rest Position*: This sketch shows the side view of the top of the thumb when it is in its rest position alongside the palm. It shows whether the thumb's front strut is parallel and properly recessed within the palm cover plate of the hand.

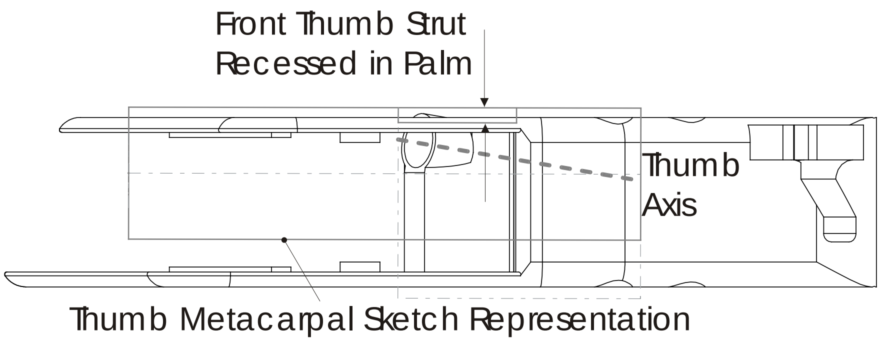

Figure 6.38 Top View of Thumb at Rest Position

The first part of the optimisation was positioning the origin of the axis. The origin corresponds with the centre of the worm gear. It's X, and Y position had to be at a minimum distance from the thumb side panel so that there was just enough room for the worm support bearings. The reason for this was the thumb had to have the minimum distance for its rear strut (base 2 length). The longer the strut was, the less anthropomorphic the thumb looked as it rotated about the palm. It did have to be long enough however that the thumb could rotate about the palm without collision.

Once the worm gear was positioned for it's X, and Y coordinates its Z offset had to be created. The worm, its motor and its drive bearing were positioned far enough away from the bottom of the top cover plate so that the motor and the support bearings did not have interferences within the palm assembly. This minimum distance would set the Z coordinate.

The vector of the thumb axis was then angled in the plane of the palm (with the main thumb axis and rest position sketch) so that it pointed to approximately the fingertip for the middle finger. This meant modifying the main axis angle variable. However there needed to be space available at the end of the axis for the front thumb strut's bearing holder. The space for this was severely restricted within the palm assembly. The only volume available was between the middle and the index fingers behind the rotation point. However this volume was limited due to the spreading motion of the index finger. When this occurred the index finger rear motors rotated to be against the middle finger. This further reduced the volume that the front thumb bearings could occupy. The thumb axis therefore had to be angled so that the thumb bearings lay directly in the centre of this volume.

The worm gear was then angled in the palm base part so that it gave the maximum angle in the vertical plane. That is the worm gear was placed in position within the palm base part so that it was angled upwards to give the maximum second axis angle. By maximising this angle the thumb would give a bigger grip angle between the thumb and the palm. It also means that the thumb would not stick out from the side of the palm so far when it is in its rest position. However the thumb bearings were not allowed to stick out of the palm base part too far otherwise they would interfere with the grip of the thumb and would give a non-anthropomorphic look to the palm assembly. Therefore the second axis angle had to be maximised within this constraint for the height of the thumb bearings.

The palm axis by this point in the iteration of the optimisation has been set. The next part was the setting of the geometry for the thumb axis in the thumb assembly. The 'base 2 length' for the thumb's rear strut was modified so as to give the necessary clearance for the thumb metacarpal past the palm cover plate in the hand assembly. The thumb also had to have the maximum rotation around the palm of the hand. The 'base 2 length' had to be sufficient for the thumb metacarpal to fit into the recess at the maximum rotation position. In this case the longer 'base 2' the further the thumb can rotate.

The 'thumb angle 2' variable then needed to be modified to give the maximum grip for the thumb in the Second Thumb Axis Sketch. It had to be large enough that this grip size was maximised when the thumb was opposite the middle finger but to prevent the thumb sticking out too far from the side of the palm when it was in the rest position. There also had to be sufficient clearance for the thumb to be away from the fingers when they spread.

The last two variables ('base 1 length' and 'thumb angle 1') dealt with how the thumb lined up with the palm when it was in the rest position. Thumb angle 1 needed to be modified so that the metacarpal lined up to be parallel with the palm of the hand. If the front strut were not recessed properly into the palm, the thumb would need its 'base 1 length' variable changed. These two variables needed to be checked when the thumb was opposing the fingers in the maximum grip position for alignment of the thumb metacarpal. If the 'thumb angle 1' was too large the thumb could be pointing away from the fingers at an angle away from the index finger.

Once the axis geometry was settled upon it was implemented in the palm assembly models (using the design table spreadsheet 'Configure') and the geometry variable values recorded. The 'Configure' program though does not modify the hand assembly motor and worm placement. The hand assembly spreadsheet had to be modified by hand for the new geometry values. The reason for this was that it was easier to modify the hand model manually and not have to rely on the program to correctly rebuild all the modified hand sub-parts. The hand assembly was also used to test the thumb for the maximum anthropomorphic rotation motion about the axis. Notes and CAD model configurations regarding the results of the motion were kept so that the geometry could be compared against previous attempts. If the motion was unacceptable or if there was insufficient clearance, then the optimisation procedure was started again with modified values for the thumb axis geometry.

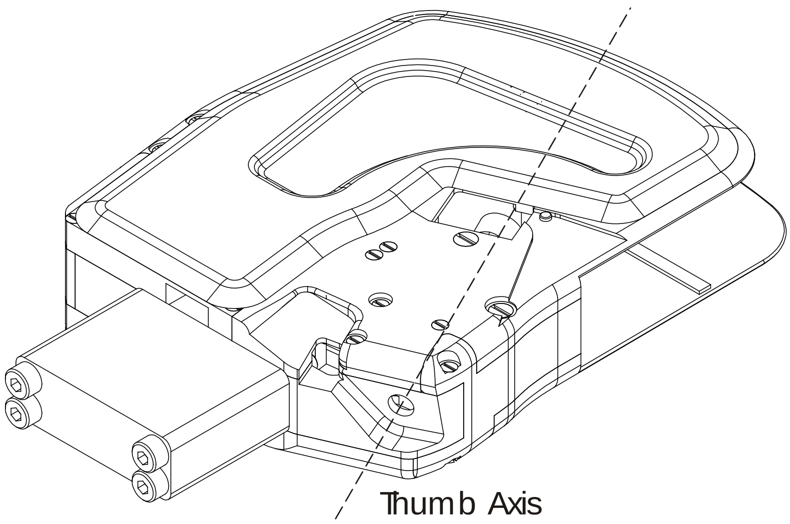

Figure 6.39 Thumb Axis in the Palm Assembly

6.4.6 Guidelines for Thumb Axis Optimisation

The guidelines that were used when optimising the thumb rotation axis have been summarised below. While these guidelines were useful, not all of them were followed at any given time. Often conflicting guidelines required that one guideline be chosen over another. In the case of the design of the best geometry for the thumb axis the functional aspects of having an increased volume of rotation was more important than the aesthetic guidelines.

6.4.6.1 Effects of changes to variables on Motion

When changes are made to the various variables that make up the thumb and the thumb axis they have an effect on the design.

If the main thumb axis angle is modified then the angle of the thumb facing the fingers at the maximum grip position will change. If the X, and Y-coordinates for the worm gear position are modified then the thumb axis will be moved about the plane of the palm. However since there is only limited room for the rotation worm gearing and the support bearings the modification would only be small. Modifying the Z-coordinate for the worm gear may cause interferences with the spreader motor or the top cover plate.

Changes to the ‘second axis angle’ would mean changes in the maximum grip position as well as the resting position of the thumb. That is if the ‘second axis angle’ is increased the thumb will no longer lie parallel with the palm cover plate when it is in the resting position. Instead it will be angled out of the palm. The thumb would be angled further upwards in the maximum grip position as well.

If ‘thumb angle 2’ is modified there will also be changes to the maximum grip position and a slight change to the angle of the thumb’s rest position. If the angle is increased there would be a larger grip angle noticeable at the maxim grip position. There would also be a greater offset angle between the thumb and the palm assembly at the rest position. The thumb would also be angled upwards away from the palm cover plate. Modification to the ‘base 2’ variable would lead to a change in the radius of the axis of rotation.

If ‘thumb angle 1’ is modified or increased then the thumb metacarpal would no longer be facing the same direction in the maximum grip position. An increase in ‘thumb angle 1’ would lead to moving the thumb outwards from the maximum grip position from the middle finger towards the index finger position. It also has the effect at the rest position of moving the thumb from its parallel position at the side of the palm. If there were an increase in its angle the thumb would slant downwards towards the top cover plate. Modification to the ‘base 1 length’ modifies the offset of the thumb metacarpal off the axis. If the thumb was in the resting position and the ‘base 1 length’ was increased the effect would be move the recess of the thumb down towards the top cover plate. The thumb would still be parallel in this case. The ‘strut separation distance’ variable controls the length between the front and rear strut that connects the thumb to the palm. It was sized so as to have the front strut bearings of the thumb positioned directly behind and between the metacarpal blocks of the middle and index fingers.

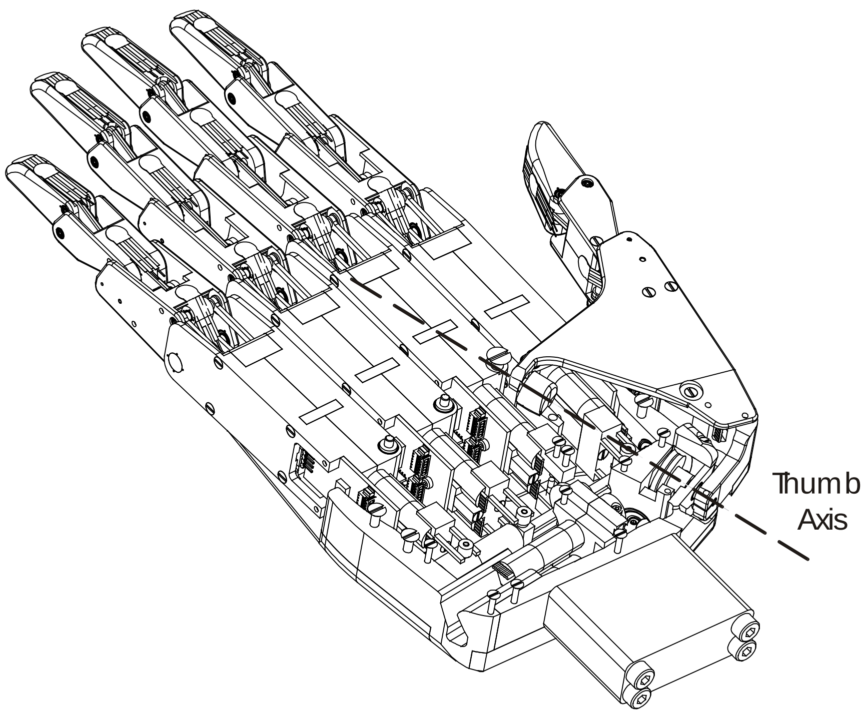

Figure 6.40 Thumb Strut Location and Connection in the Hand

6.4.6.2 Improving Aesthetic Appearance

- Reduce ‘base 2 length’ so as to have minimum clearance for the thumb’s rotation about the palm of the hand. Having the rotation worm gear as close to the thumb side as possible (Y axis) could reduce this.

- The thumb when in its rest position alongside the palm should be parallel with the palm. Its front leg strut should also be recessed in the palm (to reduce it’s profile when the thumb is at rest). The depth of recession for the strut should be around 1mm. This recession should not adversely affect the strength of the palm.

- The thumb metacarpal should be pointing toward the middle finger when it is in its maximum grip position. By having this position at the maximum grip position the thumb axis is more anthropomorphic. This direction of the metacarpal depends on both the ‘main axis angle’ and ‘thumb angle 1’. The ‘main axis angle’ sets the angle of the axis. How the metacarpal is orientated to this depends on ‘thumb angle 1’.

- The thumb axis should have the maximum ‘second axis angle’ (in the vertical plane) so as to have the best grip angle between the thumb metacarpal and the gripped object when in the maximum grip position. It should also have the second variable ‘thumb angle 2’ maximised for this.

- The ‘thumb angle 2’ though should not have the thumb stick too far out the side of the palm of the hand when in the rest position. How far the thumb sticks out depends also on the main axis angle in the palm. There should be sufficient angle so that the fingers can spread next to the extended thumb without interference.

- The thumb should have the maximum rotation so as to have the largest number of grips. The larger the working volume it can work about the more human like it will look like in operation.

6.4.6.3 Constraints

- The thumb's front strut support bearings for the axis needs to be positioned within the space between the spread index metacarpal and middle metacarpal block. It also should not protrude too far beyond the top of the palm cover plate.

- The worm and the worm gear bearings should be supported within the palm of the hand. This gives a limitation on how far across the worm can be moved in the palm so as to reduce the base 2 length of the thumb.

- The motors and the support bearings cannot interfere with the top and bottom cover plates. This is a limitation for locating the rotation motor, gears and support bearings in the Z direction within the palm assembly.

- The maximum rotation position should occur so that the side of the metacarpal rests in the recess in the middle rear of the palm cover plate. This will give the maximum allowed rotation of the thumb.

- The rest position for the thumb has a limitation on the motion of the thumb. As the thumb rotates into the rest position it's front strut will fall into the recess on the side of the palm cover plate. It will not be able to further rotate about the palm of the hand.

6.5 Results of Optimisation

The finger, thumb and thumb axis were evaluated for their motion and sizing characteristics. These results do not include the force output. Marlene Helfert is currently working on a project that should give the dynamics and gripping forces within the Canterbury Hand. The use of SolidWorks compliant motion analysis packages such as Dynamic Designer or Working Model may also be used for later analysis of the kinematics of the hand design. An approximate calculation of the force output from the extended thumb and finger position was made with a spreadsheet. The next sub-section indicates the force output for the finger and thumb linkages based on the input moment about the B4 bearing joint at the maximum curl position. This can only be considered an indication of force output, and only for a single position of the finger. It is not a final result, as there are other factors to be taken into account.

Force Output Indicator Results

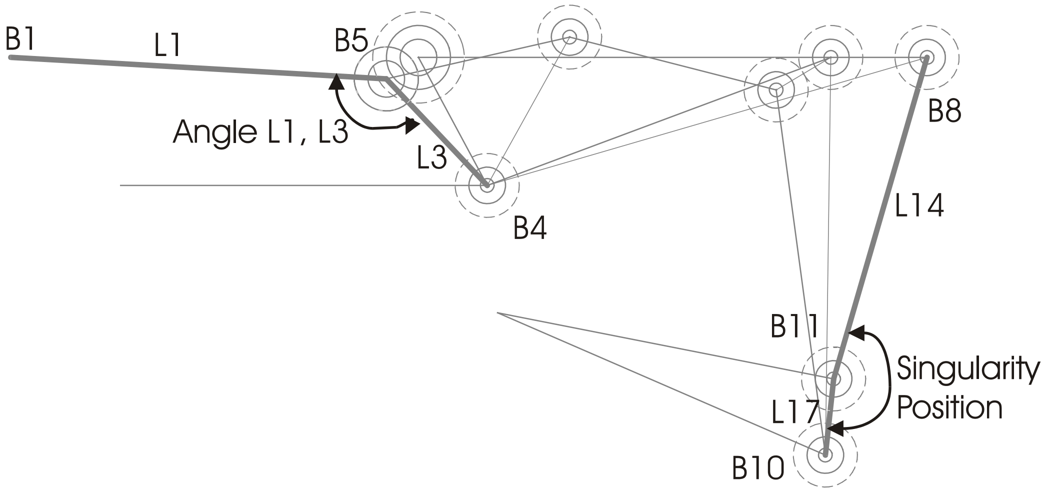

Figure 6.41 Finger Force Output Indicator Diagram

The force output for the finger curl is directly related to the input moment around bearing joint B4. The angle between links L1 (actuator link 2) and link L3 (part of the rocker link) was measured at the maximum curl position. The larger the angle the link makes at this position the less moment goes into the curl motion around the bearing joint. If the links ever achieved the singularity position of 180º there would be only a direct force on the bearing and zero moment going into the finger curl. Thus the best force output for the curl position is given by a smaller angle between these two links.

Table 6.1 Angle between L1 and L3 for the various finger geometries

Finger Geometry	*Angle between L1 and L3 (º degrees)*
Ward	141.9
Bain	150.4
Middle Maxon	136.7
Index/Ring Maxon	136.6
Little Maxon	135.2
Middle Mini	139.6
Index/Ring Mini	139
Little Mini	136.6

From these results it can be seen that the Middle and Mini finger geometries consistently have smaller angles than the Ward [1996] and Bain [1997] geometries between the L1 and L3 links. This means that at least initially they have better moments about the B4 joint bearing and potentially better force output at the fingertip.

For the thumb the output force is related to the moment about the B2 joint bearing. This moment is related to the angle the L1 link (actuator link) makes with the L3 link (part of the proximal link). The closer the links get to the singularity angle of 180º the worse the moment is at this joint bearing. Therefore the larger the angle between the two links the worse the force output out of the thumb.

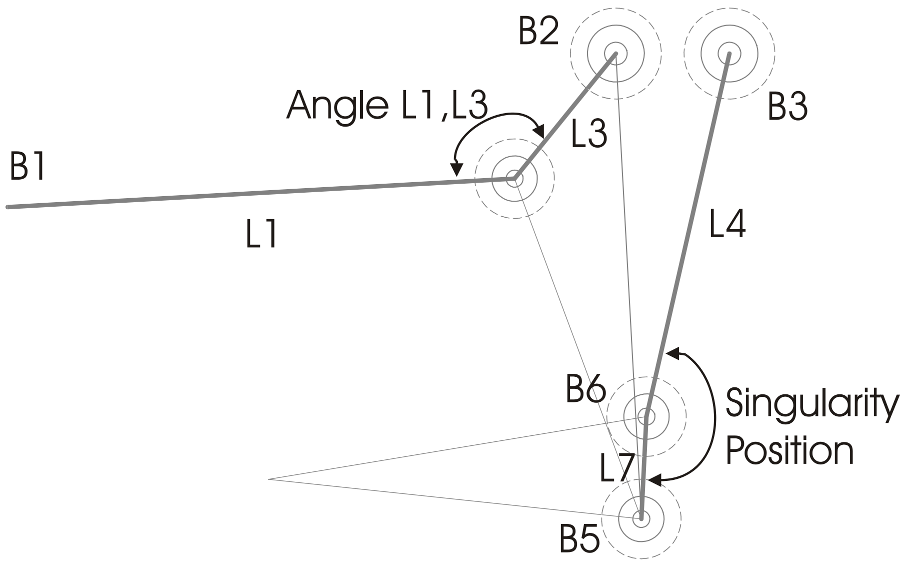

Figure 6.42 Thumb Force Output Indicator Diagram

Table 6.2 L3 Length, and Angle between L1 and L3 for the thumb geometries

Thumb Geometry	*L3 Link Length*	*Angle between L1 and L3 (º degrees)*
Bain	11.72	126.23
Maxon	14.2	132.2
Mini	12.4	137.6

From these preliminary results it can be see that the moment about the Maxon and the Mini finger geometries is reduced when compared to the Bain thumb geometry. However the L3 linkages are longer in the Maxon and Mini geometry. This means that there is a greater moment about the bearing. Also the singularity occurs earlier in the motion of the Bain thumb geometry. The resultant motion is more limited than the Maxon and Mini motor thumb geometry. Thus the maximum curl is limited and the angle between the L1 and L3 linkages reduced.

Finger Measurements

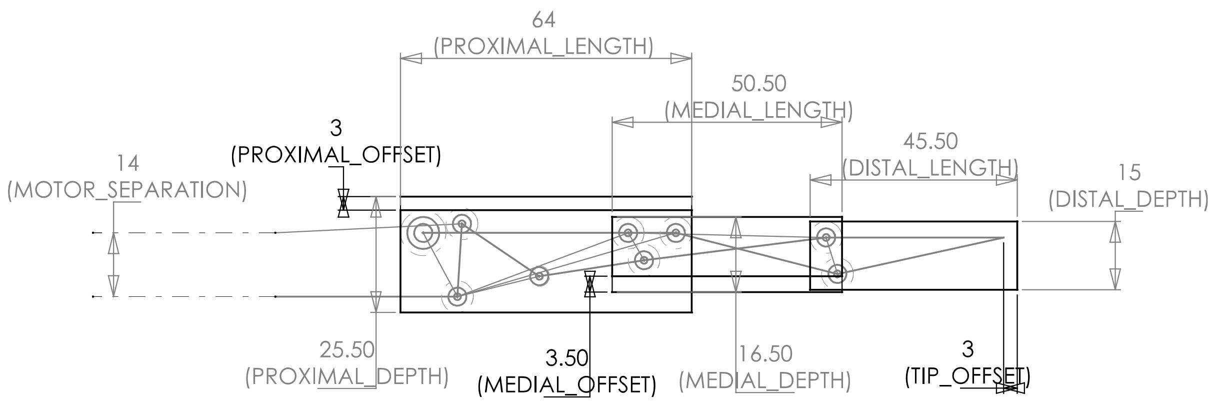

Figure 6.43 Finger Size Measurements for the Middle Maxon Finger

The finger linkages were each individually measured for their lengths and heights. The total finger length was also recorded.

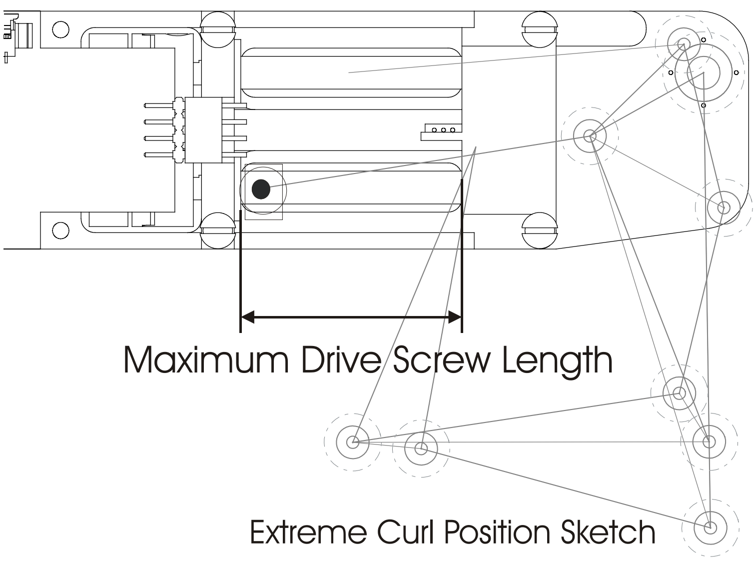

From the extreme finger sketch the drive screw length for a particular geometry can be calculated. The calculation for the drive screw length was the travel of the actuator 1 link from it rest position to its extreme curl position plus the width of the drive nut.

Figure 6.44 Method Used to Determine Finger Drive Screw Length

The measurement of the curl of the finger was measured for each phalange link. The distal curl was measured as the angle between the L12 and the L16 link at the full curl position. The medial link’s curl was measured as being the travelled angle that the L12 link makes from the extended rest position to the curl position. The Rotation sketch was used to measure the angle the proximal link (L9) travels between its extended position and its rotated position.

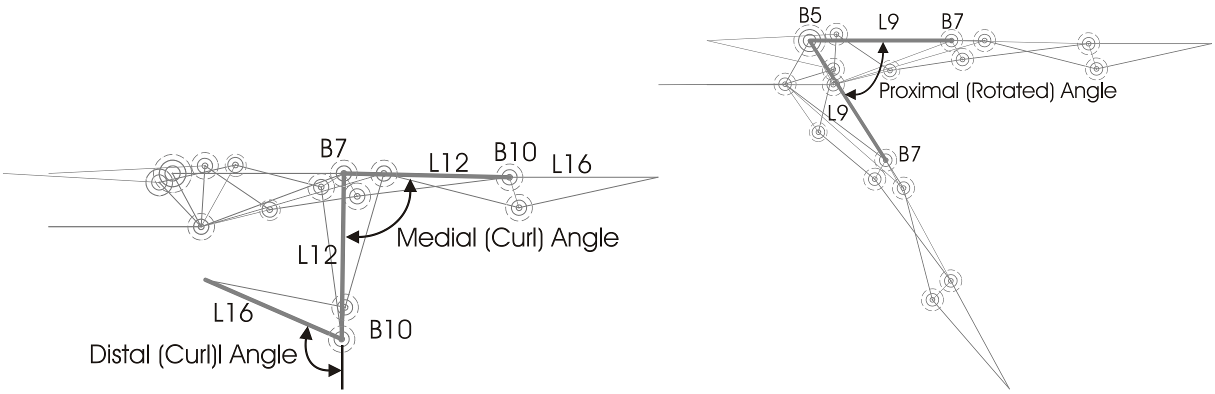

Figure 6.45 Finger Motion Measurements

Thumb

The proximal and distal thumb linkages were measured for their height and length. The thumb length as a whole was also measured.

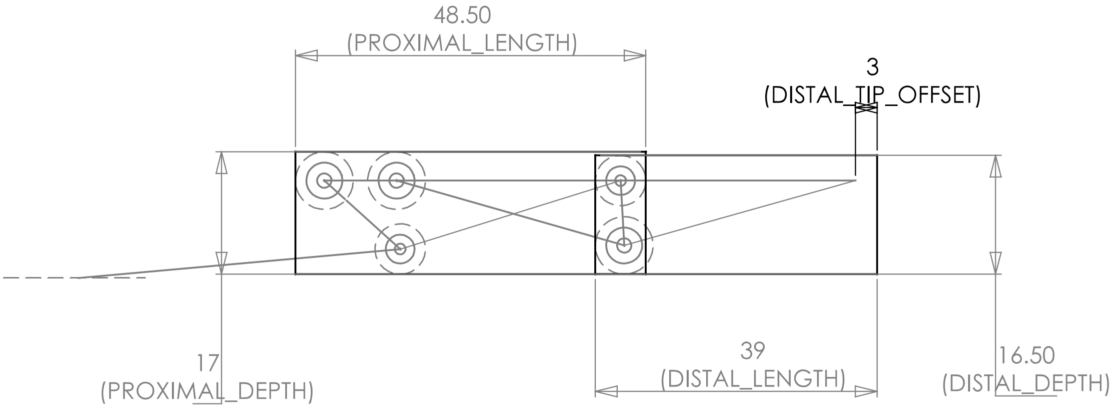

Figure 6.46 Thumb Size Measurement Example for the Bain Thumb

The curled position sketch of the thumb was used to measure the curl of the distal and proximal linkages. The distal linkage was measured as the angle between the curled L6 link (part of the distal link) and the L2 (distal driving) link. The proximal link curl was measured as the angle travelled by the L2 link (part of proximal link) from the extended thumb position to its position in the curled sketch. The drive screw length was calculated as being the distance the drive nut travels from its rest location to the curled position, plus the width of the drive nut.

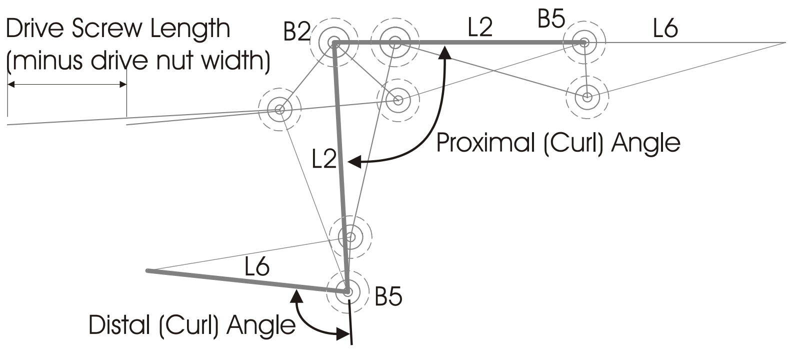

Figure 6.47 Thumb Motion Measurements

Thumb Axis

The maximum rotation of the thumb from its resting position to its maximum rotated position in the palm was measured from the hand assembly model.

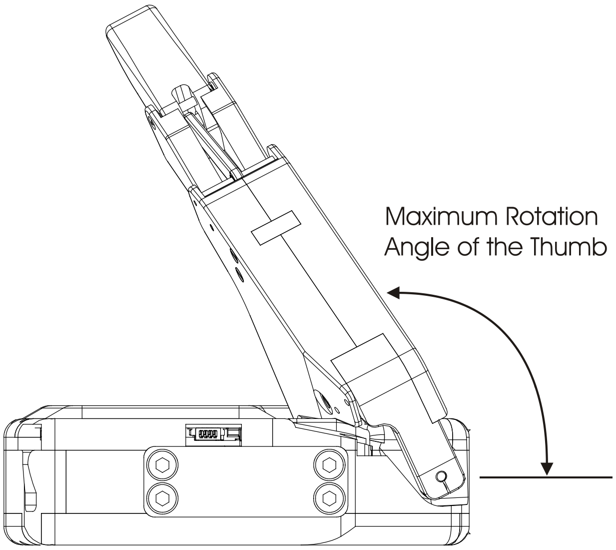

Figure 6.48 Thumb Rotation Motion Measurement

6.5.1 Finger Results

6.5.1.1 Ward Finger

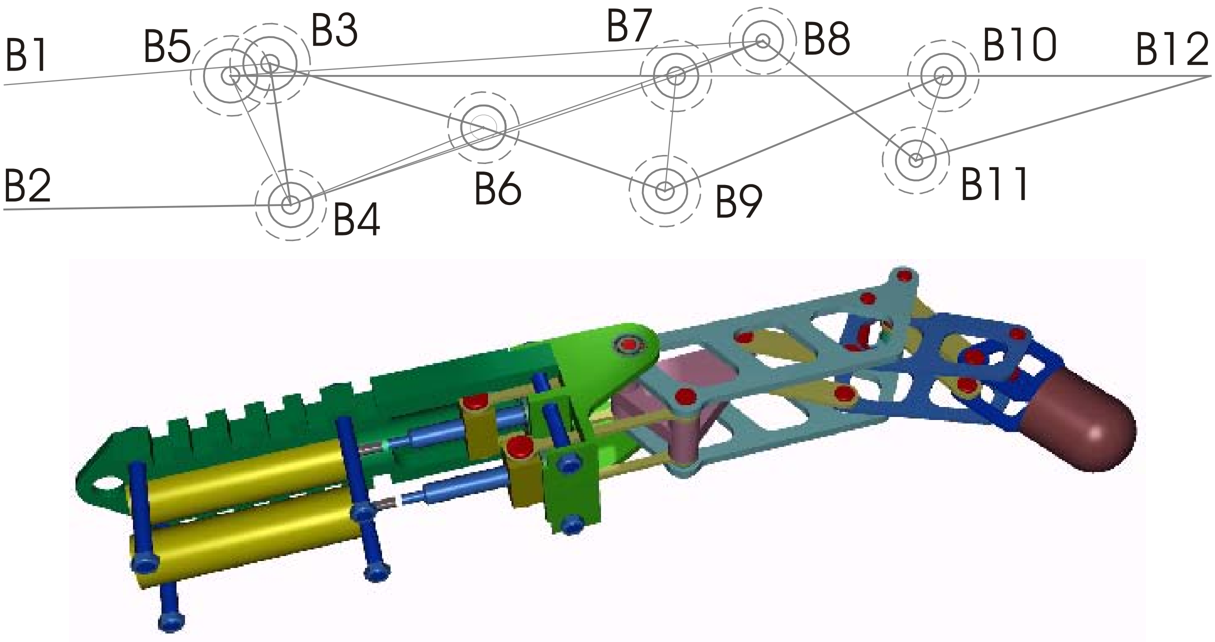

Figure 6.49 Ward's Finger Linkage Geometry and Model Design [Ward, 1996]

The following table gives the bearing geometry for the Ward [1996] finger. The Ward finger was constructed with the mini motors. However the separation between the actuator links is large enough to allow Maxon motors to be used in the current Canterbury Finger model. It should be noted that a large number of bearing types were used in the finger linkage design. This would increase the component cost. The manufacturing cost would also be increased as a larger number of tool sizes and tool changes would be needed to manufacture the linkages.

Table 6.3 Ward Finger (Maxon or Mini) Motor Geometry

Joint#	*1*	*2*	*3*	*4*	*5*	*6*	*7*	*8*	*9*	*10*	*11*	*12*
X	24.6	24.6	54.4	56.8	50	78.38	100	109.74	98.75	130	126.9	160
Y	51	65	48.6	64.5	50	55.8	50	46.07	62.94	50	59.5	50
BOD	~	~	6	2	5	2	6	2	5	2	5	~

Note: All dimensions when not otherwise stated are in millimetres.

Key

X, Y - Cartesian Joint Coordinates

BOD - Bearing Outer Diameter

The evaluation of the motions and the sizing of the Ward finger geometry are given in the table below. As can be seen the proximal link gave a rotation of 76º, the medial link 67.5º and the distal link 84.5º. The best finger geometry would be one with a 90º curl for the medial and proximal links. The distal link would be better to have greater than 90º so as to fully avoid the singularity at the L14 and L17 links.

From the evaluation it seems that the Ward finger does not have a particularly good medial curl. The distal curl was also underdeveloped. This gave the impression of a poor working area for the finger and that it could not grip very well. The proximal link motion of 76º for the finger rotation though is not too bad a result. One of the aesthetic problems the Ward finger also had was the unsightly B8 bearing in the proximal link. It stuck too far out of the proximal link and gave an unattractive looking knuckle impression when the finger curled. Ward's finger geometry has some limitations to its motion due to singularities so that it has a reduced working area.

Table 6.4 Ward Finger Geometry Evaluation

Results	*Proximal*	*Medial*	*Distal*	*Finger*	*Drive Screw*
Length (mm)	67.99	38	37	117.5	26
Height (mm)	26	22.9	17.25	~	~
Rotation (deg º)	76	67.5	84.5	~	~

6.5.1.2 Bain Optimum Finger

While Bain [1997] had created a number of geometries for the Canterbury Finger, none of them compared to his Optimum (Run 3) geometry. This finger had the best output force and motion profile of any of the other geometries. The bearing joint geometry for this finger is detailed in the below table.

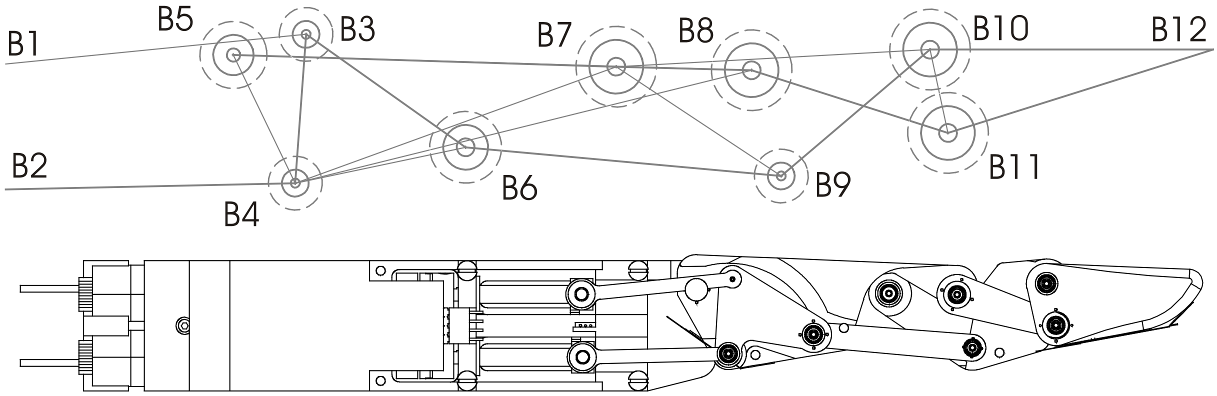

Figure 6.50 Bain's Finger Linkage Geometry and Model Design [Bain, 1997]

Table 6.5 Bain's Optimum Finger Maxon Motor Geometry

Joint#	*1*	*2*	*3*	*4*	*5*	*6*	*7*	*8*	*9*	*10*	*11*	*12*
X	24.6	24.6	58.1	56.9	50	75.9	92.7	107.8	111.1	127.7	129.7	159.3
Y	51	65	47.7	64.3	50	60.3	51.3	51.7	63.5	49.4	58.7	49.4
BOD	~	~	3	1	3	1	4.5	1.5	5	2	6	~

The Bain geometry has a finger that is of a similar length (116mm) to the Ward finger (117mm). Bain increased the length of the Medial and distal lengths to give a more anthropomorphic looking finger. The motion results of Bain's optimum finger gave the proximal link a 65.6º motion, the medial link a 72º motion and the distal link a 120.6º motion. Both the medial and distal link curls are improvements upon Ward's geometry. The distal link though has an over developed rotation of 120.6º. When looking at the curl motion of the linkages it can also be seen that the medial and distal lengths are still too short when compared to the length of the proximal link. Also when the finger is at full curl the medial link (due to the large distance from B9 to L12) covers a large portion of the distal link. This infringes on the fingers available grip area.

Table 6.6 Bain Finger Geometry Evaluation

Results	*Proximal*	*Medial*	*Distal*	*Finger*	*Drive Screw*
Length (mm)	66.05	44	39.1	116.05	26
Height (mm)	24.01	21.7	18.3	~	~
Rotation (deg °)	65.6	72	120.55	~	~

6.5.1.3 Middle Finger with Maxon Motor

The following tables represent the results of the optimisation process. The middle finger geometry is given in the table below. The first difference that is observable is that the bearings are more standardised than either the Bain or the Ward finger geometries. Also the geometry has been rounded to the nearest 0.5mm so that it is more easily manufacturable.

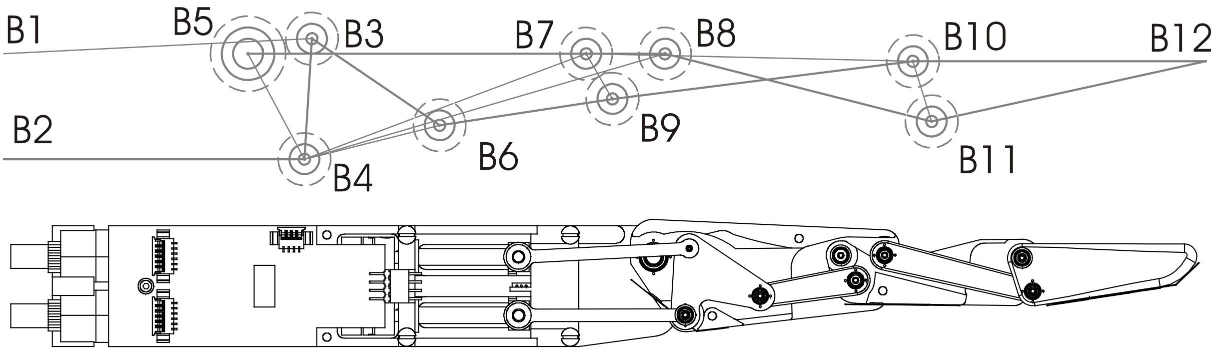

Figure 6.51 Middle Maxon Motor Finger Linkage Geometry and Model Design

Table 6.7 Middle Finger Maxon Motor Geometry

Joint#	*1*	*2*	*3*	*4*	*5*	*6*	*7*	*8*	*9*	*10*	*11*	*12*
X	50	50	91	90	825.5	108	127.5	138	131	171	173.5	210
Y	50	64	48	64	50	59.5	50	50	56	51	59	51
BOD	~	~	4	4	7	4	4	4	4	4	4	~

From the results table below it can be seen that the middle Maxon finger is also considerably longer (134.5mm). The reason for the increase in length is that the Maxon hand was considerably larger than human sized. The finger lengths (originally constrained to lengths given by Anthropometrical data) had to be scaled up to compensate for the difference.

The Proximal, Medial and Distal lengths have been balanced so that they are more similarly sized in comparison to the proximal link. The rotations of the medial and distal links are 89.5º and 112.7º respectively. This rotation was an improvement on the Ward and the Bain geometries. However the finger's (proximal) rotation motion has been decreased to 63.9º. This is only a small decrease from Bain's optimum geometry. Yet is a reasonably large change from Ward's proximal rotation of 76º. This is not a large disadvantage as further rotation of the finger is available if the position of actuator link 2 is changed.

The average height of the finger has decreased in comparison with the Ward and Bain geometries, which is an aesthetic improvement. The creation of the solid finger due to manufacturing necessity has made for a blocky looking finger. The reduction in the height of the finger has helped reduce the fingers profile, and making it appear less robotic. Like the Bain geometry the B8 bearing no longer sticks out the top of the proximal link. The overall appearance of the finger is tapered and anthropomorphic and its motion is smooth and covers a significant area.

The drive screw length has also increased by one millimetre to 27mm. By increasing the drive screw length the metacarpal length is also increased. This is a small disadvantage when compared with the increased fingers performance.

Some advantages to the Middle Maxon geometry are that the rocker has been minimised in size so that it can be enclosed within the proximal link. Also the motion of the linkages is efficient. There is less slop in the linkage motions and the coupling between the linkage systems has been enhanced so there is increased force output.

Table 6.8 Middle Maxon Finger Geometry Evaluation

Results	*Proximal*	*Medial*	*Distal*	*Finger*	*Drive Screw*
Length (mm)	63	50.5	45.5	134.5	27
Height (mm)	24.5	15	15	~	~
Rotation (deg º)	63.9	89.5	112.7	~	~

6.5.1.4 Index and Ring Finger with Maxon Motor

The Index and Ring finger geometry for the Maxon hand is given in the below table. These two fingers are similarly sized in the human hand so it was decided that they would have the same geometry.

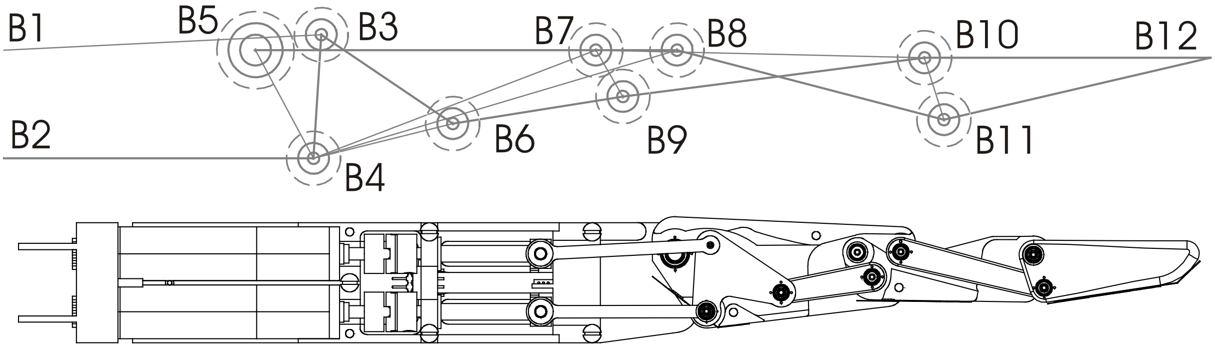

Figure 6.52 Index Maxon Motor Finger Linkage Geometry and Model Design

Table 6.9 Index/Ring Finger Maxon Motor Geometry

Joint#	*1*	*2*	*3*	*4*	*5*	*6*	*7*	*8*	*9*	*10*	*11*	*12*
X	50	50	91	90	82.5	108	126.5	137	130	169	171.5	206
Y	50	64	48	64	50	59.5	50	50	56	51	59	51
BOD	~	~	4	4	7	4	4	4	4	4	4	~

As can be seen in the evaluation table below the Index/Ring geometry is of a very similar length (130.5mm) to the Middle finger (134.5mm). The motion and the (length and height) sizing of the finger are also very similar to the Maxon finger. This is an advantage in the gripping of objects in the hand because if the fingers are as functionally and aesthetically alike the more anthropomorphic the hand will look. Functionally it also helps if the finger curls are as similar as possible for gripping such things as small diameter rods in cylindrical (heavy wrap) grasps.

Table 6.10 Index/Ring Maxon Finger Geometry Evaluation

Results	*Proximal*	*Medial*	*Distal*	*Finger*	*Drive Screw*
Length (mm)	62	49.5	43.5	130.5	27
Height (mm)	24.5	15	15	~	~
Rotation (deg ^{o})	63.9	89.5	113.1	~	~

6.5.1.5 Little Finger with Maxon Motor

The little finger geometry for the Maxon motor hand is given below.

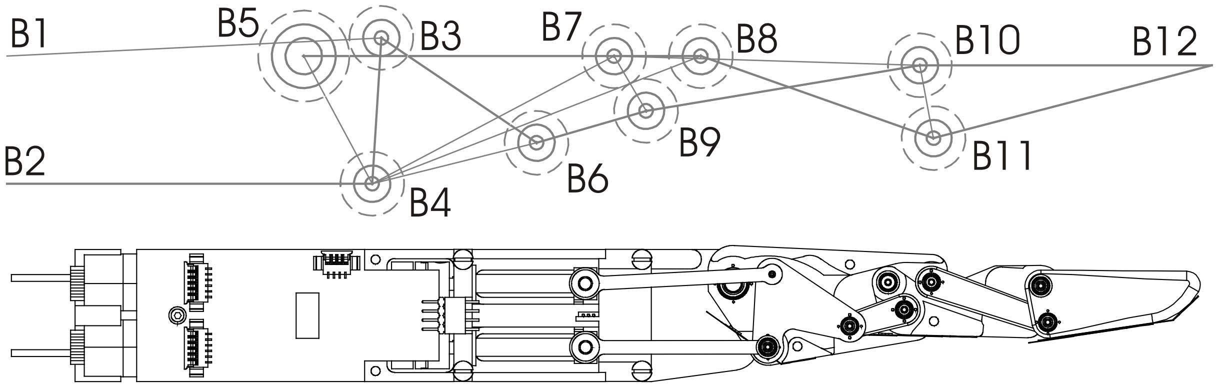

Figure 6.53 Little Maxon Motor Finger Linkage Geometry and Model Design

Table 6.11 Little Finger Maxon Motor Geometry

Joint#	*1*	*2*	*3*	*4*	*5*	*6*	*7*	*8*	*9*	*10*	*11*	*12*
X	50	50	91	90	82.5	108	116.5	126	120	150	151.5	182
Y	50	64	48	64	50	59.5	50	50	56	51	59	51
BOD	~	~	4	4	7	4	4	4	4	4	4	~

The little finger geometry was considerably shorter in length (106.5mm) than the Index, Ring and Middle finger geometries. For the hand to be anthropomorphic it had to have the fingers relatively sized to the human hand. From looking at Anthropometrics data it was found that the little finger is about 20% shorter than the middle finger.

The performance of the finger is also very similar to the other Maxon motor geometries. That is it has a 63.9º rotation for the proximal link, an 89.9º curl for the medial link and a 108.7º curl for the distal link. The distal link curl performance is slightly decreased when compared with the Index/Ring (113.1º) and Proximal (112.7º) distal curls. The aesthetic of the finger is also very similar to the other Maxon fingers for shape, width and motion.

Table 6.12 Little Maxon Finger Geometry Evaluation

Results	*Proximal*	*Medial*	*Distal*	*Finger*	*Drive Screw*
Length (mm)	51	40.5	38.5	106.5	27
Width (mm)	24.5	15	15	~	~
Rotation (deg º)	63.9	89.9	108.7	~	~

6.5.1.6 Middle Finger with Mini Motor

The other hand configuration that was created uses Mini motors to drive the finger, thumb and hand motions. The different sized motors affected the size of the hand making it slightly more compact (down the length) than the Maxon motor hand. Moving the thumb up closer to the fingers compensated for most of this extra length in the Maxon hand. However the change in hand size still meant that the geometry for the fingers and the thumb would also need to be reduced a little in size to compensate. The below table gives the geometry for the middle finger using Mini motors.

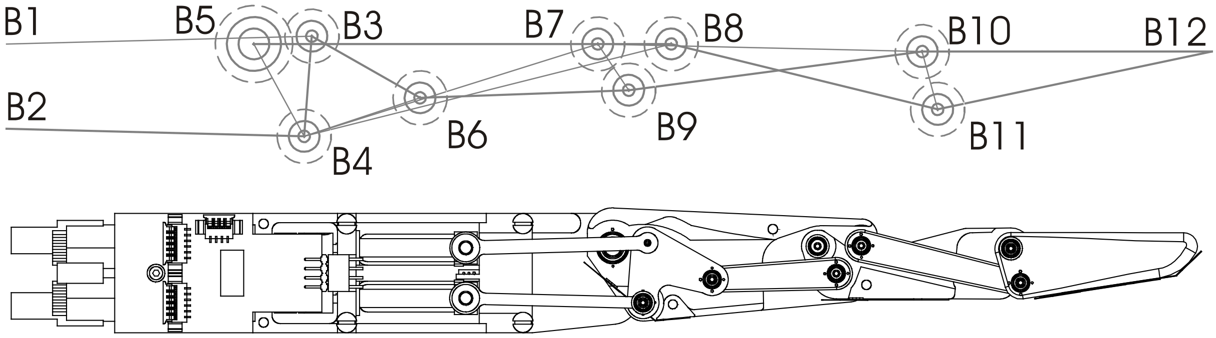

Figure 6.54 Middle Mini Motor Finger Linkage Geometry and Model Design

Table 6.13 Middle Finger Mini Motor Geometry

Joint#	*1*	*2*	*3*	*4*	*5*	*6*	*7*	*8*	*9*	*10*	*11*	*12*
X	50	50	89.5	88.5	82	103.5	126.5	136	130.5	168.5	170.5	206
Y	50	61	49	62	50	57	50	50	56	51	58.5	51
BOD	~	~	4	4	7	4	4	4	4	4	4	~

As with the previous geometries it can be seen that the bearings used in this finger geometry have been standardised and are all roughly the same size. This reduces the component and manufacture cost for the finger. Also the distance between the actuator links (Y2-Y1) has been reduced from 14mm to 11mm. This reduction is due to the smaller mini motors used in the finger metacarpal block. By reducing this distance the finger height has been reduced.

From the evaluation table below it can be seen that the finger length of 131mm. This is a reduction of only 3.5mm from the Middle Maxon motor finger geometry. The height of the middle mini finger geometry has been reduced so that the proximal link is 22.5mm and distal link is 14.5mm wide.

The motion performance of the middle mini finger geometry has decreased slightly. The rotation of the proximal link is only 59.2º. This has decreased from the 63.9º of the Middle Maxon geometry. The curl of the distal link has also decreased slightly to 109.4º. The medial link has a curl of 89.4º, which is nearly the same as previous geometry. The overall performance though decreased slightly does have other benefits. The drive screw length for example has been reduced to 24.5mmm. This corresponds in a decrease of 2.5mm of length in the metacarpal block.

Table 6.14 Middle Mini Finger Geometry Evaluation

Results	*Proximal*	*Medial*	*Distal*	*Finger*	*Drive Screw*
Length (mm)	61.5	49	44	131	24.5
Height (mm)	22.5	15	14.5	~	~
Rotation (deg º)	59.2	89.4	109.4	~	~

6.5.1.7 Index and Ring Finger with Mini Motor

The below table shows the geometry used by the Ring and the Index fingers in the Mini motor hand.

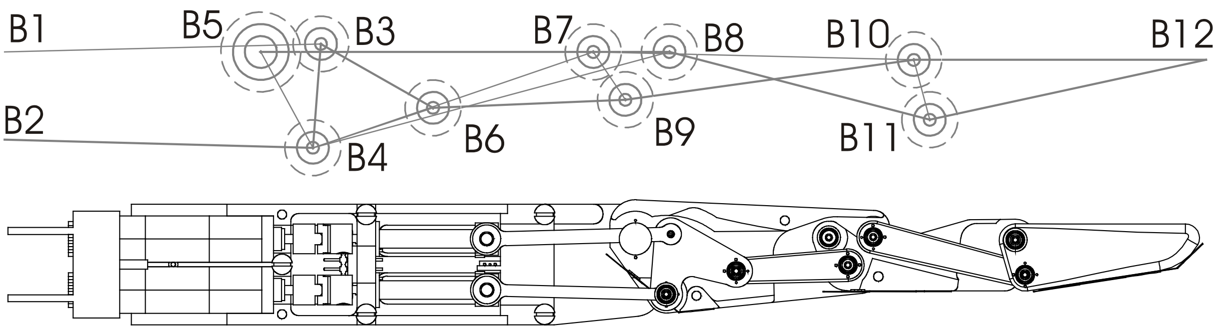

Figure 6.55 Index Mini Motor Finger Linkage Geometry and Model Design

Table 6.15 Index/Ring Finger Mini Motor Geometry

Joint#	*1*	*2*	*3*	*4*	*5*	*6*	*7*	*8*	*9*	*10*	*11*	*12*
X	50	50	89.5	88.5	82	103.5	123.5	133	127.5	163.5	165.5	200
Y	50	61	49	62	50	57	50	50	56	51	58.5	51
BOD	~	~	4	4	7	4	4	4	4	4	4	~

The index and ring Mini motor fingers are 125mm in length. This is 6mm reduction from the middle mini geometry. The heights of the fingers are very similar being 22.5mm, 15mm and 14mm for the proximal, medial and the distal link. The finger motion performance is very similar with the middle mini motor finger. The proximal link has a rotation of 59.2º, the medial link an 89.4º curl and the distal link has an 110.1º curl.

Table 6.16 Index/Ring Mini Finger Geometry Evaluation

Results	*Proximal*	*Medial*	*Distal*	*Finger*	*Drive Screw*
Length (mm)	58.5	47	43	125	24.5
Height (mm)	22.5	15	14.5	~	~
Rotation (deg º)	59.2	89.4	110.1	~	~

6.5.1.8 Little Finger with Mini Motor

The little finger geometry for the Mini motor hand is given in the table below.

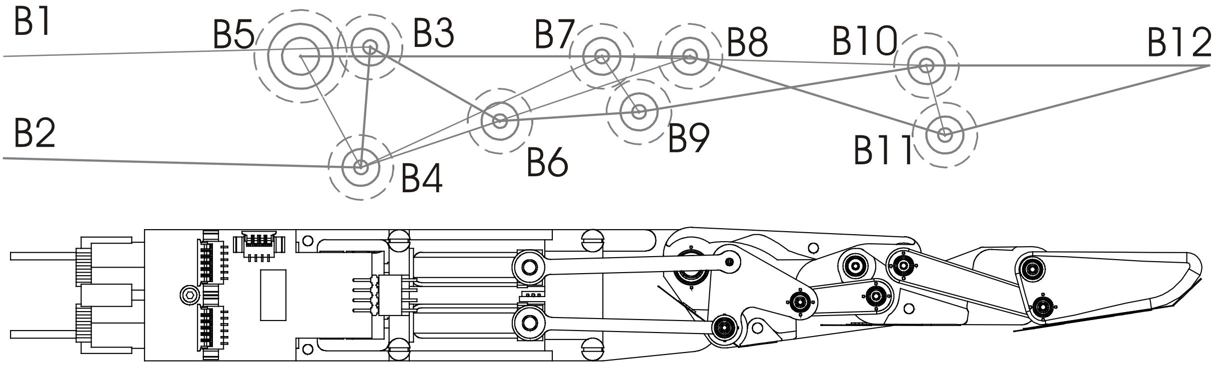

Figure 6.56 Little Mini Motor Finger Linkage Geometry and Model Design

Table 6.17 Little Finger Mini Motor Geometry

Joint#	*1*	*2*	*3*	*4*	*5*	*6*	*7*	*8*	*9*	*10*	*11*	*12*
X	50	50	89.5	88.5	82	103.5	114.5	124	118.5	149.5	151.5	180
Y	50	61	49	62	50	57	50	50	56	51	58.5	51
BOD	~	~	4	4	7	4	4	4	4	4	4	~

The little Mini finger geometry has a similar length at 105mm to the little Maxon geometry. The performance for the motion is very similar with the other mini motor finger geometries. The aesthetic appearance and anthropomorphic sizing was also kept in the design of the geometry.

Table 6.18 Little Mini Finger Geometry Evaluation

Results	*Proximal*	*Medial*	*Distal*	*Finger*	*Drive Screw*
Length (mm)	49.5	42	37	105	24.5
Height (mm)	22.5	15	14.5	~	~
Rotation (deg º)	59.2	89.4	112.2	~	~

To conclude the finger geometries were anthropomorphically sized for the new Maxon and Mini motor hand designs. The motions for the geometries were optimised so as to give the maximum prehensile interaction with the thumb. The force in the finger geometries (though not discussed in detail here) was also maximised. The bearing components, their placement and their manufacture were standardised as much as possible to reduce costs.

6.5.2 Thumb Results

6.5.2.1 Bain Thumb

The original geometry created for the Canterbury Thumb was made by Bain [1997]. The bearing geometry for the thumb linkages is shown in the table below. The thumb was then evaluated for its sizing and motion characteristics. The results of this are given in the second table.

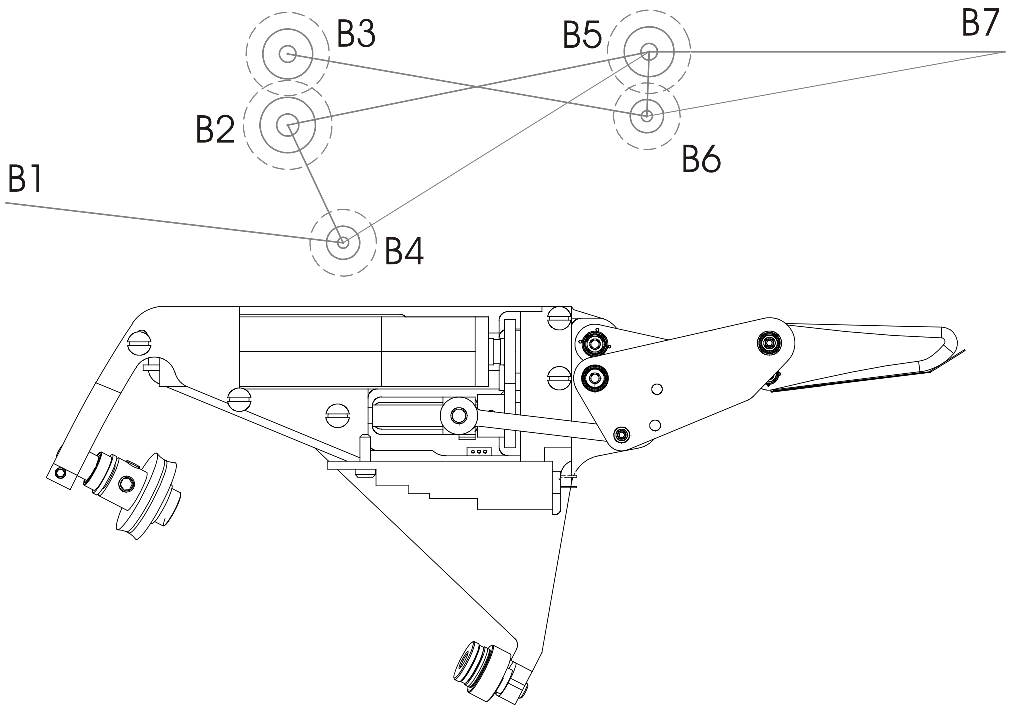

Figure 6.57 Bain Thumb Linkage Geometry and Model Design [Bain, 1997]

Table 6.19 Bain's Thumb Geometry

Joint#	*1*	*2*	*3*	*4*	*5*	*6*	*7*
X	24.6	50	50	55	82.6	82.4	114.7
Y	67	57	53.6	70.6	53.4	59.2	53.4
BOD	~	5	2	4.5	1.5	3	~

As can be seen a range of bearings of differing sizes were used in the Bain thumb geometry. This would increase the component cost. The geometry evaluation fives shows that the thumb had a limited curl. It only rotated 65.2º for the proximal link and 85.2º for the distal link curl. The best aesthetic end position for the thumb curl would have these linkages 90º with each other. Another problem with the Bain thumb was that it appeared to have an insufficient curl. The singularity at the L14 and L17 linkages occurred too early in the motion of the thumb. The distal link also appeared too long and thin in comparison with the rest of the thumb. The distal driving link (due to the location of the B3 bearing above the proximal bearing B2) also gave the thumb an uneven appearance by jutting out too far in the curl position.

Table 6.20 Bain's Thumb Geometry Evaluation

Results	*Proximal*	*Distal*	*Thumb*	*Drive Screw*
Length (mm)	40.35	38.3	71.7	20
Height (mm)	17.6	12.55	~	~
Rotation (deg º)	65.2	85.2	~	~

6.5.2.2 Thumb with Maxon Motor

The Maxon motor and Mini motor thumb linkage geometries are shown below. As part of the optimisation the same bearings were used as much as possible to reduce component cost.

Table 6.21 Thumb Maxon Motor Geometry

Joint#	*1*	*2*	*3*	*4*	*5*	*6*	*7*
X	25	59	69	69.5	100	100.5	132.5
Y	65	51.5	51.5	61	51.5	60.5	51.5
BOD	~	5	5	4	4	5	~

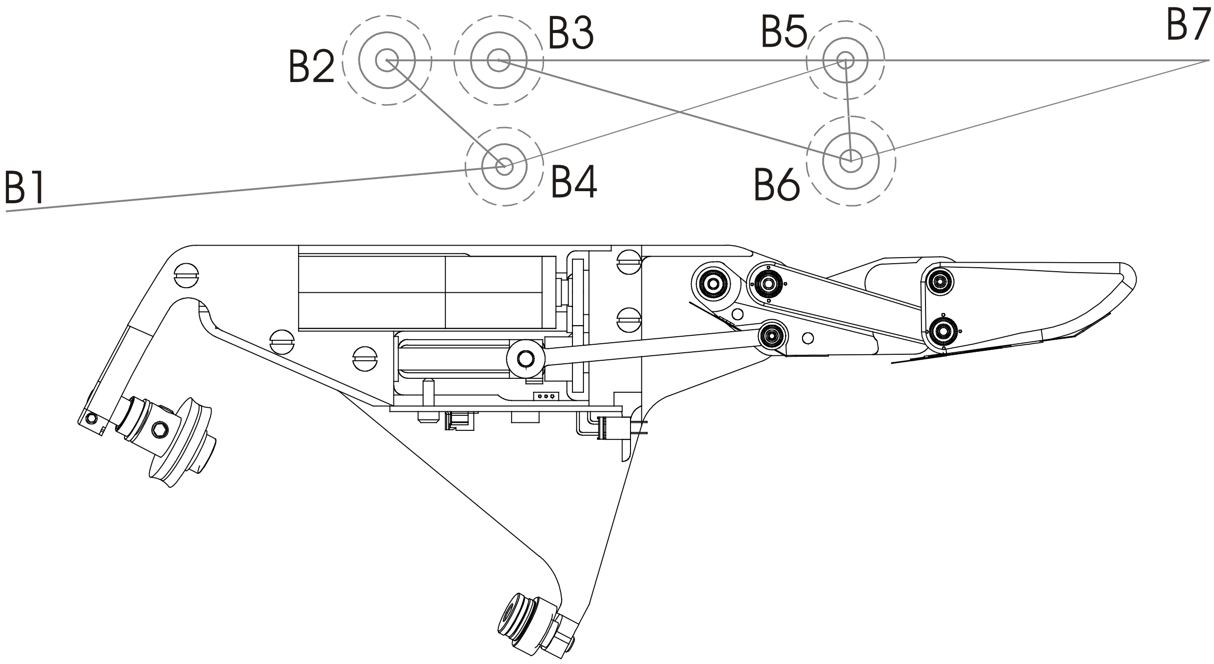

Figure 6.58 Maxon Motor Thumb Linkage Geometry and Model Design

The thumb length for the Maxon motor is very similar in size to the Bain Geometry. However the distal link was reduced in size to give a more anthropomorphic look to the linkage layout. The distal link is also wider than the Bain distal link. The reason for this is that the human thumb is nearly consistently the same thickness down its length. The design of the linkages had to incorporate this design factor for a better aesthetic appearance.

A big difference between the Bain and the Maxon thumb geometry was the curl motion of the proximal and distal linkages. The Maxon geometry has increased the linkage rotations by over 10º so that the proximal link curls 76.8º to the metacarpal and the distal link curls 97.4º to the proximal link.

Table 6.22 Maxon Thumb Geometry Evaluation

Results	*Proximal*	*Distal*	*Thumb*	*Drive Screw*
Length (mm)	45.5	34.5	73	27
Height (mm)	17.5	15	~	~
Rotation (deg º)	76.8	97.4	~	~

6.5.2.3 Thumb with Mini Motor

The Mini motor geometry is given in the table below. The Mini motor thumb is slightly shorter in length at 66.5mm than the Maxon and the Bain linkage geometries. It is very similar in width to the Maxon motor geometry.

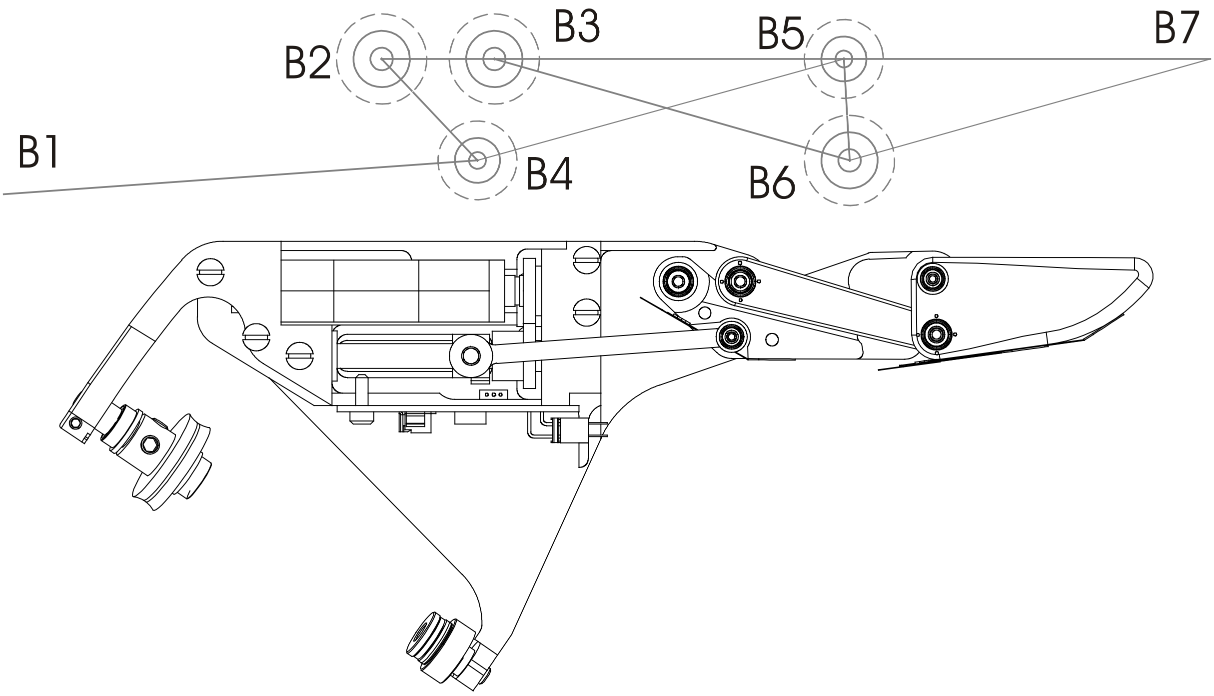

Figure 6.59 Mini Motor Thumb Linkage Geometry and Model Design

Table 6.23 Thumb Mini Motor Geometry

Joint#	*1*	*2*	*3*	*4*	*5*	*6*	*7*
X	25	58.5	68.5	67	99.5	100	132
Y	65	53	53	62	53	62	53
BOD	~	5	5	4	4	5	~

From the evaluation of the motion it can be seen that the motion characteristics for the Mini motor thumb is slightly less than the Maxon motor geometry. The proximal link rotates 74.4º and the distal link 96.6º. This is still an improvement over the Bain geometry.

Table 6.24 Mini Thumb Geometry Evaluation

Results	*Proximal*	*Distal*	*Thumb*	*Drive Screw*
Length (mm)	40.5	33.5	66.5	25.5
Height (mm)	17	15	~	~
Rotation (deg º)	74.4	96.6	~	~

To conclude the thumb geometries were optimised to give a greater interaction with the fingers. The motion was maximised and the linkages sized so as to give an anthropomorphic curling motion. The geometry was further optimised for force output (though this is not discussed here). Lastly the bearings, their location were standardised so as to reduce machining costs and time.

6.5.3 Axis Results

The results for the thumb axis for the Maxon hand and the Mini motor hand are given in the table below.

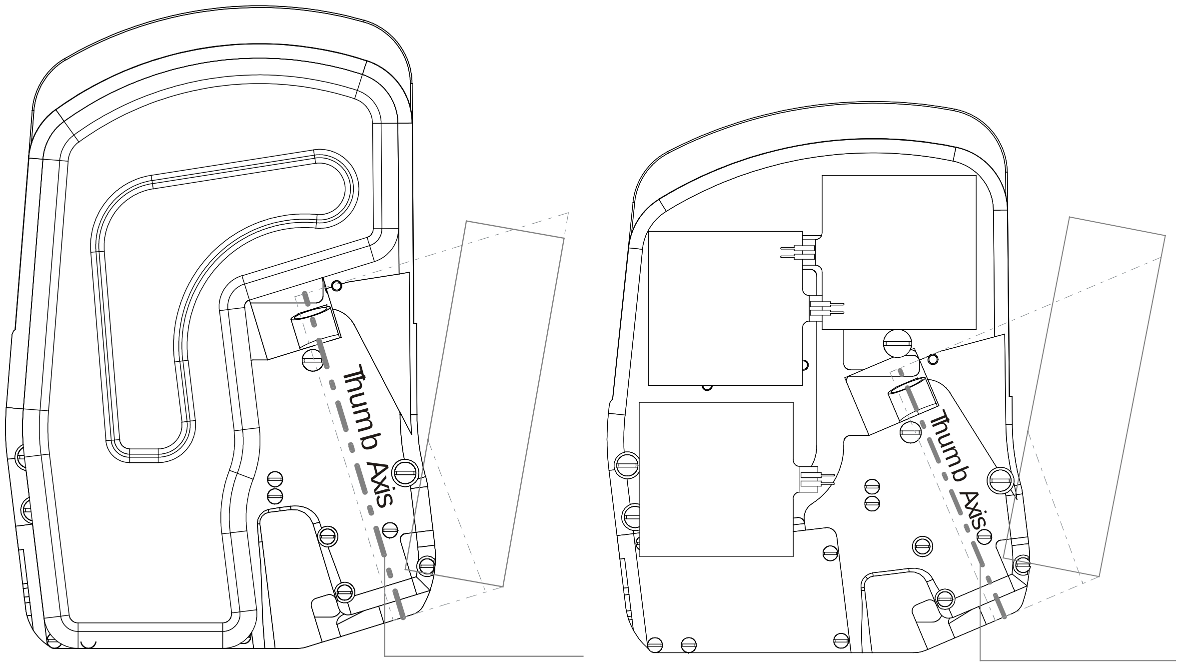

Figure 6.60 Maxon and Mini Motor Configurations of Thumb Axis in Palm Assembly

Table 6.25 Thumb Axis Geometry

Variable	*X*	*Y*	*Z*	*MainA*	*SecA*	*TA2*	*Base2*	*TA1*	*Base1*	*AxisL*
Maxon	58	29	52.5	197	99	117	30.5	100	20.65	98.5
Mini	58	30	54	203	98	124	30.5	99.5	23.68	80

<u>Key</u>

X, Y, Z - Cartesian coordinates for thumb axis vector origin.

MainA - Main thumb axis angle.

SecA - Secondary thumb axis angle.

TA1, TA2 - Thumb angle 1 and thumb angle 2.

Base1, Base2 - Base length 1 and base length 2.

AxisL - Axis length for the thumb axis. The axis length is from the back of the rear strut to the outside face of the front strut.

Table 6.26 Thumb axis Geometry Evaluation

	Rotation (º degrees)
Maxon	114.5
Mini	115.5

Since this was the first work on the Canterbury Hand as a whole there are no previous geometries to compare these results against. The results show that both the Maxon and the Mini motor hands have a very similar angular travel of approximately 115º. The motion of the thumb about the axis was approximately anthropomorphic. There was also the minimum clearance (due to the minimisation of the rear strut length) for rotation so that the thumb appeared to be a solid attachment to the hand.

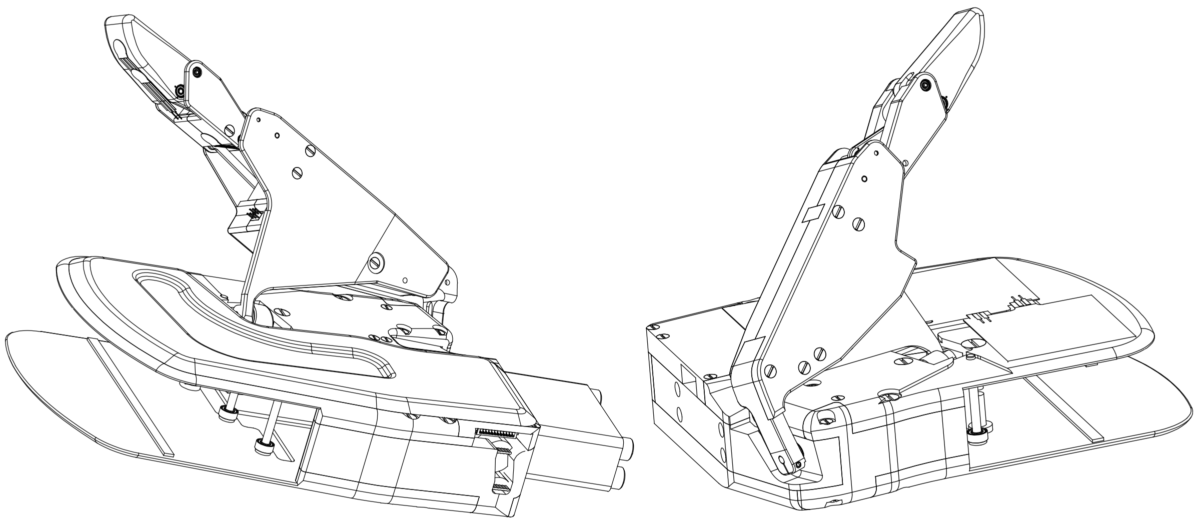

Figure 6.61 Maxon and Mini Motor Configurations of the Thumb in the Palm Assembly

6.6 Optimisation Summary

The Canterbury Hand needed to have the finger and the thumb linkage bearing geometry optimised. The thumb rotation axis also needed optimisation. Each of these problems had a number of variables that had to be manipulated to give the best results. The goals for the optimisation were to reduce the singularity effects and interferences in the hand. The grip force, the working area and the prehensile interaction needed to be maximised. The hand also had to have an anthropomorphic motion and appearance so it would be easier to use.

The optimisation process was iterative. It involved making modifications to the variables and comparing them with other geometries. Guidelines were developed to reduce the iterations needed in the optimisation process to attain the objectives. The new geometries were implemented in the hand models and design table spreadsheets by using the spreadsheet design table ‘Configure’ program. The geometries, and their evaluation for motion and sizing have been described. They were also compared against the Ward and Bain finger and thumb geometries. Overall the geometries created have superior motion, and increased anthropomorphic appearance. The optimised finger and thumb geometries will cost less and be easier to manufacture than previous designs.

Chapter 7: Conclusions and Recommendations

7.1 Summary of Work

The objective of this thesis was to parametrically design an anthropomorphic, compact, dexterous and low weight robotic manipulator. Since this was done at the University of Canterbury it was called the 'Canterbury Hand'. The hand had to utilise previously bought motors and a finger linkage arrangement that had been utilised in a prototype two degree of freedom (DOF) manipulator called the 'Canterbury Finger' [Ward, 1996].

To fulfil these objectives research was carried out to investigate the capabilities of the human hand. This was to get information for features so that the design would mimic the motions and capabilities of the human hand. Also experimental prosthetic and robotic hands were investigated to gain a perspective of the current state of the art in robotic manipulators. These hands were later compared with the finished design.

Due to the anticipated complexity of the expected design it was decided that the hand would be parametrically modelled. This was done using a Computer Aided Design (CAD) program called SolidWorks. SolidWorks is a 3D feature based parametric solid modeller that is fully associative. The design model of the hand had a number of constraints that affected how the model was to be created. For the design of the Canterbury hand the Mechanical Engineering Department had bought two different types of motors for two different hand designs.

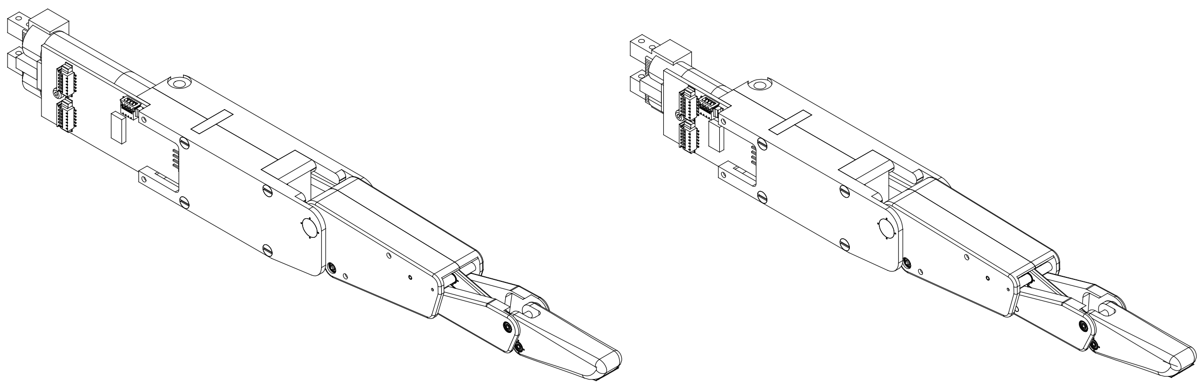

Figure 7.1 Maxon and Mini motor configurations of the Middle Finger

A dexterous robot hand was to use the Ø13mm 3 Watt DC motors from Maxon. A smaller prosthetic hand design was to use the Ø10mm 0.5 Watt DC motors from Minimotor. To save time this was implemented as two different configurations of a single CAD model of the hand. This meant that the hand design needed to be of a flexible design. The flexibility in the program was principally instigated in the model design tree using control sketches and independent design features.

Another reason for the flexibility was that the CAD model could be modified for different sized motors in a later hand design. The hand CAD model also had to be flexible for changes in the thumb rotation axis and the linkage geometry of the fingers and the thumb. This was because the hand needed to be optimised later to give the best motion and grip force possible. So that changes could be implemented spreadsheet, design tables (encapsulated within the part models) were used. They included logical equations that, depending on the geometry chosen for the bearing size, would modify the dimensions of the part designs. To implement quick changes to the (finger, thumb bearing geometry and thumb axis) geometry of the hand CAD model, a design table spreadsheet (which is a VBA program called 'Configure') was created. This program automatically changes the controlling geometry within the part design tables and then rebuilds the parts to apply the changes.

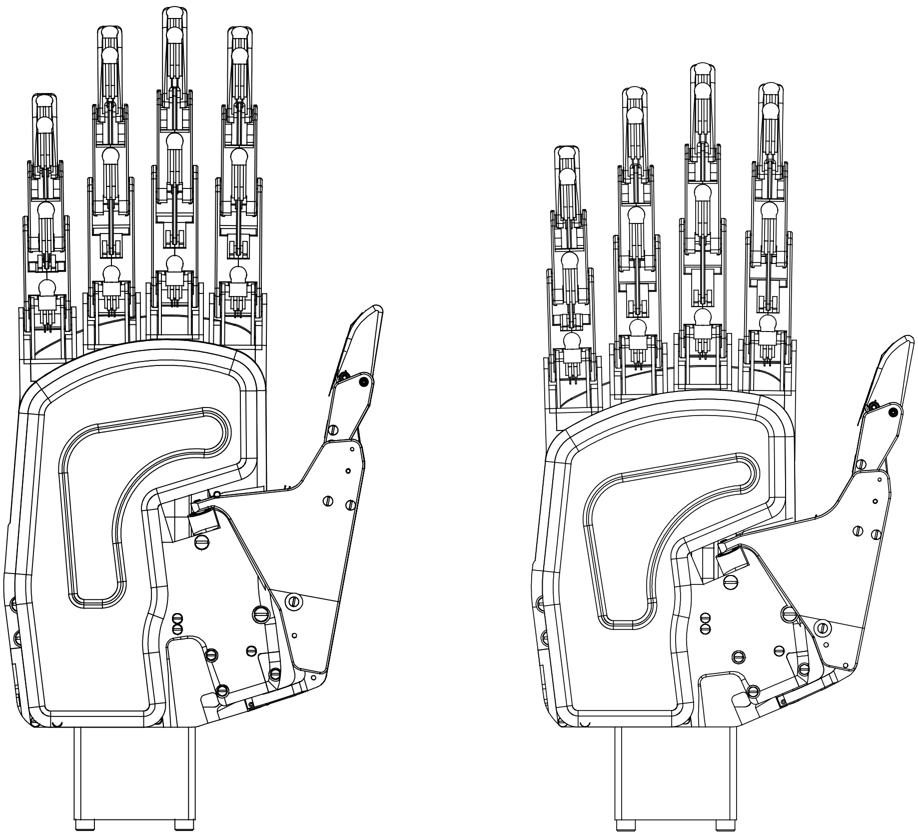

Figure 7.2 Maxon and Mini Motor Configurations of the Canterbury Hand

The final design of the Canterbury hand is an eleven DOF anthropomorphic robotic hand that has four fingers and a thumb. The fingers (2DOF each) and the thumb (1DOF) are linkages that are directly actuated by DC electric motors via a lead screw and drive nut transmission system. The finger and thumb linkage arrangements have been optimised to give them an anthropomorphic motion and appearance as well as a large working area and grip force. The hand also has a 1DOF finger spreading and a 1DOF thumb rotation mechanism. The design is very compact as it contains all the DC motors, wires and circuit boards. Lastly the hand has a wrist attachment that can be later replaced with a movable wrist mechanism or an attachment for a robotic arm.

After the design was finalised the Maxon and Mini motor hand designs were optimised. The objectives for the optimisation were the maximisation of the motions, grip force and prehensile interactions of the digits of the hand. The anthropomorphic appearance and motion of the hand was another objective of the optimisation process. Since the fingers and the thumb were made using multiple bar linkages they also had to be optimised so as to reduce the effects of singularities on their motion. This was accomplished by optimising the linkage geometry so the linkages moved within their working area, limited only by a single controlled singularity for each degree of freedom. This singularity positions was then avoided from occurring by the use of mechanical stops in the design of the model. By locating and controlling the singularity positions in the linkage geometry the bearing joint positions could then be placed/tested for maximising their motion and force output. This iterative optimisation process was carried out within SolidWorks using both test sketches and linked CAD models (using top down design) of the finger and thumb.

The thumb axis geometry was also optimised in a similar iterative process. The rotation of the thumb was not limited by singularities. Instead it was limited by the boundaries of the palm assembly. The axis was orientated so that the thumb would have an anthropomorphic rotation motion, grip opposition and resting position along side the palm. As mentioned above the geometries found from the optimisation process were implemented using the ‘Configure’ program.

7.2 Results Achieved

The end results of this thesis are the creation of a flexible multi geometry CAD solid model of the Canterbury hand. It utilises both the Maxon and Mini motors as two different hand configurations. The hand model geometries for each finger and thumb linkage bearing geometry and the thumb rotation axis alignment are controlled using a spreadsheet program called 'Configure'. This program when executed interacts with the design tables (that are encapsulated within the part models of the hand) to make predetermined design choices depending on the geometry chosen. The CAD model of the hand will be later used to create engineering drawings. These will then be used for the manufacture of the Canterbury hand. The first hand that will be created will be the Mini motor hand design. From the CAD model the characteristics for the manufactured hand designs can be estimated as being:

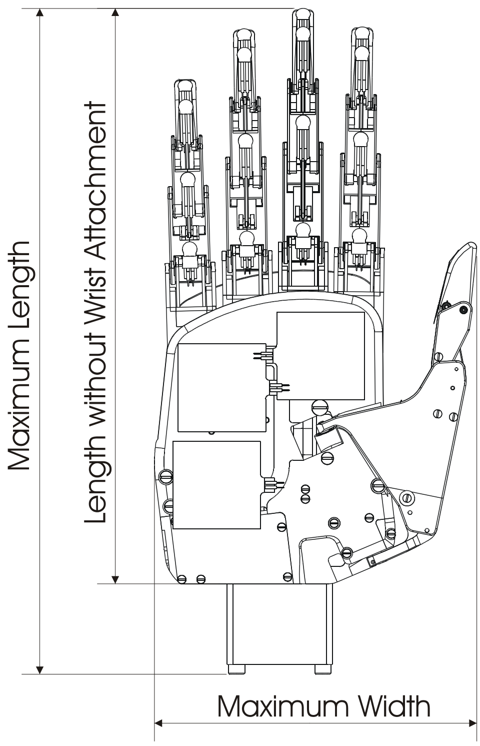

Figure 7.3 Hand Size Measurements

Table 7.1 Summary of Hand Characteristics

Hand	*Mass (kg)*	*Max. Width (mm)*	*Max. Length (mm)*	*Depth (mm)*
Maxon	2.3	166.5	326.5	37
Mini	1.8	169	300	34

Note: These dimensions are subject to change if attachments are added to the hand i.e. the wrist attachment or the palm cover.

The mass of the hand is very small when compared to international robotic hand designs. This is mainly due to many weight saving characteristics and the materials selected i.e. the high strength to weight ratio of the Aluminium material (alloy 7075). The following table gives the results for the rotation for each major phalange linkage for the fingers and the thumbs. The Middle Maxon and Mini finger results may be taken as an approximation for the Little, Index and Ring finger motions.

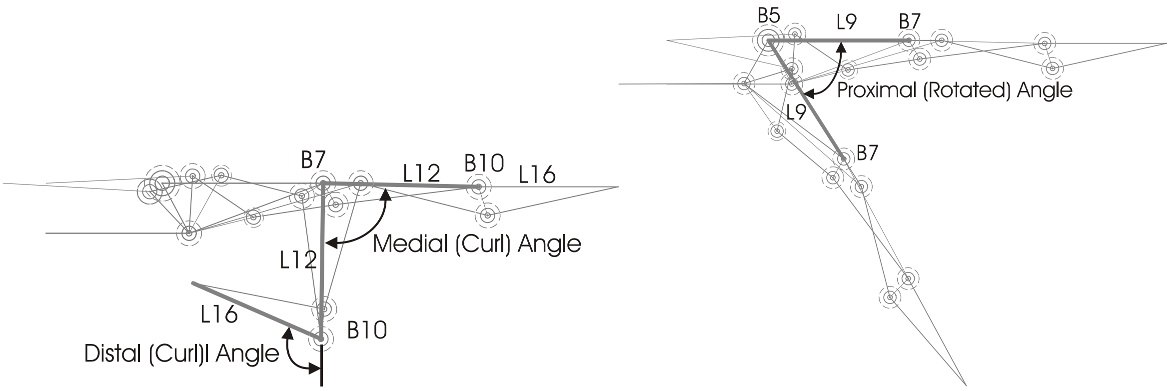

Figure 7.4 Finger Motion Measurements at Singularity Limits

Table 7.2 Summary of Finger and Thumb Optimised Motions

Movements	*Proximal (º degrees)*	*Medial (º degrees)*	*Distal (º degrees)*
Middle Maxon Finger	63.9	89.5	112.7
Middle Mini Finger	59.2	89.4	109.4
Maxon Thumb	76.8	~	97.4
Mini Thumb	74.4	~	96.6

The thumb rotation axis will give an approximate range of 114.5º rotation for the Mini thumb and 115.5º for the Maxon thumb about their respective palms. This angle is from the rest position to their maximum travel position.

7.3 Evaluation of the Design

The hand design that has resulted is a compact and reasonably dexterous anthropomorphic hand. At 11DOF its dexterity compares well with most of the experimental robotic end effectors and prosthetic hand devices. (See Appendix for detailed summaries of this research.) However it is the compactness of the design that sets it apart from these other manipulators. This is mainly due to it being directly driven (via a lead screw/drive nuts transmission system) from the DC motors. This allowed for the motors and the electrical system to be entirely contained within the hand. Once completed it will only require a DSP and battery pack to be mounted outside of the hand for it to operate. Because of its dexterity and compactness the Canterbury Hand design has potential to one day be developed as a prosthetic device. However it is estimated that the smallest (mini motor) hand design of this thesis will weigh 1.8kg. From research it was found that the human hand weighs approximately 400 to 500grams. This means that the current design of the smallest Canterbury Hand is approximately four times too heavy to be used as a prosthetic device.

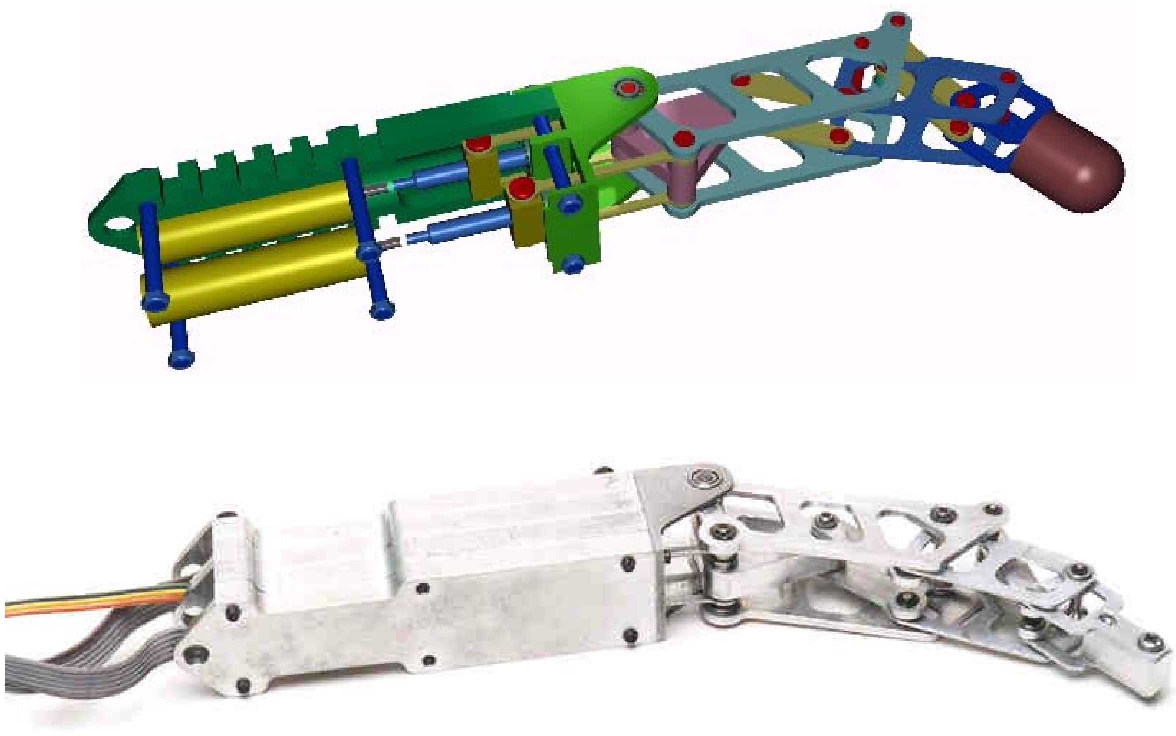

Figure 7.5 Ward's Finger Design and Manufactured Prototype

When compared with the prototype Canterbury Finger [Ward, 1996] the current design is far more anthropomorphic, simpler to manufacture and easier to assemble. The weight though similar to the Ward finger is far more balanced with a lighter metacarpal assembly (though a heavier finger). The design has created only a single force path through the linkages using common shafts at the bearing joints. This removes the potential for buckling due to unbalanced internal forces within the finger. The new finger designs also have surfaces to mount FSRs upon, and they cover the motion of the linkages within them making them far more attractive and less robotic looking.

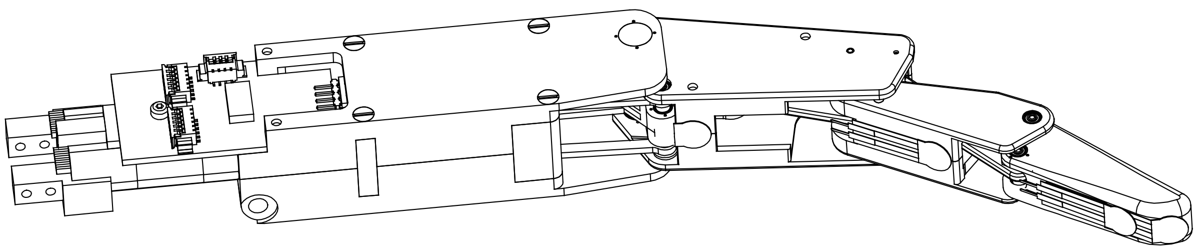

Figure 7.6 Current Design for the Middle Finger (Mini Motor Configuration)

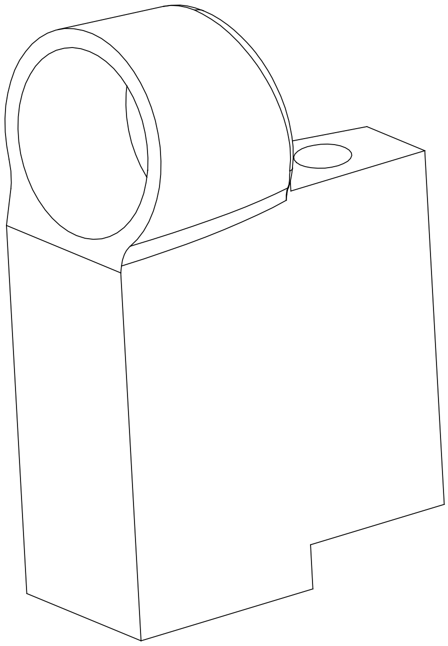

It is expected that there may be some manufacture problems with the palm assembly. However it is already as simply designed as possible while still achieving its objectives. Most of the rounded edges that appear difficult to manufacture will be created after the CNC machining using a grinding wheel. The biggest potential problem is the machining of the thumb bearing housing and the wrist connection panel. Though for maintaining a three dimensional thumb axis, and keeping the front strut's bearing housing within the palm this design is already as simply designed as possible.

Figure 7.7 Bearing Housing for Thumb's Strut Bearings.

Another anticipated problem is that the finger spreading shafts that attach the fingers to the palm assembly may not be strong enough for large loadings. If this is the case it will mean either the material of the needs to be replaced with some other stronger material or the hand should be limited to lighter objects. (It could also require that the finger spreading shafts to be replaced by fasteners to fix the fingers in place. This though is an extreme solution to only a potential problem.)

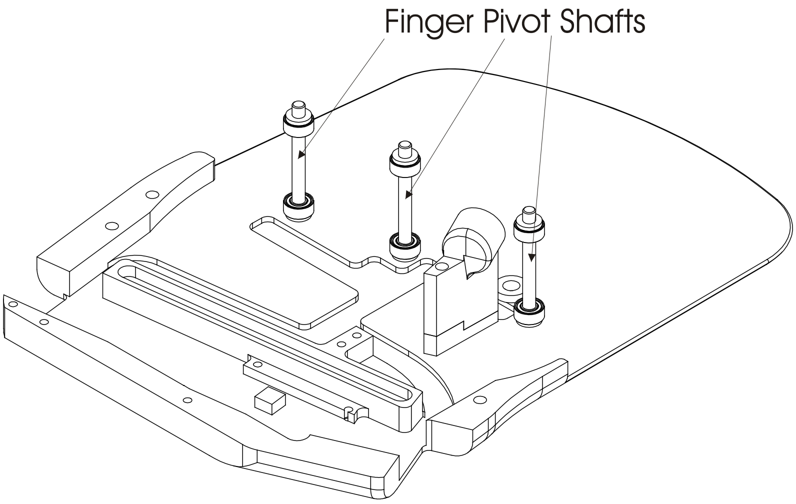

Figure 7.8 Finger Pivot Shafts and Bearing Housing on Top Cover Plate

Overall the parametric hand design is a unique anthropomorphic robotic hand. The CAD model of the hand is surprisingly easy to modify for critical dimensions. The finger and the thumb sizing and thumb rotation axis are easily modified. This is partly due to the parametric nature of the CAD program but mostly due to the careful CAD design of the features and smart design tables plus the associated interactive spreadsheet program.

7.4 Recommendations

This section will cover the recommendations for future work on the Canterbury Hand design. Currently there are several other projects that are being carried out on the Canterbury Hand. Marlene Helfert's work on the dynamic and gripping forces of the Hand, for example, may lead to further optimisation of the linkage geometry of the hand design. This potentially could affect every aspect of the manufacture of the hand from engineering drawing creation to component manufacture. There is also insufficient time for this thesis to complete these drawings and to order in components for the workshop. There is also little time available for the workshop to manufacture the hand until the end of the year.

Given these constraints though the hand will be manufactured in the near future. Drawings and components from the CAD model will soon need to be produced and ordered. However since the CAD model is completed, with referenced and fully dimensioned components these should be easily and automatically created from SolidWorks. Some time will be needed for approval from the workshop and for ordering in components. It is recommended that only a single finger be initially manufactured and tested before creating the rest of the hand. That way if there are any further problems the expenses are minimised.

Once the hand is completed it will require experimental testing (and then possible modification). It is recommended that for testing only light loadings (0.2kg to 1kg) are applied initially to the hand. The Mini motor hand will likely have difficulty with objects over one kilogram and the Maxon hand with objects of approximately five kilograms.

7.4.1 Testing

The grip force can be tested by a number of methods. The first method for measurement is similar to that which Ward [1996] described. Using the hand fixed in a vice at the wrist attachment the fingers of the hand push down on a weight measuring scale. This should give an approximation of fingertip force. The other method is to use a spring-loaded grip-measuring device, such as is used for measuring the human handgrip strength. There are many other tests the hand will be used for after these basic tests. The dexterity and motion of the fingers needs to be tested with and without loading. This would be done using different sized and textured objects. A control program will need to be created and tested for the hand, which incorporates motor position and force sensing. It would also have to be able to form pre-programmed grip patterns with the hand. The grasping of the hand using telemanipulation will also be researched and eventually tested.

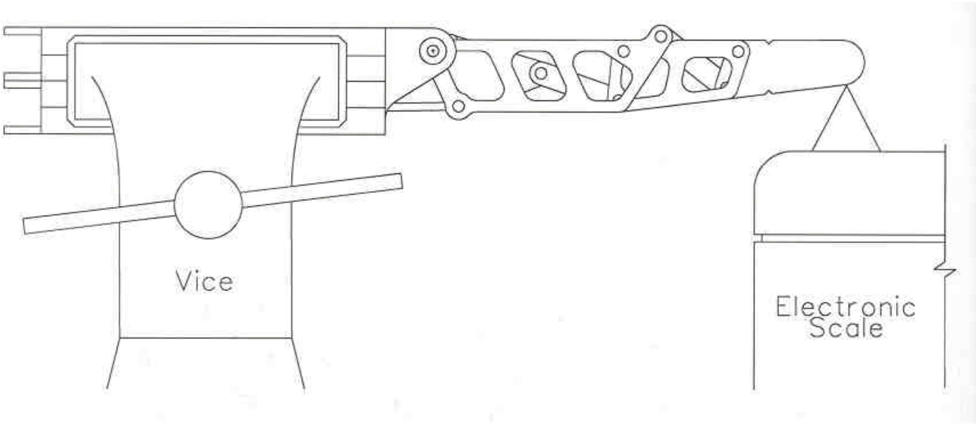

Figure 7.9 Ward's Finger Force Testing Set-up [Ward, 1996]

7.4.2 Improving Current Design

Since the hand has yet to manufactured there are various suggestions that might be added for improving the hand. It is difficult to know at this stage whether there are any weaknesses in the design. There has already been mentioned, for example, the possibility of problems with the yielding of the finger spreading shaft and replacing it with a stronger material. The benefit of having the hand as a CAD program is that it allows further tweaking for design features and optimisation. Some areas where there may be the need for modification are:

Grip Surfaces

A foam palm cover has already been designed to aid in palmar prehension with objects that rest against the palm, i.e. screwdriver. Additional foam grip surfaces need to be added to the hand design for the fingers and thumb. This will increase the gripping surface, friction and help to protect the FSRs. These surfaces may be integrated into a latex glove, which would also improve the hand's appearance.

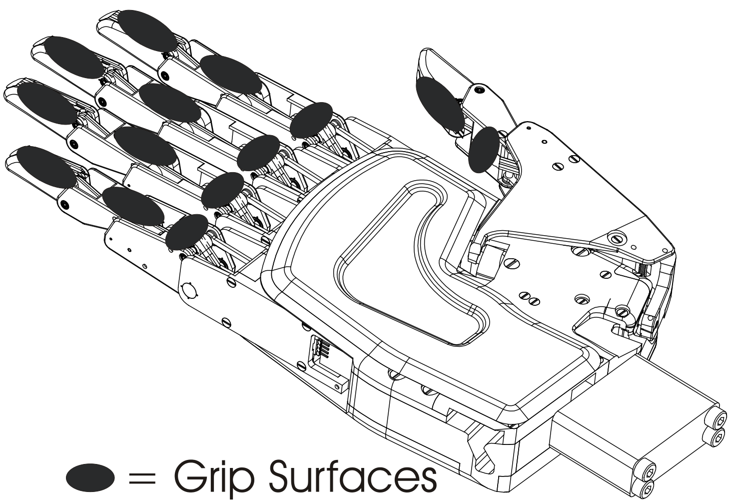

Figure 7.10 Recommended Grip Surface Locations

Force Output

If the analysis of the hand by Helfert shows problems then the fingers and the thumb may need to be re-optimised for better output force. The L13 link in the finger may need to be lengthened for example. While the results from the optimisation process are extremely good they could possibly be improved with further optimisation. Especially if done in conjunction with kinematic force analysis.

Figure 7.11 Finger Linkages with highlighted L13 Link

Weight Reduction

The weight of the two hand designs could be reduced further. New materials could be used to reduce the weight. An ideal solution would be some kind of low density, high strength, and easily machined plastic. The hand has various areas where more material could be removed to reduce the weight. Example areas are the side panels within the palm assembly as well as within the thumb metacarpal block. Internal spaces could be machined within the distal and rocker links as well. However this has to be done carefully and internally so that the aesthetic appearance of the hand isn't ruined by large see through holes and dirt doesn't enter the hand. The material removed would also have to not weaken the stability and strength of the structures of the hand. If weight reduction creates these kinds of problems it contradicts the basic design objectives.

Manufacture

The palm assembly's manufacture could be simplified in certain parts. For example a small diameter pilot hold could be manufactured through the bearing support hole in the thumb-bearing holder. This would aid in accurate drilling and reaming of the hole and allow for swarf removal. Casting could also be considered for the wrist connection panel and the thumb-bearing holder to simplify manufacture. The aluminium casting process could be combined with Rapid prototype models created from the CAD model.

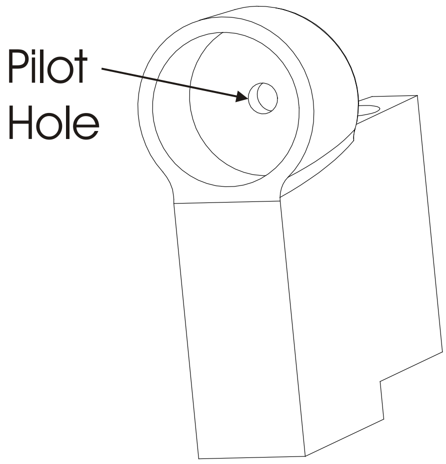

Figure 7.12 Modified Thumb Bearing Housing

Assembly

Another screw could also be added to locate the internal motor holder housing to the cover plates. This is only a preventative measure as it should already be located between various location faces. The bearing widths for the B9, and B8 bearings in the finger and the B3 bearing in the thumb could be widened to increase the width of the driving links. This would increase the strength through these linkages. The shaft locating screw at the base of the rear strut of the motor end cap could be enlarged for easier access.

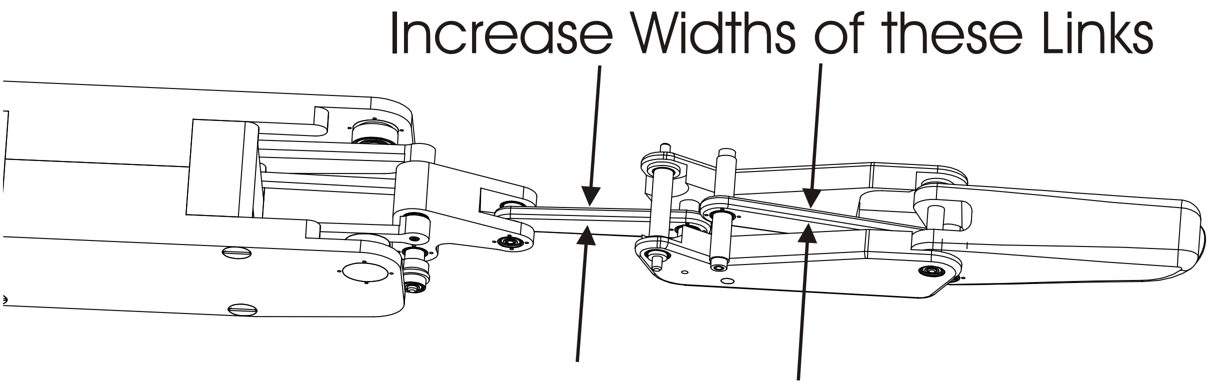

Figure 7.13 Finger Links for Improvements

Enhance Hand CAD model Interactivity

The CAD model can be modified further if need be for new motors or smaller components. A left hand can be produced from the CAD models by simply mirroring the hand components. If this were done the CAD models would be dependent on the right hand Canterbury Hand part models. For increased interactivity a GUI movement interface could be added to the hand model to replace the current control panel model. The 'Configure' program for interacting with the design tables can also be modified if new motors were to be added to the design. The structure of the palm assembly could possibly be simplified using configurations of a part instead of a base part structure.

Further Analysis

More analysis could be made for the hand. The life equations for the bronze drive nuts for example could be analysed. Even though analysis has already been made on most load bearing components it may need to be further analysed. For example the flanged support bearings for the leadscrews of the fingers and the worm gear could possibly be too small. And the support shaft for the finger spreading mechanism may not be strong enough.

These improvement suggestions will probably be unnecessary. If any problems are to occur in the creation of the hand design they will probably be from unexpected occurrences or changed requirements. For example it may be that the thumb rotates too quickly once it is tested. A larger worm wheel may need to be retrofitted into the hand to slow the hand down etc.

7.4.3 Next Generation Hand Recommendations

Future hand designs will likely utilise components and technology that is not currently available. It is expected that low weight, strong linear actuators will be developed commercially. These would be an ideal actuator for a robotic hand design. If the finger linkages can be directly driven with such an actuator it will remove the need for the lead screw. Smaller miniature bearings will become available beyond the limited ranges and types that are currently available. Plastic shell bearings as briefly researched earlier may replace the bearings in the hand. This will reduce the finger metacarpals volume and minimise the hand size. Lighter and stronger materials as they are developed will reduce weight. Distributed, precise, low powered force/tactile sensors may be developed commercially, which could mean replacing the FSRs in the hand with some kind of outer covering. Thus predicting what a future hand design will require is difficult.

However a hand design that follows this one will likely utilise this thesis as a basis for its design. The design of a complex robotic hand using a CAD program similar to the one used here is very likely. Many of the concepts used for designing the parts will be useful if the design is to be interactive and flexible to changes in geometry.

The hand design given in this thesis is limited to below the wrist. A wrist attachment device for a robotic arm will likely be a follow up project. It will need to have 2 to 3DOFs. It maybe a double active universal joint design may be utilised. Or perhaps a modified Hooks joint could be used, such as the one in the Robonaut Hand. A simple differential universal drive arrangement like the DLR hand model II may be utilised instead. Other ideas are to use a parallel platform or two revolute joints that are combined internally and externally. There are many possible solutions to this next challenge. However whatever mechanism is selected it will likely have to be internally actuated or actuated from a forearm and will have to be compact and connect to the Canterbury Hand wrist panel. After the Canterbury robotic hand development a low weight dexterous prosthetic hand using the principles developed from this thesis will be researched and created. In the compendium [Green, 2002] some general design objectives for a Canterbury Hand prosthetic device have been given. The research summarised after this in the compendium on experimental and robotic hands will also be useful for future reference and development ideas. A six-fingered hand with two thumbs may also be developed as an industrial robots end effector.

7.5 Conclusion

To conclude, this thesis has created a parametric 3D CAD model for an anthropomorphic robotic hand that has four fingers and one thumb. This design has been called the Canterbury Hand and has eleven degrees of freedom. Each of the fingers has a 2DOF motion for flexion and extension. The thumb linkages have a 1DOF curling motion. The hand has a finger spreading and thumb rotation mechanism of 1DOF each. The bearing geometry of the finger and thumb linkages, as well as the thumb rotation axis has been optimised for anthropomorphic motion, appearance and increased force output. The final hand design is low weight; and dexterous, and is able to make the generic grasp types of the human hand. This prototype prosthetic hand has applications as a teleoperated end effector for robots that work in hazardous environments, such as outer space or custom industries.

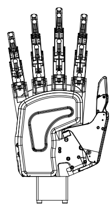

References

Articles

Al-Gallaf, E.A., Allen, A.J., and Warwick, K. (1991) Evaluation of a direct drive approach in multi-fingered robotic hands, IEE Colloquium on Robot Actuators, pp. 7/1 -7/4.

Ali, M.S., Kyriakopoulos, K.J., and Stephanou, H.E., (1993) The Kinematics of the Anthrobot-2 Dextrous Hand, 1993 IEEE International Conference on Robotics and Automation, Vol.3, pp.705-710.

Allen, P.K.; Miller, A.T.; Oh, P.Y.; Leibowitz, B.S. (1997) Using tactile and visual sensing with a robotic hand, Proceedings of the 1997 IEEE conference on Robotics and Automation, 1997. Vol. 1, pp. 676 –681.

Amato, I., (1992) In Search of the Human Touch, Science, Vol. 258, 27th November, pp1436-1437.

Ambrose, R. O. et al (2000) Robonaut: *NASA's s Space Humanoid*, Humanoid Robotics, July/August, IEEE Intelligent Systems, Vol.15, Issue: 4, July-Aug, pp.57-63.

Aramaki, S.; Shirouzu, H.; Kurono, S.; Mino, M.; Uno, Y.; Hara, K.; Tanaka, H., and Tsuruoka, T., (1999) Development of autonomous mobile humanoid robot, The 25th Annual Conference of the IEEE Industrial Electronics Society, IECON '99 Proceedings, Vol. 2, pp. 529 –534.

Atkins, D.J., Heard, D.C.Y., and Donovan, W.H., (1996) Epidemiologic Overview of Individuals with Upper Limb Los and their reported research priorities, Journal of Prosthetics and Orthotics, Vol. 8, No. 1, pp.551-536.

Baek, S.E., Lee, S.H., Heungsung, J., & Chang J. H., (1999) Design and Control of a Robotic Finger for Prosthetic Hands, Proceedings of the 1999 IEEE/RSJ International Conference on Intelligent Robots and Systems, pp.113-117.

Bailon, H., Vuskovic, M.I., and Ivokovic, B. (1995) Force Interface for the Multifingered Robotic Hand, IEEE International Conference on Systems, Man and Cybernetics, Intelligent Systems for the 21st Century, Vol. 1, pp.96-102.

Bartolini, G., and Coccoli, M., (1999) A summary of the design and realization of a robotic finger based on innovative concepts, Proceedings of the 1999 IEEE/ASME International Conference on Advanced Intelligent Mechatronics, pp. 416 –421.

Becker, J.C., and Thakor, N.V., (1988) A study of the range of motion of human fingers with application to anthropomorphic designs, IEEE Transactions on Biomedical Engineering, Vol.35, No.2, February, pp. 110-117.

Bekey, G.A., Tomovic, R., and Zeljkovic, I., (1990) Control Architecture for the Belgrade/USC Hand, in Venkataraman, S. T. and Ibrell, T. (ed.), *Dextrous Robot Hands*, Springer-Verlag, New York, pp. 136-149.

Bekey, G.A., Liu, H., Tomovic, R., Karplus, W.J., (1993) Knowledge-Based Control of Grasping in Robot Hands using Heuristics from Human Motor Skills, IEEE Transactions on Robotics and Automation, December, Vol.9, No.6, pp.709-722.

Benhamou, R., (1994) The Cover Design, *The Artificial Limb in Preindustrial France*, Society for the History of Technology, pp. 835-845.

Biagiotti, L., Melchiorri, C., and Vassura, G. (2001) Control of a robotic gripper for grasping objects in no-gravity conditions, Proceedings 2001 ICRA. IEEE International Conference on Robotics and Automation, Vol. 2, pp. 1427-1432.

Bonivento, C., Faldella, E., and Vassura, G. (1991) The University of Bologna Robotic Hand Project: current state and future developments, 91 ICAR., Fifth International Conference on Advanced Robotics, 'Robots in Unstructured Environments', Vol. 1, pp. 349 –356.

Butterfass, J., Grebenstein, M, Liu, H., and Hirzinger, G., (2001) DLR-Hand II: Next Generation of a Dextrous Robot Hand, Proceedings of the 2001 IEEE International Conference on Robotics & Automation, Seoul, Korea, May 21-26, Vol.1, pp.109-114.

Butterfass, J., Hirzinger, G., Knoch, S., and Liu, H., (1998) DLR's Multisensory Articulated Hand, *Part I: Hard- and Software Architecture*, Proceedings of the 1998 IEEE International Conference on Robotics & Automation, Leuven, Belgium, May, Vol.3, pp.2081-2086.

Caffaz, A., and Cannata, G., (1998) The Design and Development of the DIST-Hand Dextrous Gripper, Proceedings of the 1998 IEEE International Conference on Robotics & Automation, Leuven, Belgium, May, Vol.3, pp.2075-2080.

Caldwell, D.G., Kocak, O., and Andersen, U., (1995) Multi-armed Dexterous Manipulator Operation using Glove/Exoskeleton Control and Sensory Feedback, 1995 IEEE/RSJ International Conference on Intelligent Robots and Systems 95, 'Human Robot Interaction and Cooperative Robots', Vol.2, pp.567 –572.

Caldwell, D.G., and Krishna Reddy, R., (1994) A Chemo-Pneumatic Drive Source for Flexible Operation of Pneumatic Muscle Actuators, IROS '94. Proceedings of the IEEE/RSJ/GI International Conference on Intelligent Robots and Systems '94, 'Advanced Robotic Systems and the Real World', Vol.2, pp.1360-1367.

Caldwell, D.G., Medrano-Cerda, G. A., and Goodwin, M. J., (1993) Braided Pneumatic Actuator Control of a Multi-Jointed Manipulator, International Conference on Systems, Man and Cybernetics, 1993. 'Systems Engineering in the Service of Humans', Conference Proceedings, Vol.1, pp.423 –428.

Carrozza, M.C., Micera, S., Massa, B., Zecca, M., Lazzarini, R., Canelli, N., and Dario, P., (2001) The Development of a Novel Biomechatronic Hand – *Ongoing Research and Preliminary Results*, 2001 IEEE/ASME International Conference on the Advanced Intelligent Mechatronics Proceedings, 8-12 July, Corno, Italy, pp.249-254.

Chappel, P.H., and Kyberd, P.J., (1991) Prehensile control of a hand prosthesis by a Micro-controller, Journal of Biomedical Engineering Vol.13 September pp.363-369.

Chappel, P.H., Nightingale, J.M., Kyberd, P.J., and Barkhordar, M., (1987) Control of a Single Degree of Freedom Artificial Hand, Biomedical Engineering, Vol. 9, pp.273-277.

Choi, H.R., Chung, W.K., and Youm, Y., (1995) Stiffness Analysis and Control of Multifingered Robot Hands, Transactions of the ASME Journal of Dynamic Systems, Measurement and Control, September, Vol. 117, p.434-439

Choi, H.R., and Ryew, S.M., (2000) Anthropomorphic Joint Mechanism with Two Degrees of Freedom, Proceedings of the 2000 IEEE International Conference on Robotics and Automation, San Francisco, CA, April, Vol. 2, pp.1525-1530.

Congqing, W., Kui, Y., Lixin, Y., and Datai, Y., (1993) Design and Low Level Control of the USTB Multifingered Robot Hand, IEEE TENCON, Beijing, Vol.4, pp.115-118.

Coronado, J.L., Ulloa-Perez, A., Garcia-Cordova, F., and Villalba-Fernandez, J.J., (1999) Experimental development for thumb-index pinch force measurements during object manipulation with applications to robotic hands, IEEE International Conference on Systems, Man, and Cybernetics, IEEE SMC '99 Conference Proceedings, Vol. 6, pp. 786 –791.

Crisman, J.D., Kanojia, C., and Zeid, I. (1996) Graspar: *a flexible, easily controllable robotic hand*, IEEE Robotics & Automation Magazine, Vol. 3, Issue 2, June pp. 32 –38.

Crowder, R.M., (1991) Local actuation of multijointed robotic fingers, International Conference on Control, Vol. 1, pp.48-52.

Crowder, R.M., Dubey, V.N., Chappell, P.H., and Whatley, D.R., (1999) A multi-fingered end effector for unstructured environments, Proceedings of the 1999 IEEE International Conference on Robotics and Automation, Vol. 4, pp. 3038-3043.

Czinki, A., (2001) The Aachen-IFAS Robotic Hand, Ölhydraulik und Pnematik, Vol.45, No.6.

Dario, P., and Buttazzo, G., (1987) An anthropomorphic Robot Finger for Investigating Artificial Tactile perception, The International Journal of Robotics Research, Fall, Vol. 6, No. 3., pp. 25-48.

Dario, P., Laschi, C., Carrozza, M.C., Guglielmelli, E., Teti, G., Massa, B., Zecca, M., Taddeucci, D., and Lenoi, F., (2000) An Integrated Approach for the Design and Development of a Grasping and Manipulation System in Humanoid Robotics, Proceedings of the 2000 IEEE/RSJ International Conference on Intelligent Robots and Systems, pp.1-7.

Design Council (Great Britain) (1999) Hands on, Engineering, Vol.240 No.5, Great Britain, p.10.

Diftler, M.A., and Walker, I.D. (1999) Experiments in aligning threaded parts using a robot hand, IEEE Transactions on Robotics and Automation, Vol. 15, Issue 5, Oct., pp. 858 –868.

Dodds, G., Zatari, A., and Bischoff, R., (2001) Uncalibrated visual servoing for full motion dextrous robot systems with tracking cameras, Proceedings of the 2001 IEEE/RSJ International Conference on Intelligent Robots and Systems, Vol. 1, pp. 13–18.

Doersam, T., Hammerschmidt, O., and Munoz, L.A. (1997) A study on multifingered gripper control, Proceedings of the 1997 IEEE International Conference on Robotics and Automation, Vol. 2, pp. 1112 –1117.

Dream Watch (1999) T2-3D, Dream Watch, Issue 59, UK.

Dubey, V. N., Crowder, R. M., and Chappell, P. H., (2000) A robotic end effector for unstructured environments, Proceedings of the American Nuclear Society's (ANS) 7th Topical on Robotics and Remote Systems, Vol. 1, pp.452-60.

Erkmen, A.M, and Durna, M., (1998) Genetic Algorithm-Based Optimal Regrasping with the Anthrobot 5-Fingered Robot Hand, Proceedings of the IEEE International Conference on Robotics & Automation, Vol.4, May, pp.3329-3334.

Erkmen, A.M, Erkman, I., and Tekkaya, E., (2000) Optimal Initialization of Manipulation Dynamics by Vorticity Model of Robot Hand Preshaping, *Part1: Vorticity Model*, Journal of Robotic Systems, © John Wiley & Sons, Vol.17, No. 4, pp.199-212.

Erkman, I., Erkmen, A.M., Tekkaya, A.E., and Pasinlioğlu, T., (1999) Haptic Perception of Shape and Hollowness of Deformable Objects Using the Anthrobot-III Robot Hand, Journal of Robotic Systems, © John Wiley & Sons, Vol. 16, No. 1, pp.9-24.

Eusebi, A., Fantuzzi, C., Melchiorri, C.; Sandri, M., and Tonielli, A. (1994) The UB Hand II control system: design features and experimental results, IECON '94, 20th International Conference on Industrial Electronics, Control and Instrumentation, Vol. 2, pp. 782 –787.

Farooqi, M.A, Tanaka, T., Ikezawa, Y., Omata, T., and Nagata, K., (1999) Sensor Based Control for the Execution of Regrasping Primitives on a Multifingered Robot Hand, Proceedings of the 1999 IEEE International Conference on Robotics & Automation, Detroit, Michigan, May, Vol.4, pp.3217-3223.

Farry, K.A., Walker, I.D., and Baraniuk, R. G., (1996) Myoelectric Teleoperation of a Complex Robotic Hand, IEEE Transactions on Robotics and Automation, Vol.12, No. 5, October, pp.775-788.

Fisher, M., Van Der Smagt, P., and Hirzinger, G., (1998) Learning Techniques in a Dataglove Based Telemanipulation System for the DLR Hand, Proceedings of the 1998 IEEE International Conference on Robotics & Automation, Leuven, Belgium, May, Vol.2, pp.1603-1608.

Fukaya, N. Toyama, S., Asfour, T., and Dillmann, R., (2000) Design of the TUAT/Karlsruhe Humanoid Hand, Proceedings of the 2000 IEEE/RSJ International Conference on Intelligent Robots and Systems, pp.1754-1759.

Fukuda, T., Michelini, R., Potkonjak, V., Tzafestas, S., Valavanis, K., and Vukobratovic, M., (2001) How far away is "artificial man", IEEE Robotics & Automation Magazine, Vol. 8, Issue1, March, pp. 66 –73.

Fukado, O., Tsuji, T., Hiroki, S., and Kaneko, M., (1999) An EMG Controlled Human Supporting Robot Using Neural Network, Proceedings of the 1999 IEEE/RSJ International Conference on Intelligent Robots and Systems, pp.1586-1591.

Garcia-Cordova, F., Lopez-Coronado, J., and Guerrero-Gonzalez, A (1999) Design of an anthropomorphic finger using shape memory alloy springs, IEEE International Conference on Systems, Man, and Cybernetics, IEEE SMC '99 Conference Proceedings, Vol. 2, pp. 794 – 799.

Gazeau, J.P., Zeghloul, S., Arsicault, M., and Lallemand, J.P., (2001) The LMS Hand: Force and position controls in the aim of the fine manipulation of objects, Proceedings of the 2001 IEEE International Conference on Robotics & Automation, Seoul, Korea, May 21-26, Vol.3, pp.2642-2648

Graham-Rowe, D., (1999) Hands on, *Robonaut takes the risks so you don't have to,* New Scientist, New Science Publications, London, p.20.

Greenhill, S., (1993) The Digit Muscle, Industrial Robot, Vol. 20, No. 5, MCB University Press, pp.29-30.

Grupen, R.A., and Coelho, J.A., Jr. (2000) Structure and growth: *a model of development for grasping with robot hands,* Proceedings of the 2000 IEEE/RSJ International Conference on Intelligent Robots and Systems (IROS 2000), Vol. 3, pp. 1987 –1992.

Guo, G., Gruver, W.A., and Qian, X., (1991) A robotic hand mechanism with rotating fingertips and motor-tendon actuation, Conference Proceedings of the 1991 IEEE International Conference on Systems, Man, and Cybernetics, 'Decision Aiding for Complex Systems', Vol. 2, pp. 1023–1028.

Guo, G., Gruver, W.A., and Qian, X. (1992) A new design for a dexterous robotic hand mechanism, IEEE Control Systems Magazine, Vol. 12, Issue 4, Aug., pp. 35–38.

Guo, G., Zhang, J., and Gruver, W.A., (1993) Optimal Design of a six-bar linkage with one degree of freedom for an anthropomorphic three jointed finger mechanism, Proceedings of Institution of Mechanical Engineers, Vol. 207, pp. 185-190.

Hasegawa, T., Matsuoka, T., and Honda, K. (1999) Mechanical assembly by a multi-fingered robotic hand with error recovery function, (ISATP '99) Proceedings of the 1999 IEEE International Symposium on Assembly and Task Planning, pp. 232 –237.

Hasegawa, T., and Murakami, K. (2001) Finger motion planning of a multifingered manipulation with rolling contact, Proceedings of the IEEE International Symposium on Assembly and Task Planning, pp. 196 –201.

Hirose, S., and Arikawa, H., (2000) Coupled and decoupled actuation of robotic mechanisms, Proceedings of the ICRA '00, IEEE International Conference on Robotics and Automation, Vol. 1, pp. 33 –39.

Hirose, S., and Ma, S., (1991) Coupled tendon-driven multijoint manipulator, Proceedings of the 1991 IEEE International Conference on Robotics and Automation, Vol. 2, pp. 1268-1275.

Hirzinger, G., (1996) Mechatronics for a New Robot Generation, IEEE/ASME Transactions on Mechatronics, Vol.1, No.2, June, pp.149-157.

Hirzinger, G., (2001) On the interaction between human hand and robot from space to surgery, IEEE International Workshop on Robot and Human Interactive Communication, p.1.

Hirzinger, G., Brunner, B., et al (2000) Advances in Orbital Robotics, Proceedings of the 2000 IEEE International Conference on Robotics & Automation, San Francisco, CA, April, Vol.1, pp.898-907.

Hirzinger, G., Butterfass, J., et al (2000) A Mechatronics Approach to the design of light-weight arms and multifingered hands, Proceedings of the 2000 IEEE International Conference on Robotics & Automation, San Francisco, CA, April, Vol.1, pp.46-54.

Hirzinger, G., Butterfass, J., et al (2001) Space Robotics – *Driver for a New Mechatronic Generation of Light-weight Arms and Multifingered Hands*, 2001 IEEE/ASME International Conference on Advanced Intelligent Mechatronics Proceedings, 8-12 July, Como Italy, Vol.2, pp.1160-1168.

Hristu-Varsakelis, D., and Brockett, R.W. (2002) Experimenting with Hybrid Control, IEEE Control Systems Magazine , Vol. 22, Issue 1, Feb., pp. 82–95.

Hollingum, J., (1991) Japanese Robotics Displayed at Science Museum, Industrial Robot, Vol.18, No.4, pp.18-19.

Huang, H.P. and Chen C,Y, (1999) Development of a Myoelectric Discrimination System for a Multi-degree Prosthetic Hand, Proceedings of the 1999 IEEE International Conference on Robotics & Automation, Michigan, May, pp.2392-2397.

Huang, H.P., and Wei, Y.F., (1998) Control of Dextrous Hand Master with Force Feedback, Proceedings of the 1998 IEEE, International Conference on Robotics & Automation, Belgium, May, pp.687-692.

Iberall, T., (1997) Human Prehension and Dexterous Robot Hands, The International Journal of Robotics Research, Vol. 16, No. 3, June, MIT, pp.285-299.

Iberall, T., Sukhatme, G.S., Beattie, D., and Bekey, G.A., (1994) On the Development of EMG Control for a Prosthesis using a Robotic Hand, Proceedings of the IEEE Conference on Robotics and Automation, Vol. 2, pp. 1753-1758.

Iberall, T., Sukhatme, G.S., Beattie, D., and Bekey, G.A., (1994) On the Development of EMG Control for a Prosthesis using a Robotic Hand, Proceedings of the IEEE Conference on Robotics and Automation, Vol. 2, pp. 1753-1758.

Jacobsen, S.C., Wood, J.E., Knutti, D.F., and Biggers, K.B., (1986) Utah/MIT Dextrous Hand Work in Progress, in Pham, Dr D. T. and Heginbotham, Prof. W. B., (ed.), International Trends in Manufacturing Technology – Robot Grippers, IFS (Publications) Ltd., Bedford, U.K, pp.341-389.

Jägersand, M., (1999) Hierarchical Uncalibrated Predictive Display for a 16 DOF Utah/MI hand, Proceedings of the 1999 IEEE/RSJ International Conference on Intelligent Robots and Systems, Vol.1, pp.124-129.

Jau, B.M., (1992) Man-Equivalent Telepresence Through Four Fingered Human-like Hand System, Proceedings of the 1992 IEEE International Conference on Robotics and Automation, Nice, France, May, Vol.1, pp.843-848.

Jau, B.M., (1995) Dexterous Telemanipulation with Four Fingered Hand System, IEEE International Conference on Robotics and Automation, Vol.1, pp.338-343.

Kagami, S., Kuffner, J.J., Jr., Nishiwaki, K., Sugihara, T., Michikata, T., Aoyama, T., Inaha, M., and Inoue, H., (2001) Design and implementation of remotely operation interface for humanoid robot, Proceedings of the 2001 ICRA IEEE International Conference Robotics and Automation, Vol. 1, pp. 401-406.

Kaneko, M., and Imamura, N., (1991) Development of a Tendon-driven finger with single pulley-type TDT sensors, IEEE/RSJ International Workshop on Intelligent Robots and Systems IROS'91, 'Intelligence for Mechanical Systems, Osaka, Japan, November, Vol. 2, pp.752-757.

Kaneko, M., Shirai, T., and Tsuji, T., (2000) Scale-dependent grasp, IEEE Transactions on Systems, Man and Cybernetics, Part A, Vol. 30, Issue 6, Nov., pp. 806 –816.

Kawasaki, H., Komatsu, T., Uchiyama, K., and Kurimoto, T., (1999) Dextrous Anthropomorphic Robot Hand with Distributed Tactile Sensor: *Gifu Hand II*, IEEE International Conference on Systems, Man, and Cybernetics, Vol. 2, pp.782-787.

Kawasaki, H., Nakayama, K., Mouri, T., and Ito, S., (2001) Virtual Teaching Based on Hand Manipulability for Multi-Fingered Robots, Proceedings of the 2001 IEEE International Conference on Robotics & Automation, Soul, Korea, May 21-26, pp.1388-1393.

Kim; M., Kang, S., Lee, S. Chung, W., Cho, K., and Lee, C. W., (1999) Development of a Humanoid Robot CENTAUR, IEEE International Conference on Man, and Cybernetics, Vol. 4, pp. 948 –953.

Koganezawa, K., Watanabe, Y., and Shimizu, N., (1999) Antagonistic muscle-like actuator and its application to multi-d.o.f. forearm prosthesis, Advanced Robotics: The international journal of the Robotics Society of Japan, Vol. 12, pp.771-789.

Kragić, D., Miller, A.T., and Allen, P.K., (2001) Real-time Tracking Meets Online Grasp Planning, Proceedings of the 2001 IEEE International Conference on Robotics & Automation, Seoul, Korea, May 21-26, Vol.3, pp.2460-2465.

Kyberd, P., (1995) Artificial Arms: *Facts and Fantasies*, Guest lecture at the University of Canterbury.

Kyberd, P., (2000) The Intelligent Hand, IEE Review, September, pp.31-35.

Kyberd, P.J., Beard, D.J., Davey J.J., and Morrison, J.D., (1998) A Survey of Upper-Limb Prosthesis Users in Oxfordshire, Journal of Prosthetics and Orthotics, Vol. 10, No. 4, Fall.

Kyberd, P.J., and Chappel, P.H., (1993) A force sensor for automatic manipulation based on the Hall effect, Measurement, Science and Technology, Vol. 4 pp.281-287.

Kyberd, P.J., and Chappel, P.H., (1994) The Southampton Hand: *An Intelligent Myoelectric Prosthesis*, Journal of Rehabilitation, Research and Development, Vol. 31, No.4, pp326-334.

Kyberd, P.J., and Chappel, P.H., (1992) Object-Slip Detection during Manipulation using a Derived Force Vector, Mechatronics, Vol.2, No.1, pp.1-13.

Kyberd, P.J., Evans, M., and Winkel, S.T., (1998) An Intelligent Anthropomorphic Hand with Automatic Grasp, Robotica, Vol. 16, Cambridge University Press, United Kingdom, pp.531-536.

Kyriakopoulos, K.J., VanRiper, J., Zink, A., and Stephanou, H.E., (1997) Kinematic Analysis and Position/Force Control of the Anthrobot Dextrous Hand, IEEE Transactions on Systems, Man and Cybernetics, Part B: Cybernetics, Vol. 27, No. 1, February, pp.95-104.

Laliberte, T., Goselin, C.M., and Cote, G., (2001) Practical Prototyping, IEEE Robotics & Automation, Magazine, Vol. 8, No. 3, September, pp.43-52
Practical prototyping

Lane, D.M., Davies, J.B.C., Robinson, G., O'Brien, D.J., Sneddon, J., Seaton, E., and Elfstrom, A. (1999) The AMADEUS dextrous subsea hand: design, modelling, and sensor processing, IEEE Journal of Oceanic Engineering, Vol. 24, Issue 1, Jan. pp. 96–111.

LaPlante, M.P., and Carlson, D., (1996) Disability in the United States, *Prevalence and Causes*, 1992. Disability Statistics Report, No.7, US Department of Education, National Institute on Disability, University of California, San Francisco.

LeBlanc, M.A., (1973) Patient Population and Other Estimates of Prosthetics and Orthotics in the USA, Orthotics and Prosthetics, Vol. 23, No. 3, pp. 38-43.

Lee, J., Nob, C., Lee, S., Kim, M., and Park, M., (1999) Design of Masterarm based on human kinematics and its integration to humanoid robot, Proceedings of the IEEE Region 10 Conference TENCON 1999, Vol. 2, pp. 998 –1001.

Lee, Y. K., and Shimoyama, I., (1999) A skeletal framework artificial hand actuated by pneumatic artificial muscles, Proceedings of the 1999 IEEE International Conference on Robotics & Automation, Detroit, Michigan, May, pp. 926-931.

Light, C.M., Chappell, P.H., Kyberd, P.J., and Ellis, B.S., (1999) A Critical Review of Functionality Assessment in Natural and Prosthetic Hands, British Journal of occupational therapy, January, Vol. 62, No. 1, pp. 7-12.

Lim, H.-O., and Takanishi, A., (2000) Waseda biped humanoid robots realizing human-like motion, Proceedings of the 6th International Workshop on Advanced Motion Control, pp. 525 –530.

Lin, L.R., (1996) Integrating Fuzzy Control of the Dextrous National Taiwan University (NTU) Hand, IEEE/ASME Transactions on Mechatronics, Vol1. No.3, September, pp.216-229.

Lin, L.R., and Huang, H.P., (1996) Mechanism Design of a New Multifingered Robot Hand, Proceedings of the 1996 IEEE International Conference on Robotics and Automation, April, pp.1471-1476.

Lin, L.R., and Huang, H.P., (1995) DSP-Based Fuzzy Control of a Multifingered Robot Hand, IEEE International Conference on Systems, Man and Cybernetics, Intelligent Systems for the 21st Century, Vol. 4 pp.3672-3677.

Lin, L.R., and Huang, H.P., (1996) NTU Hand: *A New Design of Dexterous Hands*, Transactions of the ASME, Journal of Mechanical Design, June, Vol.120, pp.282-292.

Liu, H., Meusel, P., Butterfass, G., and Hirzinger, G., (1998) DLR's multisensory articulated hand, *Part II: The parallel torque/position control system*, Proceedings of the 1998 IEEE International Conference on Robotics & Automation, Leuven, Belgium, May, Vol.3, pp.2087-2093.

Liu, H., Butterfass, J., et al (1999) A New Control Strategy for DLR's Multisensory Articulated Hand, IEEE Control Systems, Vol.19, No.2, April, pp.47-54.

Liu, H., and Hirzinger, G., (1999) Cartesian Impedance Control for the DLR Hand, Proceedings of the 1999 IEEE/RSJ International Conference on Intelligent Robot Systems, Vol.1, pp.106-112.

Liu, H., and Hirzinger, G., (1999) Joint Torque Based Cartesian Impedance Control for the DLR Hand, Proceedings of the 1999 IEEE/ASME International Conference on Advanced Intelligent Mechatronics, September, 19-23, Atlanta, USA, pp.695-700.

Lovchik, C.S., and Diftler, M.A., (1999) The Robonaut Hand: *A Dextrous Robot Hand for Space*, Proceedings of the IEEE, International Conference on Robotics & Automation, Detroit, Michigan, May, pp.907-912.

Ma, S., Hirose, S., and Yoshinada, H. (1993) Design and experiments for a coupled tendon-driven manipulator, IEEE Control Systems Magazine, Vol. 13, Issue: 1, Feb., pp. 30–36.

Machine Design (1990) Robot hand grabs it all, May 24, p.44.

Machine Design (1992) Flexible Screw Improves Artificial Hand, November 12, p.30.

Maekawa, H., Tanie, K., and Komoriya, K., (1995) Tactile sensor based manipulation of an unknown object by a multifingered hand with rolling contact, Proceedings of the 1995 IEEE International Conference on Robotics and Automation, Vol. 1, pp. 743 –750.

Maekawa, H., Tanie, K., and Komoriya, K., (1996) Dynamic grasping force control using tactile feedback for grasp of multifingered hand, Proceedings of the 1996 IEEE International Conference on Robotics and Automation, Vol. 3, pp. 2462 –2469.

Maekawa, H.; Tanie, K.; Komoriya, K. (1997) Tactile feedback for multifingered dynamic grasping, IEEE Control Systems Magazine, Vol. 17, Issue 1, Feb., pp. 63-71.

Magee, D.J., (1992) Forearm, wrist and hand, Orthopaedic Physical Assessment, WB Saunders, London

Markenscoff. X., Ni, L., and Papadimitriou, C. H., (1990) The geometry of grasping, International Journal of Robotics Research, Vol. 9, No. 1, pp.61-74.

Martens, C., Ruchel, N., Lang, O., Ivlev, O., and Graser, A. (2001) A FRIEND for assisting handicapped people, IEEE Robotics & Automation Magazine, Vol. 8, Issue 1, March, pp. 57-65.

Matsumiya, T., Nakayama, S., Miura, Y., Chen, P., and Toyota, T., (1999) Intelligent control method for robot hand based on tactile information by double-octagon tactile sensor, IEEE SMC '99 Conference Proceedings of the IEEE International Conference on Systems, Man, and Cybernetics, Vol. 6, pp. 768–773.

Matsuoka, T., Hasegawa, T., and Honda, K., (1999) A Dexterous Manipulation System with Error Detection and Recovery by a Multi-fingered Robotic Hand, IROS '99. Proceedings of the 1999 IEEE/RSJ International Conference on Intelligent Robots and Systems Vol. 1, pp. 418–423.

Maycock, E., (2001) Engineers offer Surgeons a Hand, I Mech E, Diary of Events, January 2001, pp.1-2.

McCammon, I.D., and Jacobsen, S.C., (1994) Tactile Sensing and Control for the Utah/MIT Hand, in Venkataraman, S. T., and Iberall, T., (ed.), Dexterous Robot Hands, Springer-Verlag, New York, pp.238-266.

Michelman, P., (1998) Precision Object Manipulation with a Multifingered Robot Hand, IEEE Transactions on Robotics and Automation, Vol.14, No.1, February, pp.105-113.

Michelman, P., and Allen, P., (1993) Compliant Manipulation with a Dextrous Robot Hand, 1993 IEEE International Conference on Robotics and Automation, Vol.3, pp.711-716.

Minor, M., and Mukherjee, R., (1999) A Dexterous Manipulator for minimally invasive surgery, Proceedings of the 1999 IEEE International Conference on Robotics & Automation, Detroit, Michigan, May, Vol. 3, pp. 2057-2064.

Mokhtari, M., Didi, N., and Roby-Brami, A., (1999) A multi-disciplinary approach in evaluating and facilitating the use of the Manus robot, Proceedings of the 1999 IEEE International Conference on Robotics and Automation, Vol. 2, pp. 1071–1076.

Morita, T., Iwata, H., and Sugano, S., (1999) Development of Human Symbiotic Robot: WENDY, Proceedings of the 1999 IEEE International Conference of Robotics & Automation, Detroit, Michigan, May, Vol.4, pp.3183-3188.

Morita, T., Sugano, S., (1995) Design and Development of a new robot joint using a mechanical impedance adjustor, Proceedings of the IEEE International Conference on Robotics and Automation, Vol. 3, pp. 2469-2475.

Morita, T., and Sugano, S., (1997) Development of An Anthropomorphic Force-Controlled Manipulator WAM-10, Proceedings of the 8th International Conference on Advanced Robotics (ICAR), pp.701 –706.

Nagai, K., Eto, Y., Asai, D., and Yazaki, M. (1998) Development of a three-fingered robotic hand-wrist for compliant motion, Proceedings of the 1998 IEEE/RSJ International Conference on Intelligent Robots and Systems, Vol. 1, pp. 476–481.

Nagakubo, A., Kuniyoshi, Y., and Cheng, G., (2000) Development of a High-Performance Upper-Body Humanoid System, Proceedings of the 2000 IEEE/RSJ International Conference on Robots and Systems

Nagakubo, A., Kuniyoshi, Y., and Cheng, G., (2001) ETL-Humanoid – *A High Performance Full Body Humanoid System*, Proceedings of the 2001 IEEE/RSJ International Conference on Robots and Systems, Maui, Hawaii, USA, October 29 -November 3, pp.1087-1092.

Nahavandi, S., and Kouzani, A.Z., (2001) Artificial Hand – From a Robotic Perspective, Seventh Australian and New Zealand Intelligent Information System Conference, 18-21 November, Perth Western Australia, pp. 37-42.

Nahvi, A., Hollerbach, J.M., Xu, Y., and Hunter, I. W., (1994) An Investigation of the Transmission System of a Tendon Driven Robot Hand, Proceedings of the IEEE/RSJ/GI International Conference on Intelligent Robots and Systems '94. 'Advanced Robotic Systems and the Real World', Vol.1, pp.202-208.

Nakamura, T., Kogure, Y., and Shimamura, K., (2000) A micro operation hand and its application to microdrawing, Proceedings of the ICRA '00, IEEE International Conference on Robotics and Automation, Vol. 2, pp. 1095–1100.

Nakamura, T., Shimamura, K., and Ando, T., (2000) A magnetic suspension parallel motion hand and its application to micro processes, Proceedings of the MHS 2000, International Symposium on Micromechatronics and Human Science, pp. 157–162.

Nishiwaki, K., Sugihara, T., Kagami, S., Kanehiro, F., Inaba, M., and Inoue, H., (2000) Design and development of research platform for perception-action integration in humanoid robot: H6, Proceedings of the 2000 IEEE/RSJ International Conference on Intelligent Robots and Systems, Vol. 3, pp.1559-1564.

Northrup, S., Sarkar, N., and Kawamura, K., (2001) Biologically-inspired control architecture for a humanoid robot, Proceedings of the 2001 IEEE/RSJ, International Conference on Intelligent Robots and Systems, Vol. 2, pp.1100–1105.

Oda, M., (1999) Space robot experiments on NASDA's ETS-VII satellite-*preliminary overview of the experiment results*, Proceedings. 1999 IEEE International Conference on Robotics and Automation, Vol. 2, pp. 1390 –1395.

Ogawara, K., Kimura, H., and Ikeuchi, K., (2001) Refining hand-action models through repeated observations of human and robot behaviour by combined template matching, Proceedings, Proceedings of the 2001 IEEE/RSJ International Conference on Intelligent Robots and Systems, Vol.1, pp. 545–550.

Ohnishi, K., Tajima, T., and Saito, Y., (2000) Anthropomorphic hand control for robotic hand-arm system, 2000 IEEE International Conference on Systems, Man, and Cybernetics, Vol.2, pp.1255-1259.

Okuno, R., Yoshida, M., and Akazawa, K., (1999) Development of Myoelectric Hand Effector with Voluntarily Controlled Compliance, Proceedings of the First Joint BMES/EMBS Conference, October 13-16, Atlanta, GA, USA, p.640.

Ono. E., Kitagaki, K., and Kakikura, M., (2001) Picking up a Piece of Fabric from Layers by a Hand with 3 Fingers and a Palm, Proceedings of the 2001/RSJ International Conferences on Intelligent Robots and Systems, Hawaii, USA, Vol. 2, pp. 931–936.

Oomichi, T., Okino, A., Higuchi, M., and Waekawa, A., (1990) Development of Working Multifinger Hand Manipulator, IEEE International Workshop on Intelligent Robots and Systems, Vol.2, pp.873-880.

Otsuka, A., Tsuji, T., Fukada, O., Eisemnann Shimizu, M., and Sakawa, M., (2000) Development of an internally powered functional prosthetic hand with a voluntary closing system and thumb flexion and radial abduction, Proceedings of the 2000 IEEE International Workshop on Robot and Human Interactive Communication, September 27-29, Osaka, Japan, pp.405-410.

Pedreno-Molina, J.L., Guerrero-Gonzalez, A., Garcia-Cordova, F., and Lopez-Coronado, J., (2001) A neural estimator of object stiffness applied to force control of a robotic finger with opponent artificial muscles, IEEE International Conference on Systems, Man, and Cybernetics Vol. 5, pp.3025-3030.

Pellerin, C., (1991) The Salisbury Hand, Industrial Robot, Vol. 18, No.4, pp.25-26.

Raparelli, T., Mattiazzo, G., Maurio, S., and Velardocchia, M., (2000) Design and Development of a Pneumatic Anthropomorphic Hand, Journal of Robotic Systems, © John Wiley & Sons Inc., No. 17, Vol. 1, pp.1-15.

Ramos, A.M., Gravagne, I.A., and Walker, I.D., (1999) Goldfinger: A Non-Anthropomorphic, Dextrous Robot Hand, (1999) Proceedings of the 1999 IEEE International Conference on Robotics & Automation, Detroit, Michigan, May, Vol.2, pp.913-919.

Reynaerts, D., and Van Brussel, H., (1993) Two-fingered full envelope dexterous manipulation, Proceedings of the 1993 IEEE International Conference on Robotics and Automation, Vol. 2, pp. 436–441.

Robinson, G., Davies, J.B.C., and Jones, J.P.P. (1998) Development of the Amadeus dextrous robot end-effectors, OCEANS '98 Conference Proceedings, Vol. 2, pp. 703–707.

Robotic Hand Approaches Human Dexterity, Machine Design, June 26, 1986, pp.40-44.

Rosa, P.F.F., and Okada, T. (1995) 3-D firm grasps with the SCROLLIC gripper, Proceedings of the 1995 IEEE International Conference on Robotics and Automation, Vol. 2, pp. 1662-1667.

Rosheim, M.E., (1996) Robotic surrogate: work in progress, 1996 IEEE International Conference on Robotics and Automation, Vol. 1, pp. 399–403.

Ryew, S. and Choi, H. R., (2001) Double Active Universal Joint (DAUJ): Robotic Joint Mechanism for Humanlike Motions, IEEE Transactions on Robotics and Automation, Vol. 17, No. 3, June, Vol. 17, Issue 3, pp.290-300.

Ryew, S.M., Choi, H.R., and Chung, W.K., (2000) Robotic Finger Mechanism with New Anthropomorphic Metacarpal Joint, IECON 2000, 26th Annual Conference of the IEEE Industrial Electronics Society Vol. 1, pp. 416-421.

Ryu, J.C., and Park, C.K., (1999) A hybrid fuzzy controller design for the control of a flexible finger, SICE '99, 38th Annual Conference Proceedings of the SICE Annual, Morioka, July, pp.1233-1238.

Sacchetti, R., Davalli, A., and Schmidl, H., (1995) Advances in Upper Limb Prostheses, Proceedings of International Federation for Theory of Machines and Mechanisms, The 9th World Congress on the Theory of Machines and Mechanisms, Milan, Vol.3, pp.2209-2213.

Salisbury, J. K., (1984) Interpretation of Contact Geometry's from Force Measurements, in Robotics Research: The first International Symposium, MIT Press, pp.565-577.

Schlegl, T., and Buss, M., (1999) A Discrete-Continuous Control Architecture for Dextrous Manipulation, IEEE International Conference on Systems, Man, and Cybernetics, Vol.2, pp.860 -865.

Schlegl, T., Buss, M., Omata, T., and Schmidt, G. (2001) Fast dextrous re-grasping with optimal contact forces and contact sensor-based impedance control, Proceedings 2001 ICRA. IEEE International Conference on Robotics and Automation, Vol. 1, pp. 103 –108.

Schlegl, T., Freyberger, F., et al (1999) Compensation of Discrete Contact State Errors in Regrasping Experiments with the TUM-Hand, Proceedings of the 1999 IEEE/RSJ International Conference on Intelligent Robots and Systems, Vol.1, pp. 118 –123.

Schlemmer, M., Finsterwalder, R., Grübel, G., (1995) Dynamic trajectory optimisation in real time for moving obstacles avoidance by a ten degrees of freedom manipulator, 1995 IEEE/RSJ International Conference on Intelligent Robots and Systems 95. 'Human Robot Interaction and Cooperative Robots', Vol.3, pp.72-77.

Schneider, R., (1991) Servo pneumatic system mimics human-hand capability, Hydraulics & Pneumatics August, p.10.

Schulte, R.A., (1962) The Characteristics of the McKibben Artificial Muscle, Application of External Power in Prosthetics and Orthetics, National Academy of Sciences - National Research Council, Washington DC, Publication. 874, pp.94-115.

Schultz, S., Pylatiuk, C., and Bretthauer, G. (2001) A New Ultralight Anthropomorphic Hand, Proceedings 2001 ICRA. IEEE International Conference on Robotics and Automation, Vol. 3, pp.2437- 2441.

Science Service (1995) Science News, *Getting a grip on things*, Science Service, Vol. 147, January 7, p.15.

Seguna, C.M., and Saliba, M.A. (2001) The mechanical and control system design of a dexterous robotic gripper, ICECS 2001. The 8th IEEE International Conference on Electronics, Circuits and Systems, Vol. 3, pp. 1195–1201.

Sharma, S., and Ogot, M.M., (1997) An Inverse Dynamic Model of a Spherical Electrohydraulic Actuator for Use in a Dexterous Mechanical Hand, The International Journal of Robotics Research, Vol. 16, pp. 557-566.

Shen, Y., Liu, Y., and Li, K., (2000) Haptic Tactile Feedback in Teleoperation of a Multifingered Robot Hand, Proceedings of the 3rd World Congress on Intelligent Control and Automation, June 28-July 2, Hefei, P. R. China, pp.85-90.

Shimoga, K.B., and Khosla, P.K., (1994) Touch and Force Reflection for Telepresence Surgery, Proceedings of the 16th Annual International Engineering in Medicine and Biology Society, Engineering Advances: New Opportunities for Biomedical Engineers, Vol.2, pp.1049-1050.

Silcox, D.H., Rooks, M.D., et al., (1993) Myoelectric Prostheses, The Journal of Joint and Bone Surgery, Vol. 75-A, No.12, pp.1781-1791.

SMR (1973) Joint Replacement in the Upper Limb, Engineering in Medicine, Vol. 6, No. 3, July, pp. 90-93.

Stansfield, S.A., (1991) Robotic Grasping of Unknown Objects: A Knowledge-based approach, The International Journal of Robotics Research, MIT, Vol. 10, No. 4, August, pp. 314-321.

Steeper, H., (1993) Coming to Grips with artificial hand design, Design Engineering, March.

Sugano, S., and Kato, I., (1987) Wabot-2: *Autonomous Robot with Dexterous Finger-Arm*, Proceedings of the IEEE International Conference on Robotics and Automation, Vol.1, pp.90-97.

Sugiuchi, H., Watanabe, S., Hasegawa, Y., and Nornoto, M., (2000) A Control System for Multi-Fingered Robotic Hand with Distributed Touch Sensor, 26th Annual Conference of the IEEE Industrial Electronics Society, Vol.1, pp.434 –439.

Sugiuchi, H., Shinichiro, W., and Morino, T., (2001) Realization of Dextrous Hand Task by using Multi-Finger Dual Robot Hand, 2001 IEE/ASME International Conference on Advanced Intelligent Mechatronics Proceedings 8-12 July, Como, Italy, p.2.

Stix, G., (1998) Phantom Touch, Scientific American, October, pp.25-26.

Tanikawa, T., and Arai, T., (1999) Development of a micro-manipulation system having a two-fingered micro-hand, IEEE Transactions on Robotics and Automation, Vol. 15, Issue 1, Feb., pp. 152–162.

Teichmann, M., and Mishra, B., (2000) Reactive Robotics I: Reactive Grasping with a modified gripper and multifingered hands, The International Journal of Robotics Research, Vol. 19, No. 7, July, pp.697-708.

Tomovic, R. and Boni, G. (1962) An Adaptive Artificial Hand, IRE Transcript on Automatic Control, Vol. AC-7, No.3, pp.3-10.

Townsend, W.T., (2000) The Barrett Hand grasper – *programmably flexible part handling and assembly*, MCB-Industrial Robot Feature Article, Industrial Robot: An International Journal, Vol. 27, No. 3, pp.181-188.

Tsuji, T., Fukada, O., Shigeyoshi, H., and Kaneko, M., (2000) Bio-mimetic Impedance Control of an EMG-controlled Prosthetic Hand, Proceedings of the 2000 IEEE/RSJ International Conference on Intelligent Robots and Systems, pp.377-382.

VanRiper, J., Ali, M.S., Kyriakopoulos, K.J., and Stephanou, H.E., (1992) Description and Kinematic Analysis of the Anthrobot-2 Dextrous Hand, Proceedings of the 1992 IEEE International Symposium on Intelligent Control, pp.299-305.

Varseveld, R.B., and Bone, G.M., (1999) Design and Implementation of a Lightweight, Large Workspace Non-Anthropomorphic Dextrous Hand, Vol.121, December, Transactions of the ASME Journal of Mechanical Design, pp.480-484.

Venkataraman, S.T., and Djaferis, T.E., (1987) Multivariable Feedback Control of the JPL/Stanford Hand, Proceedings of the IEEE International Conference on Robotics and Automation, Vol. 1, pp.77-82.

Visioli, A., and Legnani, G., (2002) On the trajectory tracking control of industrial SCARA robot manipulators, IEEE Transactions on Industrial Electronics, Vol. 49, Issue 1, Feb., pp. 224 –232.

Weir, R.F., and Grahm, E.C., (2000) Development of Externally-Powered Prosthesis for Persons with Partial Hand Amputations, Proceedings of the 22nd Annual EMBS International Conference, July 23-28, Chicago, pp.427-430.

Wen-Han Qian, Hong Qiao, and Tso, S.K., (2001) Synthesizing two-fingered grippers for positioning and identifying objects, IEEE Transactions on Systems, Man and Cybernetics, Part B, Vol.: 31, Issue 4, Aug., pp. 602 –615.

Wilson, D., (1992) Giving Natural Movement to a Robotic Hand, The Chronicle of Higher Education, March 18, pp.A20-A22.

Wöhlke, G., (1994) The Karlsruhe Dextrous Hand: *Grasp Planning, Programming & Real Time Control*, Proceedings of The IEEE/RSJ Conference on Intelligent Robots and Systems, Vol. 1, pp.352-359.

Wright, A.K., and Stanistic, M.M., (1990) Kinematic Mapping between the EXOS Handmaster Exoskeleton and the Utah/MIT Dextrous Hand, IEEE International Conference on Systems Engineering, pp.101-104

Yamamoto, M., Sakai, Y., Funakoshi, Y., and Ishimatsu, T., (1999) Assistive robot hand for the disabled, IEEE SMC '99 Conference Proceedings of the IEEE International Conference on Systems, Man, and Cybernetics, Vol. 1, pp. 131-134.

Yisheng Guan; Ho, T.; Hong Zhang (2001) UA telehand: *an integrated robotic hand/simulator system for tele-manipulation via the Internet*, Proceedings of the 2001 (ICRA) IEEE International Conference on Robotics and Automation, Vol. 2, pp. 1909-1914.

Zhang, Y., Han, Z., et al, (2001) Design and Control of the BUAA Four Fingered Hand, Proceedings of the 2001 IEEE International Conference on Robotics & Automation, Seoul, Korea, May 21-26, Vol.3, pp.2517-2521.

Canterbury Hand Theses and Related Articles

Bain, Andrew R. (February 1997), Optimisation of a Two Degree of Freedom Finger using a Genetic Algorithm: *A thesis submitted for the Degree of Master of Engineering (Mechanical):* Department of Mechanical Engineering, University of Canterbury, Christchurch, New Zealand

Dunlop, G. R. and Murphy, J. D. (1993) A Universal Pulse Processing Board or Instrumentation and Machine Control, Proceedings of NELCON 1993, Auckland, New Zealand, Vol. 1, pp. 171-178.

Dunlop, G. R. and Ward, D. K., (1995) The Kinematics of a Fifteen DOF Six Fingered Hand, Proceedings of the International Federation for Theory of Machines and Mechanisms (IFToMM) – 9th World Congress on the Theory of Machines and Mechanisms, Vol.3, pp.2249-2253.

Dunlop, G. R., Bain, A. R., and Smaill, J. S., (1999) Genetic algorithm optimisation of a 2 DOF finger, Proceedings of the 10th World Congress on the Theory of Machines & Mechanisms IFToMM'99, Oulu, Finland, Vol. 3, June, pp.1015-1020.

Elliot, Rodney B (1998) Feature extraction techniques for grasp classification: *A thesis submitted in partial fulfilment of the requirements for the degree of Master of Engineering at the University of Canterbury*: Department of Mechanical Engineering, University of Canterbury, Christchurch, New Zealand

Green, C.S., (2000) Analysis of the Sensitivity of the Output Force of the Canterbury Thumb due to Machining Inaccuracy of the Joint Geometry, Report on 'Monte Carlo Simulation to Assess Risk in Engineering Design' for ENCI 606 Risk Assessment, May, Department of Mechanical Engineering, University of Canterbury, Christchurch, New Zealand

Green, C.S., (2002) Canterbury Hand Design and Background Material, Report containing supplementary material for the design of the Canterbury Hand and is a compendium to the Masters thesis "Parametric Design and Optimisation of the Canterbury Hand", Department of Mechanical Engineering, University of Canterbury, Christchurch, New Zealand

Lamalle, Didier (July 1999) Design of a Testing Device: *At the request of the Institut Français de Mécanique Avancée this project was undertaken as a practical training semester*: Department of Mechanical Engineering, University of Canterbury, Christchurch, New Zealand

Monier, Hugues and Magnier, Laurent (1993) Robot Hand – Design of a Finger: *Report prepared as part of requirements for final year undergraduate project for Mechanical Engineering Department, Ecole Nationale D'Ingenieurs, Saint-Etienne, France*: Department of Mechanical Engineering, University of Canterbury, Christchurch, New Zealand

Stewart, David M. (January 1999), Solid Modelling of the Canterbury Finger: *Research Assistant's Report for Dr G. R. Dunlop:* Department of Mechanical Engineering, University of Canterbury, Christchurch, New Zealand

Taylor, J. H. (September 1998), The Canterbury Finger: *A final year project submitted for the partial fulfilment of the requirements for the Degree of Bachelor of Engineering (Mechanical):* Department of Mechanical Engineering, University of Canterbury, Christchurch, New Zealand

Traub, Dietmar (August 1996), Weight Reduction of A Two Degree of Freedom Robotic Finger: *Technical Report:* Department of Mechanical Engineering, University of Canterbury, Christchurch, New Zealand

Ward, Derek K. (September 1996), Design of a Two Degree of Freedom Robotic Finger*: A thesis submitted for the Degree of Master of Engineering (Mechanical):* Department of Mechanical Engineering, University of Canterbury, Christchurch, New Zealand

Internet References

Allen, P., (2000) Autonomous Precision Manipulation, Columbia University Robotics Group, URL: http://www.cs.columbia.edu/robotics/projects/hands/manipulation.html

Barrett technology.com (2002), USA.
URL: http://www.barretttechnology.com/robot/index.htm

BBC News (2000) ‘Bionic’ Hand Success Hailed, Wednesday, 22 November, BBC News, Health,
URL: http://news.bbc.co.uk/hi/english/health/ newsid_1035000/1035304.stm

BBC News (2002) Israel uses a robot to disarm a suspected suicide bomber injured in an explosion near Haifa, Wednesday, 8 May,
URL: http://news.bbc.co.uk/hi/english/world/middle_east/ newsid_1976000/1976341.stm

BBC News (2002) Robot Hand for the Disabled, Health Section, Wednesday, 7 August
URL: http://news.bbc.co.uk/1/hi/health/2178226.stm

Bergeron, J., (2002) Robot hand with digital force feedback,
URL: http://www.geocities.com/androidbuilder/handbolt.html

Bernard, T.E., (2000) Data from Ergonomic Design for People at Work, Vol. 1, Table VIA-2, University of South Florida, pp 290-293.
URL: http://www.hsc.usf.edu/~tbernard/ergotools/

Bionic Hand with Fluidic Actuators, Fluid Technik, Forschungszentrum Karlsruhe, Germany,
URL: http://www.iai.fzk.de/medtech/fluid/eng/humanoide.htm

Bionic Hands for Children, March 2001, Cyber Britain Magazine,
URL: http://www.britain.or.kr/english/young/200103/

Bionic Hand for Little Conner, Saturday, 23 December 2000, Weymouth News, Newsquest Media Group
URL: http://www2.newsquest.co.uk/dorset/archive/2000/12/23/WEYMOUTH_NEWS_ NEWS11ZM.html

British Scientists Develop Bionic Hand for Children, 23 September 2000, NetLondon.com, © London Radio Service,
URL: http://www.netlondon.com/news/2000-47/ 0F977E4A17E042EE802.html

Callaghan, K., and Paget, R., (June 2001) Living in the Shadow of Robo-Sapiens, NOW.com, Gamer, © Cyber-Tech Group Ltd.
URL: http://www.now.com/feature.now?fid=1803796&cid=1023695

Cyber Britain Magazine (2000) Artificial Hand that Grasps the Problem, March, Cyber Britain Magazine,
URL: http://www.britain.or.kr/english/young/200003/np14.htm

Dassault Systems, (2002) Welcome to the CATIA's users page
URL: http://www.catia.com/

Discover (1998) Breakthroughs, *Bendbots,* Discover, Vol. 19, No.8, August, The Walt Disney Company.
URL: http://www.discover.com/august_issue/breakbendbots.html

DLR Hand II Homepage, © DLR, Institute of Robotics and Mechatronics, 2002
URL: http://www.robotic.dlr.de/HAND/

Fernandez, J., (2000) The Rice anthropomorphic hand, Houston, Texas, USA.
URL: http://www.geneticprogramming.com/jjf/hand-info.htm

Gazeau, J.P., (2000) Main mécanique ariculée à 4 doigts, Laboratoire de Mécanique des Solides de l'Université de Poitiers,
URL: http://www-lms.univ-poitiers.fr/robot/Robot.html

Humanoid Hand Project, Intelligent Robotics Lab, Vanderbilt University School of Engineering, Nashville, Tennessee, USA.
URL: http://eecs.vanderbilt.edu/CIS/IRL/html/humanoid_hand.html

Kyberd, P., The Leverhume Oxford Southampton Hand, Homepage of the Author,
URL: http://www.tagish.co.uk/losh/default.htm

Lar-Deis (2002) UB Hand 1& II, Lar-Deis, Laboratory of Automation and Robotics
URL: http://www-lar.deis.unibo.it/past-activ/ubhand/

Loncaric, J., (1991) Modular Dexterous Hand, US Patent 5,052,736, October 1, ISR.
URL: http://www.isr.umd.edu/ISR/accomplishments/028_ModularDexterousHand/

Lopez, G., Robot’s Hand, Techno Concept, Montpellier, France,
http://conceptsite.com/hand/meca_angl.html

Menzel, R., The Development of a Hydraulic Hand (SEKON), Senter for Kompetanse og Næringsutvikling,
URL: http://www.amm.mw.tu-muenchen.de/Research/Old/Bericht_e_95/node52.html

Moseley, M L., (2000) Science Fiction no more, (Barrett Hand) Cadalyst, March
URL: http://www.cadalyst.com/spectrum/spotlight/ 0300dspot/0300dspot.htm

Murphy, C., (2002) A Light-Weight Anthropomorphic Hand, Yale Hand Page, Yale University, USA.
URL: http://www.cs.yale.edu/AI/VisionRobotics/YaleHand.html

Necessary, R., and Culbert, C.,(2001) Robonaut, Homepage of NASA Robonaut,
URL: http://vesuvius.jsc.nasa.gov/er_er/html/robonaut/robonaut.html

The Official Team New Zealand Website
URL: http://xtramsn.co.nz/teamnewzealand/

Seven D.O.F. MIA Arm Page, 1997 © Sugano Laboratories, Waseda University.
URL: http://www.sugano.mech.waseda.ac.jp/wam/arm/mia1-e.htm

Smalley, E., (June 28/July5 2000) NASA grasps intricacies of human hand, TRN News,
URL: http://www.trnmag.com/Stories/062800/ NASA_Robot_Hand_062800.html

Solid Edge.com
http://134.244.209.21/

SolidWorks.com
URL: http://www.solidworks.com

Underactuated Robotic Hands, Laboratorie de robotiqu, Universite Laval, August 2002.
URL: http://wwwrobot.gmc.ulaval.ca/recherche/theme04_a.html

Woelf, K., Grasp Strategies for a Robotic Hand (SEKON), Senter for Kompetanse og Næringsutvikling,
URL: http://www.amm.mw.tu-muenchen.de/Research/Old/Bericht_e_95/node51.html

Wood, R. (2002) The Shadow Dextrous Hand/Arm, Shadow Robot Company Ltd.
URL: http://www.shadow.org.uk/products/newhand.shtml

Books

Andeen, G.B., (ed.) (1988) Robot Design Handbook, McGraw-Hill.

Boundy, A. W., (1987) Engineering Drawing, Third Edition, McGraw Hill Book Company, Sydney Australia.

Chironis, N.P., and Sclater, N., (1996) Mechanisms and mechanical devices sourcebook, Second Edition, McGraw-Hill, New York, USA.

Dreyfuss, H., (1967) Measure of man: human factors in design, Revised and expanded 2nd Edition, Whitney Library of Design, New York., USA.

Croney, J., (1971) Anthropometrics for designers, Van Nostrand Reinhold, New York, USA.

Devore, J.L., (1995) Probability and statistics for engineering and the sciences, Duxbury Press, Fourth edition, Washington, USA.

FAG (1984) FAG standard programme, FAG Kugelfischer Georg Schäfer KgaA, 1984 Edition, Schweinfurt, Germany.

Fawcett, J.N., and Burdess, J.S., (1988) Basic mechanics with engineering applications, Edward Arnold, London, UK.

Fu, K.S., Gonzalez, R.C., and Lee, C.S.G., (1987) Robotics: *control, sensing, vision, and intelligence*, McGraw-Hill, New York, USA.

Goodale, M.A., (ed.) (1990) Vision and action: the control of grasping, Ablex Publishing Corporation, Norwood, New Jersey, USA.

Iberall, T., and MacKenzie, C.L., (1990) Opposition Space and Human Prehension, in Venkataramn, S. T. and Iberall, T., (ed.), Dexterous Robot Hands, Springer-Verlag, New York, pp.15-54.

The Institution of Mechanical Engineers: Lubrication and Wear Group (1962) Eight papers on non-conventional lubricants and bearing materials such as used in nuclear engineering, Published by the Institution, Westminster, London, Great Britain.

ISO (1986) Bearings, ISO Standards Handbook 27, First Edition, Switzerland.

Jensen, P.W., (1991) Classical and modern mechanisms for engineers and inventors, Marcel Dekker, New York, USA.

Kroemer, K., Kroemer, H., and Kroemer-Elbert, K., (1994) Ergonomics: *How to design for ease and efficiency*, Prentice Hall Inc., Englewood Cliffs, New Jersey, USA.

Lundstrom, G., Lundstrom L., Anstrom, A., and Rooks, B., (ed.) (1972) Industrial robots, - *A survey: details of construction, performance, prices and applications*, originally a Swedish Report translated to English and enlarged, International Fluidics Services Ltd., Bedford, UK.

MacKenzie, C.L., and Iberall, T., (1994) The Grasping Hand, North-Holland, Amsterdam, Netherlands.

Martini, F. H., (1998) Fundamentals of Anatomy and Physiology, Prentice Hall International Inc., 4rth International Edition, Upper Saddle River, New Jersey, USA.

McCloy D., and Harris, D.M.J. (1986) Robotics: an introduction, Open University Press Milton Keynes [Buckinghamshire], Philadelphia.

Muilenburg, A.L., and LeBlanc, A., (1989) *Chapter 5*: *Body-Powered Upper-Limb Components*, Comprehensive Management of the Upper-Limb Amputee, Springer Verlag, 1st edition, January 15, 1989.

Murray, R.M., Li, Z., and Sastry, S.S., (1994) A Mathematical Introduction to Robotic Manipulation, CRC Press, Boca Raton, Florida, USA.

Neale, M.J., (ed.) (1993) Bearings: *A Tribology Handbook*, Butterworth-Heinemann Ltd., London, Great Britain.

Nieman, D.C., (1990) Fitness and Sports Medicine: An Introduction, Bull Publishing Co., Palo Alto, California, USA, p. 513.

Oberg, E., Jones, F.D., Horton, H.L., and Ryffel, H.H., (1988) Machinery's handbook: *a reference book for the mechanical engineer, designer, manufacturing engineer, draftsman, toolmaker, and machinist*, 23rd Edition, Industrial Press, New York, USA.

Panero, J., and Zelnik, M., (1979) Human dimension & interior space: a source book of design reference standards, Whitney Library of Design, New York, USA.

Pham, D.T., (ed.) and Heginbotham, W.B., (ed.) (1986) Robot grippers, IFS (Publications), Bedford.

Pheasant, S., (1986) Bodyspace: *Anthropometry, Ergonomics and Design*, Taylor and Francis Ltd, London, Great Britain.

Reichardt, J., (1978) Robots: Fact, Fiction and Prediction, Thames and Hudson Ltd.

Reynolds, D. W., (2002) Star Wars Attack of the Clones: *The Visual Dictionary*, © Lucas film Ltd., Dorling Kindersley, London, Great Britain.

Rhyder, G.H., and Bennett, M.D., (1990) Mechanics of Machines, Second Edition, Macmillan Education Ltd., Hampshire, London.

Roberts, A.D., and Lapidge, S.C., (1977) Manufacturing Processes, McGraw Hill Inc., USA.

Rosheim, M.E., (1994) Robot Evolution: The development of Anthrobotics, *"Hands"*, John Wiley& Sons Inc., New York, 1st Edition, pp.189-255.

Sauter, W.F., (1989) *Chapter 12:* Electric Paediatric and Adult Prosthetic Components, Comprehensive Management of the Upper-Limb Amputee, Springer Verlag, 1st edition, January 15, 1989.

Sears, H.H., Andrew, J.T., and Jacobsen S.C., (1989) *Chapter 18*: Experience with the Utah Arm, Hand and Terminal Device, Comprehensive Management of the Upper-Limb Amputee, Springer Verlag, 1st edition, January 15, 1989.

Shigley, J.E., (1986) Mechanical Design, Fourth Edition, McGraw Hill Inc., Singapore.

Simmons, C., and Maguire, D., (1995) Manual of Engineering Drawing to British and International Standards, Edward Arnold, London, UK.

Smith, W., (1993) Foundations of materials science and engineering, Second Edition, McGraw Hill International Editions, Engineering Mechanics Series, McGraw Hill Inc., New York, USA.

Solomon, Schmidt, and Adiagna (Unknown) Human Anatomy and Physiology, Saunders College Publishing Library

Teo, D.C., (1964) Applied linkage synthesis, Addison-Wesley Publishing Company Inc., Massachusetts, USA.

Tooley, M., (1995) PC Based Instrumentation and Control, Second Edition, Newnes, Cornwall, Great Britain.

Tsai, L-W. (1999) Robot analysis: *the mechanics of serial and parallel manipulators,* Wiley, New York, USA.

Venkataraman, S.T., and Iberall, T., (ed.) (1990) Dexterous Robot Hands, Springer-Verlag, New York, pp.83-86.and pp.151-153.

Walsh, R.A, (1994) McGraw-Hill machining and metalworking handbook, McGraw-Hill, New York, USA.

Wiebe, E.N., Miller, C.L., and Nasman, L.O., (1995) Engineering Graphics Communication, Irwin Graphics Series, Richard D. Irwin Inc., Chicago, USA.

Woodson, W.E., Tillman, B., and Tillman, P., (1992) Human factors design handbook: *information and guidelines for the design of systems, facilities, equipment, and products for human use* 2nd Edition, McGraw-Hill, New York.

Technical Catalogues

Aluminium Solutions (2001) Stock list, New Zealand, Catalogue.

Blacks Fasteners (2000) Stock list of screws, rivets, nuts, socket screws, washers, (and) bolts, Blacks Fasteners Ltd., Christchurch, New Zealand, Catalogue.

Ezo (2000) Ezo Precision Ball Bearings Catalogue, Metric Series, Sapporo Precision Inc., Japan.
(NZ Supplier: Wilson Bros. Christchurch, New Zealand)

Farnell (2002) Farnell, Farnell Electronic Components, Vol.1-3, Auckland, NZ, Catalogue.
http://www.farnell.com

Faulhaber DC motors (1994) Minimotor, Minimotor SA, Croglia, Switzerland, Catalogue.
URL: http://www.minimotor.com/

Harwin.com (2002) Harwin Inc, New Albany, USA.
URL: http://www.harwin.com/

HPC Gears (2001) Manufacturer and stock list of gear transmission products, HPC Gears Ltd., Derbyshire England, Catalogue.
URL: http://www.hpc-gears.co.uk/

Interelectric AG (1994) Maxon Motor: *drive components and systems*, Catalogue.
URL: http://www.maxonmotor.com/Catalog/index.html

Ludowici (2000) Engineering Plastic Products, Ludowici-Addington Ltd., Christchurch, Catalogue.

MicoWakefield (2001) Aluminium, MicoWakefield, New Zealand, Catalogue.

Molex.com (2002) Molex
URL: http://www.molex.com/cgi-bin/bv/molex/index_login.jsp
Nachi (2000) Ball & Roller Bearings, Nachi Fujikoshi Corporation, Tokyo, Japan, Catalogue. (NZ Suppliers: South Island Bearing Distributors Ltd., Christchurch, New Zealand)

Reliance Gear Limited (1986) Precision Drive components, *Metric and inch control and instrumentation Catalogue RG12*, Actuation and instrumentation systems and components, Reliance Gear Company Limited, UK

Reliance Gear Limited (2002) Catalogue, Reliance Gear Company Limited, UK.
URL: http://www.reliance.co.uk

RS Components (2002) RS Components, *New Zealand Catalogue*, RS Components Australasia, NZ.
URL: http://www.rswww.co.nz

SDPSI (1999) Handbook of Shafts and Couplings, Stock Drive Products Sterling Instrument, New York, USA.
URL: http://www.sdp-si.com/Sdptech_lib.htm

Solid Works (1998): Fundamentals of parametric modelling: *Intro to Solid Works mechanical design automation software:* Solid Works Corporation, Concord, Massachusetts, USA

Solid Works 98Plus (1998) Tutorial: Solid Works Corporation, Concord, Massachusetts, USA

Solid Works 99 (1999) Users Guide: Solid Works Corporation, Concord, Massachusetts, USA

Solid Works 2000 (2000) Parts, Assemblies and Drawings: *Volume I:* Solid Works Corporation, Concord, Massachusetts, USA

Solid Works 2000 (2000) Parts, Assemblies and Drawings: *Volume II:* Solid Works Corporation, Concord, Massachusetts, USA

The Solid Works web site can be found at:
URL: http://www.solidworks.com

Steel & Tube (1997) Dimensions & Properties Handbook, February 1997 Edition, Auckland, New Zealand, Catalogue.